Development and hazard assessment of nanoparticles

Sourav Bhattacharjee

FUTURE

PAST

PRESENT
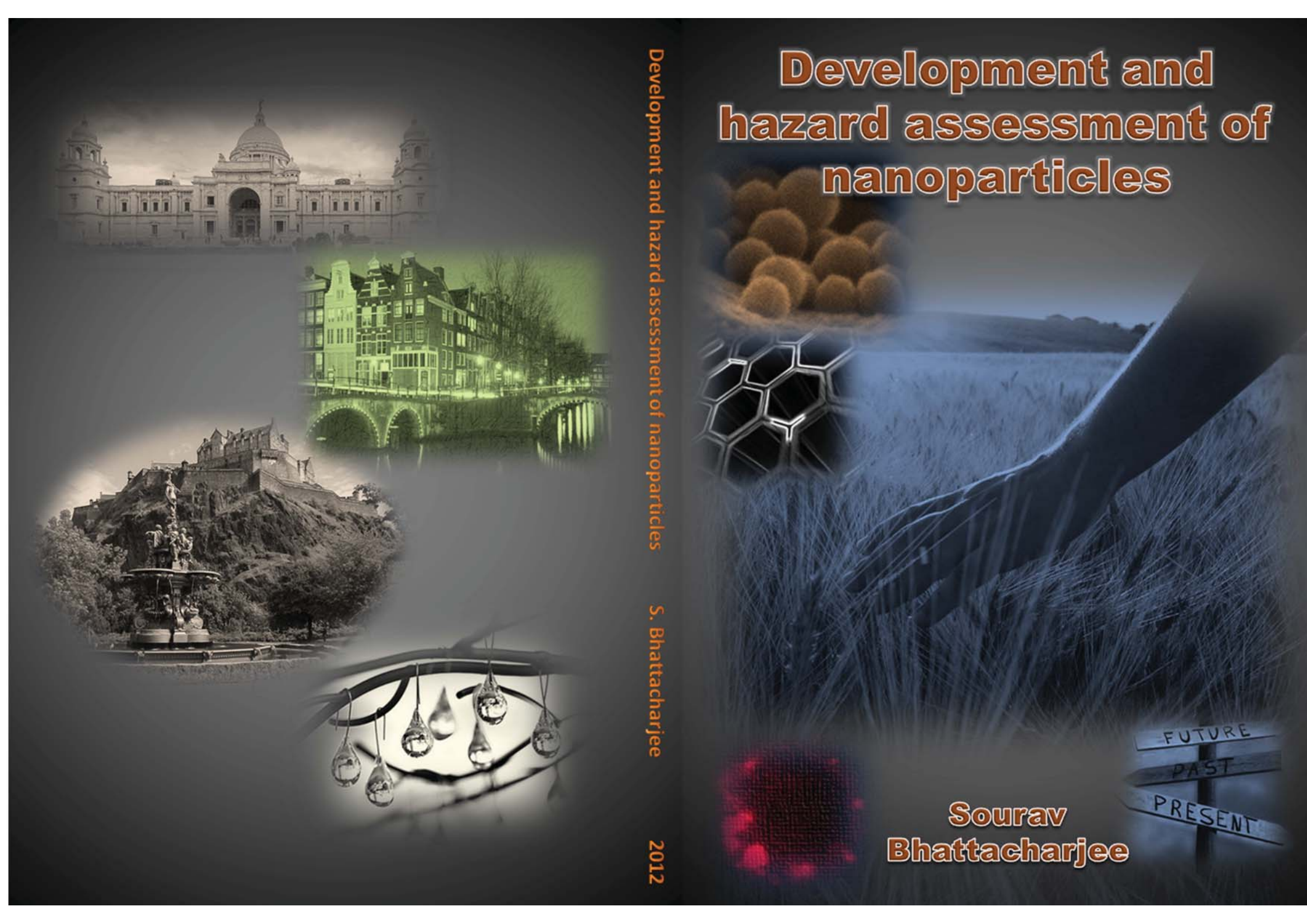
Development and hazard assessment of nanoparticles

Sourav Bhattacharjee

Thesis committee

Thesis supervisors

Prof. dr. ir. Ivonne M. C. M. Rietjens
Professor of Toxicology
Wageningen University

Prof. dr. Han Zuilhof
Professor of Organic Chemistry
Wageningen University

Thesis co-supervisors

Dr. Gerrit M. Alink
External staff member, Sub-department of Toxicology
Wageningen University

Dr. Antonius T. M. Marcelis
Assistant professor, Laboratory of Organic Chemistry
Wageningen University

Other members

Prof. Paul J. A. Borm   Zuyd University, Heerlen, The Netherlands
Prof. dr. ir. Wim E. Hennink   Utrecht University, The Netherlands
Dr. Roel P. F. Schins   IUF - Leibniz Research Institute for Environmental Medicine,
                                      Düsseldorf, Germany
Prof. dr. Aldrik H. Velders   Wageningen University, The Netherlands

Development and hazard assessment of nanoparticles

Sourav Bhattacharjee

Table of contents

Chapter 1

Introduction

Background

Although nanotechnology has gained much momentum in the last two decades, human beings have used nanotechnology from antiquity. Nanoparticles (NP) have been used for coloring pottery products by Mesopotamians in the 9th century BC[1] and medical applications of silver NP have also been known since long. Only recently the scientific community, including academia and industry, has started putting significant efforts in the development of nanotechnology. A growing interest in nanotechnology and nanotechnology-based products came with the realization that these materials show a unique range of properties that differ significantly from the bulk materials. This makes them exciting from both a scientific and application point of view.[2] With growing population and shrinking resources, mankind will be facing new and unforeseen challenges in the near future and nanotechnology has the capability of revolutionizing many facets of technology, ranging from energy generation[3] to medicine[4] and many others. The potential for applications of nanotechnology is unquestionable and hence this emerging technology will become increasingly important in the near future.

In Greek language, the word "nano" means "dwarf"[5] although considering its wide application possibilities, it can be stated that, as an emerging technology, the potential and expectations of nanotechnology are rather gigantic. In the last couple of decades, becoming an instant hit topic in the scientific community, nanotechnology has seen a tremendous surge in research as well as funding.[6] As a result of the novel inventions, new nanotechnology-based products are now-a-days getting frequently introduced into consumer market.[7] It is estimated that the market for nanotechnology industry will exceed $1.2 trillion only in the USA by 2015[2] and will keep on growing at a staggering rate.

To better understand this new state-of-the-art, it may be of importance to highlight some of the features of nanotechnology as compared to conventional technologies. It is commonly accepted that a material with at least one dimension less than 100 nm, can be considered as nanomaterial,[8] although this delineation is not an uniformly accepted definition, and efforts have been dedicated to set a specific range of sizes that define nanomaterials.[9] However, from this definition it can immediately be noted that the dimensions of nanomaterials are extremely small and fall almost within the size-domains of atoms or molecules. These small sizes often provide nanomaterials with unique properties compared to bulk materials,[10] which form the driver for further research. A specific class of nanomaterials is formed by nanoparticles (NP), i.e. objects with all three dimensions in the range of one to maximally a few hundreds of nanometers. Largely depending on the substrate and the size, these NP display an unparalleled set of optoelectronic properties (like fluorescence, high reactivity, super-conductivity, etc.). Such NP can be an embedded part of a larger solid, such as the well-studied Si NP that are formed within SiO_2 upon heating,[11] or freestanding and thus an isolable material by itself. This thesis focusses solely on the latter, as with this small size, NP pose unconventional health hazards, which were largely neither monitored nor regulated until the recent past.

The unique material features that start emerging at nanometer-scale dimensions are extraordinary.[12] It is because of these unconventional properties that nanomaterials are capable of serving purposes which can usually not be achieved with conventional or bulk materials. Due to their novel properties, nanomaterials are now getting used for multiple purposes, including cosmetics, sports equipments, clothing, drug delivery and diagnostics, etc. With more and more

unexplored fields of research converging with nanoscience, a considerable growth of the utility of this emerging technology can be forecasted.

With a highly reactive surface, NP provide ample opportunity for chemical engineering. For example, the surfaces of NP can be functionalized by DNA which can then be used for gene-delivery purposes.[13] Similarly, the surfaces of the NP (like silicon NP) can be functionalized with different end groups which render them to be carrier of different surface charges.[14] With the huge possibilities of many more uses of engineered NP, nanotechnology shows promises to influence the lives of human beings in a significant way.

Objective of the thesis

The objective of this thesis is to understand the role of surface charge and particle size in the toxicity and cellular interaction of semiconductor (like silicon) and polymer (like tri-block copolymer and polystyrene) NP.

Notable surface, physical and chemical properties of nanomaterials

The % of atoms within a particle that are expressed on the surface is inversely proportional to the size of the particle. It is because of this fact that even up to ~50 % of the atoms in a NP may be expressed on the surface,[15] and the NP present a very high surface area-to-mass ratio. This yields a highly surface-reactive material, which is prone to react with a wide variety of (bio)molecules.[16] Hence, it can be expected that the NP, by virtue of reacting with a variety of molecules, can be capable of exerting (cyto)toxicity. This makes the surface chemistry of nanomaterials of immense importance in determining the toxicity. For example, factors related to the surface - like surface charge,[17] crystallinity,[18] surface adsorption of other molecules (like protein),[19] etc. - have all been linked to the toxicity of NP.

From physical characteristics of a NP, two important observations are mentioned in relation to this thesis: 1) Due to very small size, the NP can get access to those parts of the body that are inaccessible to bigger particles (like micro particles); 2) The aspect ratio (i.e. ratio of length and width of the nanomaterial) has been found to be important in determining cytotoxicity.[20] For example, nanomaterials with a high aspect ratio, like carbon nanotubes, have been found to be cytotoxic and induce inflammatory responses, like silicosis, in human lungs.[21]

Another important characteristic of NP is that they form colloidal suspensions. However, the dispersion states of the NP in liquid, like biological cell culture medium, can vary situation-wise and dependent on their surface characteristics. It seems that depending on the environment (like concentration, dispersion medium, sonication, presence of protein, etc.) the NP can exist as monodisperse or agglomerated stages. Interestingly, the agglomeration phase of the NP had been found to influence cellular interactions and toxicity,[22] which will be discussed in more detail in the following sections.

Routes of exposure, fate and cellular uptake of NP

The exposure to the different NP can happen through multiple routes: 1) inhalational, which is the major route of exposure especially in occupational settings, like for ultrafine carbon NP;[23] 2) oral, where NP are getting used in food-based formulations, like silica NP;[24] 3) dermal, where NP are administered on the skin, like C_{60} NP in cosmetic cream preparations,[25] or titanium dioxide NP in sunscreens; 4) parenteral, when the NP are introduced in the body by parenteral routes (e.g. intravenous), like CdSe/ZnS quantum dots introduced inside the body for bioimaging purposes.[26]

The fate of the NP after entering the body depends on the local anatomy and physiology of the exposure route, as well as on the surface and physical properties of the NP. For example, after inhalational exposure, it has been shown that the NP interact with the mucous layer of the respiratory tract depending on the surface charge, particle size and other parameters (like viscosity, solubility).[27] Similarly, the interaction between food and the NP has been shown to be crucial for absorption of the NP from the gastro-intestinal tract after oral exposure.[28]

It is reported that after getting entry into the body, the NP can get access into the blood stream and circulate throughout the body. Hence, intravenous exposure gives the highest bioavailability (100 %) as this route introduces the NP directly into the blood steam. On the other hand, while the bioavailability of NP after inhalational or oral exposure seems to be less compared to the intravenous routes and depending on the composition of the NP, there is also much less control over the access of such species into the body. Unfortunately and in addition to the above, no consistent information is available on the bioavailability in case of dermal exposure, with different reports indicating contradicting bioavailability statistics.[29,30]

Irrespective of the exposure route, it has been reported that the macrophage cells were activated once the NP reached the blood stream.[31] It should be noted that blood, apart from the serum proteins, is rich in *opsonin* proteins (like immunoglobulins), which facilitates the phagocytosis of the NP. It has been shown that macrophage cells effectively phagocytosed the NP and cleared them from the blood stream.[32] However, this phenomenon also depends on the surface characteristics and the composition of the NP. For example, it was observed that surface modification of the NP with hydrophilic molecules (like polyethylene glycol/PEG) rendered the NP less phagocytosed by the macrophage cells and thus, increased their blood circulation time.[33] How this happens is still not clear, although it is suggested that with a different surface coating of NP, the group of cell membrane-bound receptors that are activated by the coated NP are also different.

Several groups of cell membrane-bound receptors (like clathrin, caveolin) had been recognized to take part in the cellular internalization of the NP.[34] However, it is not clear what are the factors that influence this interaction between the NP and the receptors. It is hypothesized that even this interaction is influenced by the surface chemistry of the NP and hence, any alteration in the surface properties (like surface charge) can change the course of interaction and in turn, can influence cellular uptake.[35]

The biodistribution and metabolism of NP inside the body are largely unclear. With the available literature, it can be seen that NP do not undergo extensive metabolism in the body through major metabolic pathways (like the cytochrome P450 system).[36] Instead, depending on the size and type of surface coating and other surface characteristics, the NP can be excreted[37] or accumulated (like in aquatic animals)[38] in the body. Recently, it was identified that NP < 5.5 nm

in size could be excreted out of the body through renal route.[39] NP gaining access into the body through inhalation can result in bioaccumulation.[40] In fact, a few nanomaterials (like carbon nanotubes) have been found to be quite biopersistent and can initiate inflammatory responses, like granuloma formation.[41]

Problem statement

With the increasing penetration of nano-based products into consumer markets, it is inevitable that consumers will be exposed to nanomaterials and especially NP.[42] From a toxicological point of view, data on the toxicological effects that these NP can exert on biological systems are rather scarce, although research in nanotoxicology has grown markedly in the last decade. Furthermore, a lack of uniformity in research protocols as well as an insufficient common minimum criteria set for such experiments can be observed.[43] The European Food Safety Authority (EFSA) has published its revised guidelines for risk assessment of nanomaterials applied in the food and feed chain in 2011, including guidelines for both in vivo and in vitro experimentation.[44] This may be pivotal in bringing back coherence within the wide variety of nanotoxicological research efforts that are currently going on. As per the EFSA guidelines, a great deal of importance has been put on the in vitro experimentation, which can be regarded as a generic shift in approach towards dealing with these unconventional risks posed by the upcoming technologies, like nanotechnology. Additionally, the EFSA strongly advocated in favor of adequate physico-chemical characterization of the NP before initiating the investigation process or making a risk assessment. The frequent lack of proper characterization of NP explains the lack of useful nanotoxicological data.[45] Different NP behave differently in different biological systems (like cell culture medium)[46] and it is important to realize what is exactly getting tested before exposing cells, or whole organisms to NP. Hence, proper characterization of the NP under the relevant testing conditions is essential in nanotoxicological research.

Although several groups have reported that NP can exert toxicity, mostly in vitro,[47-49] little is understood regarding the factors that influence such toxic effects. It is often hypothesized that various surface properties[50, 51] (like porosity, crystallinity, roughness, surface functionalization) and physical properties (like particle size)[52] influence the cytotoxicity or cellular interactions. Surface and physical properties that have been identified most often by many research groups as a factor influencing cellular interactions of NP are surface charge and particle size.[43-55] Since NP are chemically reactive through their surface groups and their biological interactions occur through a chemical interaction with biomolecules or cell constituents, anything that influences their reactivity also influences their cytotoxicity. Hence, surface charge and size both can influence the behavior of NP in cellular systems. Yet, frequently the experimental conditions are still shrouded with so much of uncertainties about the characterization of NP that it is difficult to actually form an idea regarding how surface- (like surface charge) or physical properties (like particle size) can influence the cellular interaction (like cellular uptake) of NP, or cause toxicity.

Selection of model systems

To achieve the objectives of the present thesis, the model systems to be used for the studies had to be defined especially with respect to: 1) the type of NP to be included in the studies, and 2) the biological model systems and endpoints to be used for characterizing the toxicity and cellular interactions of NP.

1) The type of NP to be included in the studies

In these studies silicon NP (Si NP), germanium NP (Ge NP) and polymeric NP (PNP) were included.

Si NP and Ge NP

Silicon NP (Si NP) and germanium NP (Ge NP), which can routinely be prepared in the size range of 2 – 20 nm, are inherently fluorescent due to *quantum confinement*.[56] As a result, Si NP/ Ge NP can be used for bioimaging purposes and have as an advantage over conventional fluorescent molecules that they do not bleach over time, even under high intensity illumination.[57]

The surfaces of different Si NP and Ge NP can further be modified with different chemical groups in order to generate NP with different properties. One possibility is *bioconjugation*, i.e. functionalization with biologically important molecules, like proteins, DNA and also antitumor drugs.[58] Due to the small size of the NP, there is a much higher surface area/volume ratio as compared to microsized particles or bulk materials,[59] which can lead to a size-dependent toxicity.

Polymeric NP (PNP)

Apart from inorganic NP, also organic NP are highly relevant. In this regard, polymeric NP (PNP) are of significant interests, specifically because of the rapidly increased control over polymer properties by advanced synthetic methods. This may lead to monomolecular PNP, or to multi-molecular PNP, in which the polymer chains are kept together by physical interactions or covalent chemical bonds. Recently, PNP prepared from tri-block copolymers that aggregate under well-defined conditions, have gained attention. Because of possible higher accessibility to different parts of the body due to smaller size compared to the microparticles, as well as significant scope for chemical engineering, PNP are presently used for multiple purposes including targeted drug delivery.[61] Given the wide range of PNP, this class of materials can provide a very exciting platform for further research.

With the rapid developments in polymer science, tri-block copolymers with well-defined monomer compositions and block lengths can be prepared using various controlled polymerization techniques. In this way, tri-block copolymer NP with different novel properties can be obtained by tuning the synthesis, using monomers with different functionalities or post-synthesis functionalizations. Perhaps the most important aspect of these tri-block copolymer PNP lies in their huge potential in *nanomedicinal* applications.[61, 62] An interesting type of PNP are those that are biodegradable. For example, PNP from polycaprolactone-PEG-polycaprolactone tri-block copolymers are biodegradable, since the PNP gradually disintegrate within the tissue

due to their conversions by proteolytic enzymes (like *matrix metalloproteinase*)[63] releasing the cargo of encapsulated drugs (like doxorubicin). Hence, these PNP can be used in targeted drug delivery.[64] These tri-block copolymers, have a hydrophobic polyester middle block and hydrophilic side blocks (like PEG_{2000}), which allows the formation of PNP via nanoprecipitation in water, yielding reverse micelle-like structures. Interestingly, by chemical engineering, multiple properties of these tri-block copolymer NP can be manipulated. For example, by simple alteration of the molecular weight of the hydrophilic side blocks (like using PEG_{400} instead of PEG_{2000}), the size of the resulting PNP can be changed. In the polyester middle block, a fluorescent probe can be incorporated, which makes the PNP fluorescent and traceable by confocal laser scanning microscopy (CLSM) in biological environments. The terminal hydroxyl moieties of the PEG molecules may be converted into other groups (like amines or acids) in order to obtain PNP with different surface charges (positive and negative) in aqueous suspensions. Thus, via highly tunable chemistry, tri-block copolymers may provide a unique set of PNP with different sizes and surface charges, along with added functional properties (like fluorescence). These tri-block copolymer NP can encapsulate hydrophobic molecules of interest (like anticancer drugs or dye molecules)[65] and after administration, can disintegrate gradually in order to release the encapsulated molecules. This has special advantages in cancer chemotherapy where the drugs used are highly toxic and a PNP-based targeted drug delivery approach will reduce the toxic side effects along with increasing the cost-efficiency of treatment.[66] Apart from tri-block copolymer NP, polystyrene NP may be an interesting class of PNP that can be employed in the investigation regarding toxicity of PNP. Wide varieties of fluorescent polystyrene NP are commercially available and hence, were tested in different sizes (50 and 100 nm) and surface charges (positive and negative). The availability of such well-characterized PNP can be exploited for further toxicological investigations.

2) The biological model systems and endpoints to be used

It should be noted that in vitro studies can indicate the toxic potential of a nanomaterial with further elucidation of the biological responses and underlying mechanisms. Of course, in vitro studies are predominantly useful for screening purposes and do not replace the in vivo study models, which are still essential in order to determine the safe exposure levels. Hence, coping with the objectives set for this thesis, both in vitro and in vivo model systems were needed. For understanding the role of surface charge and particle size in the mode of action underlying the toxicity of NP as well as in their cellular uptake, in vitro systems were more suitable. However, for validation of in vitro data, in vivo studies are generally required. In order to perform the in vitro experiments in a manner that is relevant for mammals, rat alveolar macrophage NR8383 and human colonic adenocarcinoma Caco-2 cell lines were chosen. The NR8383 cells present an adequate cellular model for in vitro studies on toxicity of different NP. As the NR8383 are macrophage cells, an impact exerted on these cells by different NP can be extrapolated to the probable effects the NP can have on the macrophage cells, which act as a line of defense against foreign pathogens. The Caco-2 cells are derived from human colonic adenocarcinoma cells and are a widely accepted in vitro cellular model for human gut enterocytes.[67] These cells can be grown on transwell inserts and when properly grown, act as an in vitro model for the human small intestinal barrier.[68] As many PNP are getting developed with

applications in food-related or oral delivery formulations in mind, Caco-2 cells and their monolayers grown on transwell inserts can be used for in vitro assessment of intestinal absorption of different PNP after oral administration. It has been amply reported before that when grown as monolayers on transwell inserts, the Caco-2 cells successfully express specific ABC (ATP binding cassette) transporters on the apical and basolateral sides of the monolayers and can be used to study the role of these transporters in cellular transport and translocation. Results from such in vitro studies on transport across an intestinal barrier can subsequently be validated by in vivo studies with rats as animal models.

Interaction of NP in biologically relevant media

It is relevant to understand how NP behave in biologically relevant media, like cell culture medium. In the recent past, a wide variety of cell lines has been tested in vitro with an equally diverse range of NP. Typically, in vitro studies use NP suspensions made in cell culture medium, like F12-K, DMEM etc., which are usually rich in protein content. Apart from the protein, such medium contains a large pool of salts, antibodies, vitamins, etc. After mixing NP with these cell culture media, these constituents, mainly protein, may get adsorbed on the surface of NP and thereby change the surface characteristics of the NP. Additionally, it can influence the dispersion of the NP. For example, it was shown that addition of fetal calf serum, as a vehicle of proteins in the cell culture medium, facilitated the monodispersity of the NP.[69] On the contrary, in absence of proteins, the NP often existed in agglomerated states. Thus, molecules present in the surroundings of the NP, influence the surface characteristics of the NP considerably and this has an effect on cytological interactions of the NP. Previously, only a few groups have investigated the production of reactive oxygen species (ROS), like superoxide, peroxide, hydroxyl radicals, after NP coming in contact with cell culture medium in cell-free systems,[70] although the results failed to show any significant induction of ROS production in such experimental systems.

Outstanding issues

A major point of debate regarding the toxicity of NP is the mechanisms by which NP cause toxicity. Traditionally, oxidative stress is regarded as the major mechanism of cytotoxicity induced by NP,[71-73] although it is only very recently that some evidences have emerged questioning the role of oxidative stress as the principal or primary mechanism of cytotoxicity.[74] It is known that NP with highly reactive surfaces can produce reactive oxygen species (ROS)[75,76] intracellularly, like hydroxyl, peroxide, superoxide radicals, etc. These ROS can exert oxidative stress on the cells resulting in cytotoxicity. However, it still needs to be settled whether intracellular ROS production is the cause of cytotoxicity or whether it is the result of preceding toxic interactions of the NP with cellular components. Several research groups identified mitochondria as one of the intracellular target organelles for especially cationic NP.[77] It is known that the mitochondrial membrane is the location of the electron transport chain (ETC).[78, 79] It was reported that especially cationic NP caused a disturbance in the electrochemical gradient across the mitochondrial membrane, increasing the permeability of the mitochondrial membrane as well as disrupting the ETC.[77,80] This has led to some discussion as to whether oxidative stress is really the primary mechanism of cytotoxicity caused by NP, because a

disruption of the ETC can be expected to result in ATP depletion and ROS production as secondary phenomena. An interesting way to investigate the significance of oxidative stress in causing cytotoxicity is to check the (protective) effects of anti-oxidants, like vitamin E and C, as well as the consequences of modification of the intracellular levels of GSH. Another approach would be to compare the cytotoxicity caused by the NP to that caused by an uncoupler of the oxidative phosphorylation, like 2,4-dinitrophenol, affecting the mitochondria and disrupting the mitochondrial ETC, or to that caused by an agent known to cause toxicity via induction of oxidative stress, like hydrogen peroxide, both in presence or absence of anti-oxidants. In this way, an idea can be obtained on the role of oxidative stress in causing cytotoxicity in comparison to the disruption of mitochondrial ETC.

Up to the work in this thesis, nothing concrete is reported on what happens as a consequence of these effects of NP on mitochondria, especially after disruption of the ETC or increased permeability of the mitochondrial membrane. For example, if the ETC is disrupted, the cellular ATP production will be hampered and the cells may not be viable any more simply due to ATP depletion. Similarly, despite the fact that some groups mentioned an increase in free intracellular free calcium level after exposure to cationic NP,[77,81] a systematic investigation trying to determine the series of events by which the toxicity arises in cells, is missing. It is possible that with increased mitochondrial membrane permeability, the calcium stored within mitochondria is released into the cell cytoplasm and triggers cellular apoptosis by cell signaling mechanisms. There are different biomarkers, such as TNF-α as pro-inflammatory marker[82] and caspase-3 as apoptosis marker,[83] which can be monitored in order to shed light on the series of events that amalgamate into the observed toxicity of NP, although an approach in this direction has not yet been adequately explored.

How NP enter different cells is largely unknown, although many hypotheses have been proposed. From the starting hypothesis that NP enter cells by simple diffusion,[84] only recently the role of cell membrane-bound receptors in cell-NP interactions has been recognized. It was shown that especially cationic NP can interact with and in fact cross the phospholipid-based biomembranes.[85] A common explanation for this behavior of cationic NP is that the electrostatic attraction between the overall negatively charged biomembranes (at physiological pH) and cationic NP facilitates the interaction between the two.[86] However, this hypothesis fails to explain the cellular uptake of anionic NP, as they should be repelled by such negatively charged membranes and hence should not (easily) enter cells. Still, it was found that even negative NP entered cells in considerable amounts.[87, 88] These findings pointed to the role of cell membrane-bound receptors in the cellular internalization of different NP. In literature, it was already reported that different NP can be internalized by receptor-mediated endocytosis pathways.[89,90] Clathrin and caveolin are two important classes of cell membrane-bound receptors that are responsible for endocytotic pathways in cells.[91, 92] It is known that these cell membrane-bound receptors are long protein molecules with embedded pockets of positive or negative charges.[93] With a reactive or charged surface, it is possible that different NP can bind to, or rather act as substrates for these receptors to initiate the receptor-mediated endocytotic process. Apart from clathrin and caveolin, other cell membrane-bound receptors (like mannose receptors in NR8383 cells)[54] can also play a role in the cell surface receptor-mediated interactions and cellular uptake of NP. Furthermore, especially cationic NP can cause a solidification of the lipid structures and thus can increase the rigidity of the cell membranes.[94, 95] On the other hand, it was found that cationic amine-terminated G5 and G7 PAMAM (polyamidoamine) dendrimers were able to

create holes in supported lipid bilayers.[96, 97] These findings point to the multitude of effects that different NP can have on cell membranes.

Outline of the thesis

This thesis presents a systematic set of in vitro and in vivo toxicological studies along with synthesis and characterization of NP aimed at understanding the role of surface charge and particle size in the toxicity and cellular interactions of NP. These studies are presented chapter-wise:

In *Chapter 1* (the current chapter), a general introduction is provided in order to give the preamble as well as to set the platform for the problem statement, aims and approaches that were undertaken in order to investigate the toxicity and bioavailability of different NP both in vitro and in vivo, as described in this thesis.

In *Chapter 2*, the cytotoxicity of well characterized, monodisperse (size 1.6 ± 0.2 nm) and intrinsically fluorescent (under UV-light excitation) Si NP with amine (positive), azide (overall neutral) and acid (negative) surface groups in the human colonic adenocarcinoma Caco-2 cell line is described.

In *Chapter 3*, the scope of the toxicity assessment of the Si NP described in the Chapter 2, was further broadened by investigating the possible induction of oxidative stress in both Caco-2 and rat alveolar macrophage NR8383 cells exposed to the differently charged Si NP. An investigation on the possible capability of cationic amine-terminated Si NP to induce ROS formation in an isolated rat liver mitochondrial fraction was also included.

In *Chapter 4*, a comparative in vitro cytotoxicity study done with both Caco-2 and NR8383 cells after exposure to Si NP and Ge NP with different surface functionalities and sizes, obtained from three acclaimed laboratories from the USA and Canada, is reported. This study was done with the aim of comparing the obtained data with the existing information on the toxicity of Si NP reported in Chapters 2 and 3, in order to understand how size and surface characteristics of Si NP or Ge NP influence their cytotoxicity.

In *Chapter 5*, the synthesis and characterization of both a fluorescent tri-block copolymer and PNP (45 ± 5 nm) derived from it, functionalized with different terminal end-groups along with their toxicity in both NR8383 and Caco-2 cells are reported. The surface charge-specific involvement of clathrin and caveolin receptors in the cellular uptake of these tri-block copolymer NP in NR8383 cells was also investigated.

In *Chapter 6*, the synthesis and characterization of tri-block copolymer NP with different sizes (sizes 45 ± 5 nm and 90 ± 5 nm) and surface charges are reported. These PNP were tested for cytotoxicity in the same way as reported for the PNP in Chapter 5 in order to compare the effects of particle size on cytotoxicity and cellular uptake of PNP. The size-specific and surface charge-specific activation of clathrin, caveolin and mannose receptors in NR8383 and Caco-2 cells, as well as induction of intracellular ROS and depletion of cellular ATP after exposure to cationic PNP were investigated.

Chapter 7 describes the surface charge-specific interaction of tri-block copolymer NP (45 ± 5 nm) of different surface charges with ABC transporters in Caco-2 monolayers grown on transwell inserts, in order to investigate the transport of these tri-block copolymer NP across an

intestinal monolayer. This study was done to further extend the knowledge on the capability of these PNP to cross the intestinal barriers and on their bioavailability in vivo.

Chapter 8, in continuation of the in vitro research reported in Chapter 7, reports an in vivo study in rats with oral exposure of fluorescent tri-block copolymer NP (size 45 ± 5 nm) as aqueous dispersions. The bioavailability and biodistribution of these PNP, as detected by fluorescence, is shown.

In *Chapter 9*, the role of oxidative stress in the mechanism of cytotoxicity of positively charged polystyrene NP is investigated based on studying the protective effects of anti-oxidants, like vitamin E and C, as well as the consequences of modification of the intracellular levels of GSH, and a comparison to similar studies with 2,4-dinitrophenol affecting the mitochondria and disrupting the mitochondrial ETC and with hydrogen peroxide, known to cause toxicity via induction of oxidative stress.

In *Chapter 10*, the role of surface charge in toxicity and cellular uptake of polystyrene NP (50 and 100 nm) along with probing the underlying mode of action of the toxicity is studied in further detail. Investigations on the surface charge-specific cytotoxicity, induction of intracellular ROS, dissipation of mitochondrial membrane permeability, increase in cytoplasmic free calcium, depletion of cellular ATP and holes caused in cell membranes by the cationic polystyrene NP mark the highlights of this chapter. Finally, the data obtained in the series of experiments in chapter 9 and 10 were summarized and an attempt is made to understand the possible cascade of events that result in the cytotoxicity of NP.

In *Chapter 11*, a discussion is included where the results as well as the lessons learned from the afore-mentioned chapters in comparison to the available literature are presented. Finally, the future perspectives of the work done are added to highlight topics of future interest that remain to be elucidated.

References

1. Mirguet C, Fredrickx P, Sciau P, Colomban P; *Phase Transit.* 2008, 81:253-266.
2. Hood E; *Environ. Health Persp.* 2004, 112(113):A740-A749.
3. Kessler R; *Environ. Health Persp.* 2011, 119(3):A120-A125.
4. Saini R, Saini S, Sharma S; *J. Cut. Aest. Surg.* 2010, 3:32-33.
5. Warheit DB; *Toxicol. Sci.* 2008, 101:183-185.
6. Horton MA, Khan A; *Nanomed-Nanotechnol.* 2006, 2:42-48.
7. Quadros ME, Marr LC; *Environ. Sci. Technol.* 2011, 45(24):10713-10719.
8. Farré M, Gajda-Schrantz K, Kantiani L, Barceló D; *Anal. Bioanal. Chem.* 2009, 393:81-95.
9. Maynard AD; *Nature* 2011, 475(7354):31.
10. Ignác C; *Adv. Colloid Interfac.* 2009, 150:63-89.
11. Biteen JS, Tchebotareva AL, Polman A, Lewis NS, Atwater HA; *Mater. Res. Soc. Symp. P.* 2003, 770:93-98.
12. Yang L, Zhang LJ, Webster TJ; *Adv. Eng. Mater.* 2011, 13:B197-B217.
13. Luo D, Saltzman WM; *Gene Ther.* 2006, 13:585-586.
14. Rosso-Vasic M, Spruijt E, van Lagen B, De Cola L, Zuilhof H; *Small* 2008, 4:1835-1841.
15. Auffan M, Rose J, Bottero JY, Lowry GV, Jolivet JP, Wiesner MR; *Nat. Nanotechnol.* 2009, 4:634-641.
16. Sager TM, Castranova V; *Part. Fibre Toxicol.* 2009, 6(15).
17. El Badawy AM, Silva RG, Morris B, Scheckel KG, Suidan MT, Tolaymat TM; *Environ. Sci. Technol.* 2011, 45:283-287.
18. Napierska D, Thomassen LCJ, Lison D, Martens JA, Hoet PH; *Part. Fibre Toxicol.* 2010, 7(39).
19. Clift MJD, Bhattacharjee S, Brown DM, Stone V; *Toxicol. Lett.* 2010, 198:358-365.
20. Poland CA, Duffin R, Donaldson K; High Aspect Ratio Nanoparticles and the Fibre Pathogenicity Paradigm. Nanotoxicity: John Wiley & Sons, Ltd; 2009. p. 61-79.
21. Lam CW, James JT, McCluskey R, Hunter RL; *Toxicol. Sci.* 2004, 77:126-134.
22. Borm PJ, Robbins D, Haubold S, Kuhlbusch T, Fissan H, Donaldson K, et al.; *Part. Fibre Toxicol.* 2006, 3(11).
23. Oberdorster G, Sharp Z, Atudorei V, Elder A, Gelein R, Lunts A, et al.; *J. Toxicol. Env. Heal. A* 2002, 65:1531-1543.
24. Peters R, Kramer E, Oomen AG, Herrera Rivera ZE, Oegema G, Tromp PC, et al.; *ACS Nano* 2012, 6:2441-2451.
25. Aschberger K, Johnston HJ, Stone V, Aitken RJ, Tran CL, Hankin SM, et al.; *Regul. Toxicol. Pharm.* 2010, 58:455-473.
26. Arya H, Kaul Z, Wadhwa R, Taira K, Hirano T, Kaul SC; *Biochem. Bioph. Res. Co.* 2005, 329:1173-1177.
27. Lai SK, Wang YY, Hanes J; *Adv. Drug Deliver. Rev.* 2009, 61:158-171.
28. Mahler GJ, Esch MB, Tako E, Southard TL, Archer SD, Glahn RP, et al.; *Nat. Nanotechnol.* 2012, 7:264-271.
29. Filon FL, Crosera M, Adami G, Bovenzi M, Rossi F, Maina G; *Nanotoxicology* 2011, 5:493-501.
30. Wu JH, Liu W, Xue CB, Zhou SC, Lan FL, Bi L, et al.; *Toxicol. Lett.* 2009, 191:1-8.

31. Kulikova GA, Parfenyuk EV, Ryabinina IV, Antsiferova YS, Sotnikova NY, Posiseeva LV, et al.; *J. Biomed. Mater. Res. A* 2010, 95A:434-439.

32. Shan XQ, Liu CS, Yuan Y, Xu F, Tao XY, Sheng Y, et al.; *Colloid Surface B* 2009, 72:303-311.

33. Torchilin VP, Trubetskoy VS, Milshteyn AM, Canillo J, Wolf GL, Papisov MI, et al.; *J. Control. Rel.* 1994, 28:45-58.

34. Iversen T-G, Skotland T, Sandvig K; *Nano Today* 2011, 6(2):176-185.

35. Arnida, Malugin A, Ghandehari H; *J. Appl. Toxicol.* 2010, 30:212-217.

36. Fröhlich E, Kueznik T, Samberger C, Roblegg E, Wrighton C, Pieber TR; *Toxicol. Appl. Pharm.* 2010, 242:326-332.

37. Burns AA, Vider J, Ow H, Herz E, Penate-Medina O, Baumgart M, et al.; *Nano Lett.* 2008, 9:442-448.

38. Zhang XZ, Sun HW, Zhang ZY, Niu Q, Chen YS, Crittenden JC; *Chemosphere* 2007, 67:160-166.

39. Choi HS, Liu W, Misra P, Tanaka E, Zimmer JP, Ipe BI, et al.; *Nat. Biotechnol.* 2007, 25:1165-1170.

40. Katsnelson BA, Degtyareva TD, Minigalieva II, Privalova LI, Kuzmin SV, Yeremenko OS, et al.; *Int. J. Toxicol.* 2011, 30:59-68.

41. Sanchez VC, Pietruska JR, Miselis NR, Hurt RH, Kane AB; *WIREs Nanomed. Nanobiotechnol.* 2009, 1:511-529.

42. Ray PC, Yu H, Fu PP; *J. Environ. Sci. Heal. C* 2009, 27:1-35.

43. Marquis BJ, Love SA, Braun KL, Haynes CL. *Analyst* 2009; 134:425-439.

44. Committee ES; *EFSA J.* 2011, 9:2140-2175.

45. Balbus JM, Maynard AD, Colvin VL, Castranova V, Daston GP, Denison RA, et al.; *Environ. Health Persp.* 2007, 115:1654-1659.

46. Garnett MC, Kallinteri P; *Occup. Med.* 2006, 56:307-311.

47. Stone V, Wilson M, Lightbody J, Donaldson K; *Environ. Health Prev. Med.* 2003;7:246-253.

48. Oberdörster G, Sharp Z, Atudorei V, Elder A, Gelein R, Kreyling W, et al.; *Inhal. Toxicol.* 2004, 16:437-445.

49. Suh WH, Suslick KS, Stucky GD, Suh Y-H; *Prog. Neurobiol.* 2009, 87:133-170.

50. Zhu Z-J, Carboni R, Quercio MJ, Yan B, Miranda OR, Anderton DL, et al.; *Small* 2010, 6:2261-2265.

51. Warheit DB, Reed KL, Sayes CM; *Inhal. Toxicol.* 2009, 21:61-67.

52. Kawata K, Osawa M, Okabe S; *Environ. Sci. Technol.* 2009, 43:6046-6051.

53. Bhattacharjee S, de Haan LHJ, Evers NM, Jiang X, Marcelis ATM, Zuilhof H, et al.; *Part. Fibre Toxicol.* 2010, 7(25).

54. Bhattacharjee S, Ershov D, Gucht Jvd, Alink GM, Rietjens IMCM, Zuilhof H, et al.; *Nanotoxicology* 2011, Early Online:1-14 (DOI: 10.3109/17435390.2011.633714)

55. Thevenot P, Cho J, Wavhal D, Timmons RB, Tang L; *Nanomed-Nanotechnol.* 2008, 4:226-236.

56. Sato K, Yokosuka S, Takigami Y, Hirakuri K, Fujioka K, Manome Y, et al.; *J. Am. Chem. Soc.* 2011, 133:18626-18633.

57. Siekierzycka JR, Rosso-Vasic M, Zuilhof H, Brouwer A; *J. Phys. Chem. C.* 2011, 115:20888-20895.

58. Sinha R, Kim GJ, Nie S, Shin DM; *Mol. Cancer Ther.* 2006, 5:1909-1917.

59. Colvin VL; *Nat. Biotechnol.* 2003, 21:1166-1170.

60. Chan JM, Valencia PM, Zhang L, Langer R, Farokhzad OC; Polymeric Nanoparticles for Drug Delivery. Cancer Nanotechnology. In: Grobmyer SR, Moudgil BM, editors.: Humana Press; 2010. p. 163-175.
61. Park JH, Lee S, Kim J-H, Park K, Kim K, Kwon IC; *Prog. Polym. Sci.* 2008, 33:113-137.
62. Rzigalinski BA, Meehan K, Davis RM, Xu Y, Miles WC, Cohen CA; *Nanomedicine* 2006, 1:399-412.
63. Nicodemus GD, Bryant SJ; *Tissue Eng. Pt. B-Rev.* 2008, 14:149-165.
64. Liu CB, Gong CY, Huang MJ, Wang JW, Pan YF, Zhang YD, et al.; *J. Biomed. Mater. Res. B* 2008, 84B:165-175.
65. Zhang Y, Zhuo RX. *Biomaterials* 2005, 26:6736-6742.
66. Gelperina S, Kisich K, Iseman MD, Heifets L; *Am. J. Resp. Crit. Care Med.* 2005, 172:1487-1490.
67. Brand W, van der Wel PAI, Rein MJ, Barron D, Williamson G, van Bladeren PJ, et al.; *Drug Metab. Dispos.* 2008, 36:1794-1802.
68. Brand W, Padilla B, van Bladeren PJ, Williamson G, Rietjens IMCM; *Mol. Nutr. Food Res.* 2010, 54:851-860.
69. Ji Z, Jin X, George S, Xia T, Meng H, Wang X, et al.; *Environ. Sci. Technol.* 2010, 44:7309-7314.
70. Apopa PL, Qian Y, Shao R, Guo NL, Schwegler-Berry D, Pacurari M, et al.; *Part. Fibre Toxicol.* 2009, 6(1).
71. Mocan T, Clichici S, Agoşton-Coldea L, Mocan L, Şimon Ş, Ilie I, et al.; *Acta Physiol. Hung.* 2010, 97:247-255.
72. Choi JE, Kim S, Ahn JH, Youn P, Kang JS, Park K, et al.; *Aquat. Toxicol.* 2010, 100:151-159.
73. Foucaud L, Goulaouic S, Bennasroune A, Laval-Gilly P, Brown D, Stone V, et al.; *Toxicol. In Vitro* 2010, 24:1512-1520.
74. Fröhlich E, Samberger C, Kueznik T, Absenger M, Roblegg E, Zimmer A, et al.; *J. Toxicol. Sci.* 2009, 34:363-375.
75. Luna-Velasco A, Field JA, Cobo-Curiel A, Sierra-Alvarez R; *Chemosphere* 2011, 85:19-25.
76. O'Farrell N, Houlton A, Horrocks BR; *Int. J. Nanomed.* 2006, 1:451-472.
77. Xia T, Kovochich M, Liong M, Zink JI, Nel AE; *ACS Nano* 2007, 2:85-96.
78. Nadia B, Wided K, Kheira B, Hassiba R, Lamia B, Rhouati S, et al.; *Acta Biol. Hung.* 2009, 60:385-398.
79. Salnikov V, Lukyánenko YO, Frederick CA, Lederer WJ, Lukyánenko V; *Biophys. J.* 2007, 92:1058-1071.
80. Alkilany A, Murphy C; *J. Nanopart. Res.* 2010, 12:2313-2333.
81. Schaeublin NM, Braydich-Stolle LK, Schrand AM, Miller JM, Hutchison J, Schlager JJ, et al.; *Nanoscale* 2011, 3:410-420.
82. Valacchi G, Pecorelli A, Mencarelli M, Maioli E, Davis P; *Toxicol. Ind. Health* 2009, 25:241-247.
83. Jeruc J, Vizjak A, Rozman B, Ferluga D; *Am. J. Kidney Dis.* 2006, 48:410-418.
84. Oberdörster G, Stone V, Donaldson K; *Nanotoxicology* 2007, 1:2-25.
85. Lin J-Q, Zheng Y-G, Zhang H-W, Chen Z; *Langmuir* 2011, 27:8323-32.
86. Vieira DB, Carmona-Ribeiro AM; *J. Nanobiotechnol.* 2008, 6:6.
87. Verma A, Uzun O, Hu Y, Hu Y, Han H-S, Watson N, et al.; *Nat. Mater.* 2008, 7:588-595.
88. Zhao F, Zhao Y, Liu Y, Chang X, Chen C, Zhao Y; *Small* 2011, 7:1322-1337.

89. Yang P-H, Sun X, Chiu J-F, Sun H, He Q-Y; *Bioconjugate Chem.* 2005, 16:494-496.

90. Jiang W, KimBetty YS, Rutka JT, ChanWarren CW; *Nat. Nanotechnol.* 2008, 3:145-150.

91. Rejman J, Bragonzi A, Conese M; *Mol. Ther.* 2005, 12:468-474.

92. Rejman J, Oberle V, Zuhorn IS, Hoekstra D; *Biochem. J.* 2004, 377:159-169.

93. Uhrig S, Coutelle O, Wiehe T, Perabo L, Hallek M, Buning H; *Gene Ther.* 2011, 19(2):210-218.

94. Zhang X, Yang S; *Langmuir* 2011, 27:2528-2535.

95. Wani MY, Hashim MA, Nabi F, Malik MA; *Adv. Phys. Chem.* 2011, 1-15.

96. Hong S, Bielinska AU, Mecke A, Keszler B, Beals JL, Shi X, et al.; *Bioconjugate Chem.* 2004, 15:774-782.

97. Mecke A, Uppuluri S, Sassanella TM, Lee D-K, Ramamoorthy A, Baker Jr JR, et al.; *Chem. Phys. Lipids* 2004, 132:3-14.

Chapter 2

Synthesis and cytotoxicity of silicon nanoparticles with covalently attached organic monolayers

Abstract

A series of highly monodisperse silicon nanoparticles (Si NP) with either positively (amine), neutral (azide) or negatively (carboxylic acid) charged covalently attached organic monolayers were synthesized and investigated for their cytotoxicity. Infrared data confirmed the presence of these covalently attached surface groups. The Si NP were characterized by absorption and fluorescence spectroscopy. The cytotoxicity was investigated in Caco-2 cells by determining the cell viability and proliferation. The EC50 values for the Si NP ranged from 20 µg/l for the amine-terminated Si NP, via 550–850 µg/l for the azide-terminated Si NP to non-toxic (no measureable EC50) for the carboxylic acid-terminated Si NP. These results indicated a trend in cytotoxicity, depending on surface charge, i.e. that positively charged Si NP were more cytotoxic than negatively charged Si NP. Interestingly, it appeared that the cytotoxicity of the amine terminated Si NP (Si NP-NH_2) depended strongly on the presence of fetal calf serum (FCS) in the medium.

Introduction

Compared to the more commonly investigated silica (SiO_2) nanoparticles (NP), silicon (Si) NP have the advantage that organic groups can be attached to the surface through a very stable covalent Si-C bond.[1,2] Compared to bulk silicon, silicon NP (Si NP) have interesting optical fluorescent properties related to their small size. *Quantum confinement* effects are expected for Si NP smaller than 5 nm,[3] which makes the study and synthesis of well-defined and monodisperse Si NP in the 1–5 nm range interesting for a variety of opto-electric applications, such as fluorescence bioimaging.[4-7] An attractive way to obtain these functionalized Si NP is by starting from H-terminated Si NP, which are then reacted with terminal alkenes to provide stable covalent Si-C bonds, similar to the preparation of functional organic groups on planar H-terminated silicon surfaces.[8-11] The method that probably yields the most well-defined Si NP is that of Tilley et al.,[12] who reported on the μg-scale synthesis of Si NP via the use of micelles in apolar solvents. These Si NP could be made alkyl-terminated and aminoalkyl-terminated.[13] Rosso-Vasic et al.[14] have further developed this method to obtain gram-scale yields of well-defined alkyl-capped Si NP with a Si-core size of 1.6 ± 0.2 nm, which now gives the ability to obtain significant amounts Si NP coated with a wide variety of functional groups, making them also suitable for a wide range of studies and biological applications.

However, little is known about the specific toxicity of NP in biological systems and human beings. Many NP proposed for sensing and diagnostics today are semiconductor quantum dots (QD) composed of core/shell particles with group II–VI or group III–V elements in the core, such as CdSe, CdTe, ZnS, GaAs and InP.[15] Many of these core metals are highly toxic in low concentrations, such as cadmium, selenium, lead and arsenic.[16, 17] The degradation of the core, an important factor in the cytotoxicity, is mostly prevented by adding a non-toxic shell to the toxic core and thereby slowing down the leakage of the toxic elements. Several studies have shown that these NP can indeed be toxic,[17,18] although the results of different toxicity studies are difficult to compare in the published literature due to differences resulting from using different methods, materials and cell lines. In contrast, Si NP have a core of silicon. The absence of toxic elements, together with the fluorescent properties and the fact that the surface can be modified with strong covalent bonds, make these NP materials potentially very useful as a platform for biomedical applications. Recently, Alsharif et al.[19] have found no evidence for in vitro cytotoxicity of alkyl-capped Si NP. Primarily the shell or surface-covering material is therefore expected to be responsible for the potential toxicity of these Si NP.

To test the cytotoxicity of the Si NP in a reproducible and quantifiable manner, two different assays were chosen in the present study. First, the colorimetric MTT (3-(4,5-dimethylthiazol-2-yl)-2,5-diphenyl tetrazolium bromide) assay was used, which is a measure for the mitochondrial metabolic activity of living cells. This test is used to monitor cell metabolic function, cell proliferation or cell activation.[20, 21] Secondly, the BrdU (5-bromo-2-deoxyuridine) immunoassay was used, which gives an indication of cell proliferation.[22]

The human colonic adenocarcinoma derived Caco-2 cell line was chosen to test the toxicity of the Si NP. Caco-2 cells can differentiate into colonic cells with a unique apico-basal conformation. Hence, these cells can be used as a model cell line for testing the toxicity of any orally administered substance. The cells are robust in nature, grow fast under laboratory

conditions and are easy to culture. The huge amount of data available in literature also makes it easier to compare the derived data with published data.

The aim of this study was to assess the influence of different surface properties, especially surface charge, of the Si NP on the cytotoxicity in Caco-2 cells. The used Si NP give the opportunity to test the role of surface charge in the cytotoxicity exhibited by NP. Similar monodisperse Si NP with amine, azide and carboxylic acid functionalities were prepared and their toxicity was tested by MTT and BrdU assays over a wide concentration range (0–2200 µg/l) in the presence and absence of fetal calf serum (FCS). Under the test-conditions, the amine-terminated Si NP were positively charged, the azide-terminated Si NP neutral and the carboxylic acid-terminated Si NP were negatively charged.

Materials and methods

Synthesis and purification of the Si NP-COOH

All chemicals were purchased from Sigma-Aldrich and employed without further purification unless specified differently. Toluene ($[H_2O \leq 0.005 \%]$, $\geq 99.7 \%$ [GC]) was dried over sodium wire overnight prior to use. Methanol was distilled and stored over anhydrous magnesium sulphate. The 3-butenoic acid was distilled and stored over molecular sieves. Dimethyl sulfoxide (DMSO) was purchased from Merck; Dulbecco's modified eagle medium (DMEM), Hank's buffered salt solution (HBSS), phosphate buffer saline (PBS), trypsin, gentamicin and non-essential amino-acids (NEAA) were purchased from Invitrogen.

For the synthesis of the NP, dry and oxygen-free conditions are essential. An argon atmosphere was used during the whole synthetic procedure. Dry toluene (100 ml) was made oxygen-free prior to use by bubbling through argon for 3 h. Tetraoctyl ammonium bromide (TOAB, $\geq 99.0 \%$; 3.0 g, 5.6 mmol) was dispersed in the toluene by 30 min of sonication. $SiCl_4$ (200 µl, 1.8 mmol) was added via an air-tight syringe, followed by 30 min of sonication. Subsequently, a 1 M $LiAlH_4$ (lithium aluminium hydride) solution in tetrahydrofuran (4.6 ml, 4.6 mmol) was injected via an air-tight syringe, followed by a further 30 min of sonication in order to form the H-terminated Si NP. Excess $LiAlH_4$ was quenched by adding dry methanol (30 ml, 740 mmol) and the reaction mixture was sonicated for 15 min. To obtain the COOH-terminated Si NP, 3-butenoic acid (4.4 ml, 0.052 mol) was added, together with a catalytic amount of chloroplatinic acid (40 µl; 0.05 M in dry methanol) and the mixture was sonicated for another 30 min. The resulting Si NP were purified by evaporation of all solvents under reduced pressure. Then the material was re-dispersed in water and solid TOAB was removed by filtration. Further purification was performed by dialysis using a regenerated cellulose membrane with molecular weight cut-off (MWCO) 3500 or 1000, and subsequent filtration through a hydrophilic 450 nm polyvinylidene fluoride membrane filter (MILLEX-HV, Millipore).

The amine-terminated (Si NP-NH$_2$) and azide-terminated (Si NP-N$_3$) Si NP were synthesized by reaction of the H-terminated Si NP with allylamine and 11-azido-undec-1-ene, respectively, as described previously and yielded Si NP with a Si core size of 1.6 ± 0.2 nm.[23]

All measurements were performed at standard pressure and at room temperature. Electronic absorption spectra were recorded in a quartz cuvette (1 cm, Hellma), using a Cary 1 UV-Vis single beam spectrophotometer and were corrected for the solvent absorption. The scan range was 600–200 nm with a scan rate of 600 nm/min.

Steady-state and time-resolved fluorescence measurements were performed on a Time-Correlating Single Photon Counting F900 spectrometer (Edinburgh Instruments), with an instrument response function for time-resolved measurements of 87 ps. All steady-state spectra were corrected for the wavelength dependent sensitivity of the detector and the source by recording reference data simultaneously. Additionally, emission spectra were corrected for Raman scattering using the solvent emission spectrum.

Time-resolved fluorescence measurements were performed with exactly the same solutions used for steady-state spectra (absorption was always adjusted to be ≤ 0.2). A pulsed light-emitting diode (λ_{ex} = 283 nm) was used as excitation source and emitted photons were collected (4096 channels) until a maximum of 104 counts was reached. Origin Pro (version 8.0) software was used to fit the data.

For Fourier-transform infrared spectroscopy (Bruker, Vector 22 FTIR spectrometer), thin films of Si NP in carbon tetrachloride solution were placed between sodium chloride crystals. For each measurement 64 scans were collected and corrected for the background signal.

Solutions of Si NP for the toxicology tests

Stock solutions of Si NP-NH$_2$ and Si NP-COOH were made in water and of Si NP-N$_3$ in DMSO. In a 24-well plate, dose-response dilutions of the stock solutions of Si NP were made using pyrogen-free water. From these solutions, two series of samples were made in the DMEM medium, either with or without 10 % heat inactivated FCS. The concentrations of the series ranged from 0–185 µg/l for Si NP-NH$_2$, 0–1700 µg/l for Si NP COOH and 0–2200 µg/l for Si NP-N$_3$.The solutions of the NP with and without FCS showed no visible signs of aggregation or precipitation. Inspection by dynamic light scattering (DLS) also showed no clear change in particle size upon adding the Si NP to the FCS solution.

Cells and treatments

The Caco-2 cells were maintained in incubators with 5 % CO$_2$ in a humidified atmosphere at 37 °C. The cells were subcultured at a ratio of 1:10 in DMEM medium in 75 cm^2 flasks. The Caco-2 cells were grown in DMEM medium, supplemented with 10 % heat-inactivated FCS and 0.1 % gentamicin. The cells were used in passage 30–40. For the exposure measurements, the cells were plated at a concentration of 1×10^5 cells/ml in a 96-well plate (100 µl/well) and were incubated for 24 h. Then the Si NP were added to the cells in different concentrations in a total volume of 100 µl. After this, the cells were incubated for another 24 h.

Toxicological assays

MTT assay. The mitochondrial metabolic activity was determined by the colorimetric MTT assay.[20] After 24 h exposure to the Si NP, 5 µl MTT solution (3-(4,5-dimethylthiazol-2-yl)-2,5-diphenyl tetrazolium bromide) in PBS (5 mg/ml) was added to each well and incubated for 4 h. Then, the medium was removed and 100 µl of DMSO was added to dissolve the formed formazan

crystals. The plates were put in the plate shaker for 5 min. The absorbances at both 562 nm and 612 nm were measured. The mitochondrial metabolic activity was expressed as the mean % of the negative control values. 0.01 % Triton X-100 was used as positive control and only DMEM medium without Si NP was used as negative control. Control tests were also done to exclude the possibility of formation of crystals after reaction between the Si NP and the MTT solution. For this, 100 μl of the tested Si NP solutions were mixed with 5 μl of MTT solution in a 96-well plate and subsequently incubated for 4 h. No crystal formation, or change in colour of the solution in the wells was observed.

BrdU assay. Cell proliferation was quantified using the colorimetric BrdU (5-bromo-2-deoxyuridine) assay (Catalogue No. 647229001, Roche Diagnostics, Penzberg, Germany). BrdU acts as a structural analogue of thymidine and will be incorporated in newly synthesized DNA during cell replication. This test indicates cell proliferation. After incubation of the Caco-2 cells with the Si NP and BrdU for 24 h, the medium containing the Si NP and BrdU was removed and the BrdU labelling solution was added to the wells and incubated for 4 h. Subsequently, the immunoassay was performed according to the protocol of the manufacturer. Cell proliferation was expressed as the mean % of the negative control values. 0.01 % Triton X-100 was used as positive control and medium without Si NP was used as negative control.

Statistical analysis

All data from MTT and BrdU assay was statistically analysed by Igor Pro 6 software from Wavemetrics Inc. Paired Student's *t*-test was performed to determine which data points are statistically significantly different from respective control values and noted with asterisk (*) sign only when $p < 0.05$. Results are shown as mean ± standard error of mean (SEM).

Results

Synthesis and characterization of Si NP

Butenoic acid-terminated Si NP (Si NP-COOH) were synthesized using the method of Zuilhof and co-workers[14] to obtain H-terminated Si NP, which were converted to carboxylic acid-terminated Si NP by the direct attachment of 3-butenoic acid. Direct attachment of the carboxylic acid has the advantage over attachment of a methyl ester[24] that subsequent ester hydrolysis is not needed. This circumvents possible incomplete hydrolysis and base-induced or acid-induced damage of the monolayer coverage, as was observed during hydrolysis of planar modified Si-surfaces.[25, 26]

The Si NP-COOH were analysed using infrared (IR)-spectroscopy (Figure 1). The peak at 1722 cm^{-1} indicated the carbonyl stretch vibration of the acid, while the broad peak around 3424 cm^{-1} indicated the carboxylic acid -OH stretch vibration. Since the peak was not broadened beyond 3000 cm^{-1}, the -COOH moieties did not form H-bonded dimers, but were largely present as free -COOH groups, which is as expected for surface-bound -COOH groups. As a result, some of them will be negatively charged (-COO^{-}) in aqueous media. The anti-symmetric and symmetric -

CH$_2$ stretching vibrations were clearly visible at 2858 and 2928 cm^{-1}. Furthermore, the -CH$_3$ stretching vibration was visible at 2956 cm^{-1}. The scissoring vibrations of the Si-C bonds were visible at 1466 cm^{-1}. There was only a very small Si-O stretch vibration visible at 1096 cm^{-1}, indicating that there is at most only a small fraction of butenoic molecules that have added to the silicon through the oxygen groups, or that a very small amount of oxidation of the silicon core has occurred.
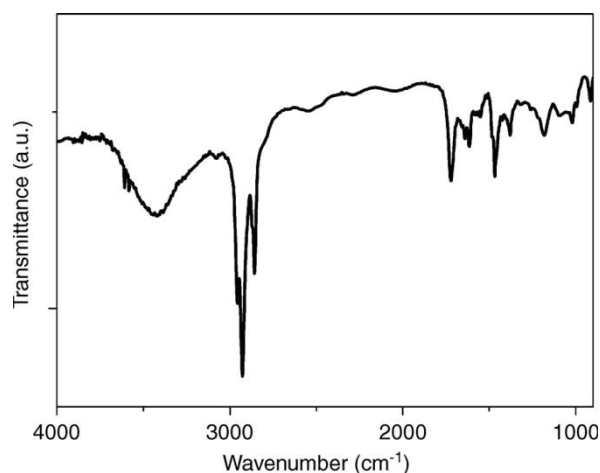

Figure 1: *IR spectrum of Si NP-COOH.*

To further characterize the Si NP, both UV-Vis absorption spectroscopy as well as steady-state and time-resolved fluorescence spectroscopies were performed. The UV-Vis absorption spectrum of the Si NP-COOH showed an absorption maximum at 278 nm. The maximum fluorescence excitation occurred at the same wavelength, whereas the emission had a maximum at 322 nm (Figure 2).
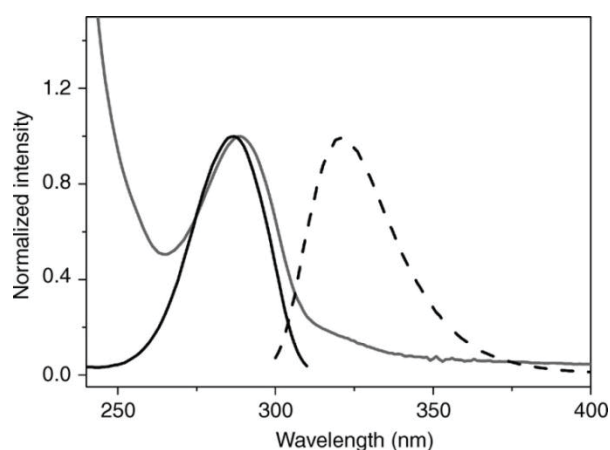
Figure 2: *Absorption (grey), excitation (black) and emission (dashed) spectra of Si NP-COOH.*

Time-resolved measurements showed that the fluorescence anisotropy decay is strictly mono-exponential. This can only be the case when all three perpendicular axes around which the Si NP can rotate are the same, i.e., when the Si NP are spherical.[14, 27] The fluorescence-related data of the Si NP are summarized in Table 1. The fluorescence lifetimes of the Si NP are calculated using a stretched exponential: $I(t) = I_0 \times \exp[-(t/\tau)^\beta]$; where $I(t)$ = fluorescence intensity at time t; I_0 = fluorescence intensity at $t = 0$; τ = fluorescence lifetime decay constant; and β = heterogeneity parameter of the sample (β = 1 means the fluorescence lifetimes of the

molecules in the sample is homogeneous). The fluorescence data showed that the emission characteristics are different (both in energy terms and rates of relaxation to the electronic ground state) for all NP under study, despite the fact that the Si-core is identical in all cases. This pointed to a clear effect of the terminal substituents on the electronic character of the NP. The effect of the terminal substituent was therefore also investigated with respect to the cytotoxicity of these NP.

Table 1: Summarized data of the luminescent properties of the studied Si NP				
Coating	Fluorescence maximum		FWHM (nm)	Fluorescence lifetime τ (ns)
	λ_{ex} (nm)	λ_{em} (nm)		
$C_3H_6NH_2$	390	475	98	4.7 ± 0.16; $\beta = 0.75$
C_3H_6COOH	278	322	32	1.30 ± 0.09; $\beta = 0.98$
$C_{11}H_{22}N_3$	280	315	57	3.13 ± 0.01; $\beta = 0.73$

FWHM, Full width half maximum; ns, nanoseconds.

Effect of Si NP-NH$_2$ on Caco-2 cells

In Figure 3A, the cell viability in the MTT assay is plotted as a function of the concentration of Si NP-NH$_2$. The cells were exposed to the Si NP-NH$_2$ in a concentration range from 0–185 µg/l, both in the presence and absence of FCS in the medium. Without FCS, cell viability did not decrease up to a concentration of 185 µg/l after 24 h of incubation. Therefore, in this concentration range of the Si NP-NH$_2$, no EC50 could be determined and Si NP-NH$_2$ showed no cytotoxic effects on the cells. When the cells were incubated in the presence of FCS, a sharp drop in cell viability was observed using concentrations of more than 11 µg/l. The EC50 value for 24 h incubation in the presence of FCS in the medium was calculated to be 20 µg/l. Figure 3B shows the effect of Si NP-NH$_2$ concentration on cell proliferation using the BrdU assay. Without the presence of FCS, no effect on the cell proliferation could be measured up to a concentration of 185 µg/l. In the presence of FCS, a gradual decrease in cell proliferation could be observed – down to ~60 % of the values compared to the negative control, where no Si NP-NH$_2$ were added.

Effect of Si NP-N$_3$ on Caco-2 cells

Figure 3C shows the Caco-2 cell viability in the MTT assay plotted as function of Si NP-N$_3$ concentration, ranging from 0–2200 µg/l, both in the presence and absence of FCS. The presence of FCS in the medium almost had no effect on the cytotoxicity of the Si NP-N$_3$. An EC50 of 850 µg/l could be determined in the presence of FCS and an EC50 of 600 µg/l in the absence of FCS. These values were much higher than the EC50 values of the Si NP-NH$_2$, indicating that the Si NP-N$_3$ were less cytotoxic than Si NP-NH$_2$ in the presence of FCS in the medium. Figure 3D shows similar effects of the Si NP-N$_3$ concentration, ranging from 0–2200 µg/l, on the Caco-2 cell proliferation in the BrdU test. Similar to the MTT assay, the presence or absence of FCS in the medium had hardly an influence on the cytotoxic effects of the Si NP-N$_3$. The calculated EC50 values were 550 µg/l in the presence of FCS and 570 µg/l in its absence.
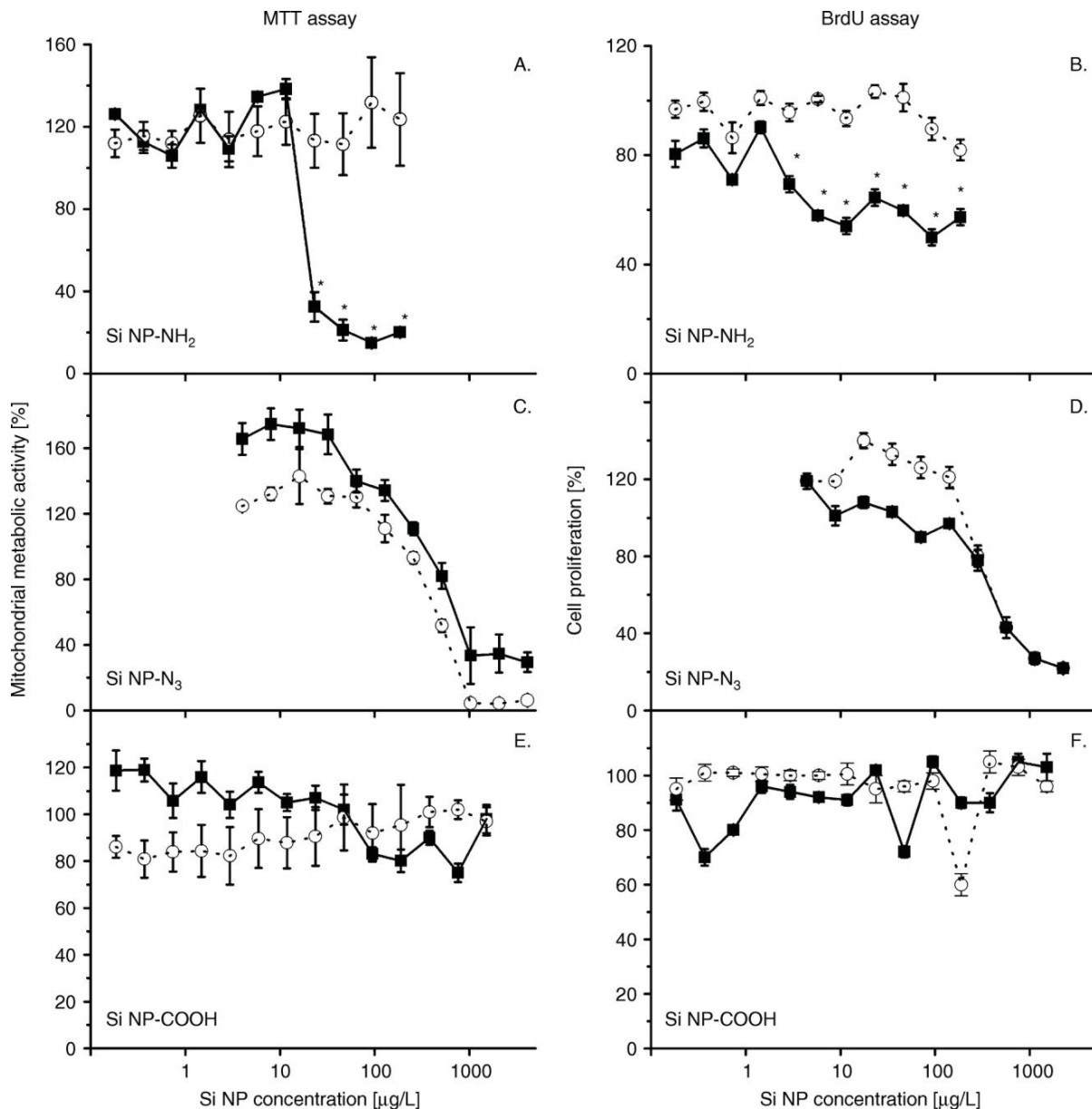
Figure 3: *Mitochondrial metabolic activity (MTT assay) and cellular proliferation (BrdU assay) of the Caco-2 cells after 24 h exposure to Si NP-NH₂ (A and B), Si NP-N₃ (C and D) and Si NP-COOH (E and F). Measurements in the presence (■) and absence (o) of FCS. Number of experiments (n) in the presence and absence of FCS: n = 12 (A and B); n = 9 (C and D); n = 8 (E and F). The asterisk sign (*) signifies statistically significantly different (p < 0.05) data from respective control values.*

Effect of Si NP-COOH on Caco-2 cells

In Figure 3E the effect of Si NP-COOH concentration, 0–1700 µg/l, on the cell viability as measured in the MTT assay and in Figure 3F, cell proliferation as measured with the BrdU assay are plotted. Remarkably, no effect of increasing concentration on the cell viability was observed even upon incubation with a Si NP-COOH concentration of 1700 µg/l. The results of the MTT assay and the BrdU assay were similar and no effect of the presence of FCS was found. These results showed that the Si NP-COOH have less cytotoxic effects on Caco-2 cells than Si NP-N₃.

Discussion

The synthetic route to make Si NP by reduction of $SiCl_4$ to obtain H-terminated Si NP, followed by a surface functionalization reaction with alkenes, was successfully further explored by making amine,[23] azide and carboxylic acid surface-modified Si NP. The maximum absorption and excitation wavelength of the Si NP-COOH were found at 278 nm and the emission maximum was at 322 nm. This is comparable to the results of Rogozhina et al.,[24] who showed that Si NP terminated with pentenoic acid, obtained by the hydrolysis of the corresponding methyl ester, had identical absorption and emission wavelengths. Furthermore, these results were also in line with computational studies by Li et al.,[28] who calculated the absorption and emission wavelengths for different sizes of Si NP capped with propionic acid. The Si NP used in this study and synthesized using the same literature method,[24] showed absorption, fluorescence excitation and emission spectra that were characteristic for the type of organic monolayer and the size of the Si NP (about 1.6 nm). The fluorescence lifetimes were also characteristic for the studied Si NP and fluorescence anisotropy measurements indicated that the particles were spherical.

An important result of the present study is that the amine-terminated Si NP-NH_2 showed cytotoxicity after exposure to Caco-2 cells for 24 h when administered together with FCS. However, they showed no cytotoxicity when administered without FCS up to concentrations of 185 µg/l. These remarkable differences in cytotoxicity caused by the absence or presence of FCS are an interesting feature that is still largely unexplained. Previous studies[29, 30] suggested that the proteins in FCS may interact with NP, so that they are better dispersed and thereby facilitate their entry into the cells, thus causing higher cytotoxic effects than in the absence of FCS. Due to the small size of the Si NP (~1.6 nm), it is thought that they are adsorbed by the proteins in FCS and that by the uptake of the FCS by the cells, the Si NP are also transported into the cells. It is known that positively charged molecules get adsorbed to the negatively charged lipid membrane of cells, e.g., shown by the interaction of the polycationic polymer chitosan with Caco-2 cells.[31] Because of the positive charge on the Si NP-NH_2, they can interact in a similar manner as chitosan with the lipid membrane of the cells and when in the cells, have interaction with negatively charged components in the cells, such as the cell membrane and DNA backbone. It is also possible that reaction with proteins in FCS makes the cationic NP more neutral by charge compensation, which might facilitate cellular uptake.

The results described above showed that the Si NP-N_3 were much less cytotoxic to the Caco-2 cells than the Si NP-NH_2. The effect of the presence or absence of FCS in the medium was less pronounced, but still visible. Furthermore, the transition from cytotoxic to non-cytotoxic concentrations is less sharp as compared to the Si NP-NH_2. The reason for this could be that the neutral Si NP-N_3 did not have extensive interactions with the lipid membrane and upon uptake, could have less toxic interactions with the contents of the cell. One of the reasons for this limited cytotoxicity could be related to the overall neutral charge of the azide ($-N=N^+=N^-$) group. The lack of cytotoxicity of the azide was also observed upon exposing cell cultures to azido-sugars for 1–3 days, after which no cytotoxic effects on the cells were observed.

The negatively charged Si NP-COOH showed no cytotoxicity to the Caco-2 cells in the current study, both in the presence and absence of FCS. This is in agreement with a study on silica nanotubes that showed negatively charged nanotubes were less harmful to cells than positively charged NH_2-coated nanotubes.[32] Although the negatively charged nanotubes still

displayed some toxicity, the Si NP-COOH, used in the present study, displayed no measurable cytotoxicity over a wide concentration range. There is one report of a toxicity study on alkyl-terminated silicon NP showing that they were non-toxic. However, these Si NP were not water-soluble and thus differed from those used in the present study. Furthermore, they were tested at only one concentration,[19] which makes comparison with our study difficult.

The cytotoxicity tests performed in this study indicated that the surface charge of the Si NP had a great influence on the cytotoxicity towards the colonic Caco-2 cells. The positively charged NH_2-terminated Si NP were cytotoxic, whereas the neutral Si NP-N_3 were moderately cytotoxic and the Si NP-COOH showed no cytotoxicity at all. Charge-dependent cellular uptake and associated toxicology has been observed previously in several studies, where positively charged molecules, such as polylysine-functionalized silica NP[33] or cationic PAMAM-dendrimers[34] were inherently taken up faster by cells than neutral molecules. In the study on PAMAM-dendrimers, it was shown that the positively charged dendrimers had a strong interaction with the negatively charged lipid bilayer, while the neutral dendrimers showed little interaction. The lipid bilayer described in that study was used as a model for the phospholipid membrane of cells. The observations were confirmed by calculations, which showed that bigger (G5 or G7; 10–13 nm diameter) dendrimers made holes in the lipid bilayer, whereas the smaller (G3; about 3.5 nm diameter) dendrimers had interactions but did not make permanent holes. A theoretical study confirmed the importance of charge in disrupting membranes by modelling of the specific interaction between these membranes and NP in general.[35] Their results indicated that the higher the charge density, the more phospholipid molecules are detached from the membrane and adsorbed on the NP surface.

Furthermore, it was shown by atomic force microscopy (AFM) studies that a wide variety of cationic NP, including cell-penetrating peptides, polycationic polymers and inorganic NP (Au-NH_2, SiO_2-NH_2) could induce disruption of supported lipid membranes. These effects were observed as formation of holes, membrane thinning and membrane erosion.[36] In contrast, a recent study on amine-modified or carboxyl-modified CdSe/ZnS QD revealed that the intravenous toxicity of the carboxyl-modified QD was much higher than of the amine-modified QD.[37] Furthermore, it was shown that QD with different surface modifications ended up in different organs in the mice. This shows that for in vivo applications of the Si NP, further studies are needed.

Interestingly, a visible increase in both mitochondrial metabolic activity and cellular proliferation was found for low concentrations of Si NP-N_3. This initial surge in activity is especially clear in the MTT assay, where it also occurred at lower concentrations than in the BrdU assay. It should be noted that mitochondrial metabolic activity and cellular proliferation are two mutually independent parameters and it is quite possible that the cytotoxicity of these Si NP affects the mitochondria of the cells before it influences cellular DNA. Similar reports have been published where an initial high mitochondrial activity was observed after exposing cells to NP or other toxic agents. Elgrabli et al.[38] first found an increased mitochondrial metabolic activity at low carbon nanotube concentrations while testing the effect of bovine serum albumin on the cytotoxicity of carbon nanotubes in A549 cells. Similar results were found by Ryman-Rasmussen et al.[39] when testing the cytotoxicity of QD on human epidermal keratinocyte (HEK) cells. Although not a NP toxicity study, Doig et al.[40] found similar results when testing the protective effects of N-methylated derivatives of amyloid-β-peptide-β (25–35) on a rat pheochromocytoma PC-12 cell line. These findings could be caused by compensatory

mechanisms that become activated within the cells to resist the toxicity of these agents at lower initial concentrations, which then gets expressed as higher proliferation values in the cytotoxicity assays.

Conclusion

The cytotoxicity of the Si NP is highly dependent on the surface charge of the coating group. In addition, the presence of FCS in the cell medium seems to enhance the cytotoxicity. Given the non-cytotoxicity of negatively charged Si NP (Si NP-COOH) and because the Si NP show photoluminescence, they may be highly promising for bioimaging applications. However, more research is required to develop Si NP which are safe and non-toxic for use in human beings.

References

1. Veinot JGC; *Chem. Commun.* 2006, 40:4160–4168.
2. Rosso-Vasic M, De Cola L, Zuilhof H; *J. Phys. Chem. C* 2009, 113(6):2235–2240.
3. Krishna MVR, Friesner RA; *J. Chem. Phys.* 1991, 95(11):8309–8322.
4. Chan WCW, Nie SM; *Science* 1998, 281(5385):2016–2018.
5. Larson DR, Zipfel WR, Williams RM, Clark SW, Bruchez MP, Wise FW, et al.; *Science* 2003, 300(5624):1434–1436.
6. Michalet X, Pinaud FF, Bentolila LA, Tsay JM, Doose S, Li JJ, Sundaresan G, et al.; *Science* 2005, 307(5709):538–544.
7. Liu W, Howarth M, Greytak AB, Zheng Y, Nocera DG, Ting AY, et al.; *J. Am. Chem. Soc.* 2008, 130(4):1274–1284.
8. Sieval AB, Linke R, Zuilhof H, Sudholter EJR; *Adv. Mater.* 2000, 12(19):1457–1460.
9. Buriak JM; *Chem. Rev.* 2002, 102(5):1271–1308.
10. Boukherroub R; *Curr. Op. Solid State Materials Sci.* 2005, 9(1–2):66–72.
11. Scheres L, Arafat A, Zuilhof H; *Langmuir* 2007, 23(16):8343–8346.
12. Tilley RD, Warner JH, Yamamoto K, Matsui I, Fujimori H; *Chem. Commun.* 2005, 14:1833–1835.
13. Warner JH, Hoshino A, Yamamoto K, Tilley RD; *Angew. Chem. Int. Ed.* 2005, 44(29):4550–4554.
14. Rosso-Vasic M, Spruijt E, van Lagen B, De Cola L, Zuilhof H; *Small* 2008, 4(10):1835–1841.
15. Chan WCW, Maxwell DJ, Gao XH, Bailey RE, Han MY, Nie SM; *Curr. Op. Biotechnol.* 2002, 13(1):40–46.
16. Derfus AM, Chan WCW, Bhatia SN; *Nano Lett.* 2004, 4(1):11–18.
17. Lewinski N, Colvin V, Drezek R; *Small* 2008, 4(1):26–49.
18. Hardman R; *Environ. Health Persp.* 2006, 114(2):165–172.
19. Alsharif NH, Berger CEM, Varanasi SS, Chao Y, Horrocks BR, Datta HK; *Small* 2009, 5(2):221–228.
20. Mosmann T; *J. Immunolog. Meth.* 1983, 65(1–2):55–63.
21. Ciapetti G, Cenni E, Pratelli L, Pizzoferrato A; *Biomaterials* 1993, 14(5):359–364.
22. Altman J, Das GD; *J. Comp. Neurol.* 1965, 124(3):319–335.
23. Rosso-Vasic M, Spruijt E, Popovic Z, Overgaag K, van Lagen B, Grandidier B, et al.; *J. Mater. Chem.* 2009, 19(33):5926–5933.
24. Rogozhina EV, Eckhoff DA, Gratton E, Braun PV; *J. Mater. Chem.* 2006, 16(15):1421–1430.
25. Linford MR, Fenter P, Eisenberger PM, Chidsey CED; *J. Am. Chem. Soc.* 1995, 117(11):3145–3155.
26. Sieval AB, Demirel AL, Nissink JWM, Linford MR, van der Maas JH, de Jeu WH, et al.; *Langmuir* 1998, 14(7):1759–1768.
27. Lakowicz JR; 2006, Principles of fluorescence spectroscopy. Singapore: *Springer*.
28. Li QS, Zhang RQ, Niehaus TA, Frauenheim T, Lee ST; *J. Chem. Theory Comput.* 2007, 3(4):1518–1526.
29. Möller W, Brown DM, Kreyling WG, Stone V; *Part. Fibre Toxicol.* 2005, 2(7).
30. Foucaud L, Wilson MR, Brown DM, Stone V; *Toxicol. Lett.* 2007, 174(1–3):1-9.

31. Schipper NGM, Olsson S, Hoogstraate JA, deBoer AG, Varum KM, Artursson P; *Pharmaceut. Res.* 1997, 14(7):923–929.
32. Nan A, Bai X, Son SJ, Lee SB, Ghandehari H; *Nano Lett.* 2008, 8(8):2150–2154.
33. Li Z, Zhu SG, Gan K, Zhang QH, Zeng ZY, Zhou YH, et al.; *J. Nanosci. Nanotechnol.* 2005, 5(8):1199–1203.
34. Mecke A, Majoros IJ, Patri AK, Baker JR, Holl MMB, Orr BG; *Langmuir* 2005, 21(23):10348–10354.
35. Ginzburg VV, Balijepailli S; *Nano Lett.* 2007, 7(12):3716–3722.
36. Leroueil PR, Berry SA, Duthie K, Han G, Rotello VM, McNerny DQ, et al.; *Nano Lett.* 2008, 8(2):420–424.
37. Geys J, Nemmar A, Verbeken E, Smolders E, Ratoi M, Hoylaerts MF, et al.; *Environ. Health Persp.* 2008, 116(12):1607–1613.
38. Elgrabli D, Abella-Gallart S, Aguerre-Chariol O, Robidel F, Rogerieux F, Boczkowski J, et al.; *Nanotoxicology* 2007, 1(4):266–278.
39. Ryman-Rasmussen JP, Riviere JE, Monteiro-Riviere NA; *J. Invest. Dermatol.* 2007, 127(1):143–153.
40. Doig AJ, Hughes E, Burke RM, Su TJ, Heenan RK, Lu J; *Biochem. Soc. Transact.* 2002, 30:537–542.

Chapter 3

Role of surface charge and oxidative stress in cytotoxicity of organic monolayer-coated silicon nanoparticles towards macrophage NR8383 cells

Based on:

Abstract

Background: Surface charge and oxidative stress are often hypothesized to be important factors in cytotoxicity of nanoparticles (NP). However, the role of these factors is not well understood. Hence, the aim of this study was to systematically investigate the role of surface charge, oxidative stress and possible involvement of mitochondria in the production of intracellular reactive oxygen species (ROS) upon exposure of rat macrophage NR8383 cells to silicon nanoparticles (Si NP). For this aim, highly monodisperse (size 1.6 ± 0.2 nm) and well-characterized Si-core NP were used with a surface charge that depends on the specific covalently bound organic monolayers: positively charged Si NP-NH_2, neutral Si NP-N_3 and negatively charged Si NP-COOH. **Results:** Positively charged Si NP-NH_2 proved to be more cytotoxic in terms of reducing mitochondrial metabolic activity and effects on phagocytosis than neutral Si NP-N_3, while negatively charged Si NP-COOH showed very little, or no cytotoxicity. Si NP-NH_2 produced the highest level of intracellular ROS, followed by Si NP-N_3 and Si NP-COOH; the latter did not induce any intracellular ROS production. A similar trend in ROS production was observed in incubations with an isolated mitochondrial fraction from rat liver tissue in the presence of Si NP. Finally, vitamin E and vitamin C induced protection against the cytotoxicity of the Si NP-NH_2 and Si NP-N_3, corroborating the role of oxidative stress in the mechanism underlying the cytotoxicity of these Si NP. **Conclusion:** Surface charge of Si NP plays an important role in determining their cytotoxicity. Production of intracellular ROS, with probable involvement of mitochondria, is an important mechanism for this cytotoxicity.

Introduction

Silicon (Si) is conventionally regarded as a non-toxic semiconductor material and Si NP are proposed as an alternative for the highly toxic heavy metal quantum dots in biological applications, such as in food industry and bioimaging.[1] However, once exposed to an aerobic atmosphere, Si NP readily get oxidized to silica (silicon dioxide; SiO_2),[2] which is reported to result in cytotoxicity.[3] The cytotoxicity of silica NP has been reported to be size dependent.[4] Data on the actual toxicity of Si NP are, however, scarce.

Recently, we developed a method for the gram-scale synthesis of Si NP,[5] which can be coated with a covalently bound organic monolayer with different surface charges.[6-8] These Si NP have a silicon core of 1.6 ± 0.2 nm, as determined by TEM.[7, 8] By attaching alkyl chains to the surface of the Si-core with amine ($-NH_2$), azide ($-N_3$) and carboxylic acid ($-COOH$) terminal moieties, Si NP with respectively positive (Si NP-NH_2), neutral (Si NP-N_3) and negative (Si NP-COOH) surface charges can be obtained. This coating prevents the oxidation of Si NP to SiO_2. Also the influence of surface charges on the cytotoxicity remains largely unresolved, although there are several research articles pointing at a possible role of surface charge in cellular uptake and/or cytotoxicity of NP. Oskuee et al.,[9] for example, reported a decrease in cytotoxicity with decreasing positive surface charge of polyethyleneimine NP. Sayin et al.[10] found that positively charged N-trimethyl chitosan NP were more cytotoxic than their negatively charged counterparts.

A brief overview of some recent articles pointing at the possible influence of surface charge of NP on their cellular uptake and/or cytotoxicity is given in Table 1, which summarizes the findings reported by different groups. The findings are based on different types of particles functionalized with different chemical groups. A consensus regarding the role of surface charge on cytotoxicity of NP is therefore hard to reach. Some research groups[11,12] observed cytotoxic effects of positively charged NP. Mayer et al.[13] reported activation of the complement system and increased hemolysis in blood samples collected from healthy donors after being exposed to positively charged polystyrene NP. Some recent publications[14-20] reported different effects of surface charges on cytotoxicity, including a higher cytotoxicity of cationic NP as compared to anionic NP. Gupta et al.[21] recently observed a reduced cytotoxicity for NP with a positive surface charge. On the other hand, other research groups[22, 23] failed to observe any significant effect of surface charge of NP on their cytotoxicity.

Previously, we reported the synthesis and cytotoxic effects of differently charged Si NP towards human colonic adenocarcinoma derived Caco-2 cells.[6] Positively charged Si NP-NH_2 exerted the highest toxicity, whereas the negatively charged Si NP-COOH were hardly toxic and the neutral Si NP-N_3 showed intermediate toxicity towards the Caco-2 cells. Unfortunately, investigations regarding the mechanisms of cytotoxicity of NP are quite limited. Also, different research groups use different experimental models. Nevertheless, oxidative stress is proposed as one of the most important mechanisms for NP mediated toxicity.[24-33] In these studies, a wide range of NP were tested in different cellular models. Still, a concerted study on the effect of surface charge on the production of intracellular ROS and subsequent oxidative stress and cytotoxicity is not available.

	Table 1				
	Brief overview of recent publications pointing at a possible role of surface charge in interaction of NP with cells				
Citation (Year)	**NP tested**	**Size of nanoparticle (nm)**	**Cell Line tested (in vitro/in vivo)**	**Endpoints studied**	**Results/Inferences**
Ruizendaal et al. (2009)[6]	Si NP with amine (+), azide (neutral) and acid (-) surface functionalization	1.6 ± 0.2	Caco-2	MTT, BrdU	Positively charged Si NP-NH$_2$ more cytotoxic than neutral Si NP-N$_3$. Negatively charged Si NP-COOH did not show toxicity.
Geys et al. (2009)[11]	Quantum dots (amine terminated, neutral, carboxylate terminated)	25	Primary alveolar epithelial cells	MTT, TEER, sodium fluorescein leakage, confocal microscopy	Surface charge did not show any influence on translocation through the cell line.
Corsi et al. (2009)[12]	Iron based magnetic nanoparticles	7 ± 3	MCF7 carcinoma cells	MTT	Anionic nanoparticles were spontaneously internalized. Cationic ones were taken up by clathrin receptor mediated endocytosis.
Sadiq et al. (2009)[13]	Aluminium oxide	179	*E. coli*	Bacterial growth, Infrared spectroscopy	Interaction between positively charged particles and bacteria was found.
Xu et al. (2009)[14]	Hemoglobin loaded polymeric NP	< 200	(MPM) cell line from SD mice	MTT, in vivo biodistribution and clearance of NP	No influence of surface charge on cytotoxicity was observed.
Nafee et al. (2009)[15]	Chitosan modified PLGA	between 150 and 250	COS-1, A549, Calu-3	MTT, LDH, ATP, TEER, SFM	Higher ζ-potential was connected with lower toxicity for COS-1, while no effect of surface charge was found for A549 cells.
Pathak et al. (2009)[16]	Branched polyethylenimine with chondroitin sulphate	between 80 and 190	HeLa, HepG2	MTT, DNA release, protein adsorption, confocal microscopy, gene transfection, radiolabelling, biodistribution	Reduction in positive charge by increasing the percentage of chondroitin sulphate decreases cytotoxicity.

Mayer et al. (2009)[17]	Polystyrene	26, 34, 62, 160, and 220	Human blood	Flow cytometry for thrombocyte and granulocyte activation, plasma coagulation assay, light microscopy, membrane integrity assay	Positive surface charge led to complement activation.
Zhang et al. (2009)[18]	Amine, PEG and carboxylic acid terminated CdSe quantum dots with ZnS shell	12 × 6	HEK	TEM, quantification of quantum dot fluorescence, immunostaining	Uptake of amine-terminated quantum dots proceeds by caveolin/clathrin pathway, while that of carboxylic acid terminated ones proceed by GPCR pathway.
Nam et al. (2009)[19]	Glycol chitosan with 5β cholanic acid	359	HeLa	Cellular uptake studies	Increase in positive charge results in enhanced uptake and distribution by clathrin, caveolin receptor mediated, macropinocytosis.
Gupta et al. (2009)[20]	Polyacrylic acid and YFa	83 ± 8	HepG2, N2a, HEK293	MTT, RBC, WBC, platelet count from blood samples, in vitro peptide release study	Positively charged particles do not have any toxic behaviour.
Kim et al. (2008)[21]	Quantum dot nanocomposites	104.5 ± 7.8	SNB19	Scanning electron microscopy, TIRF, cell viability	Cationic coating at basic pH, makes the NP more biocompatible.
Hauck et al. (2008)[22]	Gold nanorods with polyelectrolyte surface coating	18 × 40	Vi-cell, HeLa	TEM, Trypan Blue exclusion, gene expression	Only CTAB (positively charged) coated particles were toxic in absence of FCS.
Orr et al. (2007)[23]	Silica	100, 500	C10 (alveolar type II epithelial cell line)	X-ray diffraction, TEM, DIC, SEM	Positively charged particles can reach the cells through filopodia and microvilli-like structures. Positive surface charge and intact actin filaments are essential for retrograde movement of the particles.

Therefore, in the present study we systematically investigated the role of NP surface charge and oxidative stress in the rat alveolar macrophage NR8383 cell line. This cell line provides an adequate model system for studying the effect of NP on phagocytic cells, which can clarify possible effects on the innate immune response. In the current study the mechanism underlying the differential cytotoxicity of the various Si NP were investigated, with a focus on the possible role for the formation of intracellular ROS and oxidative stress. To this end, the production of intracellular ROS in both Caco-2 and NR8383 cells exposed to increasing concentrations of the differently charged Si NP was investigated. Also, the degree of protection provided by pre-incubation of the cells with the antioxidants vitamin E and vitamin C, and the possible role of Si NP-induced mitochondrial activity in the production of the intracellular ROS was studied. The results indicated how the surface charge of the Si NP influences their capability to induce intracellular ROS formation and oxidative stress and pointed at a role of mitochondria in this Si NP-induced ROS production at the subcellular level.

Materials and methods

Silicon nanoparticles (Si NP)

Si NP-NH_2 and Si NP-N_3 were prepared and characterized by methods described by Rosso-Vasic et al.[8] and Si NP-COOH were prepared by the method described by Ruizendaal et al.[6] All three Si NP were of comparable sizes with a mean Si-core diameter of 1.6 ± 0.2 nm, as determined by TEM[7,8] and all three Si NP were modified by ~25 surface groups.[5] Both Si NP-NH_2 and Si NP-COOH were dissolved in ultrapure sterile water, while the stock solution of Si NP-N_3 was dissolved in pure DMSO. The required final concentration ranges of all three Si NP were prepared by serial dilution with medium and amounted to 0 - 370 ng/ml for the Si NP-NH_2; 0 - 2200 ng/ml for the Si NP-N_3, and 0 - 3000 ng/ml for the Si NP-COOH, which were the final tested concentration ranges for each of the assays described in this paper, unless otherwise mentioned. No aggregation of these particles was observed with time in medium with DLS for at least two weeks and the solutions were vortexed at least for 1 min before use. The solutions were filtered through 0.2 μm cellulose filters before cytotoxicity assays to maintain sterility. The amount of DMSO in the wells containing Si NP-N_3 was calculated to be < 1 % (v/v), at which concentration no cytotoxic effect of the DMSO was observed.

Cell Lines and tissue fractions

NR8383 cells

Rat alveolar macrophage cells were obtained from ATCC (Manassas, VA). The cells were cultured in 150 cm² cell culture flasks with 25 ml F12-K culture medium (Gibco 21127) supplemented with 10 % (v/v) heat-inactivated FCS in a humidified atmosphere containing 5 % CO_2 at 37 °C.

Caco-2 cells

The human colonic adenocarcinoma cells were obtained from ATCC (Manassas, VA). The cell line was cultured in a humidified atmosphere containing 5 % CO_2 at 37 °C in DMEM medium supplemented with 10 % (v/v) heat-inactivated FCS, 1 % (v/v) NEAA and 0.1 % (v/v) gentamicin.

Isolation of the mitochondrial fraction from rat liver tissue

A Wistar rat of body weight 200 - 250 g was sacrificed by decapitation following anesthesia with isoflurane. The liver was excised at 4 °C and homogenized in ice-cold saline using a Potter homogenizer with 20 - 25 strokes. The homogenized tissue was then centrifuged at 500 g for 10 min at 4 °C. The supernatant was then removed and the pellet, after being weighed, was re-suspended in ice-cold saline and centrifuged at 10.000 g for 10 min at 4 °C. The supernatant was removed again and the pellet containing the isolated mitochondrial fraction was suspended in phosphate buffered saline (PBS) at 3 mg pellet/ml concentration with the addition of 0.4 mM glutamate and 0.4 mM NAD^+ as substrates for mitochondrial oxidative phosphorylation. The mitochondrial fraction was then kept in an incubator at 37 °C with 5 % CO_2 atmosphere for 4 h to ensure initiation of mitochondrial respiration.

MTT assay

Cytotoxicity of Si NP

An NR8383 cell suspension was collected and centrifuged at 140 g for 5 min before resuspending the cell pellet in medium followed by counting and adjusting the cellular concentration to 2 × 10^5 cells/ml. The cells were then seeded in a 96-well plate (50 µl/well) and the plate was kept in a 5 % CO_2 incubator at 37 °C for 24 h. Next day, 50 µl of serial dilutions of Si NP were added to the wells to obtain the required final concentrations of Si NP and then incubated for 24 h. After 24 h, 5 µl of MTT solution in PBS (5 mg/ml) was added to each well and the plate was incubated for another 4 h. Then 100 µl of pure DMSO was added to each well to dissolve the formazan crystals. Now the absorption of each well was measured at 562 nm in a 96-well plate reader and the background absorption at 612 nm was subtracted. Mitochondrial metabolic activity for each concentration of Si NP was expressed as % of corresponding negative control reading. Medium without Si NP and medium with Triton-X (0.01 %) were used as negative and positive controls, respectively. Control experiments were done to exclude a possible reaction between MTT reagent and Si NP. Additional control experiments were performed with stoichiometrically equivalent amounts of the coating materials (allylamine in case of Si NP-NH_2, 10-undecenyl azide in case of Si NP-N_3 and 1-butenoic acid in case of Si NP-COOH) to exclude cytotoxicity arising from the coating material molecules, possibly remaining in the stock solutions of Si NP as impurities. However, at these concentrations no cytotoxic effects were found for these coating compounds.

Protection by cellular pre-incubation with vitamin E

NR8383 cells were plated as described above (1×10^4 cells/well; 50 µl/well) in F12-K medium containing 100 µM vitamin E. After 24 h, 50 µl of serial dilutions of Si NP were added to the wells to obtain the required final concentrations of Si NP (the final concentration of vitamin E upon addition of the Si NP was reduced to 50 µM/well). Upon incubation for another 24 h MTT reagent was added and the MTT assay was performed as described above. Control experiments were run with vitamin E only or Si NP only; both showed no activity in the MTT test.

Protection by cellular pre-incubation with vitamin C

NR8383 cells were plated in a 96-well plate (1×10^4 cells/well; 50 µl/well) in F12-K medium and after 22 h, vitamin C was added to reach a concentration of 1 mM vitamin C. After 2 more h of incubation, 50 µl of serial dilutions of Si NP were added to the wells to obtain the required final concentrations of Si NP (this reduced the final concentration of vitamin C to 500 µM). Upon incubation for another 24 h, MTT reagent was added and the MTT assay was performed as described above. Control experiments were run with vitamin C only or Si NP only; both showed no activity in the MTT test.

Phagocytic Index measurement

A NR8383 cell suspension (2×10^5 cells/ml) was plated in a 96-well plate (50 µl/well) in F12-K medium, followed by addition of 50 µl/well of serial dilutions of Si NP to obtain the required final concentrations of Si NP. Plain F12-K medium without Si NP and medium containing 100 µM $CuSO_4$ were used as negative and positive controls, respectively. After 24 h, the cells were exposed to yellow green fluorescent latex beads (1 µm size) at a ratio of beads to cells in each well of 50:1. After 4 h of incubation, counting samples were taken from the wells and viewed first under a fluorescent microscope to visualize the fluorescent beads, followed by bright field view to visualize the cells [see *Appendix A*]. Also samples were taken out of each well to assess the cell viability by *Trypan Blue Exclusion* test. The phagocytic index was determined by calculating the average number of fluorescent beads phagocytosed per viable cell and expressed as % of the negative control.

DCFH-DA assay

NR8383 cells

The cell suspension was adjusted to 2×10^5 cells/ml and seeded in a 96-well plate (50 µl/well) in F12-K medium. 50 µl/well of serial dilutions of Si NP in F12-K medium were added to obtain the required final concentrations of Si NP. A final concentration of 10 mM H_2O_2 was used as positive control and F12-K medium without Si NP as negative control. After 6 h of exposure to the Si NP, 5 µl of a 20 mM solution of DCFH-DA were added to each well and the plates were incubated for another 18 h in a 5 % CO_2 atmosphere at 37 °C. The fluorescence was then measured on a fluorometer at 485 nm excitation and 538 nm emission wavelengths. The fluorescence induction factor for each concentration of Si NP was calculated by dividing the reading of each well by the average reading of the negative control and expressed as %. Control experiments were performed by incubating the Si NP at their test concentrations with DCFH-DA

in the absence of cells to check the possibility of a positive fluorescence reading caused by reaction with Si NP alone.

Caco-2 cells

The cells were suspended in DMEM medium to a concentration of 1×10^5 cells/ml after trypisinization and were plated in a 96-well plate (100 μl/well). After 24 h, the cells were exposed to 100 μl/well of final concentrations of Si NP. Following another 6 h of Si NP exposure, 5 μl of a 20 mM solution of DCFH-DA were added. The plate was further incubated for 18 h before measurement of the fluorescence was carried out as described above. Control experiments were performed by incubating the Si NP at their test concentrations with DCFH-DA in the absence of cells to check the possibility of a positive fluorescence reading caused by reaction with Si NP alone.

Effect on isolated mitochondrial fraction

The isolated mitochondrial fraction (3 mg pellet/ml in PBS) was plated in a 96-well plate (50 μl/well) and serial dilutions of Si NP and 5 μl of DCFH-DA probe were added. The plate was incubated for 90 min at 37 °C in a humidified 5 % CO_2 atmosphere. The plate was then measured at 485 nm excitation and 538 nm emission wavelength. Medium without Si NP and with 75 μM 2,4-dinitrophenol (DNP) in DMSO were used as negative and positive controls, respectively. Results were expressed as % of negative control.

Statistical analysis

Data were analysed with Origin Pro (version 8.0) graphing software. For statistical analysis a student's *t*-test was performed and data with $p < 0.05$ (compared to negative control, except for Figure 5) are marked with an asterisk (*) sign. Each data point represents the average from three independent experiments (n = 3) and is presented as the arithmetic mean ± standard error of mean (SEM).

Results

Figure 1 shows the cytotoxic effect of increasing concentrations of various Si NP on NR8383 cells, as detected by the reduction in the mitochondrial metabolic activity (MTT assay) of these cells after 24 h exposure. Si NP-NH_2 showed the highest cytotoxicity (EC50 value = 12 ng/ml) followed by Si NP-N_3, which were cytotoxic at relatively higher concentrations (EC50 value = 270 ng/ml). Si NP-COOH failed to show any cytotoxicity up to concentrations of 3000 ng/ml (Table 2). The effects of increasing concentrations of the differently charged Si NP on the phagocytic index of NR8383 cells upon 24 h of exposure are shown in Figure 2. Exposure to Si NP-NH_2 and Si NP-N_3 resulted in a concentration-dependent decrease in the phagocytic index. The EC50 value for Si NP-NH_2 was 60 ng/ml and for Si NP-N_3 it was 320 ng/ml (Table 2). Exposure to Si NP-COOH did not result in a decrease in phagocytosis index, but surprisingly, even resulted in a steady increase in the phagocytosis index up to ~130 % of the control values.
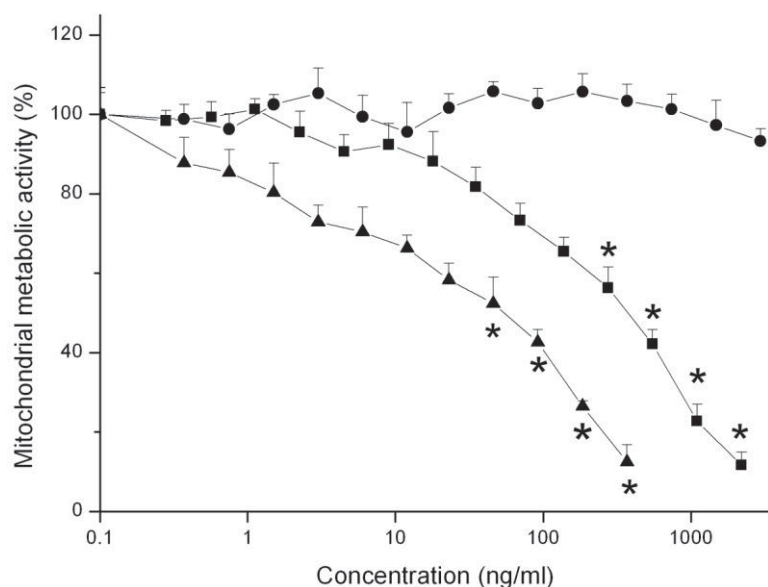
Figure 1: *Effect of 24 h exposure of NR8383 cells to increasing concentrations of Si NP-NH$_2$ (▲), Si NP-N$_3$ (■) and Si NP-COOH (●) on mitochondrial metabolic activity (measured by the MTT assay). Error bars show standard error of mean (n = 3). The asterisk (*) sign signifies p < 0.05.*
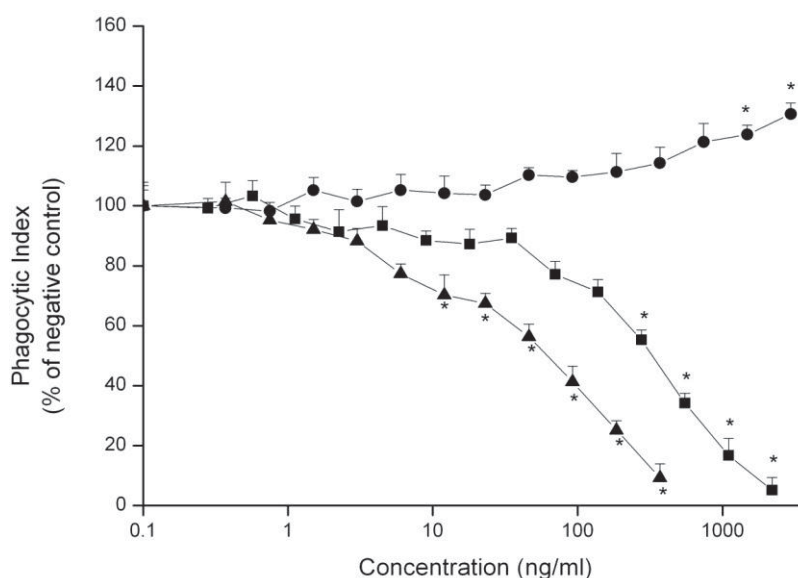

Figure 2: *Effect of 24 h exposure of NR8383 cells to increasing concentrations of Si NP-NH$_2$ (▲), Si NP-N$_3$ (■) and Si NP-COOH (●) on phagocytosis (measured as the phagocytic index). Error bars show standard error of mean (n = 3). The asterisk (*) sign signifies p < 0.05.*

In Figure 3A the intracellular ROS production (measured by DCFH-DA assay) in NR8383 cells after 24 h exposure to various Si NP is shown. Exposure of NR8383 cells to Si NP-NH$_2$ resulted in a dose-dependent increase in intracellular ROS production (EC50 value = 22 ng/ml). Upon exposure to Si NP-N$_3$, also an increase in intracellular ROS production was observed (EC50 value = 190 ng/ml), although the rate of intracellular ROS production was lower than that observed upon exposure of the NR8383 cells to Si NP-NH$_2$ (Table 2). Upon exposure of the NR8383 cells to Si NP-COOH, no increase in intracellular ROS production was observed. In Figure 3B, the intracellular ROS production (measured by DCFH-DA assay) in Caco-2 cells after 24 h exposure to various Si NP is shown. Upon exposure to Si NP-NH$_2$, intracellular ROS production started at low concentrations and then grew rapidly reaching a plateau at concentrations above 46 ng/ml (EC50 value = 18 ng/ml; Table 2). For Caco-2 cells exposed to Si NP-N$_3$, intracellular ROS production increased significantly at concentrations above 50 ng/ml and increased up to higher concentrations (EC50 value = 310 ng/ml; Table 2). For Caco-2 cells exposed to Si NP-COOH, no increase in intracellular ROS production was observed.
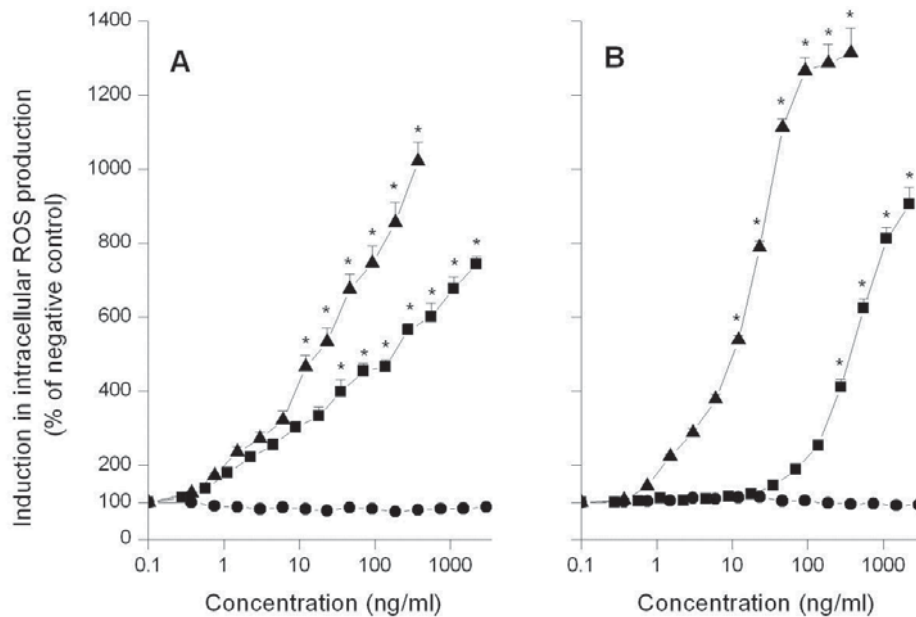
Figure 3: Induction of ROS production (measured using the DCFH-DA assay) in NR8383 (A) and Caco-2 (B) cells after 24 h exposure to increasing concentrations of Si NP-NH$_2$ (▲), Si NP-N$_3$ (■) and Si NP-COOH (●) on phagocytosis (measured as the phagocytic index). Error bars show standard error of mean (n = 3). The asterisk (*) sign signifies p < 0.05.

In Figure 4, ROS production (measured by DCFH-DA assay) upon 90 min incubation of an isolated rat liver mitochondrial fraction with different Si NP is shown. Incubation with Si NP-NH$_2$ resulted in a concentration-dependent increase in ROS production, which started at concentrations as low as 6 ng/ml. The calculated EC50 value for Si NP-NH$_2$ induced mitochondrial ROS production was 80 ng/ml (Table 2). Incubation of the mitochondrial fraction with Si NP-N$_3$ resulted in a concentration-dependent increase in ROS formation starting at 90 ng/ml, with an EC50 value of 1050 ng/ml (Table 2). No increase in ROS production was found for the Si NP-COOH, even for concentrations as high as 3000 ng/ml.

In Figure 5A, the effects of the antioxidants vitamin E and C on the cytotoxicity in NR8383 cells upon 24 h exposure to Si NP-NH$_2$ are depicted. Pre-incubation of the NR8383 cells with vitamin E resulted in a significant reduction in the Si NP-NH$_2$-induced cytotoxicity with EC50 values of 12 ng/ml and 60 ng/ml ($p < 0.05$) for NR8383 cells not pre-incubated with antioxidants (control) and cells pre-incubated with 100 µM vitamin E, respectively (Table 2). Although a higher EC50 value of 32 ng/ml was found for NR8383 cells pre-incubated with 1 mM of vitamin C in comparison to NR8383 cells not pre-incubated with antioxidants (control), the magnitude of reduction in cytotoxicity for 1 mM vitamin C was less than pre-incubation of NR8383 cells with 100 µM vitamin E (EC50 value = 60 ng/ml; Table 2). The effects of vitamins E and C on the cytotoxic effects of Si NP-N$_3$ in NR8383 cells are shown in Figure 5B. For cells exposed to Si NP-N$_3$, vitamin C offered a significant protection, whereas pre-incubation of the cells with vitamin E did not result in protection against the cytotoxicity of the NP. The corresponding EC50 values for Si NP-N$_3$ were 270 ng/ml, 310 ng/ml and 510 ng/ml ($p < 0.05$), respectively, for NR8383 cells not pre-incubated with antioxidants (control), cells pre-incubated with 100 µM vitamin E and cells pre-incubated with 1 mM vitamin C.
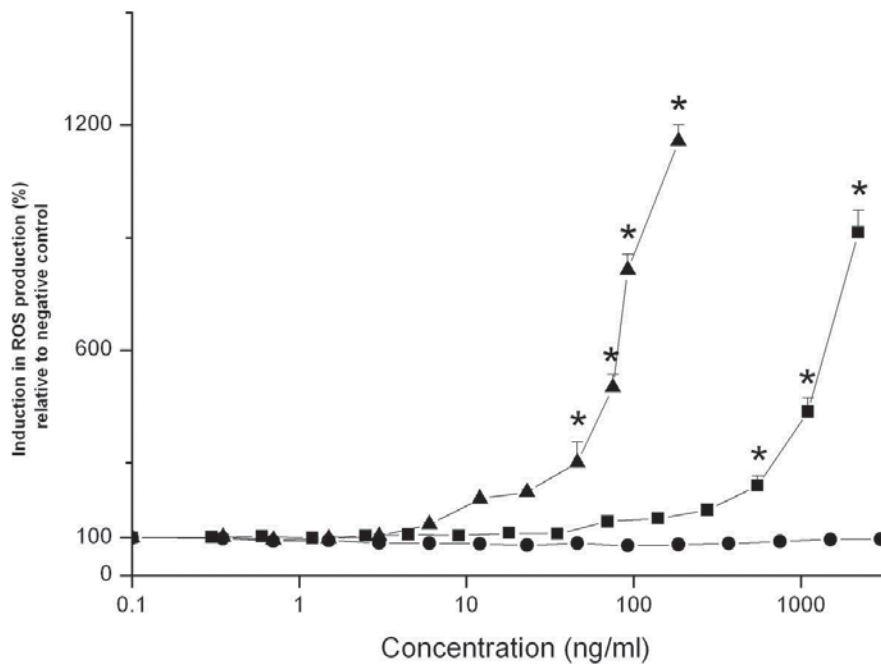
Figure 4: Induction of ROS production (measured using the DCFH-DA assay) upon 90 min incubations of an isolated rat liver mitochondrial fraction to increasing concentrations of Si NP-NH₂ (▲), Si NP-N₃ (■) and Si NP-COOH (●). Error bars show standard error of mean (n = 3). The asterisk (*) sign signifies p < 0.05.
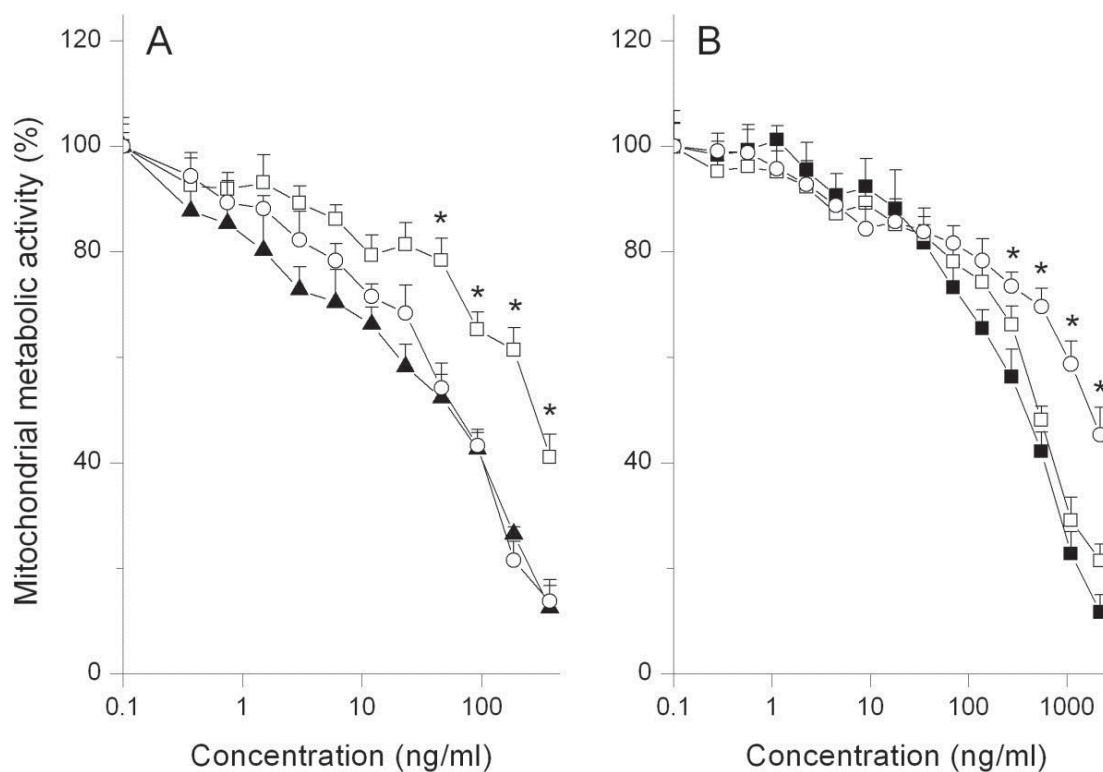

Figure 5: Protective effect of pre-incubation of NR8383 cells with vitamin E (□) and vitamin C (○) against cytotoxicity (measured using the MTT assay) after 24 h exposure to serial dilutions of (A) Si NP-NH₂ (▲) and (B) Si NP-N₃ (■). Error bars show standard error of mean (n = 3). The asterisk (*) sign signifies p < 0.05 (compared to data without anti-oxidants).

Discussion

The surface charge of NP plays an important role in their interaction with cells and cytotoxicity. In this paper, the role of surface charge on cytotoxicity was studied and mechanistic factors (like oxidative stress) causing this cytotoxicity were probed. The main conclusions are that positively charged Si NP-NH$_2$ are more cytotoxic towards NR8383 cells both in terms of reducing mitochondrial metabolic activity and phagocytosis, than neutral Si NP-N$_3$, while negatively charged Si NP-COOH showed very little or no cytotoxicity. Si NP-NH$_2$ produced most intracellular ROS followed by Si NP-N$_3$, with no ROS produced by Si NP-COOH. Part of this ROS production probably originated from mitochondria, as a similar trend in ROS production was observed in NR8383 cells and in incubations of isolated rat liver mitochondrial fractions with Si NP. The Si NP-NH$_2$ and Si NP-COOH were slightly more hydrophilic than Si NP-N$_3$. However, since the difference in cytotoxicity and ROS production was much larger between Si NP-NH$_2$ and Si NP-COOH than between Si NP-NH$_2$ or Si NP-COOH and Si NP-N$_3$, we conclude that surface charge was much more important than differences in hydrophilicity or hydrophobicity.

Table 2				
The EC50 values (ng/ml) of different Si NP obtained from experiments reported in this article				
Assay	Parameter	Reference figure	Si NP-NH$_2$	Si NP-N$_3$
MTT	Mitochondrial metabolic activity	Figure 1	12	270
Phagocytosis Index	Induction Factor	Figure 2	60	320
DCFH-DA	Intracellular ROS production	Figure 3A (NR8383)	22	170
		Figure 3B (Caco-2)	18	310
DCFH-DA	ROS production (from isolated mitochondrial fraction)	Figure 4	80	1050
MTT (in presence of antioxidants vitamin E and vitamin C)	Mitochondrial metabolic activity	Figure 5 (for Vitamin E)	60	310
		Figure 5 (for Vitamin C)	32	510

The role of ROS was also reflected in the protection against cytotoxicity by Si NP upon pre-treatment of the NR8383 cells with vitamin E and C. Interestingly, pre-treatment of the NR8383 cells with vitamin E showed more protection towards Si NP-NH$_2$ than vitamin C, while vitamin C showed more protection towards Si NP-N$_3$. The mechanism behind this difference may be related to the nature of the ROS formed and/or the location(s) and mechanism(s) of this ROS formation, although the results of the present study reveal that in both cases, mitochondrial ROS production is likely involved. Pan et al.[34] previously reported different protective effects offered by different antioxidants (N-acetylcysteine, glutathione, triphenylphosphine monosulphonate and vitamin C) while studying the cytotoxic effects of gold NP on HeLa cells.

The relatively higher cytotoxicity of Si NP-NH$_2$ as compared to Si NP-N$_3$ or Si NP-COOH is in agreement with our previous study, where similar effects of these Si NP were observed on human colonic adenocarcinoma-derived Caco-2 cells.[6] Shiohara et al.[35] recently reported the synthesis and cytotoxicity of Si NP with different functionalized surfaces containing amine, epoxide, diene and diol terminated alkyl chains. These authors also reported a higher toxicity of amine-terminated Si NP as compared to the other Si NP. However, the functional groups of their Si NP were mostly different from our Si NP. Also, their Si NP were substantially larger (~4 nm in size), more polydisperse and prepared by a different synthetic technique. Goodman et al.[36] tested the cytotoxicity of cationic and anionic monolayer-coated gold NP on Cos-1 cells and found that cationic particles were toxic, whereas the anionic particles were not toxic at all, which matches our observation as well. Table 1 presents an overview of additional literature studies on NP, showing the role of surface charge on cellular interaction, including cellular uptake and cytotoxicity. It seems that the findings reported in these studies can be summarized to an overall match to our results since, mostly positive charged NP were cytotoxic, although the cytological and experimental models used and endpoints studied in these reported studies were quite different from the ones we applied.

Our data also showed that positively charged Si NP-NH$_2$ and the neutral Si NP-N$_3$ decreased the phagocytic activity in NR8383 cells, but surprisingly revealed that the negatively charged Si NP-COOH increased the phagocytic index significantly. Although the precise mechanism of this phenomenon is not fully understood, several indications have been reported in the literature that suggested that this in fact is not an unexpected phenomenon. One study reported comparable results for etoposide-incorporated tripalmitin NP with positive and negative surface charges.[37] That study showed that in rats, after 24 h of intravenous administration, the concentration of positively charged particles in blood was ~1.64 times that of negatively charged ones. Sengupta et al.[38] showed that etoposide-incorporated cationic liposomes attained a longer $t_{1/2}$ in blood than anionic liposomes containing etoposide, due to a decreased phagocytic activity of macrophages for cationic particles that is not seen in the case of anionic particles. A similar charge-dependent increase (for negatively charged liposomes) or decrease (for positively charged liposomes) of phagocytosis of liposomes containing stearylamine was reported by Levchenko et al.[39] Comparable results were reported by Aoki et al.[40] while investigating the disposition kinetics of liposomes with encapsulated methyl-2-amino-6-palmitoyl-D-glycoside. They found that the surface charge of liposomes is an important factor for phagocytosis of liposomes by the reticule-endothelial system: positively charged liposomes decreased phagocytosis, while negatively charged ones did not affect phagocytosis. It should be noted that all studies quoted above[37-40] were bioavailability studies and only potentially non-toxic NP were tested irrespective of their surface charge. Furthermore, in most of these studies

no proper cytotoxicity tests were performed simultaneously with the bioavailability experiments.

As the Si NP-COOH proved to exert very little or no cytotoxicity at the tested concentrations, the induction of phagocytosis by negatively charged Si NP-COOH may be compared with similar findings reported in the above-mentioned studies. However, these findings should not be compared with our results on positively charged Si NP-NH$_2$, which are cytotoxic within the tested concentration range. Hence, the decrease in phagocytic capability of NR8383 cells after exposure to positively charged Si NP-NH$_2$ is the result of the positive surface charge and NP cytotoxicity, but does not reflect an absence or induction in cellular uptake. A possible explanation for the induction of phagocytosis by negatively charged NP is given by Hernandez-Caselles et al.,[41] who reported better binding of *opsonin* serum proteins with negatively charged NP than with positively charged NP. As a result, negatively charged NP get more covered with *opsonin* proteins, which stimulates phagocytosis by macrophages. It should be noted that the cell culture medium F12-K used in our experiments had fetal calf serum, which contained *opsonin* proteins (like immunoglobulins) in it as well.

In order to get more insight in the mechanism behind the cytotoxicity of Si NP towards NR8383 and Caco-2 cells, we assessed the production of intracellular ROS. From our results it is evident that positively charged Si NP-NH$_2$ were more efficient in producing intracellular ROS than the neutral Si NP-N$_3$, which produced ROS only at much higher concentrations and then negatively charged Si NP-COOH, that did not produce any intracellular ROS at all. Xia et al.[42] did an extensive study on murine macrophage RAW 264.7 cells with a broad range of NP (including metal oxides like titanium dioxide, fullerols, carbon black and amine terminated polystyrene nanoparticles/PS-NH$_2$) and found that only carbon black and cationic PS-NH$_2$ were able to generate intracellular ROS production. ROS production by cationic PS-NH$_2$ is in line with our study where Si NP-NH$_2$ were also able to induce production of intracellular ROS. Stone et al.[43] also mentioned oxidative stress as an important mechanism for cytological injury caused by NP. Previously, Foucaud et al.[44] showed that carbon black ultrafine particles are capable of producing ROS in biologically relevant medium (like cell culture medium). Additionally, there are several other reports in which oxidative stress has been identified as an important mechanism for cytotoxicity of NP.[45-47] Subsequently, we investigated the capability of mitochondria to act as a source for nanoparticle-induced ROS production, since mitochondria have previously been recognized as a probable subcellular target of NP.[48] The results of our study revealed that mitochondria might indeed interact and contribute to the intracellular ROS production induced by NP. Karataş et al.[49] also reported that the mitochondrial membrane may be a target for NP interaction. They used an isolated mitochondrial fraction from A549 lung cancer cells incubated with negatively charged 13 nm gold NP and studied the interaction with surface-enhanced Raman scattering (SERS). Using AFM and TEM, they also demonstrated interaction of the gold NP with the mitochondrial membrane. There is one more report[34] in which 1.4 nm and 15 nm gold NP were tested on HeLa cells. The 1.4 nm gold NP were coated with triphenylphosphine sulphonate groups and their cytotoxic effect on the mitochondrial membrane potential ($\Delta\Psi_m$) was compared with bigger 15 nm gold NP. However, that study focused more on the size effect of gold NP on the mitochondrial membrane potential and did not report the effect of surface charge of NP in interaction of the NP with the mitochondrial membrane. To the best of our knowledge, the present study is the first one to show production of ROS directly from mitochondria when exposed to NP. The observation that incubation of the

mitochondrial fraction with positively charged Si NP-NH$_2$ produced more ROS than incubation with neutral Si NP-N$_3$ and negatively charged Si NP-COOH is in agreement with findings reported by Xia et al.[42] With electron microscopy, they saw that positively charged NH$_2$-PS nanospheres completely disrupted the morphology of mitochondria after 16 h of exposure, while negatively charged COOH-PS nanospheres did not cause any harm to the mitochondria. They also reported a dissipation in mitochondrial membrane potential ($\Delta\Psi_m$) with NH$_2$-PS, but not for COOH-PS nanospheres. These data suggest that the interaction of cationic NP with mitochondrial membranes exerts significant toxic effects.

Conclusion

The present study demonstrates the importance of surface charge in the cytotoxicity of NP. Dose-dependent and surface charge-dependent production of intracellular ROS further emphasizes the role of oxidative stress as an important mechanism for cytotoxicity. Mitochondria are likely the target organelles for Si NP in the production of intracellular ROS. The negative Si NP-COOH showed potential for further biological applications, whilst positive Si NP-NH$_2$ should be applied with care.

References

1. Derfus AM, Chan WCW, Bhatia SN; *Nano Lett.* 2004, 4:11-18.
2. Klauser F, Stijepovic R, Endstrasser N, Jaksch S, Memmel N, Scheier P; *Surf. Sci.* 2009, 603:2999-3004.
3. Park J, Gu L, Maltzahn GV, Ruoslahti E, Bhatia SN, Sailor MJ; *Nat. Mater.* 2009, 8(4):331-336.
4. Burns AA, Vider J, Ow H, Herz E, Penate-Medina O, Baumgart M, Larson SM, Wiesner U, Bradbury M; *Nano Lett.* 2009, 9(1):442-448.
5. Rosso-Vasic M, Spruijt E, van Lagen B, De Cola L, Zuilhof H; *Small* 2008, 4(10):1835-1841.
6. Ruizendaal L, Bhattacharjee S, Pournazari K, Rosso-Vasic M, de Haan LHJ, Alink GM, Marcelis ATM, Zuilhof H; *Nanotoxicology* 2009, 3(4):339-347.
7. Rosso-Vasic M, De Cola L, Zuilhof H; *J. Phys. Chem. C* 2009, 113:2235-2240.
8. Rosso-Vasic M, Spruijt E, Popovi Z, Overgaag K, van Lagen B, Grandidier B, Vanmaekelbergh D, Domínguez-Gutiérrez D, De Cola L, Zuilhof H; *J. Mater. Chem.* 2009, 19:5926-5933.
9. Oskuee RK, Dehshahri A, Shier WT, Ramezani M; *J. Gene. Med.* 2009, 11(10):921-932.
10. Sayin B, Somavarapu S, Li XW, Thanou M, Sesardic D, Alpar HO, Senel S; *Int. J. Pharm.* 2008, 363(1-2):139-148.
11. Nafee N, Schneider M, Schaefer UF, Lehr CM; *Int. J. Pharm.* 2009, 381(2):130-139.
12. Hauck TS, Ghazani AA, Chan WC; *Small* 2008, 4(1):153-159.
13. Mayer A, Vadon M, Rinner B, Novak A, Wintersteiger R, Fröhlich E; *Toxicology* 2009, 258(2-3):139-147.
14. Sadiq IM, Chowdhury B, Chandrasekaran N, Mukherjee A; *Nanomedicine* 2009, 5(3):282-286.
15. Xu F, Yuan Y, Shan X, Liu C, Tao X, Sheng Y, Zhou H; *Int. J. Pharm.* 2009, 377(1-2):199-206.
16. Pathak A, Kumar P, Chuttani K, Jain S, Mishra AK, Vyas SP, Gupta KC; *ACS Nano* 2009, 3(6):1493-1505.
17. Zhang LW, Monteiro-Riviere NA; *Toxicol. Sci.* 2009, 110(1):138-155.
18. Nam HY, Kwon SM, Chung H, Lee SY, Kwon SH, Jeon H, Kim Y, Park JH, Kim J, Her S, Oh YK, Kwon IC, Kim K, Jeong SY; *J. Control. Release* 2009, 135(3):259-267.
19. Kim BY, Jiang W, Oreopoulos J, Yip CM, Rutka JT, Chan WC; *Nano Lett.* 2008, 8(11):3887-3892.
20. Orr G, Panther DJ, Phillips JL, Tarasevich BJ, Dohnalkova A, Hu D, Teeguarden JG, Pounds JG; *ACS Nano* 2007, 1(5):463-475.
21. Gupta K, Singh VP, Kurupati RK, Mann A, Ganguli M, Gupta YK, Singh Y, Saleem K, Pasha S, Maiti S; *J. Control. Release* 2009, 134(1):47-54.
22. Geys J, De Vos R, Nemery B, Hoet PH; *Am. J. Physiol. Lung. Cell. Mol. Physiol.* 2009, 297(5):L903-L911.
23. Corsi F, De Palma C, Colombo M, Allevi R, Nebuloni M, Ronchi S, Rizzi G, Tosoni A, Trabucchi E, Clementi E, Prosperi D; *Small* 2009, 5(22):2555-2564.
24. Shvedova AA, Castranova V, Kisin ER, Schwegler-Berry D, Murray AR, Gandelsman VZ, Maynard A, Baron PJ; *J. Toxicol. Environ. Health A* 2003, 66(20):1909-1926.
25. Xia T, Korge P, Weiss JN, Li N, Venkatesen MI, Sioutas C, Nel A; *Environ. Health Perspect.* 2004, 112(14):1347-1358.

26. Green M, Howman E; *Chem. Commun.* 2005, (1):121-123.

27. Hussain SM, Hess KL, Gearhart JM, Geiss KT, Schlager JJ; *Toxicol. in Vitro* 2005, 19(7):975-983.

28. Sayes CM, Gobin AM, Ausman KD, Mendez J, West JL, Colvin VL; *Biomaterials* 2005, 26(36):7587-7595.

29. Foster KA, Galeffi F, Gerich FJ, Turner DA, Muller M; *Prog. Neurobiol.* 2006, 79(3):136-171.

30. Lin W, Huang YW, Zhou XD, Ma Y; *Int. J. Toxicol.* 2006, 25(6):451-457.

31. Limbach LK, Wick P, Manser P, Grass RN, Bruinink A, Stark WJ; *Environ. Sci. Technol.* 2007, 41(11):4158-4163.

32. Monteiller C, Tran L, MacNee W, Faux S, Jones A, Miller B, Donaldson K; *Occup. Environ. Med.* 2007, 64(9):609-615.

33. Schubert D, Dargusch R, Raitano J, Chan SW; *Biochem. Biophys. Res. Commun.* 2006, 342(1):86-91.

34. Pan Y, Leifert A, Ruau D, Neuss S, Bornemann J, Schmid G, Brandau W, Simon U, Jahnen-Dechent W; *Small* 2009, 5(18):2067-2076.

35. Shiohara A, Hanada S, Prabakar S, Fujioka K, Lim TH, Yamamoto K, Northcote PT, Tilley RD; *J. Am. Chem. Soc.* 2010, 132(1):248-253.

36. Goodman CM, McCusker CD, Yilmaz T, Rotello VM; *Bioconjugate Chem.* 2004, 15(4):897-900.

37. Reddy LH, Sharma RK, Chuttani K, Mishra AK, Murthy RR; *AAPS. J.* 2004, 6(3):e23.

38. Sengupta S, Tyagi P, Velpandian T, Gupta YK, Gupta SK; *Pharmacol. Res.* 2000, 42(5):459-464.

39. Levchenko TS, Rammohan R, Lukyanov AN, Whiteman KR, Torchilin VP; *Int. J. Pharm.* 2002, 240(1-2):95-102.

40. Aoki H, Sun C, Fuji K, Miyajima K; *Int. J. Pharm.* 1995, 115:183-191.

41. Hernandez-Caselles T, Villalain J, Gomez-Fernandez JC; *Mol. Cell Biochem.* 1993, 120:119-126.

42. Xia T, Kovochich M, Brant J, Hotze M, Sempf J, Oberley T, Sioutas C, Yeh JI, Wiesner MR, Nel AE; *Nano Lett.* 2006, 6(8):1794-1807.

43. Stone V, Donaldson K; *Nat. Nanotechnol.* 2006, 1(1):23-24.

44. Foucaud L, Wilson MR, Brown DM, Stone V; *Toxicol. Lett.* 2007, 174(1-3):1-9.

45. Wilson MR, Lightbody JH, Donaldson K, Sales J, Stone V; *Toxicol. Appl. Pharmacol.* 2002, 184(3):172-179.

46. Donaldson K, Aitken R, Tran L, Stone V, Duffin R, Forrest G, Alexander A; *Toxicol. Sci.* 2006, 92(1):5-22.

47. Brown DM, Donaldson K, Borm PJ, Schins RP, Dehnhardt M, Gilmour P, Jimenez LA, Stone V; *Am. J. Physiol. Lung Cell Mol. Physiol.* 2004, 286(2):L344-L353.

48. Li N, Sioutas C, Cho A, Schmitz D, Misra C, Sempf J, Wang M, Oberley T, Froines J, Nel A; *Environ. Health Perspect.* 2003, 111(4):455-460.

49. Karataş ÖF, Sezgin E, Aydin Ö, Çulha M; *Colloids Surf. B Biointerfaces* 2009, 71(2):315-318.

50. Supino R; In Vitro Toxicity Testing Protocols. Vol. 43. Edited by S. O'Hare and C. K. Atterwill. *Humana Press*, Totowa, NJ.

Chapter 4

The cytotoxicity of surface-functionalized silicon and germanium nanoparticles : the dominant role of surface charges

Abstract

A comparative cytotoxicity study, quantifying nine different cellular endpoints, was performed with a broad series of monodisperse, well characterized silicon (Si) and germanium (Ge) nanoparticles (NP) with various surface functionalizations. Human colonic adenocarcinoma Caco-2 and rat alveolar macrophage NR8383 cells were used, to clarify the toxicity of this series of NP. The surface coating on the NP appeared to dominate the cytotoxicity: the cationic NP exhibited cytotoxicity, whereas the carboxylic acid-terminated and hydrophilic PEG- or dextran-terminated NP did not. Within the cationic Si NP, smaller Si NP were more toxic than bigger ones. Manganese-doped (1 % Mn) Si NP did not show any added toxicity, which favours their further development for bioimaging. Iron-doped (1 % Fe) Si NP showed some added toxicity, which may be due to the leaching of Fe^{3+} ions from the core. A silica coating seemed to impart toxicity, in line with the reported toxicity of silica. Intracellular mitochondria seem to be a target organ for the toxic NP since a dose-, surface charge- and size-dependent imbalance of the mitochondrial membrane potential ($\Delta\Psi_m$) was observed. Such imbalance leads to a series of other cellular events for cationic NP, like decreased mitochondrial membrane potential ($\Delta\Psi_m$) and ATP production, induction of ROS generation, increased cytoplasmic Ca^{2+} content, production of TNF-α and enhanced caspase-3 activity. Taken together, the results explain the toxicity of Si NP/ Ge NP largely by their surface characteristics, provide insight in the mode of action underlying the observed cytotoxicity and give directions on synthesizing non-toxic Si and Ge NP, as this is crucial for bioimaging and other applications in for example, the field of medicine.

Introduction

Nanoparticles (NP) with their unconventional properties,[1] and ability to interact with a wide variety of biomolecules, have the potential to revolutionize medicine, including diagnostics and therapeutics.[2,3] Unfortunately, often the applicability of different NP is hampered by their toxicity.[4,5] Hence, there is a rapidly growing interest in understanding the toxicity of such NP in more detail, with the aim to control and minimize this toxicity.

Semiconductor quantum dots (SCQD), like silicon NP (Si NP) or germanium NP (Ge NP), have recently received significant attention because they can be made into multipotent and biocompatible NP.[6,7] Si NP or Ge NP can be used as vehicles for drug delivery,[8] but perhaps the most exciting application of SCQD can be foreseen in the field of bioimaging.[9,10] The Si NP or Ge NP, due to their very small sizes (< 5 nm) and intrinsic fluorescence, enjoy an edge over other NP (like polymer NP (PNP)[11] and carbon NP[12]) that need to be functionalized to be fluorescent.

The potential to provide intrinsically non-toxic NP also makes Si and Ge NP highly interesting systems. Unlike many PNP or carbon NP, Si NP and Ge NP are non-biopersistent and exhibit sufficient biodegradability.[13-15] For example, in human beings, Si is converted to orthosilicic acid/$Si(OH)_4$ and is excreted in the urine.[15,16] Moreover, since they can be synthesized with diameters < 5 nm, the sizes of Si NP and Ge NP are often below the size threshold for renal clearance for NP (< 5.5 nm) enabling renal elimination.[17] In addition, unlike the popular but intrinsically toxic Cd-based bioimaging agents, such as CdSe/ZnS quantum dots (QD),[15] Si or Ge are mostly non-toxic. In line with this, it has been reported for a set of well-characterized, monodisperse (size 1.6 ± 0.2 nm) and fluorescent Si NP,[18,19] that Si NP may display toxicity or non-toxicity, against human colonic adenocarcinoma Caco-2 and rat alveolar macrophage NR8383 cells, depending on their surface functionalization ($Si-C_3H_6-NH_2$, $Si-C_4H_8-N_3$ and $Si-C_{11}H_{22}-COOH$).[9,18,20,21] It was found that cationic $Si\ NP-NH_2$ were toxic,[21,22] while the anionic Si NP-COOH displayed no discernible toxicity in two different toxicity tests (MTT and BrdU).[21]

It has been proposed that the surface properties of NP determine their interactions with biological systems,[23-25] although little data based on systematic investigations are available. Fortunately, a wide array of synthetic methods has become available for the preparation of surface-functionalized Si NP and Ge NP.[26,27] Therefore, a comparative study is now possible, in which the toxicity of the different Si NP and Ge NP can be determined with respect to their surface characteristics. This can help to gain insight in how surface factors of these NP can influence the toxicity. To obtain a generally applicable hypothesis, we therefore performed a systematic investigation in which, a large series of Si NP and Ge NP with different properties (sizes, synthetic origin and surface functionalities) were tested for their possible adverse cellular effects.

Rat alveolar macrophage NR8383 and human colonic adenocarcinoma Caco-2 cells provide two adequate in vitro testing models for the Si NP and Ge NP. The NR8383 lung cells, being macrophage cells, act as the first line of defense against air-borne foreign pathogens and a toxic effect imparted on them by the NP, can give an idea on how the NP can influence the innate immune system. Similarly, eyeing the increasing number of food-based applications of different NP (like silica NP), Caco-2 cells being a human colonic cell line, can be an excellent model to test cytotoxicity and extrapolate the data to in vivo situations. Due to the ample reported data on the

toxicity of NP on these two cell lines,[11,20,28] a systematic and comparative toxicity testing with a mechanistic perspective can be performed. It is yet not fully clear what might be the mechanism of cytotoxicity for NP. Although oxidative stress has been recognized as a mechanism,[29,30] some recent reports counter this view and identified intracellular mitochondria as the target and perhaps the starting point of cytotoxicity.[11] Bhattacharjee et al.[20] have shown that an isolated mitochondrial fraction from rat liver, produced reactive oxygen species (ROS) after being exposed to cationic Si NP-NH$_2$. A recent hypothesis to explain the cytotoxicity of especially the cationic NP is that the cationic NP can interfere with the mitochondrial membrane and decouple the electron transport chain (ETC).[31,32] This in turn may lead to an induction of intracellular ROS (like superoxides, peroxides, hydroxyls) production as well as to leaching out of the sequestered calcium from the mitochondria into the cytoplasm. Interestingly, this can lead to a cytoplasmic free calcium overload and initiation of apoptotic cascades. Additionally, a de-coupling of the ETC can cause a decreased cellular ATP production, which may compromise the cellular viability.

The objective of the current paper is thus to investigate the cytotoxicity of a broad series of Si and Ge NP. To this aim, the following features were measured in both the NR8383 and Caco-2 cells after 24 h exposure to the different Si NP or Ge NP: 1) cell viability by MTT assay,[33] 2) cell proliferation by BrdU assay,[21] 3) induction of ROS from isolated rat liver mitochondrial fraction by DCFH-DA assay,[20] 4) change in mitochondrial membrane potential ($\Delta\Psi_m$),[31] 5) cellular ATP content,[31] 6) cellular ROS production by DCFH-DA assay,[20] 7) cytoplasmic free Ca^{2+} concentration,[34] 8) caspase-3 activity[31] as a biomarker for apoptotic pathways and 9) production of TNF-α,[35] as a pro-inflammatory marker. Finally, the obtained data were assembled to propose a series of events that ultimately lead to the toxicity (or lack thereof) of surface-functionalized Si and Ge NP and to provide directions to obtain non-toxic Si and Ge NP.

Materials and methods

Si NP and Ge NP

The fully characterized different Si NP and Ge NP were obtained as aqueous dispersions. Exposure ranges of the different Si NP and Ge NP (concentration 0-100 µg/ml) were prepared by mixing the aqueous dispersion of NP with cell culture media (F12-K or DMEM).

NR8383 cells

Rat alveolar macrophage (NR8383) cells were obtained from ATCC (Manassas, VA). The NR8383 cells were cultured in 150 cm^2 cell culture flasks with 25 ml F12-K culture medium (Gibco 21127) supplemented with 10 % (v/v) heat inactivated fetal calf serum (FCS) in a humidified atmosphere containing 5 % CO$_2$ at 37 °C.[11, 20] The cells were sub-cultured every two weeks. Cells with passage numbers 30-40 were used.

Caco-2 cells

The Caco-2 cells were obtained from ATCC (Rockville, MD) and were cultured in DMEM medium (Gibco), fortified with 10 % (v/v) heat-inactivated fetal calf serum (FCS) and 50 mg/ml gentamicin, in a humidified atmosphere at 5 % CO_2 and 37 °C in 75 cm^2 flasks.[11, 20] After reaching ~70 % confluence, the Caco-2 cells were sub-cultured, after rinsing with phosphate buffered saline (PBS), using trypsin (Gibco, Paisley, UK). Only cells within passage numbers 30-40 were used.

MTT assay

A. NR8383 cells. In this assay, the mitochondrial activity is determined photometrically by measuring the amount of MTT salt converted to insoluble formazan crystals by mitochondrial reductase enzymes. An NR8383 cell suspension was collected and centrifuged at 140 *g* for 5 min before resuspending the cell pellet in medium followed by counting and adjusting the cellular concentration to 2×10^5 cells/ml.[20] The cells were then seeded in a 96-well plate (50 µl/well) and the plate was kept in a 5 % CO_2 incubator at 37 °C for 24 h. Next day, 50 µl of serial dilutions of Si NP or Ge NP were added to the cells to obtain the required final concentration range (0-100 µg/ml) of Si NP or Ge NP and then the plates were incubated for 24 h. After 24 h, 5 µl of MTT (3-(4,5-dimethylthiazol-2-yl)-2,5-diphenyl tetrazolium bromide) solution in PBS (5 mg/ml) was added to each well and the plate was incubated for another 4 h. Then 100 µl of pure DMSO was added to each well to dissolve the formazan crystals. Now the absorption of each well was measured at 562 nm in a 96-well plate reader and the background absorption at 612 nm was subtracted. Mitochondrial metabolic activity for each concentration of Si NP was expressed as % of the value of the corresponding negative control. F12-K medium without NP and medium with Triton-X (0.01 %) were used as negative and positive controls, respectively. Control experiments were done to exclude a possible reaction between MTT salt and Si NP or Ge NP by mixing test concentration of the Si NP or Ge NP with MTT reagent.

B. Caco-2 cells. The Caco-2 cells were plated at a concentration of 10^5 cells/ml in a 96-well plate (100 µl/well) and were incubated for 24 h.[20] Then the Si NP or Ge NP were added to the cells in a total volume of 100 µl at final exposure concentrations of 0-100 µg/ml. After this, the cells were incubated for another 24 h. After 24 h exposure to the Si NP or Ge NP, 5 µl MTT solution in PBS (5 mg/ml) was added to each well and incubated for 4 h. Then, the medium was removed and 100 µl of DMSO was added to dissolve the formed formazan crystals. The plates were put in the plate shaker for 5 min. The absorbance at both 562 nm and 612 nm was measured. The mitochondrial metabolic activity was expressed as the mean percentage of the negative control values (0 µg/ml). 0.01 % Triton-X was used as positive control and DMEM medium without Si NP or Ge NP was used as negative control. Control tests were also done to exclude interfering reactions between the NP and the MTT solution.

BrdU assay

A. NR8383 cells. The NR8383 cells were plated and exposed to Si NP or Ge NP (final exposure concentration 0-100 µg/ml) as described before. Cell proliferation was quantified using the colorimetric BrdU (5-bromo-2-deoxyuridine) assay (Catalogue No. 647229001, Roche Diagnostics, Penzberg, Germany). BrdU acts as a structural analogue of thymidine and will be incorporated in newly synthesized DNA during cell replication and hence indicates cell proliferation.[21] After 24 h incubation with NP and BrdU, 100 µl of the BrdU labeling solution was added to each well followed by an incubation for 4 h. The immunoassay was then performed as instructed by the manufacturer. A 0.01 % Triton-X solution in F12-K medium was used as positive control and F12-K medium without Si NP or Ge NP was used as negative control.

B. Caco-2 cells. The Caco-2 cells were plated and exposed to Si NP or Ge NP as described before.[21] After incubation of the Caco-2 cells with the Si NP or Ge NP and BrdU for 24 h, the medium containing the Si NP or Ge NP and BrdU was removed and the BrdU labeling solution was added to the wells and incubated for 4 h. Subsequently, the immunoassay was performed according to the protocol of the manufacturer. Results were expressed as the mean percentage of the negative control (0 µg/ml) values. 0.01 % Triton-X (in DMEM) and DMEM medium without Si NP or Ge NP were used as positive and negative controls, respectively.

Induction of ROS from isolated mitochondrial fraction from rat liver by DCFH-DA assay

An isolated mitochondrial fraction from rat liver tissue was prepared as described before.[20] The isolated mitochondrial fraction (3 mg pellet/ml in PBS) was plated in a 96-well plate (50 µl/well) and serial dilutions of Si NP or Ge NP and 5 µl of 20 mM DCFH-DA (2',7'-dichlorofluorescein diacetate) probe (Catalogue No. D6883/ Sigma Aldrich Chemie BV) was added. The plate was incubated for 90 min at 37 °C in a humidified 5 % CO_2 atmosphere. The plate was then measured at λ_{ex} = 485 nm and λ_{em} = 538 nm. Medium without Si NP or Ge NP and with 75 µM DNP (2,4-dinitrophenol) in DMSO were used as negative and positive controls, respectively. Results were expressed as % of negative control (0 µg/ml).

Measurement of the mitochondria membrane potential ($\Delta\Psi_m$)

The NR8383 and Caco-2 cells were plated as described above and exposed to serial test concentrations of NP (0 - 100 µg/ml). The mitochondrial membrane potential ($\Delta\Psi_m$) was then measured by a commercially available kit from Invitrogen (MitoProbe™ Transition Pore Assay Kit; Catalogue No. M34153) and the results were expressed as % of the negative control (0 µg/ml). A 100 µM solution of F12-K or DMEM medium containing ionomycin and medium without NP were used as positive and negative controls, respectively.

Measurement of intracellular ATP content

The NR8383 and Caco-2 cells were seeded in a 96-well plate and exposed to different Si NP or Ge NP as mentioned before. After 24 h, the intracellular ATP content of each well was

measured by a commercial ATP measuring kit (Sigma Aldrich, Product No. FLASC) and results were expressed as % of the negative control (0 µg/ml). Cells exposed to medium without NP and to medium with 75 mM DNP were used as negative and positive controls, respectively.

Measurement of cytoplasmic free Ca²⁺ content

The NR8383 and Caco-2 cells were plated and exposed to the serial test concentration range of Si NP/ Ge NP before measuring the cytoplasmic free calcium content by a commercially available kit from the Invitrogen (Fluo-4 Direct™ Calcium Assay Kit; Catalogue No. F10472). Only F12-K or DMEM medium without NP (0 µg/ml) was used as negative control and the results were expressed as % of the negative control.

Measurement of intracellular ROS by DCFH-DA assay

A. NR8383 cells. The cell suspension was adjusted to 2×10^5 cells/ml and seeded in a 96-well plate (50 µl/well) in F12-K medium. 50 µl/well of serial dilutions of Si NP or Ge NP in F12-K medium were added to obtain the required final concentrations of Si NP or Ge NP. A final concentration of 10 mM H_2O_2 in F12-K medium was used as positive control and F12-K medium without NP as negative control. After 6 h of exposure to the Si NP or Ge NP, 5 µl of a 20 mM solution of DCFH-DA were added to each well and the plates were incubated for another 18 h in a 5 % CO_2 atmosphere at 37 °C. The fluorescence was then measured at λ_{ex} = 485 nm and λ_{em} = 538 nm. The fluorescence induction factor for each concentration of Si NP or Ge NP was then calculated by dividing the reading of each well with the average reading of the negative control (0 µg/ml) and expressed as %. Control experiments were performed by incubating the Si NP or Ge NP at their test concentrations with DCFH-DA in the absence of cells to check the possibility of a positive fluorescence reading caused by reaction with NP alone.

B. Caco-2 cells. The cells were suspended in DMEM medium to a concentration of 1×10^5 cells/ml after trypsinization and were plated in a 96-well plate (100 µl/well). After 24 h, the cells were exposed to 100 µl/well of final concentrations of Si NP or Ge NP. Following another 6 h, 5 µl of a 20 mM solution of DCFH-DA in DMSO was added to each well. The plate was further incubated for 18 h before measurement of the fluorescence was carried out as described above. Control experiments were performed by incubating the Si NP or Ge NP at their test concentrations with DCFH-DA in the absence of cells to check the possibility of a positive fluorescence reading caused by reaction with Si NP or Ge NP alone.

Measurement of TNF-α

The NR8383 and Caco-2 cells were seeded in a 96-well plate and exposed to different Si NP or Ge NP as mentioned before. After 24 h, the TNF-α content of each well was measured by a commercial TNF-α measuring kit (Invitrogen, Catalogue No. KRC3011) and results were expressed as % of negative control (0 µg/ml). Medium without NP and medium with 0.1 µg/ml lipopolysaccharide were used as negative and positive controls, respectively.

Measurement of caspase-3 activity

With prior plating and exposure of the NR8383 and Caco-2 cells to serial test concentrations of Si NP or Ge NP, the caspase-3 levels were measured by a commercially available kit from Sigma Aldrich Chemie BV (Catalogue No. CASP3C). Results were expressed as % of negative control (0 μg/ml).

Statistical analysis

The data were analyzed and plotted with the Origin Pro (Version 8.0) software. The results were presented as arithmetic mean of three independent observations (n = 3) ± standard error of mean.

Results and Discussion

The Si NP and Ge NP

The Si NP and Ge NP under investigation were obtained via four different synthetic approaches [18, 21,36-38] in order to have a diverse mix of NP with a wide range of surface properties. These NP were all prepared from a Si or Ge core, which were subsequently surface-functionalized with different groups. The detailed characterization data including the abbreviations used for each of them are given in Table 1. This collection of Si NP and Ge NP could be classified into four groups based on their sources: (1) Si NP (1.6 ± 0.2 nm), synthesized from $SiCl_4$, with surface functionalizations of amine (Si(1.6) NP-NH_2), carboxylic acid (Si(1.6) NP-COOH) and azide (Si(1.6) NP-N_3).[18, 21] These Si(1.6) NP showed emission in the blue region upon excitation with UV light and their toxicity or lack thereof, has been reported before.[20, 21] These data are added for reference. The Si(1.6) NP-NH_2 were the only cytotoxic NP within these three Si(1.6) NP, whereas the Si(1.6) NP-COOH did not show any cytotoxicity up to 3 μg/ml concentration.[20, 21] The Si(1.6) NP-N_3 were toxic only at higher concentrations of > 2 μg/ml. (2) Amine-terminated Si NP (3.9 ± 1.3 nm) synthesized from *Zintl* salts (NaSi$_{1-x}$, x = 0.05, 0.1, 0.15), further on referred to as: Si(3.9) NP-NH_2. The synthetic route used allowed the doping of these Si NP with 1 % manganese (Si/Mn(3.9) NP-NH_2) or 1 % iron (Si/Fe(3.9) NP-NH_2). These three Si NP were then also coated with dextran, referred to as Si(3.9) NP-NH_2-Dex, Si/Mn(3.9) NP-NH_2-Dex and Si/Fe(3.9) NP-NH_2-Dex. (3) Ge NP (average size 7.5 ± 2.5 nm) with surfaces functionalized with polyethylene glycol (Ge NP-PEG) or N,N,N-trimethyl-3(1-propyne) ammonium iodide (Ge NP-TMPA) and Si NP, surface-functionalized with PEG (Si NP-PEG). (4) Si NP (average size 2.1 ± 0.6 nm) functionalized with undecenylic acid (Si NP-UDA) or linked via a dodecyl chain to a coating of poly(maleic anhydride)-based amphiphilic polymer (Si NP-Pol)[38], or silica (Si NP-Sil)[39] with average sizes of 17.8 ± 0.4 nm and 35 ± 5 nm, respectively. All the Si NP and Ge NP were well characterized. More extensive characterization of the NP involved can be found elsewhere.[21, 36, 37] For the cluster of Si(1.6) NP-NH_2, Si(1.6) NP-COOH and Si(1.6) NP-N_3, the published reports[20, 21] already provided us with knowledge on the toxicity which will be discussed in later sections. In the next group comprising of Si(3.9) NP-NH_2, Si/Mn(3.9) NP-NH_2,

Si/Fe(3.9) NP-NH$_2$ and dextran coated Si(3.9) NP-NH$_2$-Dex, Si/Mn(3.9) NP-NH$_2$-Dex, Si/Fe(3.9) NP-NH$_2$-Dex, the comparison can be useful in several ways. As this group contained Si(3.9) NP-NH$_2$ bigger in size than Si(1.6) NP-NH$_2$, an indication of the influence of NP size on their cytotoxicity can be obtained. The toxicity of the Mn or Fe doped Si(3.9) NP can be compared to both Si(1.6) NP-NH$_2$ and Si(3.9) NP-NH$_2$ to find if the Mn or Fe dopants had any added toxic effects. This is important to learn, as the Si/Mn(3.9) NP-NH$_2$ and Si/Fe(3.9) NP-NH$_2$ have tremendous potential to be developed as bioimaging agents in the future and hence, an exacerbated toxicity is undesirable. The dextran-coated Si NP gave an interesting scope to compare the toxicity and find out whether the dextran coating can alleviate the toxicity. For the following group of Ge NP-PEG, Ge NP-TMPA and Si NP-PEG, a comparative investigation may reveal several important things. It has been claimed before that the balance between the hydrophilicity and hydrophobicity of NP surface coatings is important for the NP to exert cytotoxicity.[40,41] The Ge NP-PEG, Ge NP-TMPA, Si NP-Pol and Si NP-PEG differ in hydrophilicity and hence, an idea can be developed on the role of hydrophilicity on the toxic effects of Si NP or Ge NP. Furthermore, to investigate what effect the addition of PEG to the surface has, the toxicity of Si NP-PEG can be compared with Si(1.6) NP-NH$_2$ or Si(3.9) NP-NH$_2$. In case of the group of Si NP-UDA and Si NP-Sil, it is relevant to investigate if toxicity is detected, in spite of the fact that the Si NP-Sil had a non-toxic Si-core, as silica is often reported to be toxic.[42,43]

MTT assay

The MTT assay measures the mitochondrial metabolic activity of the cells and this can be expressed as % cell viability of the negative control. In this study, the MTT assay was performed on both NR8383 and Caco-2 cells exposed to serial dilutions of Si NP or Ge NP (Figure 1) for 24 h. From the results, it could be seen that only Si(3.9) NP-NH$_2$, Si/Mn(3.9) NP-NH$_2$, Si/Fe(3.9) NP-NH$_2$, Ge NP-TMPA and Si NP-Sil caused a dose-dependent reduction in cell viability, whereas the remaining Si NP/ Ge NP did not show any toxicity within the tested concentration range (0 - 100 µg/ml). In a study by Bhattacharjee et al.,[20, 21] among the Si(1.6) NP-NH$_2$, Si(1.6) NP-N$_3$ and Si(1.6) NP-COOH, only Si(1.6) NP-NH$_2$ was found to be toxic, followed by Si(1.6) NP-N$_3$ though only at comparatively high concentrations (> 2 µg/ml). While the toxicity of amine-terminated NP is thus in line with previous observations, it is noteworthy that the addition of Mn-dopant did not cause any increased toxicity of Si/Mn(3.9) NP-NH$_2$ in comparison to Si(3.9) NP-NH$_2$. Such an increased toxicity upon doping was, however, observed for the iron-doped Si/Fe(3.9) NP, which may be attributed to the leaching out of Fe ions from the Si-core to the cellular environment or to the NP surfaces, being responsible for the concomitant increase in overall toxicity. Perhaps the most relevant finding of this test was that coating the NP with PEG or dextran reduced the toxicity to nearly nil, even if the NP was doped with Fe or Mn. Apparently, the coating effectively blocks any leaching out in the case of Fe-doped Si NP and/or removes any toxicity of the remaining amine-groups or surfaced Fe ions 'hidden' under the polymeric coating. The EC50 values of all the NP measured by the MTT assay are given in Table 2 for comparison.

Table 1: *Data on different Si NP and Ge NP used in this study.*

NP	Surface Functionalization	Dopant	Size (nm)	Abbreviations used	Graphical presentation
Si NP	Si-C$_3$-NH$_2$		1.6 ± 0.2	Si(1.6) NP-NH$_2$[9]	
	Si-C$_{11}$-N$_3$	No		Si(1.6) NP-N$_3$	
	Si-C$_4$-COOH			Si(1.6) NP-COOH[21]	
Si NP	Si-C$_3$-NH$_2$	No	3.9 ± 1.3	Si(3.9) NP-NH$_2$[37]	
		Mn (1 %)		Si/Mn(3.9) NP-NH$_2$[36]	
		Fe (1 %)		Si/Fe(3.9) NP-NH$_2$	
Si NP	Si-C$_3$-NH$_2$-Dex	No dopant	3.9 ± 1.3	Si(3.9) NP-NH$_2$-Dex	
		Mn (1 %)		Si/Mn(3.9) NP-NH$_2$-Dex	
		Fe (1 %)		Si/Fe(3.9) NP-NH$_2$-Dex	

Cytotoxicity of surface functionalized Si NP and Ge NP
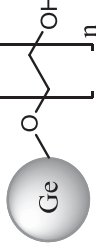
|					Structure
Ge NP	*Ge-PEG*		*Ge NP-PEG*		
	Ge-TMPA	*No*	*Ge NP-TMPA*	7.5 ± 2.5	
Si NP	*Si-PEG*		*Si NP-PEG*		
	Si-undecenylic acid		*Si NP-UDA*	2.1 ± 0.6 *(core)*	
Si NP	*Si-C$_{12}$-Pol*		*Si NP-Pol*[38]	17.8 ± 0.4 *(hydro-dynamic)*	
	Si-C$_{12}$-Sil		*Si NP-Sil*	35 ± 5	
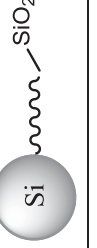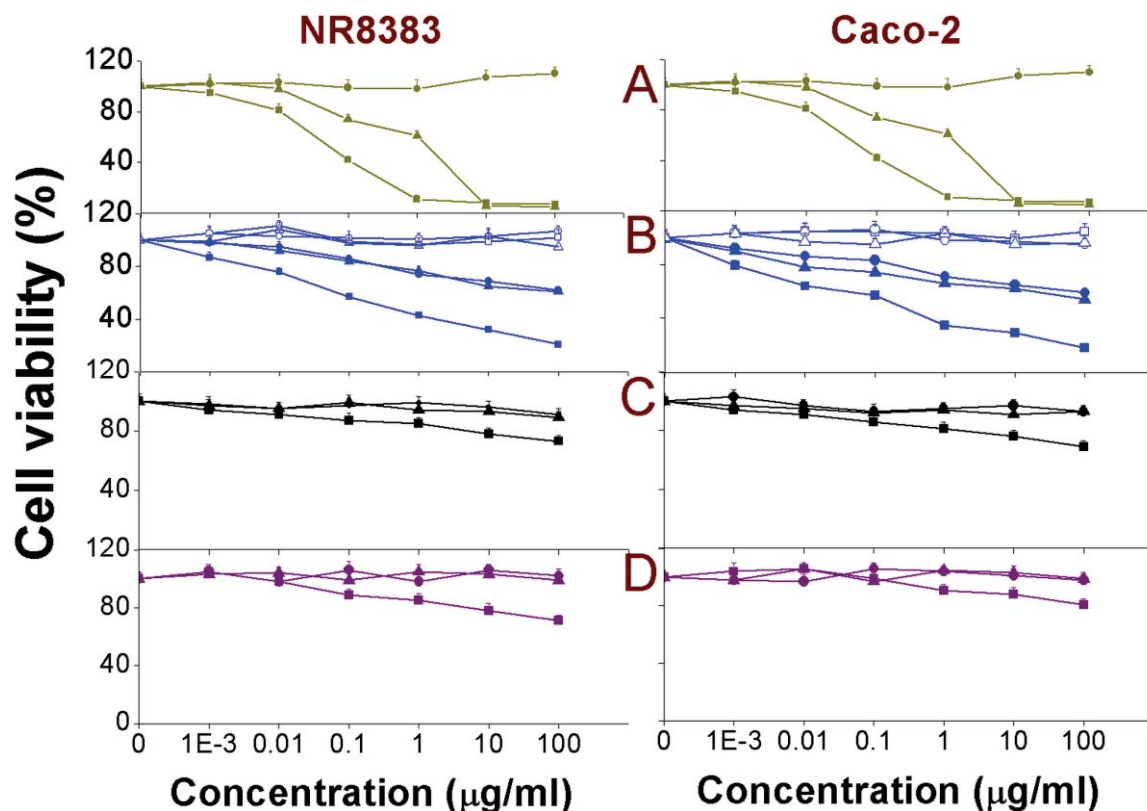
Figure 1: *MTT assay on NR8383 and Caco-2 cells after 24 h exposure to: (A) Si(1.6) NP-NH₂ (■),*
Si(1.6) NP-N₃ (▲) and Si(1.6) NP-COOH (●); (B) Si/Fe(3.9) NP-NH₂ (■), Si(3.9) NP-NH₂ (▲),
Si/Mn(3.9) NP-NH₂ (●), Si/Fe(3.9) NP-NH₂-Dex (□), Si(3.9) NP-NH₂-Dex (Δ) and Si/Mn(3.9) NP-
NH₂-Dex (○); (C) Ge NP-TMPA (■), Ge NP-PEG (▲) and Si NP-PEG (●); (D) Si NP-Sil (■), Si NP-UDA
(▲) and Si NP-Pol (●). Results are shown as mean ± SEM (n = 3).

BrdU assay

5-Bromo-2-deoxyuridine (BrdU) is a structural analogue of the thymidine base of DNA and gets incorporated within the strands of the DNA of proliferating cells and the amount of incorporated BrdU can then be measured spectrophotometrically.[44] As an adjunct to the MTT assay, which gives an idea on the effect on mitochondrial metabolic activity, the BrdU assay displays a DNA-based degree of continuing cell divisions, with the results presented as % of the negative control. The results obtained after 24 h exposure of NR8383 and Caco-2 cells towards different Si NP and Ge NP are shown in Figure 2 and the EC50 values are given in Table 2. From Figure 2, it can be seen that apart from the amine-terminated Si(3.9) NP-NH₂, Si/Mn(3.9) NP-NH₂, Si/Fe(3.9) NP-NH₂ and Ge NP-TMPA, only Si NP-Sil were slightly cytotoxic, which matched well with the MTT assay data. The Si/Mn(3.9) NP-NH₂ did not show any added toxicity over Si(3.9) NP-NH₂, which encourages their further development as imaging agents. The Si/Fe(3.9) NP-NH₂ again showed enhanced toxicity compared to the Si(3.9) NP-NH₂, which – as discussed with the MTT assay – can be an effect of the leaching Fe^{3+} ions from the core to the cellular environment or NP surfaces. In line with what was observed in the MTT assay, the dextran coating curbed the toxicity of not only Si/Fe(3.9) NP-NH₂, but also of the Si(3.9) NP-NH₂ and

Si/Mn(3.9) NP-NH$_2$. The slight toxicity of Si NP-Sil can be attributed to the silica shell of these NP. All the other Si NP/Ge NP were found to be non-toxic. In contrast to the positively charged NP, the -OH or -COOH terminated Si NP/ Ge NP did not show any effect on cell proliferation.[45] A possible reason behind lesser cytotoxicity is the comparatively reduced cellular uptake of anionic NP compared to the cationic NP. Various groups have observed such surface charge-dependent cellular uptake[11, 46, 47] and this phenomenon could also affect the toxicity of NP and the role of surface properties in it.
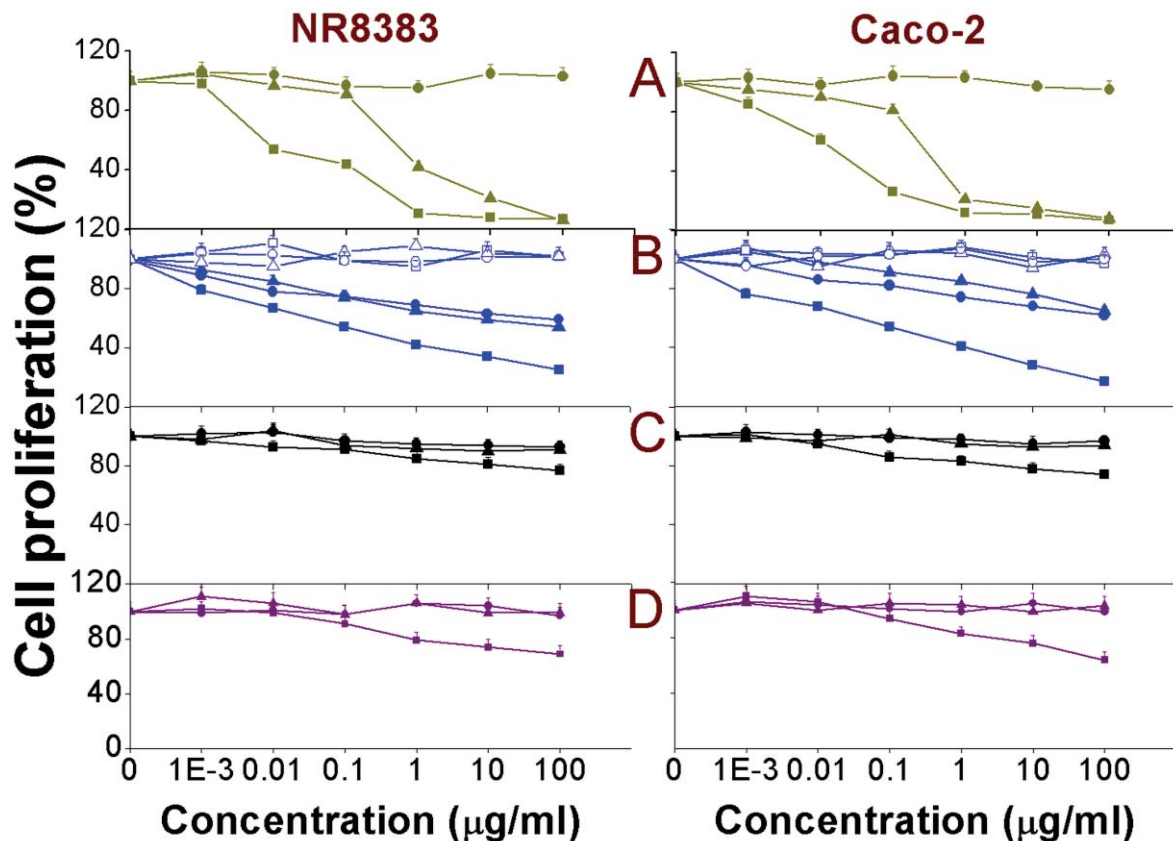

Figure 2: BrdU assay on NR8383 and Caco-2 cells after 24 h exposure to: (A) Si(1.6) NP-NH$_2$ (■), Si(1.6) NP-N$_3$ (▲) and Si(1.6) NP-COOH (●); (B) Si/Fe(3.9) NP-NH$_2$ (■), Si(3.9) NP-NH$_2$ (▲), Si/Mn(3.9) NP-NH$_2$ (●), Si/Fe(3.9) NP-NH$_2$-Dex (□), Si(3.9) NP-NH$_2$-Dex (Δ), and Si/Mn(3.9) NP-NH$_2$-Dex (○); (C) Ge NP-TMPA (■), Ge NP-PEG (▲) and Si NP-PEG (●); (D) Si NP-Sil (■), Si NP-UDA (▲) and Si NP-Pol (●). Results are shown as mean ± SEM (n = 3).

Induction of Reactive Oxygen Species (ROS) from isolated rat liver mitochondrial fraction by DCFH-DA assay

The mitochondrial fraction of liver tissue from a Wistar rat was prepared as reported before[20] and these isolated mitochondria were incubated with serial dilutions of Si NP and Ge NP. DCFH-DA was used for the detection of reactive oxygen species (ROS). DCFH-DA is cleaved by nonspecific intramitochondrial esterases[48] to form DCFH. DCFH is further oxidized by ROS to form the fluorescent compound DCF (2',7'-dichlorofluorescein), which was then measured (λ_{ex} =

485 nm; λ_{em} =538 nm); the results are shown in Figure 3 and the EC50 values are given in Table 2.
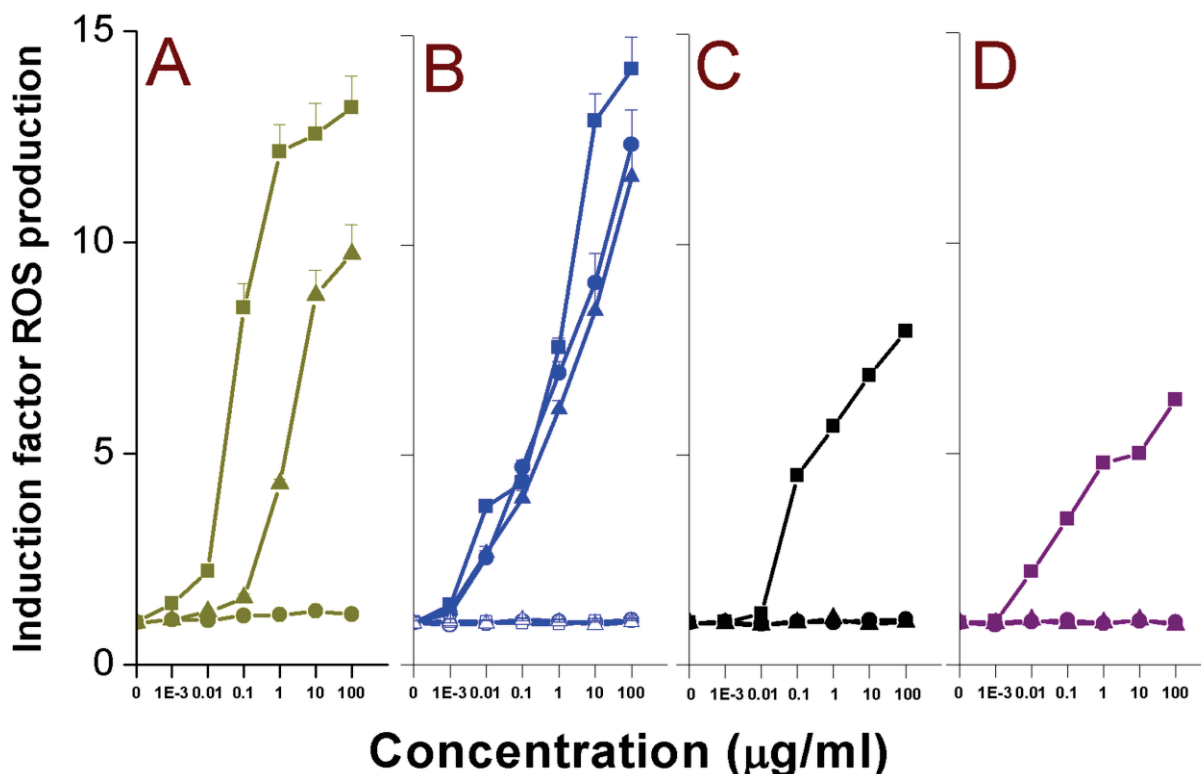

Figure 3: *DCFH-DA assay on isolated rat liver mitochondrial fraction after 1.5 h exposure to: (A) Si(1.6) NP-NH₂ (■), Si(1.6) NP-N₃ (▲) and Si(1.6) NP-COOH (●); (B) Si/Fe(3.9) NP-NH₂ (■), Si(3.9) NP-NH₂ (▲), Si/Mn(3.9) NP-NH₂ (●), Si/Fe(3.9) NP-NH₂-Dex (□), Si(3.9) NP-NH₂-Dex (Δ) and Si/Mn(3.9) NP-NH₂-Dex (○); (C) Ge NP-TMPA (■), Ge NP-PEG (▲) and Si NP-PEG (●); (D) Si NP-Sil (■), Si NP-UDA (▲) and Si NP-Pol (●). Results are shown as mean ± SEM (n = 3).*

From our data, it is clear that only the cationic Si(3.9) NP-NH₂, Si/Mn(3.9) NP-NH₂, Si/Fe(3.9) NP-NH₂, Ge NP-TMPA and the hydroxyl-capped Si NP-Sil induced ROS production upon incubation with the isolated mitochondrial fraction. PEG-terminated Ge and Si NP displayed no discernible ROS production. The ROS production induced by all the Si(3.9) NP-NH₂, Si/Mn(3.9) NP-NH₂ and Si/Fe(3.9) NP-NH₂ were decreased to almost none by the covalently bound dextran coating. How cationic NP show enhanced ROS production when incubated with isolated mitochondria is not fully understood, although as hypothesized for the outer cell membrane, electrostatic interaction between the negative lipid bilayer membranes and positive NP may be a cause. Such interaction between mitochondria and especially cationic polystyrene NP has been noted before,[31] although to the best of our knowledge, this is one of the first cases where such an interaction between intracellular mitochondria and semiconductor quantum dots were shown.

Measurement of mitochondrial membrane potential ($\Delta\Psi_m$)

The change of the mitochondrial membrane potential ($\Delta\Psi_m$) can be an important parameter in understanding the mechanism of toxicity of NP. A change in $\Delta\Psi_m$ indirectly showed the alteration in the mitochondrial membrane permeability and might caused disruption of the electron transport chain (ETC). This may subsequently yield a decrease in ATP production and induction of ROS production. The $\Delta\Psi_m$ in both the NR8383 and Caco-2 cell lines was measured after 24 h exposure to different Si NP and Ge NP, and the results along with the corresponding EC50 values are shown in Figure 4 and Table 2, respectively. Only exposure of the cells to the cationic amine-terminated NP as well as to the Si NP-Sil resulted in a decrease in the $\Delta\Psi_m$ in contrast to exposure of the cells to anionic or PEG-terminated Si NP and Ge NP. Interestingly, a dextran coating over the Si(3.9) NP-NH$_2$, Si/Mn(3.9) NP-NH$_2$ and Si/Fe(3.9) NP-NH$_2$ minimized also the effects on $\Delta\Psi_m$.
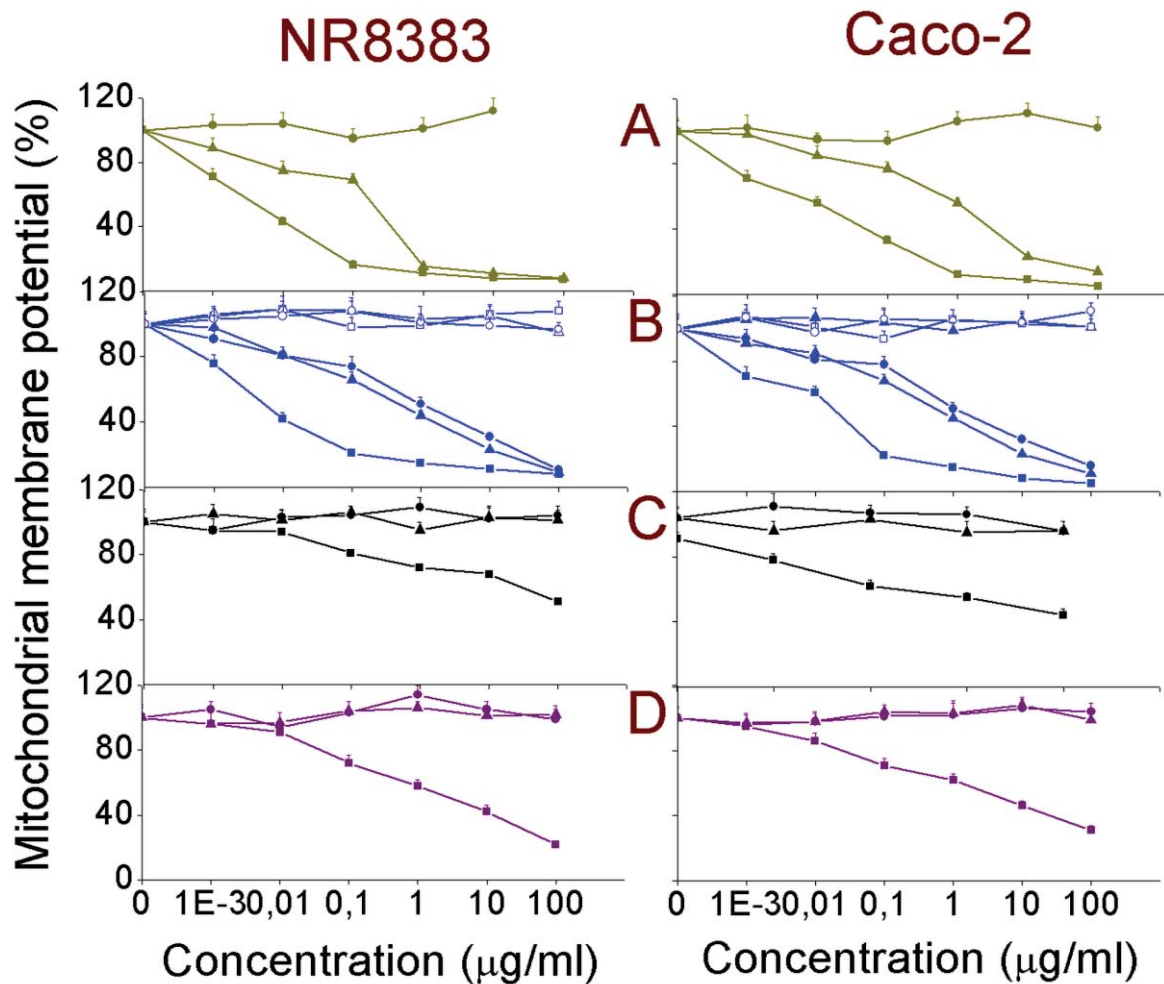

Figure 4: *Mitochondrial membrane potential ($\Delta\Psi_m$) in NR8383 and Caco-2 cells after 24 h exposure to : (A) Si(1.6) NP-NH$_2$ (■), Si(1.6) NP-N$_3$ (▲) and Si(1.6) NP-COOH (●); (B) Si/Fe(3.9) NP-NH$_2$ (■), Si(3.9) NP-NH$_2$ (▲), Si/Mn(3.9) NP-NH$_2$ (●),Si/Fe(3.9) NP-NH$_2$-Dex (□), Si(3.9) NP-NH$_2$-Dex (Δ) and Si/Mn(3.9) NP-NH$_2$-Dex (○); (C) Ge NP-TMPA (■), Ge NP-PEG (▲) and Si NP-PEG (●); (D) Si NP-Sil (■), Si NP-UDA (▲) and Si NP-Pol (●). Results are shown as mean ± SEM (n = 3).*

Measurement of intracellular ATP production

To investigate more deeply the effects of the interaction of the different Si NP and Ge NP with mitochondrial membranes and the probable disruption of the ETC, the intracellular ATP content was measured. The results are shown in Figure 5 and the EC50 values are given in Table 2. In line with the observations made before, only exposure to the cationic Si(1.6) NP-NH_2, Si(3.9) NP-NH_2, Si/Mn(3.9) NP-NH_2, Si/Fe(3.9) NP-NH_2, Ge NP-TMPA, apart from the Si(1.6) NP-N_3 and Si NP-Sil, resulted in a decrease in intracellular ATP production.
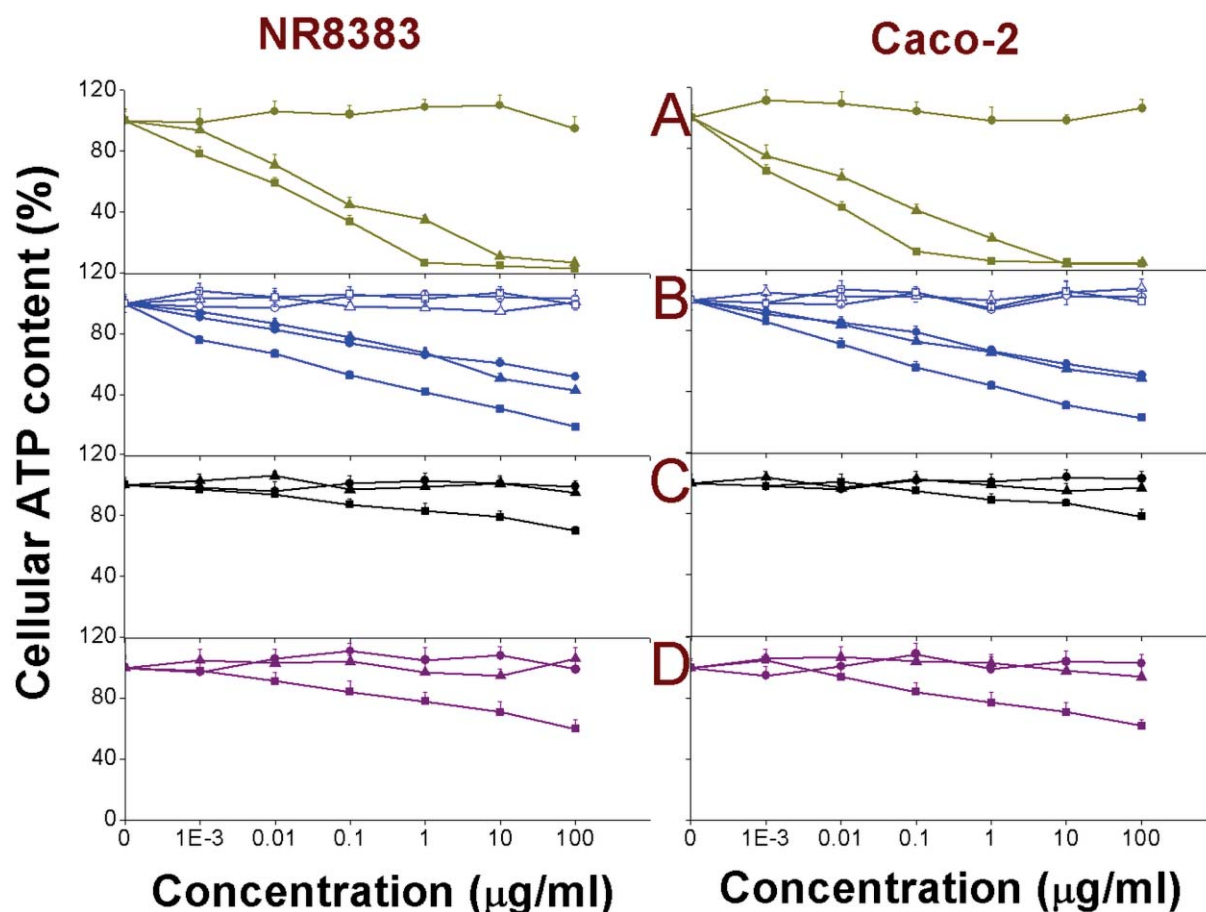

Figure 5: *Cellular ATP content in NR8383 and Caco-2 cells after 24 h exposure to: (A) Si(1.6) NP-NH_2 (■), Si(1.6) NP-N_3 (▲) and Si(1.6) NP-COOH (●); (B) Si/Fe(3.9) NP-NH_2 (■), Si(3.9) NP-NH_2 (▲), Si/Mn(3.9) NP-NH_2 (●), Si/Fe(3.9) NP-NH_2-Dex (□), Si(3.9) NP-NH_2-Dex (Δ) and Si/Mn(3.9) NP-NH_2-Dex (○); (C) Ge NP-TMPA (■), Ge NP-PEG (▲) and Si NP-PEG (●); (D) Si NP-Sil (■), Si NP-UDA (▲) and Si NP-Pol (●). Results are shown as mean ± SEM (n = 3).*

This further strengthened our hypothesis that the interaction of cationic NP with the outer layer of mitochondrial membranes disrupts the ETC, which then results in a decreased ATP production. Interestingly, depletion of ATP can be a contributing factor to the toxicity of the Si NP or Ge NP. In line with the MTT and the BrdU assay data, the dextran coating basically removed the toxicity of Si(3.9) NP-NH_2, Si/Mn(3.9) NP-NH_2 and Si/Fe(3.9) NP-NH_2. While similar

findings have been reported for 60 – 300 nm polystyrene NP[31] and polydisperse (6 – 20 nm) starch-coated Ag NP,[49] this is the first report of the effect of NP with different surface charges on the cellular ATP production for NP that are smaller than the critical diameter of 5.5 nm, which is required for efficient renal clearance.[18]

Measurement of cytoplasmic free Ca²⁺

The cytoplasmic free calcium concentration is important in many aspects regarding the physiology of the cells. An increased free calcium content can not only disturb the ionic contents (K^+, Na^+, etc.) of the cellular cytoplasm, but can also trigger the apoptotic cascade that leads to programmed cell death. Here, the NR8383 and Caco-2 cells were exposed for 24 h to different test concentrations (0 - 100 µg/ml) of Si NP and Ge NP and cytoplasmic free Ca^{2+} levels were quantified. The results are shown in Figure 6. The corresponding EC50 values are given in Table 2. The cationic NP and Si NP-Sil showed mild to moderate increase in cytoplasmic free calcium (order: Si/Fe(3.9) NP-NH₂ > Si(1.6) NP-NH₂ = Si/Mn(3.9) NP-NH₂ > Si(1.6) NP-N₃ > Ge NP-TMPA > Si NP-Sil) whereas no such increase could be seen for the anionic NP or PEG-terminated and dextran-coated NP.
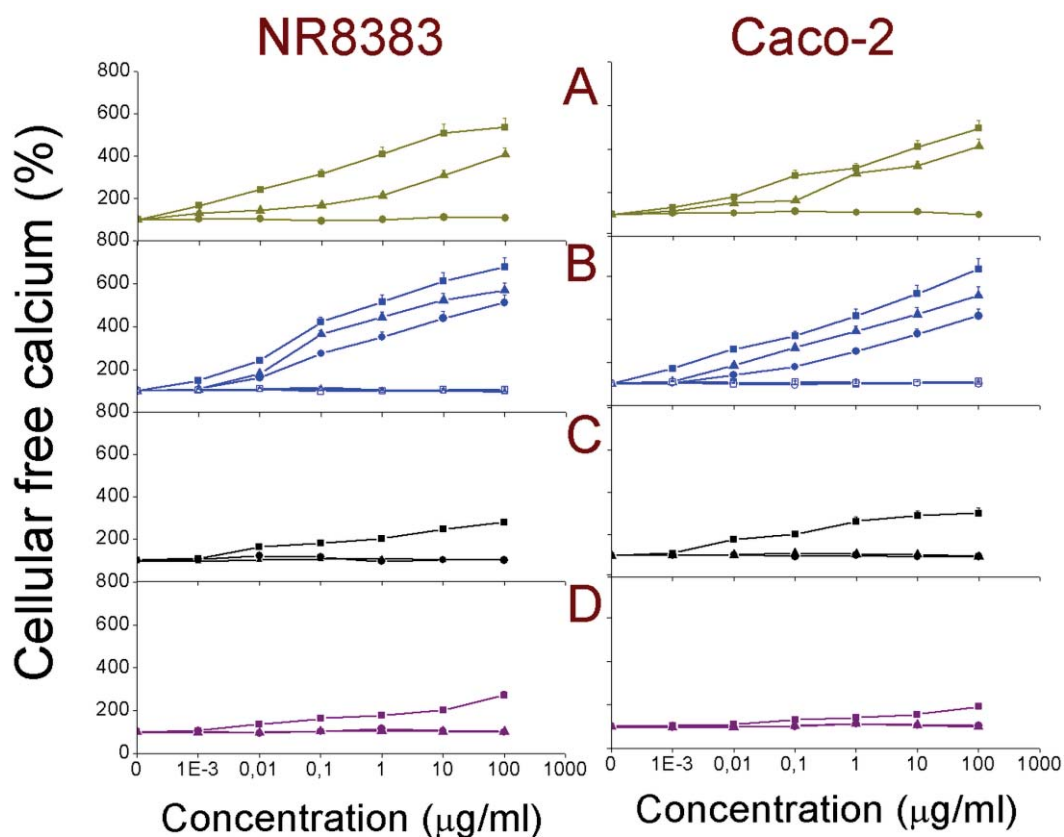
Figure 6: *Cellular free calcium in NR8383 and Caco-2 cells after 24 h exposure to: (A) Si(1.6) NP-NH₂ (■), Si(1.6) NP-N₃ (▲) and Si(1.6) NP-COOH (●); (B) Si/Fe(3.9) NP-NH₂ (■), Si(3.9) NP-NH₂ (▲), Si/Mn(3.9) NP-NH₂ (●), Si/Fe(3.9) NP-NH₂-Dex (□), Si(3.9) NP-NH₂-Dex (Δ) and Si/Mn(3.9) NP-NH₂-Dex (○); (C) Ge NP-TMPA (■), Ge NP-PEG (▲) and Si NP-PEG (●); (D) Si NP-Sil (■), Si NP-UDA (▲) and Si NP-Pol (●). Results are shown as mean ± SEM (n = 3).*

Measurement of intracellular ROS production

In order to better understand our findings of especially cationic NP causing induction of ROS production in mitochondria along with causing a reduction in the cellular ATP concentration, the intracellular ROS concentration was measured. With data pointing towards possible damage caused by cationic Si NP and Ge NP on the mitochondrial membrane and decoupling of the ETC, it is possible that the exaggerated production of ROS may cause oxidative stress. Several groups have hypothesized oxidative stress as the mechanism of NP cytotoxicity,[50-52] although the source of ROS is still not clear. It is possible that damaged mitochondria with compromised outer membrane integrity can be a source for the production of intracellular ROS. This would also suggest that intracellular oxidative stress is rather a secondary mechanism, which appears as a follow-up event to that of the mitochondrial interaction with cationic Si NP or Ge NP. The results of the DCFH-DA assay performed to measure the intracellular ROS production are shown in Figure 7, with the EC50 values given in Table 2. In line with previous results, exposure of the cells to Si NP-Sil and the cationic Si(3.9) NP-NH$_2$, Si/Mn(3.9) NP-NH$_2$, Si/Fe(3.9) NP-NH$_2$ and Ge NP-TMPA resulted in an increase in intracellular ROS production. The negatively charged Si (1.6) NP-COOH, Si NP-UDA, and the dextran- or PEG-coated Si or Ge NP did not induced ROS production.
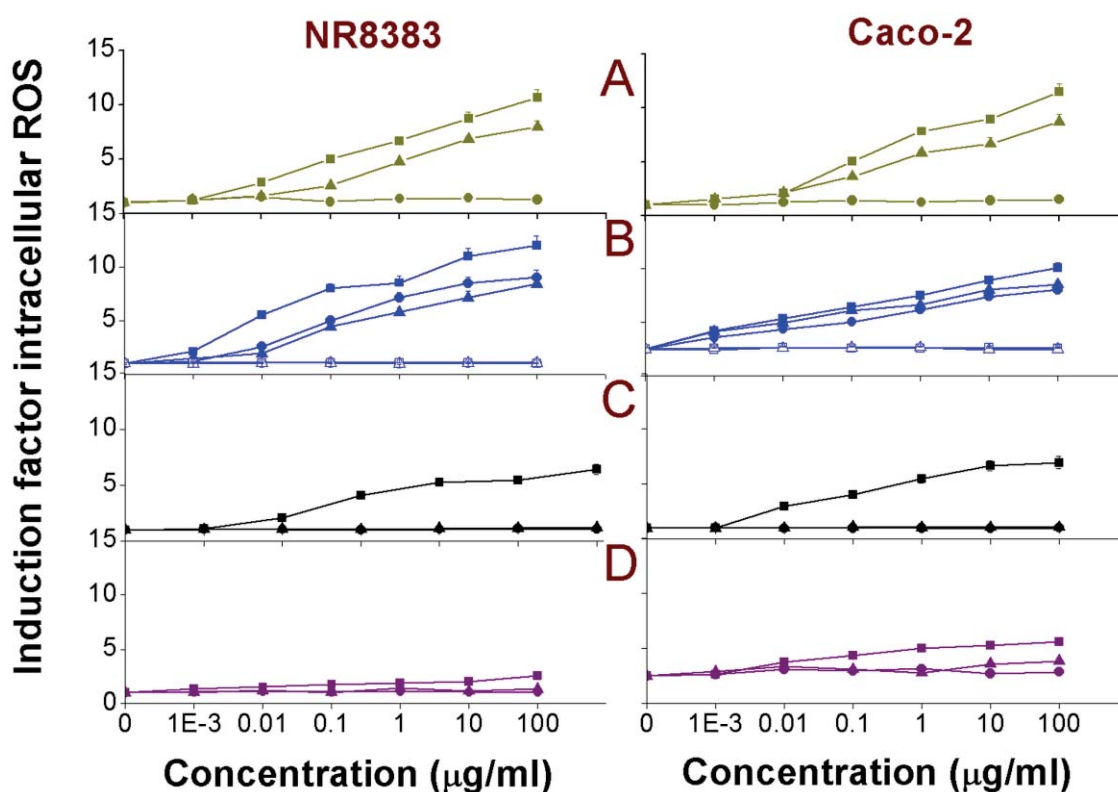
Figure 7: *DCFH-DA assay on NR8383 and Caco-2 cells after 24 h exposure to: (A) Si(1.6) NP-NH$_2$ (■), Si(1.6) NP-N$_3$ (▲) and Si(1.6) NP-COOH (●); (B) Si/Fe(3.9) NP-NH$_2$ (■), Si(3.9) NP-NH$_2$ (▲), Si/Mn(3.9) NP-NH$_2$ (●), Si/Fe(3.9) NP-NH$_2$-Dex (□), Si(3.9) NP-NH$_2$-Dex (Δ) and Si/Mn(3.9) NP-NH$_2$-Dex (○); (C) Ge NP-TMPA (■), Ge NP-PEG (▲) and Si NP-PEG (●); (D) Si NP-Sil (■), Si NP-UDA (▲) and Si NP-Pol (●). Results are shown as mean ± SEM (n = 3).*

Cytotoxicity of surface functionalized Si NP and Ge NP

Table 2: *The EC50 values (μg/ml) for different Si NP/ Ge NP obtained for the various endpoints reported in this article.*

Experiment	Figure	Si(1.6) NP-NH₂		Si(1.6) NP-N₃		Si(3.9) NP-NH₂		Si/Mn(3.9) NP-NH₂		Si/Fe(3.9) NP-NH₂		Ge NP-TMPA		Si NP-Sil	
		NR8383	Caco-2	NR8383	Caco-2	NR8383	Caco-2	NR8383	Caco-2	NR8383	Caco-2	NR8383	Caco-2	NR8383	Caco-2
MTT	1	0.012[20]	0.014[21]	0.27[20]	0.31[21]	0.38	0.16	0.4	0.17	0.07	0.03	0.17	0.16	0.12	0.58
BrdU	2	0.02	0.011[21]	0.26	0.28[21]	0.15	0.12	0.16	0.14	0.08	0.05	0.22	0.21	0.18	0.37
Ψ_m	4	0.02	0.017	0.18	0.31	0.19	0.21	0.18	0.22	0.09	0.08	0.17	0.22	0.23	0.41
ATP	5	0.01	0.02	0.11	0.14	0.16	0.15	0.17	0.16	0.04	0.06	0.19	0.2	0.33	0.45
Cytoplasmic free Ca²⁺	6	0.05	0.04	0.19	0.17	0.18	0.21	0.13	0.18	0.08	0.07	0.15	0.27	0.28	0.39
ROS (DCFH-DA)	7	0.022[20]	0.018[20]	0.17[20]	0.31[20]	0.21	0.22	0.2	0.23	0.09	0.08	0.18	0.19	0.29	0.34
TNF-α	8	0.1	0.2	0.18	0.28	0.18	0.19	0.22	0.21	0.08	0.11	0.19	0.21	0.33	0.39
Caspase-3	9	0.11	0.24	0.21	0.26	0.16	0.24	0.18	0.23	0.09	0.15	0.22	0.18	0.27	0.48

Experiment	Figure	Si(1.6) NP-NH₂	Si(1.6) NP-N₃	Si(3.9) NP-NH₂	Si/Mn(3.9) NP-NH₂	Si/Fe(3.9) NP-NH₂	Ge NP-TMPA	Si NP-Sil
DCFH-DA (isolated mitochondria fraction)	3	0.08[20]	1.05[20]	0.28	0.29	0.12	0.11	0.34

Measurement of TNF-α

As a result of the oxidative stress and the injury inflicted by the different ROS radicals, an inflammatory response can be anticipated. The cytokine TNF-α (tumor necrosis factor-alpha or cachectin) is a pro-inflammatory biomarker that can be measured to identify an inflammatory response (see Figure 8). Only the amine-terminated NP (Si(1.6) NP-NH$_2$, Si(3.9) NP-NH$_2$, Si/Mn(3.9) NP-NH$_2$, Si/Fe(3.9) NP-NH$_2$, Ge NP-TMPA) and Si NP-Sil caused an induction in the TNF-α production. The corresponding EC50 values are given in Table 2.
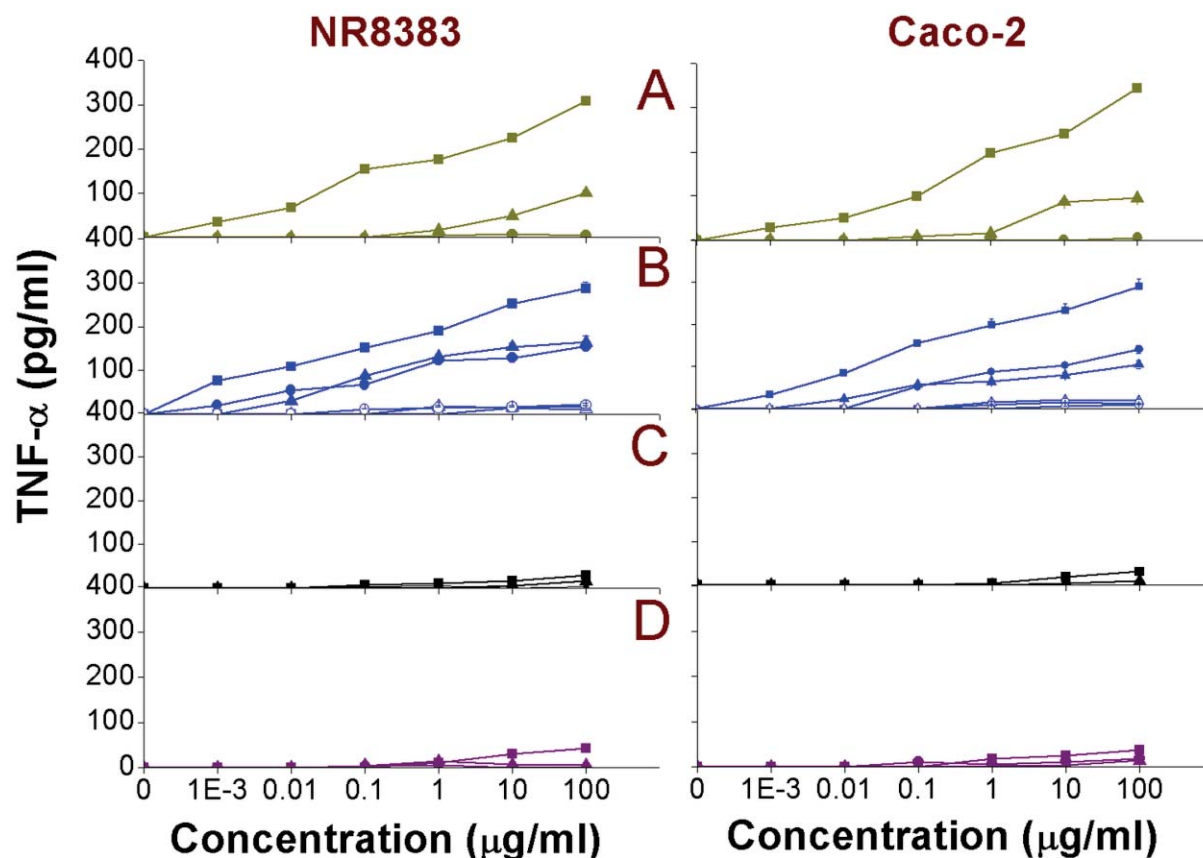

Figure 8: Cellular TNF-α in NR8383 and Caco-2 cells after 24 h exposure to: (A) Si(1.6) NP-NH$_2$ (■), Si(1.6) NP-N$_3$ (▲) and Si(1.6) NP-COOH (●); (B) Si/Fe(3.9) NP-NH$_2$ (■), Si(3.9) NP-NH$_2$ (▲), Si/Mn(3.9) NP-NH$_2$ (●), Si/Fe(3.9) NP-NH$_2$-Dex (□), Si(3.9) NP-NH$_2$-Dex (Δ) and Si/Mn(3.9) NP-NH$_2$-Dex (○); (C) Ge NP-TMPA (■), Ge NP-PEG (▲) and Si NP-PEG (●); (D) Si NP-Sil (■), Si NP-UDA (▲) and Si NP-Pol (●). Results are shown as mean ± SEM (n=3).

Measurement of caspase-3 enzyme

The caspase-3 enzyme is an important biomarker for the apoptotic (self-programmed cell death) cascade. The caspase-3 activity was measured in NR8383 and Caco-2 cells after 24 h exposure to the different Si NP and Ge NP and the results are shown in Figure 9 with the EC50 values enlisted in Table 2. In line with the data obtained from the previously mentioned results in this paper, apart from the Si NP-Sil, only exposure to the cationic Si NP/Ge NP resulted in an

increase of the caspase-3 activity. The observed order was Si/Fe(3.9) NP-NH$_2$ > Si(1.6) NP-NH$_2$ = Si/Mn(3.9) NP-NH$_2$ > Si(1.6) NP-N$_3$ > Si(3.9) NP-NH$_2$ > Ge NP-TMPA > Si NP-Sil, but the differences between these NP were all relatively small. Characteristically, the Fe-containing NP yielded the highest caspase-3 induction. On the other hand, none of the anionic NP, dextran-coated or PEGylated NP showed any increase of the caspase-3 activity.
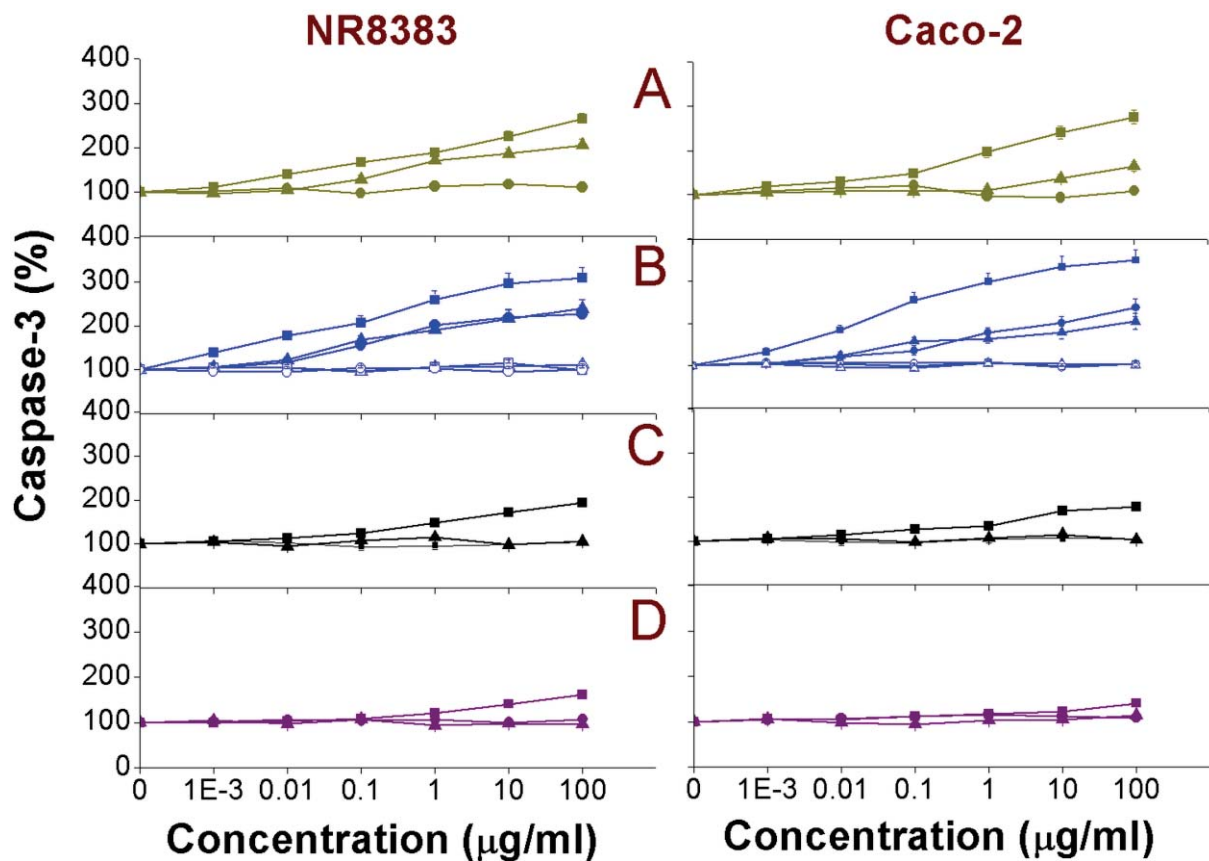

Figure 9: *Cellular caspase-3 activity in NR8383 and Caco-2 cells after 24 h exposure to: (A) Si(1.6) NP-NH$_2$ (■), Si(1.6) NP-N$_3$ (▲) and Si(1.6) NP-COOH (●); (B) Si/Fe(3.9) NP-NH$_2$ (■), Si(3.9) NP-NH$_2$ (▲), Si/Mn(3.9) NP-NH$_2$ (●), Si/Fe(3.9) NP-NH$_2$-Dex (□), Si(3.9) NP-NH$_2$-Dex (Δ) and Si/Mn(3.9) NP-NH$_2$-Dex (○); (C) Ge NP-TMPA (■), Ge NP-PEG (▲) and Si NP-PEG (●); (D) Si NP-Sil (■), Si NP-UDA (▲) and Si NP-Pol (●). Results are shown as mean ± SEM (n=3).*

Analysis of toxicity tests

Upon comparison, it can be seen that, apart from Si NP-Sil, only cationic Si NP/Ge NP induced signs of cytotoxicity and effects on the nine endpoints evaluated in this study. The surface charge of NP has been hypothesized to be an important factor in cytotoxicity of NP.[25, 53-55] Typically, positive NP were found to be toxic whereas the anionic ones were not, which is in agreement with the current data. A detailed discussion on why positive surface charge-containing NP are toxic in contrast with the negative NP is beyond the scope of this chapter. However, it can be stated that positive NP get electrostatically attracted towards the negative cell membrane,[56] thereby initiating cell membrane-bound receptor-mediated interactions and

possibly also cell signaling cascades.[31] Within the group of amine-terminated Si NP, the smaller Si(1.6) NP-NH$_2$, in line with previously reported relationships between the size and toxicity of NP,[57-60] were found to be more toxic than the bigger Si(3.9) NP-NH$_2$. One possible explanation for this size-dependence of toxicity of NP is that smaller NP can have better access to different parts of the cells. Additionally, smaller NP have more reactive surface area.[61]

It was interesting to find that Mn-doped Si/Mn(3.9) NP-NH$_2$ did not show a higher cytotoxicity than either of the Si(3.9) NP-NH$_2$. This result is exciting in view of the potential of Mn-doped Si NP for bimodal bioimaging.[36] However, the Fe-doped Si/Fe(3.9) NP-NH$_2$ did show a higher cytotoxicity than Si(3.9) NP-NH$_2$. It was already reported that Fe has a tendency to leach out from the core of NP as ions and cause toxicity.[62] The toxicity caused by the Fe^{3+} ions can be due to first their reduction to Fe^{2+} (by acidic lysosomes) and then reacting with mitochondrial and nuclear hydrogen peroxide to produce ROS via Fenton reaction.[63, 64] Remarkably, the toxicity could be diminished significantly when the Si/Fe(3.9) NP-NH$_2$ was coated by a covalently linked dextran coating. The dextran coating also abolished the toxicity of the other two toxic Si NP: Si(3.9) NP-NH$_2$ and Si/Mn(3.9) NP-NH$_2$. This showed that a surface coating with a biocompatible material, like dextran, can strongly reduce the overall toxicity and perhaps even turn the NP (nearly) non-toxic. The Si NP-Sil showed signs of toxicity although the toxicity was comparatively much lower. It has been reported that silica NP are toxic,[42, 43, 65] and this can also be linked to the toxicity of Si NP-Sil. It was highly relevant to note that the carboxylic acid-terminated and hydroxyl-terminated Si NP-PEG, Ge NP-PEG, Si NP-UDA and Si NP-Pol did not show any toxicity within the tested concentration range. It has been reported that negative Si NP were much less toxic compared to the positive ones.[20-22] This may be due to the fact that negative NP get repelled by the negatively charged cell membranes, which hinders their cellular interactions. It has also been observed that the positive and negative NP followed different endocytic uptake patterns in cells via activation of distinct groups of cell membrane receptors.[45, 60, 66, 67] Interestingly, the interactions between lipid bilayer membranes and cationic NP are of the same nature as the interactions between mitochondria and charge-bearing NP. It is reported that cationic NP caused an imbalance of the normal electrochemical gradient (80 - 130 mV)[68] across the outer mitochondrial membrane[69] and thus yielded an ionic imbalance and increased permeability. This can cause decoupling of ETC and cause an increase of intracellular ROS as well as a depletion of intracellular ATP production. Therefore we studied the effect of these NP on the mitochondrial membrane potential and on the intracellular ATP production.

A silica coating on an intrinsically less or non-toxic Si-core would be of both chemical and toxicological interest investigating the effect of surface coating on toxicity of NP as silica NP have been reported to be toxic.[70] For such hybrid SiO$_2$/Si NP, the presence of an organic coating is relevant, as this allows tuning of the hydrophilicity/hydrophobicity of the surfaces, which is reported to play an important role in the cellular interaction and uptake. Silica NP have been reported to cause induction of intracellular ROS,[71,72] increase in the cytosolic free calcium concentration[73] and increased damage to the intra-nuclear DNA.[74] It is reported that cationic NP (Si[21] and ZnO/CeO$_2$[34]) induced intracellular ROS production and this matched with the current data. However, how these ROS are formed is yet unclear. It is possible that with reactive nature, NP can react with a wide variety of biomolecules inducing production of oxygen and nitrogen radicals or that they are the result of uncoupling of oxidative phosphorylation as such. A mitochondrial involvement in such induction of ROS production seems to be a feasible explanation. It should also be mentioned here that the high induction of ROS production

following the exposure to the Si/Fe(3.9) NP-NH$_2$ may be due to the leaching of Fe^{3+} ions from the core to the NP surface or cellular environment. The results obtained from the TNF-α measurements pointed towards damage caused by the ROS and showed that the inflammatory behavior of the cells is a response to the toxic effects caused by the NP. It is documented in literature that especially cationic NP (of different compositions, like lipids[75] or gelatin[76]) can cause an induction of TNF-α. Our data on the currently studied inorganic NP are in line with the available literature.

Interestingly, an inverse relationship between the inflicted toxicity and size of the NP can also be observed here, as the induction of TNF-α was found to be larger for the smaller Si(1.6) NP-NH$_2$ compared to the bigger Si(3.9) NP-NH$_2$, which is in line with literature available for polystyrene[77] or metallic NP.[53] The induction of TNF-α by the cationic Si NP, found in the present study, also strengthened the idea that the inflammatory responses of the cells are caused by various radicals and ions. This can be pivotal in understanding the mechanism of cytotoxicity of different NP.

Compilation of the available data and strategy to design more biocompatible Si NP or Ge NP

An analysis of the reported data in this article can not only lead to a better understanding of the mode of action underlying the cytotoxicity of these NP, but may also help to develop smarter Si NP or Ge NP in future. In this article, we tried to show that the cell-NP interaction can be evaluated on the basis of their surface properties and hence it is of utmost importance that the surface chemistry of both the exposed cells and the NP are known in detail. It has been reported that NP interact preferentially with cell membrane-bound receptors.[11] In fact, by computational chemistry, the characteristics of these types of interactions between the cell membrane and NP have recently been probed.[78] Besides that, cationic surface charge has been recognized as an important factor in causing toxicity of NP. A surface charge-dependent cellular uptake pattern, with cationic NP showing higher cellular uptake compared to the anionic ones,[11] has also been observed. Interestingly, these two phenomena may be counteracting each other, as for targeted drug delivery it is important that the NP combine a high cellular uptake with minimal toxicity. Hence, the finding that cationic NP are usually more toxic can be a limiting factor for their possible applications in biological systems.

Recently, it was shown that an alleviation of the toxicity of cationic NP could be achieved by increasing the steric bulk around the positive charge of the NP.[11] In the current study, the positive charge on the Ge NP-TMPA was also sterically hindered and by simple comparison of EC50 values, it can be stated that in equivalent amounts, the toxicity of these Ge NP-TMPA was lesser than that of the other amine-terminated NP. Although this is just only the second example of such reduced toxicity, increasing the steric bulk around positive surface charges may thus be an interesting way of decreasing the toxicity of cationic NP. More research is surely desired here to further delineate this phenomenon.

It is also important to have an idea of the surface functionalization of the NP, as from our data it can be observed that a silica coating over a Si-core imparted toxic effects. Similarly, a coating with biocompatible dextran almost annulled the toxic effects of amine-terminated Si(3.9) NP-NH$_2$, Si/Mn(3.9) NP-NH$_2$ and Si/Fe(3.9) NP-NH$_2$. It is possible that the cells recognize

the dextran moieties on the NP surface and hence, the cell-NP interactions are immediately channeled in a different route, like activation of a different set of receptors. This is important to note, as it may provide some initial guidelines for functionalizing the surfaces of Si NP/Ge NP which are targeted for biological applications. A review of literature on the toxicity of the coating materials as well as some control experiments with only the coating material, can give initial predictions on the toxicity of NP coated with the respective material.

Taken together, an indication towards surface reactivity-oriented interactions between the NP and the cells can be obtained. It suggests to analyze the interactions between the cells and the NP on the basis of chemical interactions possible between them. It is reported in literature that different cell lines show dissimilar responses after being exposed to similar doses of the same NP for the same time points,[31] which can be due to the fact that diverse cell lines express different cell membrane-bound receptors in varying quantities.[52] The interaction of NP with cell membrane-bound receptors are quite specific and a variation in the amount of receptor protein expressed can also result in a variation of the exhibited toxicity. The battery of tests performed in the present study also enables us in getting a clearer picture of the mechanism of toxicity of NP.

A schematic diagram showing the proposed mechanism of cytotoxicity of cationic Si NP or Ge NP is given in Figure 10. It seems that the mitochondria play a pivotal role in the entire mechanistic cascade of toxicity, where especially the cationic NP, by creating damage to the normal physiology of the outer membrane of mitochondria, propel a series of events (like dissipation of ATP production, induction of ROS generation, cytoplasmic free calcium upload, oxidative stress, inflammatory response and finally triggering of apoptotic reactions) that ultimately sum up as the observed compromised viability of the cells.

In summary, in this article we have demonstrated by comparing the data obtained from a series of systematically varied Si NP and Ge NP that have been subjected to a systematic set of toxicological in vitro experiments, that the toxicity of Si NP and Ge NP is dominated by their surface chemistry. Whereas positively charged NP display some toxicity, carboxylic acid-coated, dextran-coated and PEG-coated Si and Ge NP display no toxicity in a rat lung and human colon cell lines. Such surface-functionalized Si NP or Ge NP are of interest because of their intrinsic fluorescence, modifiable surfaces, minimally toxic cores and tunable doping with MRI-active elements, such as Mn and Fe. Given the right coating, these are thus highly attractive materials for biological and medical applications. Of course, it is not only looks (outside), but also size that matters: only smaller NP (< 5.5 nm) are typically effectively cleared via the kidneys.[17] Therefore, further research into Si or Ge NP with a relatively small core, some bio-inert, neutral coating and possibly dopants for bimodal bioimaging seems highly attractive. In addition, if an effective renal clearance is undesired, Si NP and Ge NP do provide access to materials that combine a substantial larger size with minimal intrinsic toxicity. Finally, with this systematic set of toxicological investigations, a clearer idea on the mechanism of cytotoxicity could be achieved, which puts intracellular mitochondria as one of the important target organs for the toxicity of NP.
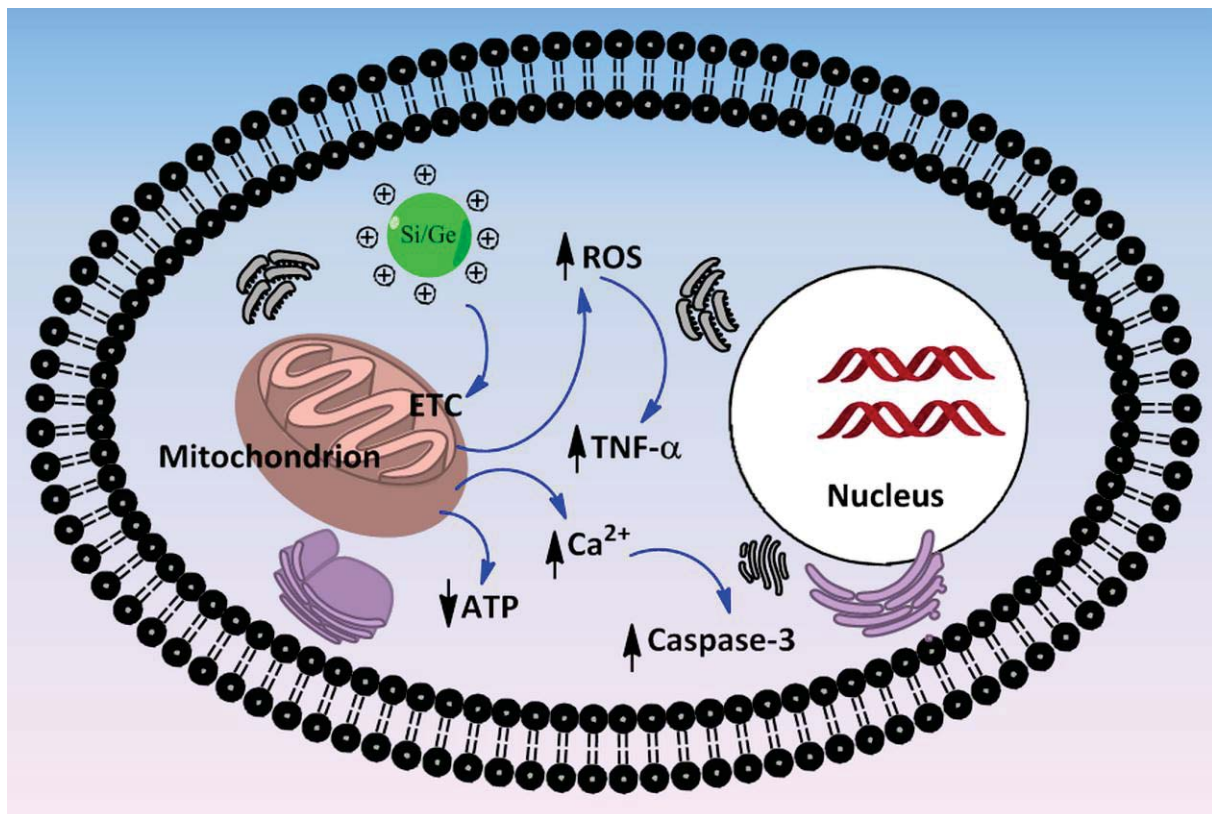
Figure 10: *Schematic diagram showing the proposed mechanism of cytotoxicity for cationic Si and Ge NP.*

References

1.   Luo XL, Morrin A, Killard AJ, Smyth MR; *Electroanalysis* 2006, 18 (4), 319-326.

2.   Lee JH, Huh YM, Jun Y, Seo J, Jang J, Song HT, et al.; *Nat. Med.* 2007, 13 (1), 95-99.

3.   Zhang L, Gu FX, Chan JM, Wang AZ, Langer RS, Farokhzad OC; *Clin. Pharmacol. Ther.* 2007, 83 (5), 761-769.

4.   Buzea C Pacheco I, Robbie K; *Biointerphases* 2007, 2 (4), MR17-MR71.

5.   Lanone S, Rogerieux F, Geys J, Dupont A, Maillot-Marechal E, Boczkowski J, et al.; *Part. Fibre Toxicol.* 2009, 6(14).

6.   Iga AM, Robertson JHP, Winslet MC, Seifalian AM; *J. Biomed. Biotechnol.* 2007.

7.   Xing Y Rao JH; *Cancer Biomark.* 2008, 4(6), 307-319.

8.   Abramowitz S; Quantum Dots: Their Use in Biomedical Research and Clinical Diagnostics. In Handbook of Biosensors and Biochips, John Wiley & Sons, Ltd: 2008.

9.   Rosso-Vasic M, Spruijt E, Popovic Z, Overgaag K, van Lagen B, Grandidier B, et al.; *J. Mater. Chem.* 2009, 19 (33), 5926-5933.

10.   Oku T, Nakayama T, Kuno M, Nozue Y, Wallenberg LR, Niihara K, et al.; *Mater. Sci. Eng. B* 2000, 74 (1–3), 242-247.

11.   Bhattacharjee S, Ershov D, Gucht Jvd, Alink GM, Rietjens IMCM, Zuilhof H, et al.; *Nanotoxicology* 2011, DOI:10.3109/17435390.2011.633714, 1-14.

12.   Chandra S, Das P, Bag S, Laha D, Pramanik P; *Nanoscale* 2011, 3.

13.   Kim D, Park S, Lee JH, Jeong YY, Jon S; *J. Am. Chem. Soc.* 2007, 129:7661-7665.

14.   Ballou B, Lagerholm BC, Ernst LA, Bruchez MP, Waggoner AS; *Bioconjugate Chem.* 2004, 15:79-86.

15.   Derfus AM, Chan WCW, Bhatia SN; *Nano Lett.* 2004, 4:11-18.

16.   Popplewell JF, King SJ, Day JP, Ackrill P, Fifield LK, Cresswell RG, et al.; *J. Inorg. Biochem.* 1998, 69:177-180.

17.   Choi HS, Liu W, Misra P, Tanaka E, Zimmer JP, Ipe BI, et al.; *Nat. Biotechnol.* 2007, 25:1165-1170.

18.   Rosso-Vasic M, Spruijt E, van Lagen B, De Cola L, Zuilhof H; *Small* 2008, 4:1835-1841.

19.   Warner JH, Hoshino A, Yamamoto K, Tilley RD; *Angew. Chem. Int. Edi.* 2005, 44:4550-4554.

20.   Bhattacharjee S, de Haan LHJ, Evers NM, Jiang X, Marcelis ATM, Zuilhof H, et al.; *Part. Fibre Toxicol.* 2010, 7(25).

21.   Ruizendaal L, Bhattacharjee S, Pournazari K, Rosso-Vasic M, de Haan LHJ, Alink GM, et al.; *Nanotoxicology* 2009, 3:339-347.

22.   Shiohara A, Hanada S, Prabakar S, Fujioka K, Lim TH, Yamamoto K, et al.; *J. Am. Chem. Soc.* 2009, 132:248-253.

23.   Asati A, Santra S, Kaittanis C, Perez JM; *ACS Nano* 2010, 4:5321-5331.

24.   Schaeublin NM, Braydich-Stolle LK, Schrand AM, Miller JM, Hutchison J, Schlager JJ, et al.; *Nanoscale* 2011, 3:410-420.

25.   El Badawy AM, Silva RG, Morris B, Scheckel KG, Suidan MT, Tolaymat TM; *Environ. Sci. Technol.* 2010, 45:283-287.

26.   Shirahata N; *Phys. Chem. Chem. Phys.* 2011, 13:7284-7294.

27.   Siekierzycka JR, Rosso-Vasic M, Zuilhof H, Brouwer AM; *J. Phys. Chem. C* 2011, 115:20888-20895.

28. Scherbart AM, Langer J, Bushmelev A, van Berlo D, Haberzettl P, van Schooten FJ, et al.; *Part. Fibre Toxicol.* 2011, 8(31).

29. Nel A, Xia T, Mädler L, Li N; *Science* 2006, 311:622-627.

30. Zhu X, Zhou J, Cai Z; *Mar. Pollut. Bull.* 2011, 63:334-338.

31. Xia T, Kovochich M, Liong M, Zink JI, Nel AE; *ACS Nano* 2007, 2:85-96.

32. Xia T, Kovochich M, Liong M, Mädler L, Gilbert B, Shi H, et al.; *ACS Nano* 2008, 2:2121-2134.

33. Uboldi C, Bonacchi D, Lorenzi G, Hermanns MI, Pohl C, Baldi G, et al.; *Part. Fibre Toxicol.* 2009, 6(18).

34. Simon M, Barberet P, Delville M-H, Moretto P, Seznec H; *Nanotoxicology* 2011, 5:125-139.

35. Xia T, Kovochich M, Brant J, Hotze M, Sempf J, Oberley T, et al.; *Nano Lett.* 2006, 6:1794-1807.

36. Zhang X, Brynda M, Britt RD, Carroll EC, Larsen DS, Louie AY, et al.; *J. Am. Chem. Soc.* 2007, 129:10668-10669.

37. Zhang XM, Neiner D, Wang SZ, Louie AY, Kauzlarich SM: Fabrication of Silicon-based Nanoparticles for Biological Imaging - art. no. 644804. *Colloidal Quantum Dots for Biomedical Applications II* 2007, 6448:44804-44804.

38. Hessel CM, Rasch MR, Hueso JL, Goodfellow BW, Akhavan VA, Puvanakrishnan P, et al.; *Small* 2010, 6:2026-2034.

39. Regli S, Kelly JA, Veinot JGC; *Mater. Res. Soc. Symp. Proc.* 2011, 1359:149-154.

40. Hoshino Y, Koide H, Furuya K, Haberaecker WW, Lee S-H, Kodama T, et al.; *Proc. Natl. Aca. Sci.* 2012, 109:33-38.

41. Rivera Gil P, Oberdörster G, Elder A, Puntes V, Parak WJ; *ACS Nano* 2010, 4:5527-5531.

42. Lin W, Huang Y-w, Zhou X-D, Ma Y; *Toxicol. Appl. Pharmacol.* 2006, 217:252-259.

43. Yu T, Malugin A, Ghandehari H; *ACS Nano* 2011, 5:5717-5728.

44. Prasad BR, Nikolskaya N, Connolly D, Smith TJ, Byrne SJ, Gerard VA, et al.; *J. Nanobiotechnol.* 2010, 8:7.

45. Nel AE, Madler L, Velegol D, Xia T, Hoek EMV, Somasundaran P, et al.; *Nat. Mater.* 2009, 8:543-557.

46. Yue Z-G, Wei W, Lv P-P, Yue H, Wang L-Y, Su Z-G, et al.; *Biomacromolecules* 2011, 12:2440-2446.

47. Arvizo RR, Miranda OR, Thompson MA, Pabelick CM, Bhattacharya R, Robertson JD, et al.; *Nano Lett.* 2010, 10:2543-2548.

48. Tazawa H, Fujita C, Machida K, Osada H, Ohta Y; *Arch. Biochem. Biophys.* 2009, 481:59-64.

49. AshaRani PV, Low Kah Mun G, Hande MP, Valiyaveettil S; *ACS Nano* 2008, 3:279-290.

50. Kim S, Choi JE, Choi J, Chung K-H, Park K, Yi J, Ryu D-Y; *Toxicol. In Vitro* 2009, 23:1076-1084.

51. Müller L, Riediker M, Wick P, Mohr M, Gehr P, Rothen-Rutishauser B; *J. R. Soc. Interface* 2010, 7:S27-S40.

52. Auffan M, Rose J, Wiesner MR, Bottero J-Y; *Environ. Pollut.* 2009, 157:1127-1133.

53. Schrand AM, Rahman MF, Hussain SM, Schlager JJ, Smith DA, Syed AF; *Wiley Interdiscip. Rev. Nanomed. Nanobiotechnol.* 2010, 2:544-568.

54.   Mura S, Hillaireau H, Nicolas J, Le Droumaguet B, Gueutin C, Zanna S, et al.; *Int. J. Nanomed.* 2011, 6:2591-2605.

55.   Bhattacharjee S, Ershov D, Islam MA, Kämpfer AM, Gucht Jvd, Alink GM, et al.; *Submitted* 2012.

56.   Verma A, Stellacci F; *Small* 2010, 6:12-21.

57.   Pan Y, Neuss S, Leifert A, Fischler M, Wen F, Simon U, et al.; *Small* 2007, 3:1941-1949.

58.   Prabhu BM, Ali SF, Murdock RC, Hussain SM, Srivatsan M; *Nanotoxicology* 2010, 4:150-160.

59.   Lin Y-S, Haynes CL; *J. Am. Chem. Soc.* 2010, 132:4834-4842.

60.   Bhattacharjee S, Ershov D, Fytianos K, Gucht Jvd, Alink GM, Rietjens IMCM, et al.; *Part. Fibre Toxicol.* 2012, 9(11).

61.   Auffan M, Rose J, Bottero J-Y, Lowry GV, Jolivet J-P, Wiesner MR; *Nat. Nanotechnol.* 2009, 4:634-641.

62.   Bouwmeester H, Poortman J, Peters RJ, Wijma E, Kramer E, Makama S, et al.; *ACS Nano* 2011, 5:4091-4103.

63.   Voinov MA, Pagán JOS, Morrison E, Smirnova TI, Smirnov AI; *J. Am. Chem. Soc.* 2010, 133:35-41.

64.   Singh N, Jenkins GJ, Asadi R, Doak SH; *Nano Rev.* 2010, 1.

65.   Jin Y, Kannan S, Wu M, Zhao JX; *Chem. Res. Toxicol.* 2007, 20:1126-1133.

66.   Lynch I, Salvati A, Dawson KA; *Nat. Nanotechnol.* 2009, 4:546-547.

67.   Vácha R, Martinez-Veracoechea FJ, Frenkel D; *Nano Lett.* 2011, 11:5391-5395.

68.   Kleiner D, Fitzke E; *BBA-Biomembranes* 1981, 641:138-147.

69.   Goodman CM, McCusker CD, Yilmaz T, Rotello VM; *Bioconjugate Chem.* 2004, 15:897-900.

70.   Ariano P, Zamburlin P, Gilardino A, Mortera R, Onida B, Tomatis M, et al.; *Small* 2011, 7:766-774.

71.   Napierska D, Thomassen LCJ, Lison D, Martens JA, Hoet PH; *Part. Fibre Toxicol.* 2010, 7(39).

72.   Merchant RK, Peterson MW, Hunninghake GW; *J. Appl. Physiol.* 1990, 68:1354-1359.

73.   Chen J, Armstrong LC, Liu SJ, Gerriets JE, Last JA; *Toxicol. Appl. Pharmacol.* 1991, 111:211-220.

74.   Schins RPF, Duffin R, Hohr D, Knaapen AM, Shi TM, Weishaupt C, et al.; *Chem. Res. Toxicol.* 2002, 15:1166-1173.

75.   Kedmi R, Ben-Arie N, Peer D; *Biomaterials* 2010, 31:6867-6875.

76.   Zwiorek K, Bourquin C, Battiany J, Winter G, Endres S, Hartmann G, et al.; *Pharm. Res.* 2008, 25:551-562.

77.   Liu Y, Li W, Lao F, Liu Y, Wang L, Bai R, et al.; *Biomaterials* 2011, 32:8291-8303.

78.   Zhang S, Li J, Lykotrafitis G, Bao G, Suresh S; *Adv. Mat.* 2009, 21:419-424.

Chapter 5

Surface charge-specific cytotoxicity and cellular uptake of tri-block copolymer nanoparticles

Abstract

A series of monodisperse (45 ± 5 nm) fluorescent nanoparticles from tri-block copolymers (polymeric nanoparticles (PNP)) bearing different surface charges were synthesised and investigated for cytotoxicity in NR8383 and Caco-2 cells. The positive PNP were more cytotoxic and induced a higher intracellular reactive oxygen species (ROS) production than the neutral and negative ones. The cytotoxicity of positive PNP with quaternary ammonium groups decreased with increasing steric bulk. The intracellular uptake and cellular interactions of these different PNP were also tested in NR8383 cells by confocal laser scanning microscopy (CLSM), which revealed higher cellular uptake for positive than for negative PNP. Also positive PNP were found to interact much more with cell membranes, whereas the negative PNP were internalised mainly by lysosomal endocytosis. Uptake of positive PNP decreased with increasing steric bulk around the positive charge. A surface charge-specific interaction of clathrin for positive PNP and caveolin receptors for negative PNP was observed. These findings confirm that surface charge is important for the cytotoxicity of these PNP, while they also point to considerable additional effects of the steric shielding around positive charges on cytotoxicity of PNP.

Introduction

With the rapid growth of nanotechnology and its bio-applications, human exposure to nanomaterials is dramatically increasing.[1] Hence, there are widespread concerns about the possible harmful effects that nanomaterials and specifically non-aggregated nanoparticles (NP), can exert on living organisms. The small size, high surface area and reactivity of NP can pose new and unconventional types of health risks as compared with similar but bigger particles or bulk materials. It has been postulated that due to their small size, NP can access parts of the body that are inaccessible for bigger particles. Combined with their higher reactivity due to the high surface area and therefore higher % of molecules expressed on the surface, NP can pose a bigger threat at a lower dose when compared to bigger particles,[2] although little experimental data exist to substantiate this hypothesis.

Surface charge has recently been recognised as an important factor in determining the cytotoxicity of NP.[3-6] However, as investigations on cytotoxicity have been performed on a broad range of NP and the diversity of the investigated cytotoxicity end points is large, it is not easy to draw general conclusions. A complicating factor is that in many studies poorly characterised NP were used. Performing a study on cellular uptake and cytotoxicity on a well-characterised homologous series of polymeric nanoparticles (PNP) with systemic variation in surface charge and shielding of that charge will add improved mechanistic insight in the role of surface charge in these cellular processes and effects of PNP.

So far, positive NP are claimed to be more cytotoxic than negative ones with few exceptions.[7] A common hypothesis is that positive NP interact more strongly with cells than negative ones, because of the electrostatic attraction towards the negatively charged cell membranes.[8-11] Unfortunately, this hypothesis proved to be insufficient in explaining several recent findings. For example, Asati et al.[12] and Xia et al.[13] reported surface charge-dependent cytotoxicity and cellular uptake for both positive and negative NP. In contrast to positive NP, negative NP should be repelled by the negative cell membrane, which in turn should restrict their intracellular uptake. Thus, the hypothesis mentioned above does not explain the uptake of negative NP.

Apart from the charge itself (positive or negative), the steric shielding of the charge may also play an important role, but surprisingly nothing has been reported on this. While in nearly all studies on positively charged NP, primary amines were used as positively charged surface groups, in only one study on dendrimers,[14] secondary and tertiary amines were also investigated. This study indicated that the cytotoxicity of dendrimers with primary amines as surface groups was higher than of similar dendrimers with secondary and tertiary amines as surface groups.

The surface charge-specific intracellular uptake of different NP is also of importance; it has been claimed that surface charge can affect cellular uptake of NP.[15-17] Interestingly, several groups reported on the crucial role of cell surface receptors in cellular interactions and intracellular uptake of NP.[13, 18] This means that in order to better understand the role of surface charge in cytotoxicity of NP, cellular uptake via cell surface receptors also has to be taken into account. However, systematic investigations on these aspects are still missing.

Several reports indicated that oxidative stress, resulting from the induction of intracellular reactive oxygen species (ROS) production, may be relevant for the cytotoxicity of NP.[19-21] Unfortunately, it still remains unclear whether induction of intracellular ROS production is the

cause or rather the result of cytotoxicity and through which mechanism(s) this is caused. Several publications indicated an effect of surface charge of NP on intracellular ROS production. Recently, we showed that silicon NP bearing positive surface charges, induced ROS production in isolated rat liver mitochondrial fractions in vitro.[5] Xia et al.[3] reported that amine-terminated positively charged polystyrene latex beads altered the membrane potential of intracellular mitochondria and caused formation of vacuoles upon 16-24 h exposure. In an another recent article,[13] it was reported that these amine-terminated latex beads caused ATP depletion in cells, which indirectly pointed towards impairment of the mitochondrial electron transport chain. These effects might indeed be caused by induction of intracellular ROS production, whereas on the other hand, disruption of the oxidative phosphorylation reaction chain due to the presence of PNP may also be the cause for ROS production and ATP depletion. All these reports pointed towards surface charge of NP as being important in cellular interaction, cellular uptake and the mode of action for cytotoxicity of NP. Increased use of tuneable NP in drug and imaging probe delivery can be foreseen in nanomedicine and bioimaging. PNP allow easy variation of their composition via the toolbox of organic chemistry and are therefore excellent materials for investigation of factors that play a role in cellular uptake and cytotoxic effects and can thus provide guidelines for the development of safe PNP. By chemical engineering, many physico-chemical properties including the surface charge of PNP can be varied, which then may be used in studying the effects on cytotoxicity.[22] Moreover, the use of fluorescent PNP enables the study of cellular uptake and intracellular localization.

The PNP used in this study were derived from PEG_{2000}-PHA-PEG_{2000} of which the terminal hydroxyl groups have been converted into carboxylic acid, amine or ammonium groups and the poly(hexamethylene adipate) (PHA) middle block was labelled with a fluorescent dye. PNP from these tri-block copolymers are considered to be biodegradable and can be used as vehicles for encapsulation and release of compounds, like the antioxidant quercetin.[23] The surface charge-specific cytotoxicity, intracellular ROS production and intracellular uptake patterns of these well-characterized and fluorescent ~45-nm size PNP with different surface charges were systematically investigated in rat alveolar macrophage NR8383 and human colonic adenocarcinoma Caco-2 cell lines. These cell lines are especially relevant as lung cell macrophages are the first line of body defence against foreign pathogens. Therefore, the effects of these PNP on NR8383 cells could indicate how NP interact with this part of the body immune system. Studies on Caco-2 cells are useful to assess the toxicity of NP to intestinal cells following oral administration, because Caco-2 cells are generally accepted as a model for intestinal cells.[24] Finally, the role of charge of PNP on the cellular uptake by clathrin and caveolin cell surface receptors was studied using confocal laser scanning microscopy (CLSM) and selective inhibitors of clathrin- and caveolin-mediated uptake. Taken together, this study was performed to systematically investigate how surface charge and steric shielding of the charge affect the cellular uptake and cytotoxicity of different PNP. All PNP were synthesized from tri-block copolymers with the same length and the same content of fluorescent probe in the hydrophobic polyester middle block. As a result, they differed only in the nature of their terminal functional groups. It was demonstrated how surface charge influences cytotoxicity and cellular uptake of PNP and this was related to different internalization pathways. The data obtained from this study shed light on the influence of surface charge of NP on their cellular uptake, intracellular localization and cytotoxicity.

Materials and methods

Synthesis of tri-block copolymer PEG$_{2000}$-PHA-PEG$_{2000}$ with fluorescent probe

The fluorescent probe was synthesized and characterized as reported previously.[25] A dry, three-necked 100 ml round-bottom flask containing properly grinded and dried 1,6-hexanediol (2.0 g; 17 mmol) and 0.1 mg of fluorescent probe was fitted with a reflux condenser and flushed with dry nitrogen for 30 min. The flask was heated on an oil bath of 120 °C with gentle stirring until the 1,6-hexanediol melted. To the mixture 50 µl of triethylamine was added, followed by drop-wise addition of 3.28 g (17.8 mmol) of dry adipoyl chloride. The mixture was gently stirred at 120 °C for 48 h until no more HCl was produced. Now, excess of well-dried PEG$_{2000}$ was added at 120 °C and the reaction mixture was stirred gently for another 48 h. The resulting viscous mixture was poured into 50 ml of dry ether and the precipitate was filtered and washed repeatedly with dry ether. The precipitate was then stirred with 100 ml of distilled water and centrifuged at 4000 rpm for 4 min. This process was repeated thrice. The polymer was finally dried by overnight freeze drying and characterised by ^{1}H NMR (Bruker Avance III 400 MHz NMR spectrometer; CDCl$_3$), infrared spectroscopy, DSC (differential scanning calorimetry), SEC (size exclusion chromatography) and UV–Vis spectroscopy.

Synthesis of fluorescent PEG$_{2000}$-PHA-PEG$_{2000}$ polymer with different end groups

Conversion to amines

In a dry, three-necked 100 ml round-bottom flask fitted with a reflux condenser, 400 mg (0.03 mmol) of polymer was heated at 120 °C until it melted. While stirring, 11.2 mg (0.1 mmol) of chloroacetyl chloride was slowly added. Stirring of the reaction mixture was continued for another 6 h. For conversion to the amine-terminated polymers, the mixture was cooled and 6.8 mg of 25 % w/w aqueous ammonia (0.1 mmol of ammonia) was added. For conversion to the dimethylethanolammonium-terminated polymers, 8.9 mg (0.1 mmol) of dimethylethanolamine was added at 120 °C. For conversion to the pyridinium-terminated polymers, 7.9 mg (0.1 mmol) of pyridine was added at 120 °C. All mixtures were allowed to stir for another 12 h before workup. The polymers were purified and dried as described above.

Conversion to acid

In a similar experimental setup as mentioned above, 10 mg (0.1 mmol) of succinic anhydride was added in portions to 400 mg (0.03 mmol) of molten polymer and allowed to react for 12 h at 120 °C. The purification was performed as described above.

Estimation of terminal hydroxyl group conversion with trichloroacetyl isocyanate[26]

In an NMR tube with polymer sample dissolved in CDCl$_3$, 10 µl of trichloroacetyl isocyanate (TAIC) was added and the tube was vortexed for 5 min. After reaction for 10 min, ^{1}H NMR

spectra were recorded and the peak appearing at δ = 4.43 ppm was integrated and compared with the value obtained from unmodified polymer to obtain the conversion rates.

Synthesis and characterization of NP

NP were prepared by the nanoprecipitation method, using a slight modification of the method described by Khoee et al.[23] A slightly warm (40 °C) solution of 10 mg of tri-block copolymer in 2 ml tetrahydrofuran (THF) was injected into 10 ml of vigorously stirred ultrapure water in an open beaker. The dispersion was stirred for another 30 min. The THF was then removed under reduced pressure and the aqueous dispersion was filtered through 0.2 μm cellulose filters. The size of the PNP was determined by DLS (dynamic light scattering) and the surface potential by ζ-potential (Malvern Zetasizer) measurements at different pH values.

Scanning Electron Microscopy

A clean circular cover glass of 8 mm diameter (Menzel, Brauschweig, Germany) was fitted on a sample holder by carbon adhesive tabs (EMS Washington USA). An aqueous suspension of PNP (50 μl) was put on the glass and the water was allowed to evaporate until the PNP that remained behind were completely dried. The dry sample was sputter coated with 2 nm tungsten (MED 020, Leica, Vienna, Austria). Samples were analysed at 2 kV at room temperature in a field emission scanning electron microscope (Magellan 400, FEI, Eindhoven, the Netherlands).

Cell lines

Rat alveolar macrophage (NR8383) and human colonic adenocarcinoma (Caco-2) cells were obtained from ATCC (Manassas, VA). The NR8383 and Caco-2 cells were cultured in 150 cm^2 cell culture flasks with 25 ml F12-K culture medium (Gibco 21127) and DMEM medium, respectively supplemented with 10 % (v/v) heat-inactivated FCS and 0.1 % (v/v) gentamicin, in humidified atmosphere containing 5 % CO_2 at 37 °C.

Cytotoxicity measurement by MTT assay

NR8383 cells

An NR8383 cell suspension was centrifuged at 140 *g* for 5 min before resuspending the cell pellet in medium followed by counting and adjusting the cellular concentration to 2×10^5 cells/ml. The cells were then seeded in a 96-well plate (50 μl/well) and the plate was kept in a 5 % CO_2 incubator at 37 °C for 24 h. Next day, 50 μl of serial dilutions of different PNP in water were added to the cells to obtain the required final concentrations. The plate was further incubated for another 24 h, after which 5 μl of 3-(4,5-dimethylthiazol-2-yl)-2,5-diphenyltetrazolium bromide (MTT) solution in PBS (5 mg/ml) was added to each well and the

plate was incubated for another 4 h. To each well, 100 µl of pure DMSO was added to dissolve the formazan crystals. The absorption of each well was measured at 562 nm in a 96-well plate reader and the background absorption at 612 nm was subtracted. Mitochondrial metabolic activity for each concentration of PNP was expressed as % of the corresponding negative control reading. Medium without PNP and medium with Triton-X (0.01 %) were used as negative and positive controls, respectively.

Caco-2 cells

The Caco-2 cells were plated at a concentration of 10^5 cells/ml in a 96-well plate (100 µl/well) and were incubated at 37 °C for 24 h. Different PNP in water were then added to the cells (100 µl/well) to achieve the final concentrations followed by further incubation of 24 h at 37 °C. Each well was then carefully emptied without dislodging the precipitated crystals and the crystals were dissolved in pure DMSO (100 µl/well). Each well was measured as mentioned above.

Measurement of intracellular ROS by 2′,7′-dichlorofluorescein diacetate assay

NR8383 cells

The cell suspension was adjusted to 2×10^5 cells/ml and seeded in a 96-well plate (50 µl/well) in F12-K medium. Serial dilutions of PNP (50 µl/well) in F12-K medium were added to obtain the required final concentrations of PNP. A final concentration of 10 mM H_2O_2 was used as positive control and F12-K medium without PNP as negative control. After 6 h of exposure to the PNP, 5 µl of a 20 mM solution of DCFH-DA (2′,7′-dichlorofluorescein diacetate) in DMSO was added to each well and the plates were incubated for another 18 h in a 5 % CO_2 atmosphere at 37 °C. The fluorescence was then measured on a fluorometer at 485 nm excitation and 538 nm emission wavelengths. The fluorescence induction factor for each concentration of PNP was calculated by dividing the reading of each well by the average reading of the negative control and expressed as percentage. Control experiments were performed by incubating the PNP at their test concentrations with DCFH-DA in the absence of cells to check the possibility of a positive fluorescence reading caused by reaction of DCFH-DA with PNP alone.

Caco-2 cells

The cells were suspended in DMEM medium to a concentration of 10^5 cells/ml after trypsinization and were plated in a 96-well plate (100 µl/well). After 24 h, the cells were exposed to 100 µl/well of final concentrations of different PNP. Following another 6 h of PNP exposure, 5 µl of a 20 mM solution of DCFH-DA were added to each well. The plate was further incubated for 18 h before measurement of the fluorescence was carried out as described above.

Inhibition of endocytosis in NR8383 cells and analysis by CLSM

For performing CLSM, a drop of the NR8383 cell suspension was mounted on a glass slide and viewed through an oil immersion lens of a confocal microscope (Zeiss). For assessment of the average fluorescence intensity, readings from 30 individual cells (for each type of PNP) from 10 different fields and 10 different samples in focus were used. All the measurements were done at the same excitation wavelength (λ_{ex} = 488 nm), emission wavelength (λ_{em} = 543 nm), focal plane, aperture size and image gain. For comparison purposes, maximum intensity projection from all the slices was done. The figures from 4′,6′-diamidino-2-phenylindole (DAPI) staining and CLSM pictures were overlaid by *ImageJ* software. To exclude any background fluorescence, control samples of NR8383 cells not exposed to the different PNP were also investigated by CLSM. These NR8383 cells did not show any auto-fluorescence at the excitation wavelength of 488 nm. The nuclei of the NR8383 cells were stained by DAPI and visualised under UV excitation (λ_{ex} = 366 nm). To inhibit endocytosis by low temperatures (4 °C), NR8383 cells were seeded and exposed to 1 μg/ml concentration of PNP-NH$_2$, PNP-OH and PNP-COOH in a 96-well plate as mentioned above and were both pre-incubated and incubated at 4 °C. Endocytosis was also blocked by exposing the NR8383 cells to a mixture of 50 mM 2-deoxyglucose and 10 mM sodium azide for 30 min at 37 °C before being centrifuged and generously washed with PBS at least three times to remove the exposure medium. The cells were then plated and exposed to different PNP at 37 °C as described before. Clathrin and caveolin receptor-mediated endocytosis was inhibited by exposing the NR8383 cells to 450 mM sucrose and 1 μM methyl-β-cyclodextrin (MβCD), respectively for 30 min, before being plated, washed and exposed to different PNP at 37 °C as mentioned above.

Statistical analysis

Data were analysed with Origin Pro (version 8.0) graphing software. For statistical analysis, a Student's *t*-test was performed and data with $p < 0.05$ (compared with negative control) were marked with an asterisk (*) sign. Each data point represents the average from three independent experiments (n = 3) and is presented as the arithmetic mean ± standard error of mean (SEM).

Results

Synthesis and characterization of PEG$_{2000}$-PHA-PEG$_{2000}$ with fluorescent probe

The synthesis of the PEG$_{2000}$-PHA-PEG$_{2000}$ polymer is depicted in Figure 1. From ^{1}H NMR data of the polymer (see *Appendix B*), the molecular weight was estimated to amount to 12.5 kDa, which was in agreement with the data obtained from SEC (see *Appendix B*). The polydispersity index (of polymer) of 1.53 matched the findings of Khoee et al.[23] (Table 1).
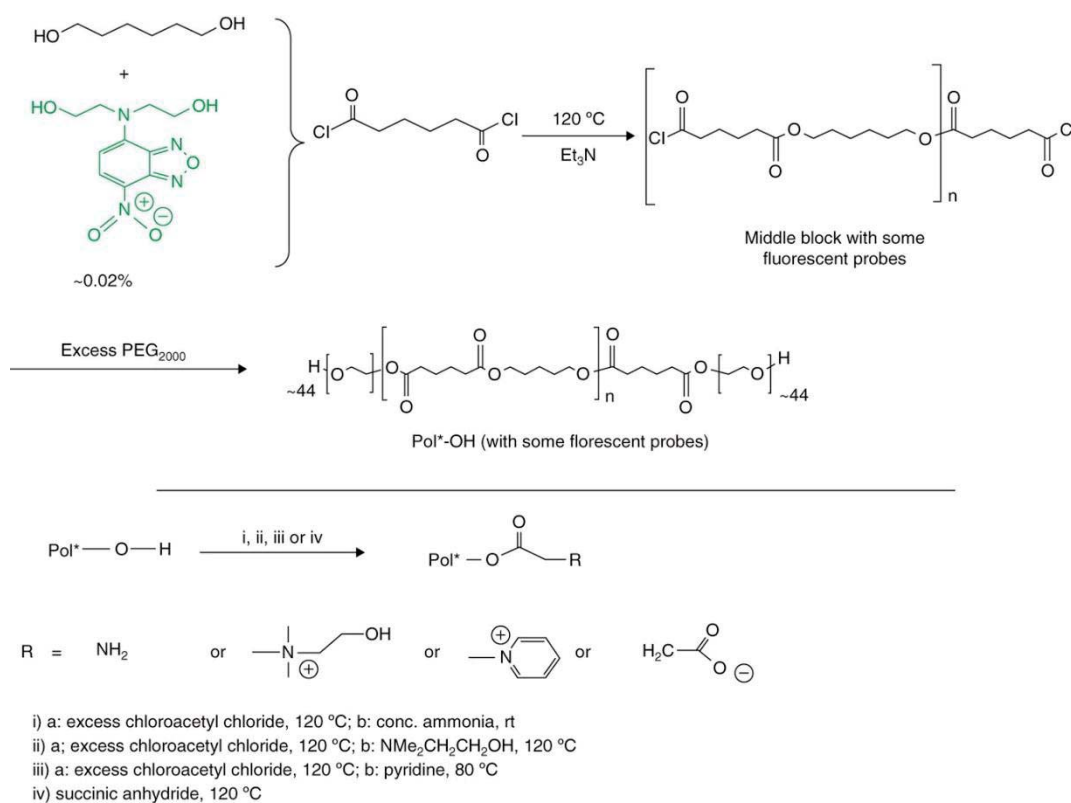
Figure 1: *Scheme of synthesis of PEG$_{2000}$-PHA-PEG$_{2000}$ polymer with fluorescent probe and further conversion of the terminal hydroxyl moieties to various functional end groups.*

Conversion of terminal hydroxyls to different functional end groups

The terminal hydroxyl groups of PEG$_{2000}$-PHA-PEG$_{2000}$ were converted to different amines and ammonium groups by first reacting with chloroacetyl chloride and subsequently adding concentrated ammonia (yielding: Pol-NH$_2$), N,N-dimethyl-ethanolamine (yielding: Pol-DMEA) or pyridine (yielding: Pol-Py). The resulting polymers had positively charged terminal groups, either pH-dependent through the -NH$_2$ group or with a permanent, pH-independent charge through the –N$^+$(CH$_3$)$_2$CH$_2$CH$_2$OH or pyridinium group. Similarly, polymers with negatively charged carboxylate terminal groups were obtained upon reaction of the terminal hydroxyl groups with succinic anhydride. The degree of conversions of the terminal hydroxyl groups were assessed through reaction with TAIC. Reaction of TAIC[26] with terminal hydroxyl groups gives a peak in the ^{1}H NMR spectrum at 4.43 ppm, which can be used to quantify the conversion (Table 1 and *Appendix B*). The data regarding the characterization of PEG$_{2000}$-PHA-PEG$_{2000}$ polymer including the conversion of the terminal hydroxyl groups to different functional groups as well as a summary of all the reactions are presented in Table 1 and Figure 1, respectively. The melting points of each polymer were determined by DSC and were found to be ~43 °C for all polymers. The ^{1}H NMR spectrum of the polymer with pyridinium end groups is provided as supplemental information (see *Appendix B*). Since all polymers were prepared from the same batch and the molecular weights do not change much due to the modification reactions, the content of the fluorescent groups was approximately the same in all polymers.

Table 1. Data for PEG$_{2000}$-PHA-PEG$_{2000}$ polymer and end-group conversions.					
Polymer	**Molecular weight (kDa)**	**Melting point**	**PDI**	**Converted to**	**Conversion terminal-OH (%; determined by TAIC)**
PEG$_{2000}$-PHA-PEG$_{2000}$	^{1}H NMR 1.25 × 10^4	43 °C	1.53	Pol-NH$_2$	~85
				Pol-DMEA	~90
	SEC 1.26 × 10^4			Pol-Py	80
				Pol-COOH	>90

PDI, Polydispersity index; TAIC, Trichloroacetyl isocyanate.

Synthesis and characterization of different PNP

The different PNP were prepared by a nanoprecipitation technique, where a solution of polymer in THF was injected into vigorously stirred water, converting Pol-X to PNP-X (X = NH$_2$, N$^+$(CH$_3$)$_2$CH$_2$CH$_2$OH, pyridinium, COOH) to obtain a stable clear aqueous dispersion of PNP with a size of 45 ± 5 nm for each type of PNP, as determined by DLS. Scanning electron microscopy (Figure 2) as well as atomic force microscopy (AFM) (see *Appendix B*) confirmed the presence of particles of this size. Time-dependent DLS measurements confirmed that these PNP did not have a strong tendency to aggregate in water within 48 h of preparation. The occasional clustering of the particles, as seen in Figure 2, is mostly an artefact resulting from sample preparation for scanning electron microscopy, i.e. drying of droplets containing particles under vacuum. The size and size dispersion of the different PNP were also measured in cell culture media (DMEM and F12-K) enriched with 10 % FCS. In both media with 10 % FCS, all PNP showed an increase in size due to protein adsorption on their surfaces, although the cationic PNP increased relatively more in size than the anionic ones (Table 2). While performing the cellular experiments, the PNP dilutions were vortexed for 5 min before adding to the wells. The content of fluorescent dye in the different PNP was comparable. This can be derived from the fact that UV–Vis measurements showed that solutions of the different PNP prepared at the same concentration have within 5 % the same absorption at 465 nm.
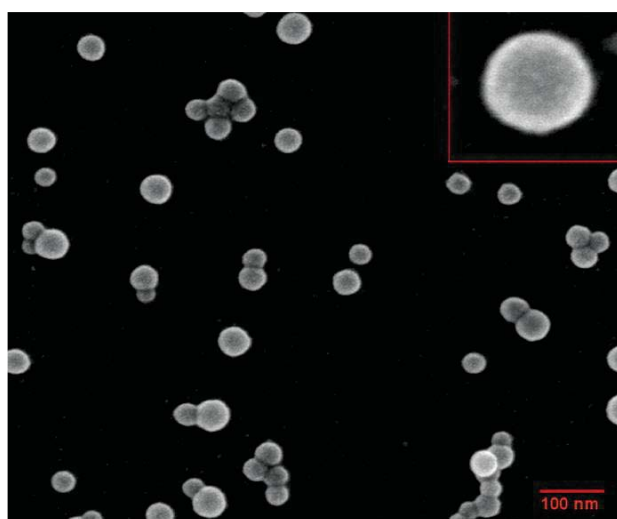

Figure 2: Scanning electron microscopy image of monodisperse (45 ± 5 nm)PNP; insert: high-resolution image of an individual particle. Scale bar show 100 nm.

The ζ-potentials of the different PNP were measured at different pH values, ranging from 3 to 11 and the results are shown in Figure 3. As expected, the PNP-NH$_2$ showed a decrease in positive ζ-potential with increasing pH (pK$_a$ ~9). However, variation in pH hardly showed an effect on the positive ζ-potential of the ammonium-terminated PNP, PNP-DMEA and PNP-Py. For PNP-COOH, negative ζ-potentials were obtained at normal physiological pH and as expected, the negative ζ-potential values approached zero at lower pH values (pK$_a$ ~5). PNP derived from unmodified PEG$_{2000}$-PHA-PEG$_{2000}$ polymer (PNP-OH) yielded slightly negative ζ-potential values, which possibly resulted from remaining hydrolysed acid chloride moieties in the middle block.
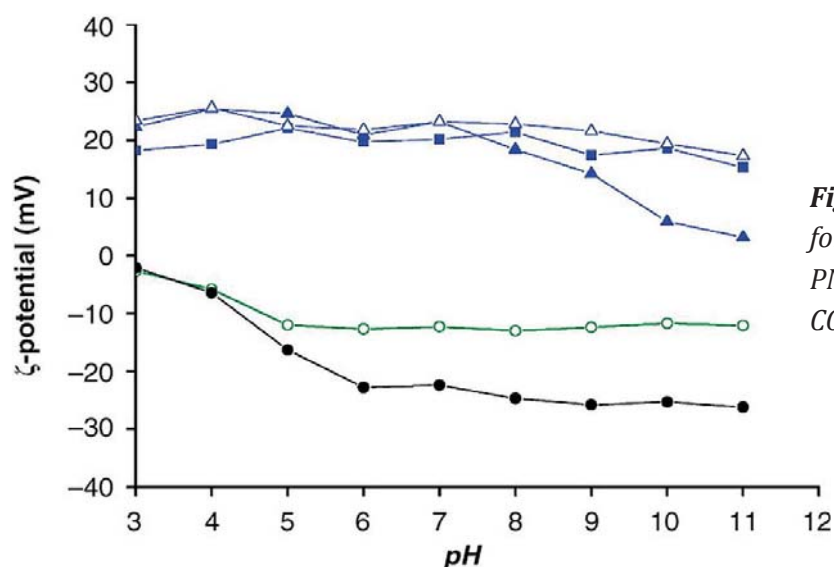
Figure 3: pH-dependent ζ-potentials for PNP-NH$_2$ ($\blacktriangle$), PNP-DMEA ($\blacksquare$), PNP-Py ($\triangle$), PNP-OH ($\circ$) and PNP-COOH ($\bullet$) in water.

Table 2. Summary of DLS data of different PNP dispersed in water and in both cell culture media (DMEM and F12-K).

Type of PNP	Size in water (nm) (PDI)	Size in DMEM (nm) (after 1 h)	Size in F12-K (nm) (after 1 h)
PNP-NH$_2$	45 ± 5 (0.016)	98 ± 5	106 ± 5
PNP-DMEA	45 ± 5 (0.02)	92 ± 6	101 ± 4
PNP-Py	45 ± 5 (0.023)	89 ± 5	90 ± 6
PNP-OH	45 ± 5 (0.021)	78 ± 5	79 ± 5
PNP-COOH	45 ± 5 (0.022)	73 ± 5	67 ± 5

DLS, Dynamic light scattering.

Evaluation of the cytotoxicity of nanoparticles by MTT assay

The cytotoxicity of the different PNP was tested in NR8383 and Caco-2 cells (Figure 4) using the MTT assay in the concentration range of 0–400 µg/ml after 24 h exposure. This assay measures the mitochondrial metabolic activity of the cells, which was then compared with the mitochondrial metabolic activity of the negative control and expressed as cell viability (%).

Exposure of the cells to positively charged PNP caused a concentration-dependent increase in cytotoxicity, whereas exposure to the negatively charged ones did not result in cytotoxicity. Among the positive PNP, the cytotoxicity decreased in the order: PNP-NH$_2$ > PNP-DMEA > PNP-Py for both NR8383 and Caco-2 cells (see Table 3). The positive control (0.01 % Triton-X) showed 0.01 % viability compared with negative control (100 %).
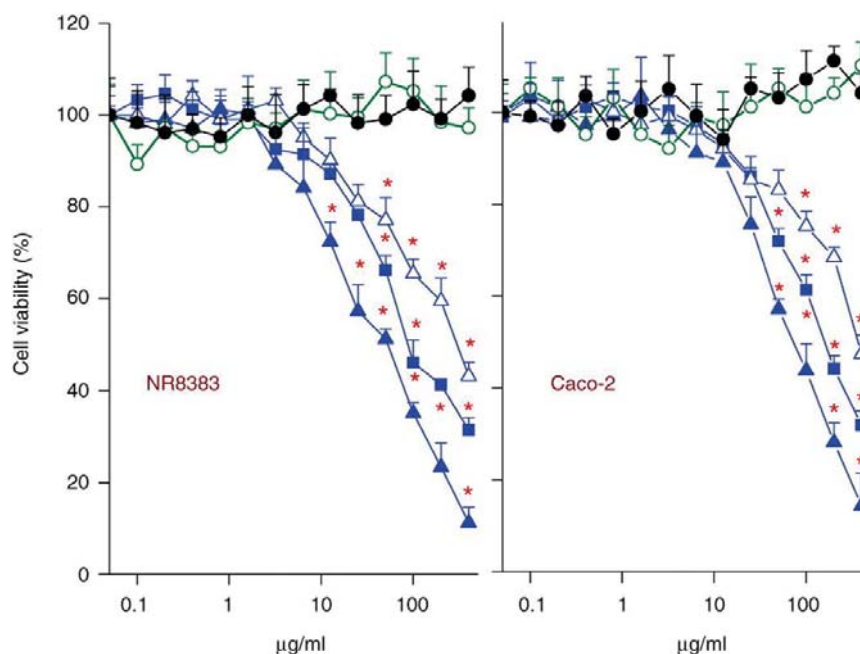

Figure 4: *Cytotoxicity assessment of PNP-NH$_2$ (▲), PNP-DMEA (■), PNP-Py (Δ), PNP-OH (○) and PNP-COOH (●) on cell viability measured by the MTT assay in NR8383 and Caco-2 after 24 h exposure. The * symbols indicate data points that are statistically significantly different (p < 0.05) from negative control (0 μg/ml).*

Table 3. *The EC50 values (μg/ml) obtained from different assays after 24 h of exposure of NR8383 and Caco-2 cells to different positively charged PNP.*

Assay	Parameter	Reference Figure	Cell line	PNP-NH$_2$	PNP-DMEA	PNP-Py
MTT	Cell viability	Figure 4	NR8383	31	50	64
			Caco-2	54	75	121
DCFH-DA	Intracellular ROS production	Figure 5	NR8383	13	16	28
			Caco-2	21	29	31

Assessment of intracellular ROS production by DCFH-DA assay

All the positive PNP, i.e. PNP-NH$_2$, PNP-DMEA and PNP-Py, were able to induce intracellular ROS production in both NR8383 and Caco-2 cells, whereas negative PNP, i.e. PNP-OH and PNP-COOH, did not (Figure 5). Furthermore, in both NR8383 and Caco-2 cells, the strongest induction of intracellular ROS production was found with PNP-NH$_2$, followed by PNP-DMEA and then PNP-

Py. These results matched the MTT assay results and showed the relation between oxidative stress and cytotoxicity. The positive control (10 mM H_2O_2) showed ~643 % of intracellular ROS production compared with negative control (100 %).
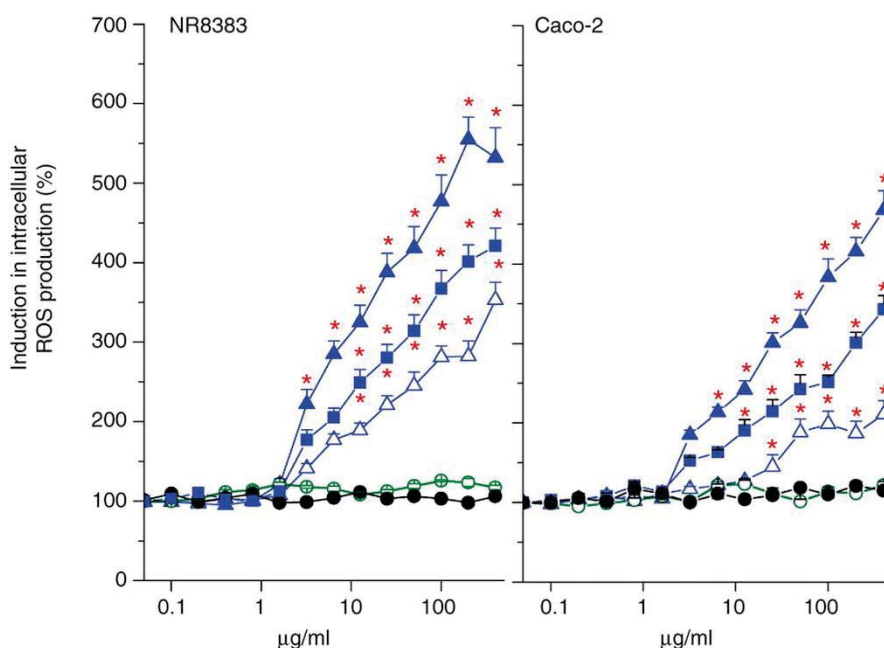

Figure 5: *Induction in intracellular reactive oxygen species (ROS) production in NR8383 and Caco-2 cells after 24 h exposure to PNP-NH$_2$ (▲), PNP-DMEA (■), PNP-Py (Δ), PNP-OH (○) and PNP-COOH (●). The * symbols indicate data points that are statistically significantly different (p < 0.05) from negative control (0 μg/ml).*

Assessment of intracellular uptake and localization of different PNP in NR8383 cells by CLSM

The cellular uptake and localization of three positive PNP-NH$_2$, slightly negative PNP-OH and negative PNP-COOH after 24 h exposure in NR8383 cells were investigated by CLSM. The results are shown in Figure 6. Under normal incubation conditions (37 °C), the positive PNP-NH$_2$ showed increased uptake levels and more interaction with the cellular periphery as compared with negative PNP. Interaction with the cellular periphery can be seen as a halo at the cell surface. DAPI staining was used to visualise intracellular ds-DNA (nucleus). Furthermore, the pictures obtained from CLSM, bright-field and DAPI staining were overlaid to visualize the intracellular distribution of different PNP (Figure 6). For the positive PNP-NH$_2$, the pictures revealed an interaction with the cellular nucleus. To confirm that the PNP were inside the cells, *z*-stack imaging from multiple slices were taken to facilitate maximal intensity projection as well as three-dimensional views of the cells. A detailed CLSM study demonstrated that positive PNP-NH$_2$ showed more interaction with all cellular regions than PNP-OH and PNP-COOH. Whereas PNP-OH and PNP-COOH were mainly present in the cytoplasm, positive PNP-NH$_2$ were also present in relatively high concentrations in the cell nucleus and at the cell membrane (upper panels of Figure 7).
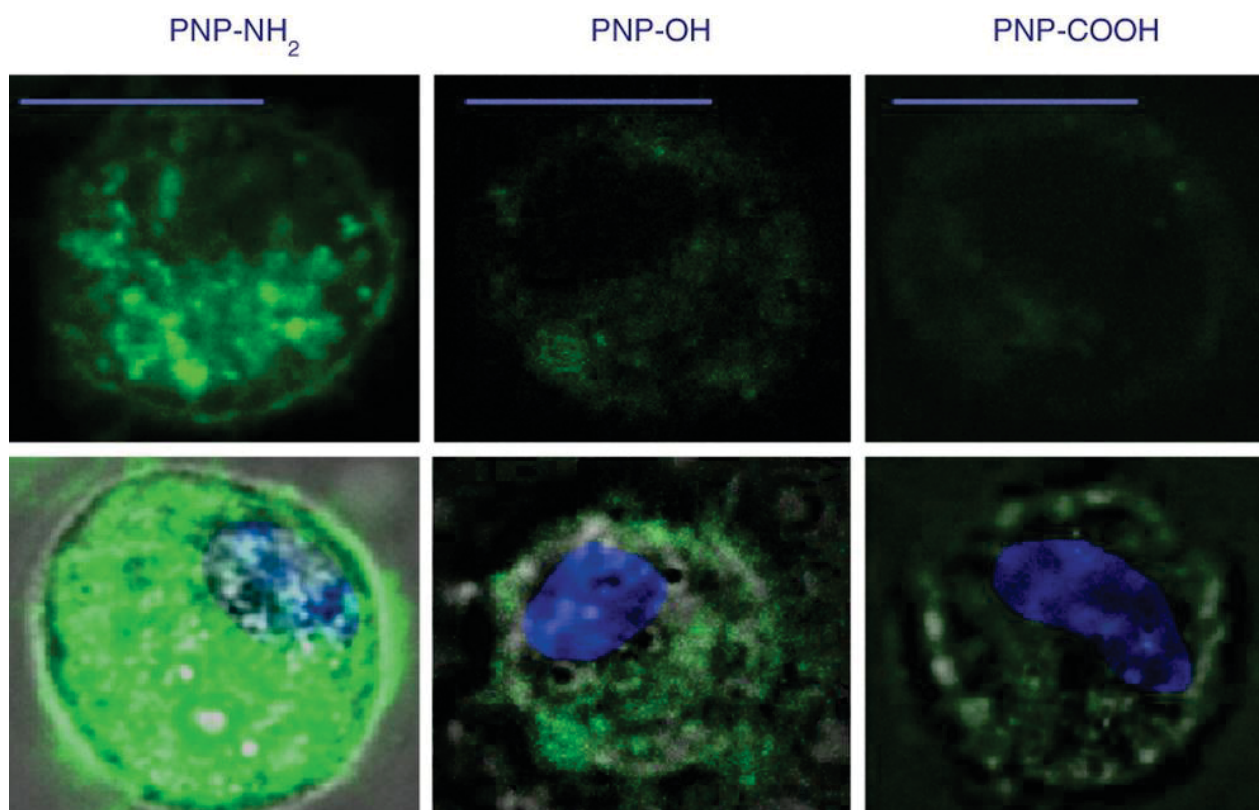
*Figure 6: Upper panel: CLSM pictures of NR8383 cells after 24 h exposure to 1 μg/ml concentrations of positive PNP-NH₂, slightly negative PNP-OH and negative PNP-COOH (λ_{ex} = 488 nm). **Lower panel**: overlay pictures of confocal laser scanning microscopy, bright-field and 4′,6′-diamidino-2-phenylindole (DAPI) staining.*

Also positive PNP-NH$_2$ were internalised more into the cells than PNP-OH and PNP-COOH upon exposure for 24 h. Internalisation of positive PNP varied with the steric bulk around the positive charge and followed the order: PNP-NH$_2$ > PNP-DMEA > PNP-Py (bottom panel of Figure 7). Furthermore, the EC50 values derived from the MTT data (Table 3) showed that no EC50 values could be ascertained for PNP-OH and PNP-COOH in spite of the fact that both PNP-OH and PNP-COOH showed cellular uptake.

To investigate the uptake process of PNP in more detail, normal endocytotic processes were inhibited either by blocking the metabolic activities including ATP production by performing the experiments at a lower temperature of 4 °C (middle panel of Figure 8) or by exposing the cells to a mixture of 50 mM 2-deoxyglucose and 10 mM sodium azide (lower panel of Figure 8).[12] It was observed that in both experiments, the cellular uptake for all three PNP decreased, although the decrease was much more pronounced for PNP-OH and PNP-COOH (90 %) than for PNP-NH$_2$ (45 %). The statistical analysis of the results obtained from blocking endocytosis is provided as supplemental information (see *Appendix B*).
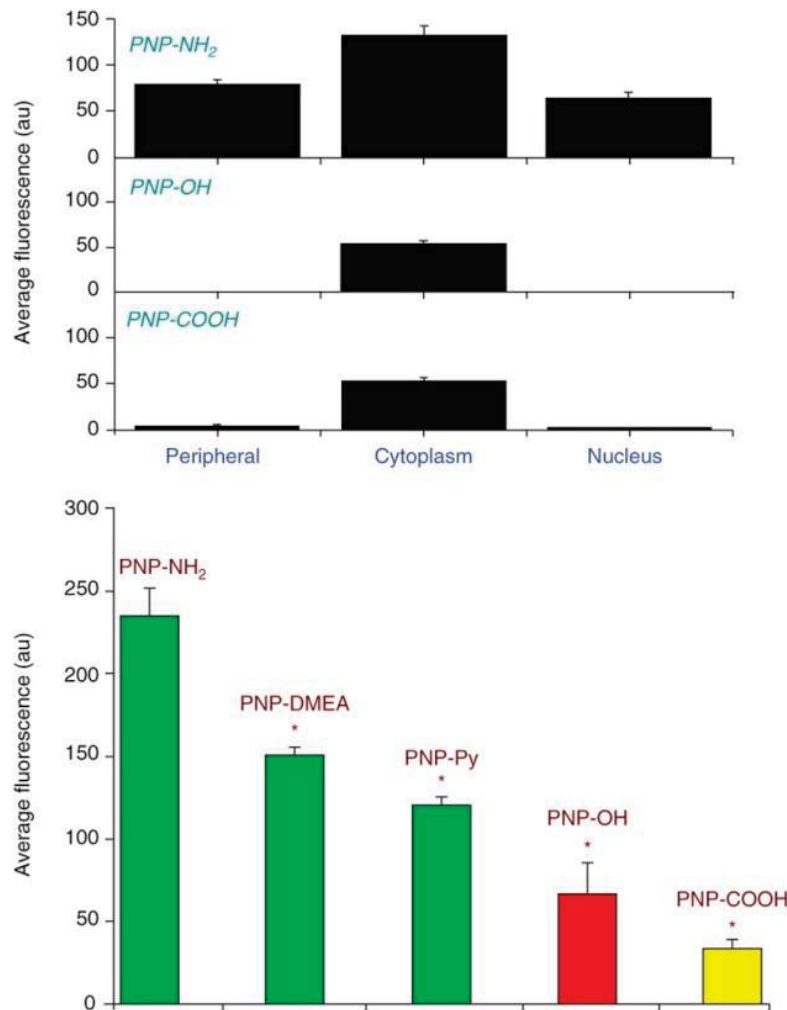
Figure 7: *Intracellular uptake and localisation of different PNP in NR8383 cells after 24 h exposure assessed from fluorescence measurements (λ_{ex} = 488 nm). The upper panel shows the localization of different PNP at different cellular compartments. The lower panel shows the relative cellular uptake of different PNP. Scale bars show 10 μm. Results are calculated from an average of 20 independent fields (30 cells) and are shown as mean ± SEM (n = 6). The * indicate data points that are statistically significantly different from PNP-NH₂ (p < 0.05).*

Assessment of the role of clathrin and caveolin receptors in the surface charge-specific intracellular uptake of different PNP

Upon blocking the clathrin receptors, the NR8383 cells showed an ~85 % decrease in cellular uptake of positive PNP-NH₂. For PNP-OH and PNP-COOH, only a small decrease (~20 %) in cellular uptake was observed (middle panel of Figure 9). However, upon blocking the caveolin receptors, an opposite trend was observed, i.e. the intracellular uptake of positive PNP-NH₂ was much less hampered (~20 %) as compared with that of PNP-OH and PNP-COOH (bottom panel of Figure 9), which decreased by >90 %. The statistical analysis of the results obtained from blocking endocytosis is provided as supplemental information (see *Appendix B*).
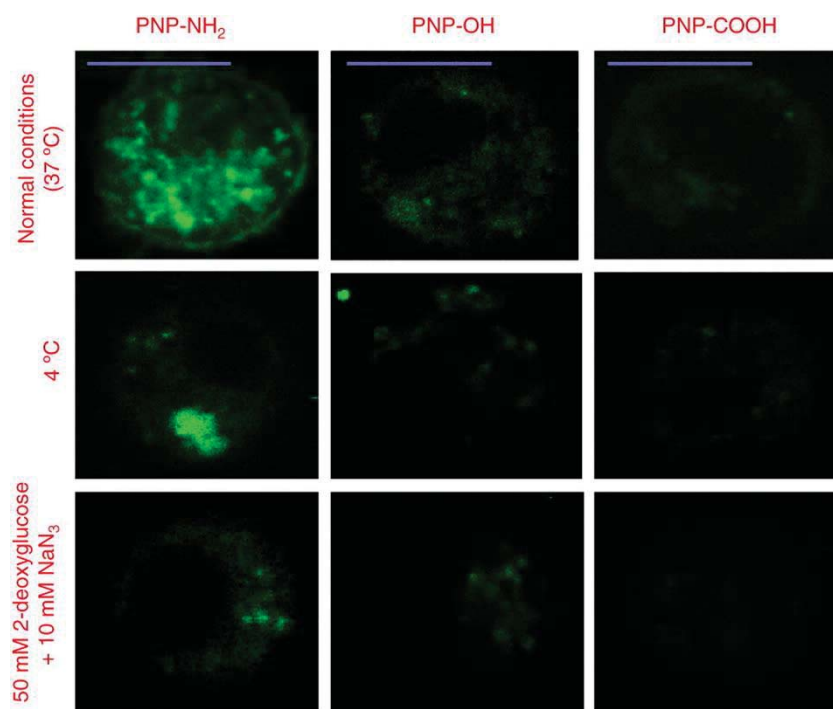
Figure 8: *CLSM pictures of NR8383 cells after 24 h exposure to PNP-NH₂, PNP-OH and PNP-COOH (λ_{ex} = 488 nm). Upper panel shows images obtained under normal experimental conditions (37 °C) whereas other panels show images obtained after inhibition of endocytosis by low temperature (4 °C; middle panel) and administration of 2-deoxyglucose and sodium azide (lower panel). Scale bars show 10 μm.*
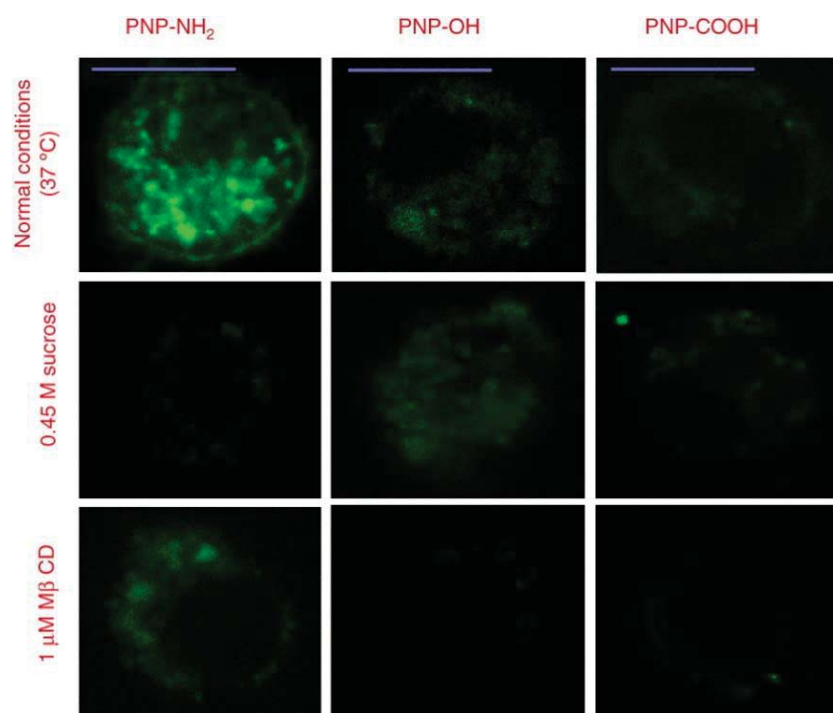

Figure 9: *CLSM pictures of NR8383 cells after 24 h exposure to PNP-NH₂, PNP-OH and PNP-COOH (λ_{ex} = 488 nm). The upper panel shows the results obtained under normal experimental conditions (37 °C) whereas the middle and lower panel show results under inhibition of endocytosis by blocking the clathrin and caveolin receptors with 450 mM sucrose and 1 μM MβCD, respectively. Scale bars show 10 μm.*

Discussion

Surface charge of NP is one of the important factors influencing cellular interaction of PNP, although very little is reported on this topic. To investigate, we hypothesised that surface charge influences not only cytotoxicity but also cellular uptake of PNP including their intracellular distribution. In order to facilitate our investigation, we successfully synthesized and characterized fluorescent tri-block copolymer PNP (size ~45 nm) with different surface charges. Our data showed that positive PNP were more cytotoxic than the negative ones. Most recent articles, in which the effects of surface charge on cytotoxicity of NP were studied, claimed that positive NP were more cytotoxic than negative ones.[27-29] Previously, we also reported a higher cytotoxicity for positively charged silicon NP than for neutral and negatively charged silicon NP (1.6 ± 0.2 nm).[5, 6] There are only a few exceptions reported,[7, 30] where indications were found that negative NP could be more cytotoxic than positive ones. Thubagere et al.[7] studied the interactions of 20 and 40 nm polystyrene NP with positive and negative surface charges on Caco-2 monolayers by CLSM and fluorescence spectroscopy. They observed lower cell viability and higher cellular uptake of NP for cells exposed to negatively charged NP than for cells exposed to positively charged ones. However, these results were based only on fluorescence measurements on Caco-2 monolayers grown on transwell inserts. This method is very different from our approach of determining cytotoxicity using MTT assays. This makes a comparison with our results difficult. Similarly, Saxena et al.[30] reported cytotoxicity of single-walled carbon nanotubes that were acid-functionalized to yield a negative surface charge without testing positively charged carbon nanotubes. Since the NP used in this study were completely different from our PNP and other aspects like shape may play a role, a comparison with our results is hampered.

Recently, some reports have appeared about the interaction of NP with intracellular mitochondria that pointed towards an interaction of positive NP with mitochondria, hampering normal mitochondrial functioning.[3, 31-33] Surface charge-dependent interactions of PNP with cell membranes have been reported before by different groups.[34-36] Data derived from computer simulations of the interaction of differently charged NP with artificial bilayer lipid membranes within an in vitro setup showed that the interactions of NP with cells could be more complicated and also case specific.[37] These simulation data indicated that cationic gold NP could alter the integrity of the cell membrane and create pores in it, whereas the neutral and negative NP could not. An interesting finding of our study is the difference in cytotoxicity of the three different positive PNP, i.e. PNP-NH$_2$, PNP-DMEA and PNP-Py. It has been reported that primary amines were more cytotoxic than secondary and tertiary amines.[38] However, nothing was reported so far whether the same holds for NP with permanently positively charged surface groups. It can be expected that the ammonium/pyridinium-terminated PNP, which carry a positive charge that is permanent but also sterically somewhat buried, are more shielded and sterically hindered while approaching the cell membranes than the amine-terminated PNP. These results also indicate that a charge-driven differential membrane interaction of the PNP with the cell membrane plays a crucial role in their cytotoxicity. Very recently, Kim et al.[39] reported a similar trend of decreased cytotoxicity of amine-modified gold NP (2.5 ± 0.4 nm) with increasing steric shielding of the positive charge in the human breast cancer MCF-7 cell line thereby increasing the biocompatibility of these gold NP.

To investigate the cytotoxicity of the PNP in more detail, the production of intracellular ROS after exposure to different PNP was determined by the DCFH-DA assay. Induction of intracellular reactive oxygen radicals leading to oxidative stress has been identified by many groups as a possible mechanism of NP cytotoxicity.[40-44] Recently, Xia et al.[13] showed that cationic polystyrene NP were able to deplete the cellular ATP content. Interestingly, they also pointed towards an ROS-mediated change in the mitochondrial membrane potential ($\Delta\Psi_m$). It is unclear yet whether oxidative stress is the cause or merely an effect of the disruption of the normal mitochondrial function resulting in both ATP depletion and ROS production. However, a conclusion in favour of ROS being the mechanism of cytotoxicity should not be made. More data are required to elucidate whether intracellular ROS production is a cause or rather a consequence of toxicity.

From the CLSM data it could be seen that positive PNP showed stronger interactions with the cellular periphery. Similar results were previously reported by Rosso-Vasic et al.[45] who also found strong interactions of amine-terminated silicon NP with the cellular periphery. By contrast, the PNP-OH and PNP-COOH displayed only diffuse uptake and did not show any particular preference for intracellular localisation. It was confirmed by *z*-stack imaging that these NP were actually present inside the cells and not only on the surface. In contrast, the *z*-stack image of an NR8383 cell exposed to PNP-NH$_2$ (provided as supplemental information; see *Appendix B*) showed strong interaction of the PNP with the cell surface. Verma et al.[46,47] observed a stronger interaction of cationic NP with cell membranes compared with anionic ones as studied by CLSM. Apart from the overall electrostatic attraction of positive NP with the negative surface charge of the cell membrane, it was also hypothesised that the cationic charges facilitate interactions of NP with anionic binding sites on the cell membrane, like sialic acid residues.[48] This interaction results in binding of the positive NP to the cell membrane, which may ultimately result in their translocation across the membrane. The present study reveals that in addition to the nature of the charge, also the shielding of the charge by bulky groups may affect the membrane translocation, since uptake of NP by the NR8383 cells decreased with increasing steric shielding, i.e. cellular uptake of positive PNP decreased in the order PNP-NH$_2$ > PNP-DMEA > PNP-Py. However, for the negatively charged particles, the affinity of the NP for the negative cell membrane is much less. For this situation, we assumed that internalization of negative NP occurred via clustering of the NP in localized positive pockets in the cell membrane. Shi et al.[49] suggested that endocytotic processes like pinocytosis or simple diffusion are important pathways for cellular uptake of negative NP. In order to correlate the cytotoxicity of different PNP (positive and negative) on the basis of their internal cellular concentrations, the EC50 values were compared with the ratio of intracellular uptake of different PNP (ratio of intracellular uptake of PNP-NH$_2$: PNP-OH : PNP-COOH = 1 : 0.3 : 0.14). It was found that the positive PNP-NH$_2$ were intrinsically more cytotoxic than the negative PNP-OH and PNP-COOH as both PNP-OH and PNP-COOH failed to show cytotoxicity in spite of cellular uptake. This revealed that the positive PNP were intrinsically more cytotoxic compared with the other PNP and that the higher toxicity of positive PNP is in part due to the higher intrinsic toxicity once they have entered the cells. It should be taken into account, however, when making this comparison based on intracellular concentrations, that differences in cellular uptake of PNP are part of the overall mechanisms underlying differences in cytotoxicity and thus contribute to overall differences in cytotoxicity between differently charged PNP.

To investigate the role of endocytosis, the endocytotic processes in NR8383 cells were blocked either by incubating the cells at 4 °C or by exposing the cells to a mixture of 2-

deoxyglucose and sodium azide. Both methods inhibited ATP production within the cells and thus all energy-dependent endocytotic processes were inhibited. The inhibition of endocytosis severely hampered the cellular uptake of PNP-OH and PNP-COOH, whereas the uptake of positive PNP-NH$_2$ was not so much influenced. These experiments showed the differential importance of active transport mechanisms in the cellular uptake of different PNP. However, as even blocking of the endocytosis could not completely prevent the uptake of PNP (especially for positive PNP-NH$_2$), it is apparent that the intracellular internalization of these PNP involved more than one process. This is an important finding as it provides additional insight into the mode of cellular uptake of NP. Recently, the interactions between cell membranes and positive NP were studied using an in vitro modelling system. In one experiment, positively charged poly(amidoamine) (PAMAM) dendrimers of different generations were found to produce holes in a suspended lipid bilayer, whereas the anionic PAMAM dendrimers failed to do so.[50] It was also reported that these holes enabled the rapid internalisation of dendrimers inside the cells.[51] The stronger interaction of cationic NP compared with anionic ones and the ability of the cationic NP to form holes in lipid bilayers, have also been reported by others.[52, 53] It was also reported that positive NP reduced the flexibility of the cell membrane by making the liquid phase of the lipid membrane more rigid.[54] This finding has been supported by experiments with NP of different compositions.[55] With the help of AFM, Vasir et al.[56] demonstrated that the adhesive force between positive NP and a cell membrane is much higher than negative NP, implying the importance of surface charge.

We investigated the role of clathrin and caveolin receptors in cellular uptake of different PNP and found an overall surface charge-specific preference of different PNP towards these receptors (clathrin receptors for positive and caveolin receptors for negative PNP). Various groups reported on the role of clathrin-mediated and caveolin-mediated endocytosis in the cellular uptake of NP.[57-60] However, no systematic studies on the role of these receptors in a macrophage cell line have been reported so far. In this study, the surface charge-specific role of clathrin and caveolin receptors was investigated in NR8383 cells. A 450 mM sucrose solution was used to provide the necessary hypertonic atmosphere for inhibiting the clathrin receptors by causing polymerisation of these receptor proteins.[61] Similarly, a 1 μM solution of methyl-β-cyclodextrin (MβCD) was used to selectively block the caveolin receptors.[13] The MβCD causes sequestration of sterols from the lipid rafts of the caveolae resulting in its blockade. Harush-Frenkel et al.[62] found a similar dominant role for clathrin receptor-mediated endocytosis when they exposed HeLa cells to differently charged PEGylated NP. They reported activation of clathrin-dependent endocytosis for cationic NP, which was not observed for anionic NP. In a separate study, Huth et al.[63] found a clathrin receptor-mediated activation of endocytosis by cationic polyethyleneimine-coated NP. Similar findings were reported for Caco-2 cells.[64] These findings underline the complex nature of interactions that cells can undergo when they are exposed to charged PNP. While additional investigations are surely required to outline mechanistic details, our observations clarify the role of two of the factors (surface charge and degree of steric shielding around the charge) that are important in the cytotoxicity of PNP.

Conclusion

A series of monodisperse fluorescent tri-block copolymer NP (45 ± 5 nm) with different surface charges (positive, slightly negative and negative) and varying steric shielding around the

positive charges (e.g. $-NH_3^+$, $-N^+(CH_3)_2CH_2CH_2OH$ and pyridinium) were prepared and characterized. A systematic investigation of their cytotoxicity and cellular interactions including intracellular uptake was performed. It was found that the positive charge-bearing PNP were more cytotoxic than the negative ones. Also, by increasing the steric shielding of the positive charge-bearing groups, a lower cytotoxicity was found. Oxidative stress was found to be an important phenomenon associated with cytotoxicity of positive PNP. Positive PNP were interacting more strongly with the cell membrane and displayed a much higher cellular uptake efficiency than negative PNP. Endocytosis was found to be an important mechanism for internalisation of different PNP by the cells, with the positive PNP getting internalized predominantly by clathrin receptor-mediated and negative PNP by caveolin receptor-mediated endocytosis. These findings confirm that surface charge is important for the cytotoxicity of these PNP, while they additionally point to considerable additional effects of the steric bulk around the positive charges on PNP cytotoxicity.

References

1. Clift MJ, Bhattacharjee S, Brown DM, Stone V; *Toxicol. Lett.* 2010, 198:358–365.
2. Krug HF, Wick P; *Angew. Chem.* 2011, 50:1260–1278.
3. Xia T, Kovochich M, Brant J, Hotze M, Sempf J, Oberley T; *Nano Lett.* 2006, 6:1794–1807.
4. Nemmar A, Hoylaerts MF, Hoet PH, Vermylen J, Nemery B; *Toxicol. Appl. Pharmacol.* 2003, 186:38–45.
5. Bhattacharjee S, de Haan LHJ, Evers NM, Jiang X, Marcelis ATM, Zuilhof H, et al.; *Part. Fibre Toxicol.* 2010, 7:25.
6. Ruizendaal L, Bhattacharjee S, Pournazari K, Rosso-Vasic M, de Haan LHJ, Alink GM, et al.; *Nanotoxicology* 2009, 3(4):339–347.
7. Thubagere A, Reinhard BM; *ACS Nano* 2010, 4:3611–3622.
8. Dif A, Henry E, Artzner F, Baudy-Floc'h M, Schmutz M, Dahan M; *J. Am. Chem. Soc.* 2008, 130:8289–8296.
9. Zhang L, Granick S; *Nano Lett.* 2006, 6:694–698.
10. Yan X, He Q, Wang K, Duan L, Cui Y, Li J; *Angew. Chem. Int. Ed.* 2007, 46:2431–2434.
11. Wang B, Zhang L, Bae SC, Granick S; *Proc. Natl. Acad. Sci.* 2008, 105:18171–18175.
12. Asati A, Santra S, Kaittanis C, Perez JM; *ACS Nano* 2010, 4:5321–5331.
13. Xia T, Kovochich M, Liong M, Zink JI, Nel AE; *ACS Nano* 2008, 2:85–96.
14. Schatzlein AG, Zinselmeyer BH, Elouzi A, Dufes C, Chim YTA, Roberts CJ; *J. Control. Rel.* 2005, 101:247–258.
15. Xiao Y, Forry SP, Gao X, Holbrook RD, Telford WG, Tona A; *J. Nanobiotechnology* 2010, 8:13.
16. Osaka T, Nakanishi T, Shanmugam S, Takahama S, Zhang H; *Colloids Surf. B* 2009, 71:325–330.
17. Kemp SJ, Thorley AJ, Gorelik J, Seckl MJ, O´Hare MJ, Arcaro A; *Am. J. Respir. Cell Mol. Biol.* 2008, 39:591–597.
18. Yang P, Sun X, Chiu J, Sun H, He Q; *Bioconjugate Chem.* 2005, 16:494–496.
19. Green M, Howan E; *Chem. Commun.* 2005, 1:121–123.
20. Sayes CM, Gobin AM, Ausman KD, Mendez J, West JL, Colvin VL; *Biomaterials* 2005, 26:7587–7595.
21. Lin W, Huang YW, Zhou XD, Ma Y; *Int. J. Toxicol.* 2006, 25:451–457.
22. Kwon S, Kim H, Ha J, Lee S; *J. Ind. Eng. Chem.* 2011, 17:259–263.
23. Khoee S, Hassanzadeh S, Goliaie B; *Nanotechnology* 2007, 18:17.
24. Brand W, Schutte MW, Williamson G, van Zanden JJ, Cnubben NHP, Groten JP; *Biomed. Pharmacother.* 2006, 60:508–519.
25. Gentili PL, Mugnaia M, Bussotti L, Righini R, Foggi P, Cicchi S; *J. Photochem. Photobiol. A* 2007, 187:209–221.
26. Loccufier J, Bos MV, Schacht E; *Polym. Bull.* 1991, 27:201–204.
27. Hauck TS, Ghazani AA, Chan WC; *Small* 2008, 4:153–159.
28. Mayer A, Vadon M, Rinner B, Novak A, Wintersteiger R, Frohlich E; *Toxicology* 2009, 258:139–147.
29. Orr G, Panther DJ, Phillips JL, Tarasevich BJ, Dohnalkova A, Hu D; *ACS Nano* 2007, 1:463–475.

30. Saxena RK, Williams W, McGee JK, Daniels MJ, Boykin E, Gilmour MI; *Nanotoxicology* 2007, 1:291–300.
31. Li N, Sioutas C, Cho A, Schmitz D, Misra C, Sempf J; *Environ. Health Perspect.* 2003, 111:455–460.
32. Karatas OF, Sezgin E, Aydin O, Culha M; *Colloids Surf. B* 2009, 71:315–318.
33. Pan Y, Leifert A, Ruau D, Neuss S, Bornemann J, Schmid G, et al.; *Small* 2009, 5:2067–2076.
34. Cho EC, Xie JW, Wurm PA, Xia YN; *Nano Lett.* 2009, 9:1080–1084.
35. Villanueva A, Canete M, Roca AG, Calero M, Veintemillas-verdaguer S, Serna CJ; *Nanotechnology* 2009, 20:115103.
36. Martin AL, Bernas LM, Rutt BK, Foster PJ, Gillies ER; *Bioconjugate Chem.* 2008, 19:2375–2384.
37. Lin J, Zhang H, Chen Z, Zhng Y; *ACS Nano* 2010, 4:5421–5429.
38. Goodwin LG, Richards WHG, Udall V; *Br. J. Pharmacol.* 1957, 12:468–474.
39. Kim C, Agasti SS, Zhu Z, Isaacs L, Rotello V; *Nat. Chem.* 2010, 2:962–965.
40. Stone V, Donaldson K; *Nat. Nanotechnol.* 2006, 1:23–24.
41. Foucaud L, Wilson MR, Brown DM, Stone V; *Toxicol. Lett.* 2007, 174:1–9.
42. Wilson MR, Lightbody JH, Donaldson K, Sales J, Duffin R, Stone V; *Toxicol. Appl. Pharmacol.* 2002, 184:172–179.
43. Donaldson K, Aitken R, Tran L, Stone V, Duffin R, Forrest G; *Toxicol. Sci.* 2006, 92:5–22.
44. Brown DM, Donaldson K, Borm PJ, Schins RP, Dehnhardt M, Gilmour P; *Am. J. Physiol. Lung Cel Mol. Physiol.* 2004, 286:L344–L353.
45. Rosso-Vasic M, Spruijt E, Popovic Z, Overgaag K, van Lagen B, Grandidier B; *J. Mater. Chem.* 2009, 19:5926–5933.
46. Verma A, Uzun O, Hu Y, Hu Y, Han H, Watson N; *Nat. Mater.* 2008, 7:588–595.
47. Verma A, Stellacci F; *Small* 2010, 6:12–21.
48. Alberts AJB, Lewis J, Raff M, Roberts K, Walter P; 2002. Molecular Biology of the Cell. Garland Science, Taylor and Francis group. New York.
49. Shi X, Thomas TP, Myc LA, Kotlyar A, Baker JR; *Phys. Chem. Chem. Phys.* 2007, 42:5712–5720.
50. Leroueil PR, Hong SY, Mecke A, Baker JR, Orr BG, Holl MMB; *Acc. Chem. Res.* 2007, 40:335–342.
51. Hong SP, Bielinska AU, Mecke A, Keszler B, Beals JL, Shi XY; *Bioconjugate Chem.* 2004, 15:774–782.
52. Huang WM, Han XJ, Wang EK; *J. Electrochem. Soc.* 2003, 150:E218–E221.
53. Parimi S, Barnes TJ, Prestidge CA; *Langmuir* 2008, 24:13532–13539.
54. Mecke A, Lee DK, Ramamoorthy A, Orr BG, Holl MMB; *Langmuir* 2005, 21:8588–8590.
55. Hong SP, Leroueil PR, Janus EK, Peters J, Kober MM, Islam MT; *Bioconjugate Chem*. 2006, 17:728–734.
56. Vasir JK, Labhasetwar V; *Biomaterials* 2008, 29:4244–4252.
57. Huang M, Ma Z, Khor E, Lim LY; *Pharm. Res.* 2002, 19:1488–1494.
58. Panyam J, Labhasetwar V; *Pharm. Res.* 2003, 20:212–220.
59. Foster KA, Yazdanian M, Audus KL; *J. Pharm. Pharmacol.* 2001, 53:57–66.
60. Vrecl M, Anderson L, Hanyaloglu A, McGregor AM, Groarke AD, Milligan G; *Mol. Endocrin.* 1998, 12:1818–1829.

61. Suh H, Jeong B, Rathi R, Kim SW; *J. Biomed. Mater. Res.* 1998, 42:331–338.

62. Harush-Frenkel O, Debotton N, Benita S, Altschuler Y; *Biochem. Biophys. Res. Commun.* 2007, 353:26–32.

63. Huth S, Lausier J, Gersting SW, Rudolph C, Plank C, Welsch U; *J. Med. Genet.* 2004, 6:923–936.

64. Ma Z, Lim LY; *Pharm. Res.* 2003, 20:1812–1819.

Chapter 6

Cytotoxicity and cellular uptake of tri-block copolymer nanoparticles with different size and surface characteristics

Abstract

Background. Polymeric nanoparticles (PNP) are becoming increasingly important in nanomedicine and food-based applications. Size and surface characteristics are often considered to be important factors in the cellular interactions of these PNP although, systematic investigations on the role of surface properties on cellular interactions and toxicity of PNP are scarce. **Results.** Fluorescent, monodisperse tri-block copolymer nanoparticles with different sizes (45 and 90 nm) and surface charges (positive and negative) were synthesized, characterized and studied for uptake and cytotoxicity in NR8383 and Caco-2 cells. All types of PNP were taken up by the cells. The positive smaller PNP_{45} (45 nm) showed a higher cytotoxicity compared to the positive bigger PNP_{90} (90 nm) particles including reduction in mitochondrial membrane potential ($\Delta\Psi_m$), induction of reactive oxygen species (ROS) production, ATP depletion and TNF-α release. The negative PNP did not show any cytotoxic effect. Reduction in mitochondrial membrane potential ($\Delta\Psi_m$), uncoupling of the electron transfer chain in mitochondria and the resulting ATP depletion, induction of ROS and oxidative stress may all play a role in the possible mode of action for the cytotoxicity of these PNP. The role of receptor-mediated endocytosis in the intracellular uptake of different PNP was studied by confocal laser scanning microscopy (CLSM). Involvement of size and charge in the cellular uptake of PNP by clathrin (for positive PNP), caveolin (for negative PNP) and mannose receptors (for hydroxylated PNP) were found with smaller PNP_{45} showing stronger interactions with the receptors than bigger PNP_{90}. **Conclusion.** The size and surface characteristics of PNP (45 and 90 nm with different surface charges) play a crucial role in cellular uptake. Specific interactions with cell membrane-bound receptors (clathrin, caveolin and mannose) leading to cellular internalization were observed to depend on size and surface properties of the different PNP. These properties of the nanoparticles also dominate their cytotoxicity, which was analyzed for many factors. The effective reduction in the mitochondrial membrane potential ($\Delta\Psi_m$), uncoupling of the electron transfer chain in mitochondria and resulting ATP depletion, induction of ROS and oxidative stress likely all play a role in the mechanisms behind the cytotoxicity of these PNP.

Introduction

With the rapid appearance of nanotechnology-based products on the consumer market, human exposure to nanoparticles (NP) is unavoidable.[1] However, a serious lack of knowledge regarding the health and safety issues of these nanotechnology-based products is genuinely felt. A very important question in nanotoxicological research concerns the factors that determine the cytotoxicity of nanomaterials. Obviously, one of the factors is related to particle size. Due to their small size, NP have a high surface area to mass ratio, which may play a role in the interactions of NP with biomolecules (proteins, cell wall constituents, etc.) and in mechanisms underlying their toxicity when compared to undissolved bulk material. These mechanisms can involve chemical reactions and physical adsorption processes with different biomolecules. Both can ultimately lead to cellular uptake[2] and (cyto)toxic effects.[3] So far, little is also known on the mechanism of cellular uptake and intracellular distribution of different NP inside cells, and how factors like size can influence these.

Currently, many applications are foreseen in fields like NP-based drug delivery and bioimaging,[4-6] and for food-based applications.[7] Especially for drug delivery applications, the use of polymeric nanoparticles (PNP) is emerging as promising.[8] Recent advancements in polymer science allow synthesis of well-defined polymers (including tri-block copolymers) that can be tailor-made for specific purposes, like drug or food ingredient delivery through synthesis and use of biodegradable polymers. Additionally, these tri-block copolymers can be tagged with fluorescent probes to render them fluorescent and thus, traceable in biological environments. Thus, PNP derived from the tri-block copolymer can be utilized in the encapsulation of drugs or bioactive food ingredients, and hence can be exciting for drug or food ingredient delivery and sustained release preparations. Although much research is done on the synthesis of biologically valuable PNP, knowledge is lacking on how chemical and physical characteristics, like size and charge, influence the toxicity and bio-interactions of these PNP.

Therefore, it is essential to investigate how size and charge affect the cytotoxicity as well as other facets of NP-cell interactions, like cellular uptake. In order to interpret the results of such studies, it is essential that the investigated NP are well-characterized and comparable, so that only the size is different, while other factors like composition, surface groups, charge, etc. remain constant. Therefore, in this study particular care was taken that both the polymers and the PNP prepared thereof are well-defined and well-characterized to ensure that differences in biological properties only result from size differences for particles with the same surface groups.

The mechanism of nanomaterial toxicity is not completely clear, and it is possible that more than one mechanism is involved. Literature supports oxidative stress as being an important factor in the mechanism.[9-15] However, it remains to be established if oxidative stress is the mechanism underlying the NP induced cytotoxicity or a phenomenon accompanying this cytotoxicity. Recently, it was recognized that mitochondria can interact with charged NP, which can then influence the electron transport chain (ETC),[16] although the mechanism underlying this interaction and its exact consequences remain largely unknown. It is possible that due to the damage on the mitochondrial membrane as well as the disruption of the ETC caused by the PNP, the resulting oxidative stress may cause the production of different cytokines (like tumor necrosis factor-α/TNF-α),[17] which in turn is known to be a biomarker of inflammation.

Previously, it was postulated that NP can enter cells by passive diffusion[18] or adhesion.[19] However, this model has proven inadequate in explaining several findings. For example, this

model fails to explain why negative NP, which should be repelled by the negative cell membrane, can enter cells in overwhelming amounts.[20,21] Recently, receptor-mediated endocytosis was found to be crucial for the cellular uptake of different NP.[2,22,23] It is possible that cellular uptake of different PNP occurs through different cell membrane-bound receptors, like clathrin and caveolin receptors. These NP-receptor interactions have been related to antigen-antibody coupling reactions.[24] It is hypothesized that surface-functionalized and charge-bearing NP present an "epitope"-like structure, which is recognized and bound to the binding sites of different cell membrane-bound receptors. This initiates a cascade of reactions by which the NP are internalized. Therefore, a detailed investigation on the role of NP-receptor interactions in the cellular uptake of NP is justified with an aim to understand how size and surface charge influences cytotoxicity as well as cellular uptake of different PNP. The cellular in vitro models chosen were rat macrophage NR8383 cells and human colonic adenocarcinoma-derived Caco-2 cells. They represent models for two important targets for NP toxicity upon oral exposure including the innate immune response by phagocytosing cells and human enterocytes.

In this article, a method is described for the synthesis of well-characterized fluorescent PNP of different sizes (45 and 90 nm) and different surface charges from their corresponding tri-block copolymers. The presence of a fluorescent probe in the interior of the PNP makes investigations like bioimaging through confocal laser scanning microscopy (CLSM) possible. The influence of size and charge of the PNP on cytotoxicity as well as on intracellular uptake was studied with a variety of cytotoxicological tools. The influence of cell membrane-bound receptors in the internalization of PNP was investigated with receptor blocking studies and further visualization with CLSM.

Materials and methods

Synthesis of the fluorescent tri-block copolymers

The fluorescent probe, 4-(diethanolamino)-7-nitro-benzo[1,2,5]oxadiazole, was synthesized and characterized as reported in literature.[25] For the synthesis of Pol_{400}, a dry 100 ml three-necked round-bottom flask containing properly grinded and dried 1,6-hexanediol (2.0 g; 17 mmol) and 0.1 mg of fluorescent probe ($\sim 4 \times 10^{-4}$ mmol) was fitted with a reflux condenser and flushed with dry nitrogen for 30 min. Subsequently, the flask was heated on an oil bath at 120 °C with gentle stirring until the hexanediol melted. Then 50 μl of dry triethylamine was added to the mixture followed by drop-wise addition of 3.28 g (17.8 mmol) of dry adipoyl chloride. The mixture was gently stirred at 120 °C for 48 h until no more HCl was produced. Then, excess (40 g; 100 mmol) of PEG_{400} (carefully dried under reduced pressure) was added at 120 °C and the reaction mixture was heated while stirring for another 48 h. The resulting viscous mixture was poured into 50 ml of dry ether and the precipitate was filtered and washed repeatedly with dry ether. The precipitate was then stirred with 100 ml of distilled water and centrifuged at 900 rpm for 4 min. This process was repeated thrice. The resulting polymer was finally dried by overnight freeze drying and characterized by ^{1}H NMR (Bruker Avance III 400 MHz NMR spectrometer; $CDCl_3$), IR (infrared) spectroscopy, DSC, SEC and UV-Vis spectroscopy. Pol_{2000} with the same fluorescent probe was synthesized and characterized as described previously.[4]

Synthesis of fluorescent Pol$_{400}$ and Pol$_{2000}$ polymers with different end groups

A. Conversion to amines

In a dry three-necked 100 ml round-bottom flask fitted with a reflux condenser, 0.03 mmol of Pol$_{400}$ (330 mg) was heated at 120 °C until it melted. Then 11.2 mg (0.1 mmol) of chloroacetyl chloride was added slowly under stirring. The mixture was then stirred for 6 h. For conversion to the amine-terminated polymers, the mixture was cooled and 6.8 mg of 25 % (w/w) aqueous ammonia (0.1 mmol of ammonia) was added. The mixture was allowed to stir for another 12 h before workup. The polymer was purified and dried as mentioned before for Pol$_{400}$. Similarly, Pol$_{2000}$ with amine terminal groups was obtained.[4]

B. Conversion to acid

In a similar experimental set up as mentioned for the conversion to the amines, 10 mg (0.1 mmol) of succinic anhydride was added in portions to 0.03 mmol of molten Pol$_{400}$ polymer and allowed to react for 12 h at 120 °C. The purification was performed as described above.

C. Estimation of terminal hydroxyl group conversion with trichloroacetyl isocyanate (TAIC)

In an NMR tube with Pol$_{400}$ polymer sample dissolved in CDCl$_3$, 10 µl of TAIC was added and the tube was vortexed for 5 min.[4] Then after another 10 min, ^{1}H NMR spectra were recorded and the peak appearing at $\delta = 4.43$ ppm was integrated and compared with the value obtained from unmodified polymer to obtain the conversions of the terminal -OH groups.[26]

Synthesis and characterization of nanoparticles (NP)

NP were prepared by the nanoprecipitation method using a slight modification of the method described by Khoee et al.[27] First, 10 mg of tri-block copolymer (Pol$_{400}$ or Pol$_{2000}$ to obtain PNP$_{90}$ and PNP$_{45}$, respectively) were dissolved in 2 ml THF with mild heating (~35 °C) and the solution was then injected into 10 ml of vigorously stirred ultrapure water in an open beaker.[4] The dispersion was stirred for another 30 min. Then THF was removed under reduced pressure and the aqueous dispersion was filtered through 0.2 µm cellulose filters. Essentially no material remained on the filter. These stock solutions were diluted in measuring flasks to obtain solutions with well-defined concentrations. The hydrodynamic radius of the PNP, both in aqueous dispersions and in F12-K and DMEM cell culture media were determined by DLS at 90° and their ζ-potential was obtained with a Malvern Zetasizer. The cell culture mediums (F12-K and DMEM) were also checked by DLS and ζ-potential measurements. While the DLS failed to measure any

particulate material > 5 nm in size, the ζ-potential measurements varied between -5 to -10 mV, which can be attributed to the anionic protein molecules originating from the FCS. The serial dilutions of PNP in F12-K or DMEM media were also checked by DLS to exclude any agglomeration of PNP occurring within the tested concentration range. The probability of monomers of the tri-block copolymer leaking out of the PNP resulting in the disintegration of the PNP was excluded by both the SEC and DLS performed at different intervals.

Scanning Electron Microscopy

A clean circular cover glass, 8 mm diameter, (Menzel, Braunschweig, Germany) was fitted on a sample holder by carbon adhesive tabs (EMS, Washington, USA) and 50 μl of an aqueous suspension of PNP was put on the glass and the water was allowed to evaporate until the PNP that remained behind were completely dried.[4] The dry sample was sputter-coated with 2 nm tungsten (MED 020, Leica, Vienna, Austria). Samples were analysed at 2 kV at room temperature in a field emission scanning electron microscope (Magellan 90, FEI, Eindhoven, the Netherlands).

Cell lines

Rat alveolar macrophage (NR8383) and human colonic adenocarcinoma (Caco-2) cells were obtained from ATCC (Manassas,VA).[14,15] The NR8383 and Caco-2 cells were cultured in 150 cm^2 cell culture flasks with 25 ml F12-K culture medium (Gibco 21127) and DMEM medium, respectively, both supplemented with 10 % (v/v) heat-inactivated foetal calf serum (FCS) and 0.1 % (v/v) gentamicin, in a humidified atmosphere containing 5 % CO_2 at 37 °C.

Cytotoxicity measurement by MTT assay

A. NR8383 cells. An NR8383 cell suspension was centrifuged at 140 *g* for 5 min before re-suspending the cell pellet in F12-K medium followed by counting and adjusting the cellular concentration to 2×10^5 cells/ml. The cells were then seeded in a 96-well plate (50 μl/well) and the plate was kept in a 5 % CO_2 incubator at 37 °C for 24 h. Subsequently, 50 μl of serial dilutions of freshly prepared and well-vortexed different PNP_{90} in F12-K medium were added to the cells to obtain the required final concentrations.[14,15] The concentration range of 0-400 μg/ml was chosen because these concentrations appeared to detect the differences in toxic responses of the cells to the different PNP. This was followed by incubation for another 24 h after which 5 μl of MTT solution in PBS (5 mg/ml) was added to each well and the plate was incubated for another 4 h. Then 100 μl of pure dimethylsulfoxide (DMSO) was added to each well to dissolve the formazan crystals. As the NR8383 cells are a suspension cell line, the medium in the wells of the 96-well plates could not be evacuated before addition of DMSO to the wells as also described before.[28] The absorption of each well was measured at 562 nm in a 96-well plate reader and the background absorption at 612 nm was subtracted. Mitochondrial metabolic activity for each concentration of PNP was expressed as % of the corresponding negative control reading.

Medium without PNP and medium with Triton-X (0.01 %) were used as negative and positive controls, respectively. Additional control experiments were performed in order to exclude a possible interference with the absorption by the PNP themselves by measuring the absorbance values in a similar set-up after mixing MTT reagent as well as only F12-K medium with different dilutions of PNP_{90}.

B. Caco-2 cells. The Caco-2 cells were plated at a concentration of 10^5 cells/ml in a 96-well plate (100 µl/well) and were incubated at 37 °C for 24 h.[14,15] Then different freshly prepared and well-vortexed PNP_{90} in DMEM medium were added to the cells (100 µl/well) to achieve the final concentrations followed by further incubation of 24 h at 37 °C. 5 µl of MTT solution (in PBS) was then added to each well followed by an incubation of 4 h. Each well was then carefully emptied (because unlike NR8383 the Caco-2 cells attach to the bottom of the wells) without dislodging the precipitated crystals and the crystals were dissolved in pure DMSO (100 µl/well). Finally, each well was measured as mentioned above. Control experiments, as mentioned before, were also done.

C. Phagocytic index measurement in NR8383 cells

An NR8383 cell suspension (2×10^5 cells/ml) was seeded in a 96-well plate (50 µl/well) in F12-K medium, followed by addition of 50 µl/well of serial dilutions of freshly prepared and well-vortexed PNP_{90} in F12-K medium to obtain the required final test concentrations of PNP.[14,15] Plain F12-K medium without PNP_{90} and medium containing 100 µM $CuSO_4$ were used as negative and positive controls, respectively. After 24 h, the cells were exposed to yellow-green fluorescent latex beads (1 µm size) at a ratio of beads to cells in each well of 50:1. After 4 h of incubation, counting samples were taken from the wells and viewed first under a fluorescent microscope to visualize the fluorescent beads, followed by bright-field view to visualize the cells. Samples were also taken out of each well to assess the cell viability by trypan blue exclusion test. The phagocytic index was determined by calculating the average number of fluorescent beads phagocytosed per viable cell and expressed as % of the negative control. Control experiments were run with only PNP in absence of fluorescent latex beads (1 µm) and no phagocytic vacuole inside the NR8383 cells could be seen.

Measurement of intracellular ROS by DCFH-DA assay

A. NR8383 cells. The cell suspension was adjusted to 2×10^5 cells/ml and seeded in a 96-well plate (50 µl/well) in F12-K medium. 50 µl/well of serial dilutions of freshly prepared and well-vortexed PNP_{90} in F12-K medium were added to obtain the required final test concentrations of PNP. A concentration of 10 mM H_2O_2 was used as positive control, and F12-K medium without PNP as negative control. After 6 h of exposure to the PNP, 5 µl of a 20 mM solution of DCFH-DA was added to each well and the plates were incubated for another 18 h in a 5 % CO_2 atmosphere at 37 °C. The fluorescence was then measured in a fluorometer (λ_{ex} = 485 nm and λ_{em} = 538 nm). The fluorescence induction factor for each concentration of PNP_{90} was calculated by dividing the reading of each well by the average reading of the negative control and expressed as %. Control

experiments were performed by incubating the PNP_{90} at their test concentrations with DCFH-DA in the absence of cells to check the possibility of a positive fluorescence reading caused by reaction of DCFH-DA with PNP_{90} alone.[14,15]

B. Caco-2 cells. The cells were suspended in DMEM medium to a concentration of 10^5 cells/ml after trypsinization and were seeded in a 96-well plate (100 μl/well). After 24 h the cells were exposed to 100 μl/well of final concentrations of freshly prepared and well-vortexed different PNP_{90} in DMEM medium. Following another 6 h of PNP_{90} exposure, 5 μl of a 20 mM solution of DCFH-DA was added to each well. The plate was further incubated for 18 h before measurement of the fluorescence was carried out as described above.

Measurement of mitochondrial membrane potential (ΔΨ$_m$)

The NR8383 and Caco-2 cells were plated and exposed to serial dilutions of freshly prepared and well-vortexed PNP of both sizes (45 and 90 nm) as mentioned before. The mitochondrial membrane potential ($\Delta\Psi_m$) was measured by a commercially available kit from Invitrogen (MitoProbe™; Transition Pore Assay Kit; Catalogue No. M34153) and expressed as % of negative control (0 μg/ml). A 100 μM solution of ionomycin in DMSO (supplied with the kit) and F12-K or DMEM medium without PNP were used as positive and negative controls, respectively.

Measurement of intracellular ATP content

The NR8383 and Caco-2 cells were seeded in a 96-well plate and exposed to different freshly prepared and well-vortexed PNP_{90} and PNP_{45} as mentioned before. After 24 h the intracellular ATP content of each well was measured by a commercial ATP measuring kit (Sigma Aldrich, Product No. FLASC) and results were expressed as % of negative control. Cells exposed to medium without PNP and to medium with 75 mM 2,4-DNP (2,4-dinitrophenol) were used as negative and positive controls, respectively.

Measurement of TNF-α release in NR8383 cells

The NR8383 cells were seeded in a 96-well plate and exposed to different concentrations of freshly prepared and well-vortexed PNP_{90} of each type, as mentioned above. After 24 h the supernatants were collected, centrifuged at 1000 g for 10 min, and then spectrophotometrically analysed for the TNF-α content with a commercial rat TNF-α kit (Invitrogen), using the procedure from the manufacturer's manual. Medium without PNP and medium with 0.1 μg/ml lipopolysaccharide (LPS)[29] were used as negative and positive controls, respectively.

Confocal laser scanning microscopy (CLSM)

For performing CLSM, a drop of the NR8383 or Caco-2 cell suspension was placed on a glass slide and viewed through an oil immersion lens (100×) of a confocal microscope (Zeiss Exciter). For assessment of the average fluorescence intensity, readings from 20 individual cells from five different optical fields (for each PNP_{90}) in focus selected from five separate experiments (n = 5) were used. All the measurements were done at the same excitation wavelength (λ_{ex} = 488 nm and λ_{em} = 543 nm), laser power, pinhole opening and detector gain. To exclude any background fluorescence, control samples of NR8383 or Caco-2 cells not exposed to the different PNP_{90}, were also investigated by CLSM. These NR8383 or Caco-2 cells did not show any background fluorescence. Non-fluorescent PNP_{90} were also tested to exclude any additional fluorescence from the PNP.

Effect of inhibition of endocytosis

A. Inhibition of endocytosis by performing the experiment at 4 °C

The NR8383 and Caco-2 cells (after trypsinization) were seeded and exposed to non-toxic 1 µg/ml concentrations of different PNP_{90} in a 96-well plate as mentioned above and were both pre-incubated and incubated at 4 °C. Results of the CLSM images (λ_{ex} = 488 nm; λ_{em} = 543 nm) were compared to results from similar incubations performed at 37 °C.[4] A figure of colony of NR8383 cells that have taken up fluorescent $PNP_{90}\text{-}NH_2$ is provided as supplementary information (see *Appendix C*). Control experiments with cells exposed to PNP without a fluorescent probe (non-fluorescent PNP) of similar sizes and surface groups were done. Non-fluorescent PNP in absence of cellular system were also tested by CLSM and did not show any fluorescence signal. The results for PNP_{90} were then compared with PNP_{45}.[4]

B. Inhibition of endocytosis by exposure to a mixture of 2-deoxyglucose and sodium azide

An NR8383 or Caco-2 cell suspension was exposed to a mixture of 50 mM 2-deoxyglucose and 10 mM sodium azide[30] for 30 min at 37 ºC before being centrifuged and generously washed with PBS at least three times to remove the exposure medium. Finally, the cells were plated and exposed to different PNP_{90} at 37 °C as described before. The results for PNP_{90} were then compared with PNP_{45}.[4]

Inhibition of clathrin and caveolin receptor-mediated endocytosis

The NR8383 and Caco-2 cells were exposed to 450 mM sucrose (to inhibit clathrin receptors)[31] or to 1 µM methyl-beta-cyclodextrin (MβCD) (to inhibit caveolin receptors)[32] for 30 min before being washed, plated and exposed to different PNP_{90} at 37 °C. Control experiments were done by incubating the cells with 10 µg/ml of Alexa Fluor 488 nm-conjugated transferrin (known substrate for clathrin/ λ_{ex} = 495 nm and λ_{em} = 519 nm)[33] or 5 µg/ml of Alexa Fluor 488 nm-conjugated cholera toxin subunit-B (known substrate for caveolin/ λ_{ex} = 495 nm and λ_{em} = 519 nm)[33] for 30 min on ice followed by thorough washing with PBS thrice and then performing CLSM on the cells in order to confirm the blockade of the clathrin and caveolin receptors. It was

seen that the inhibitors used (sucrose and MβCD) could block > 90 % of the normal uptake of transferrin or cholera toxin for both the cell lines (see *Appendix C*) without any additional cytotoxicity. The results for PNP_{90} were then compared with PNP_{45}.[4]

Inhibition of mannose receptor mediated endocytosis

The NR8383 cells were exposed to a 2 mg/ml concentration of α-mannan for 2 h in order to inhibit the mannose receptors[34] before being washed, plated and exposed to different PNP_{90} and PNP_{45} at 37 °C.

Statistical analysis

Data were analysed with Origin Pro (version 8.0) graphing software. For statistical analysis a student's *t*-test was performed and data with $p < 0.05$ (compared to negative control) were marked with an asterisk (*) sign. Each data point represents the average from three independent experiments (n = 3) (for CLSM studies n = 5) and is presented as the arithmetic mean ± standard error of mean (SEM). While comparing the effect of size, the results for PNP_{45} and PNP_{90} were also mutually compared and only the statistically significantly different ($p < 0.05$) data between the two were marked by "†" sign.

Results

Synthesis of the fluorescent tri-block copolymers

Synthesis of fluorescent polyethylene glycol₄₀₀-polyhexylene adipate-polyethylene glycol₄₀₀ [PEG₄₀₀-PHA-PEG₄₀₀] (Pol₄₀₀) polymer

The reaction scheme for the synthesis of Pol_{400} is depicted in Figure 1. The synthesis is similar to the previously reported[4] synthesis of fluorescent Pol_{2000} polymer [polyethylene glycol₂₀₀₀-polyhexylene adipate-polyethylene glycol₂₀₀₀]. From proton nuclear magnetic resonance (^{1}H NMR) (see *Appendix C*) analysis of the polymer, an estimation of the molecular weight (~9 kDa) was made, which was in agreement with the data obtained from size exclusion chromatography (SEC) (see *Appendix C*). From the infrared (IR) spectrum of the polymer (see *Appendix C*) the carbonyl (C=O) stretch from the polyester middle block could easily be seen at 1737 cm^{-1}. From these combined data, it is inferred that the middle block has about 35-40 repeating units. From SEC, a polydispersity index (PDI = M_w/M_n where M_w = molecular weight; M_n = relative molecular weight) of 1.47 was obtained for Pol_{400} (Table 1). Based on the average chain length of the polymer molecules as well as the initial amount of probe, it is estimated that roughly ~1 % of the polymer molecules contained a fluorescent probe, embedded in the hydrophobic middle block.
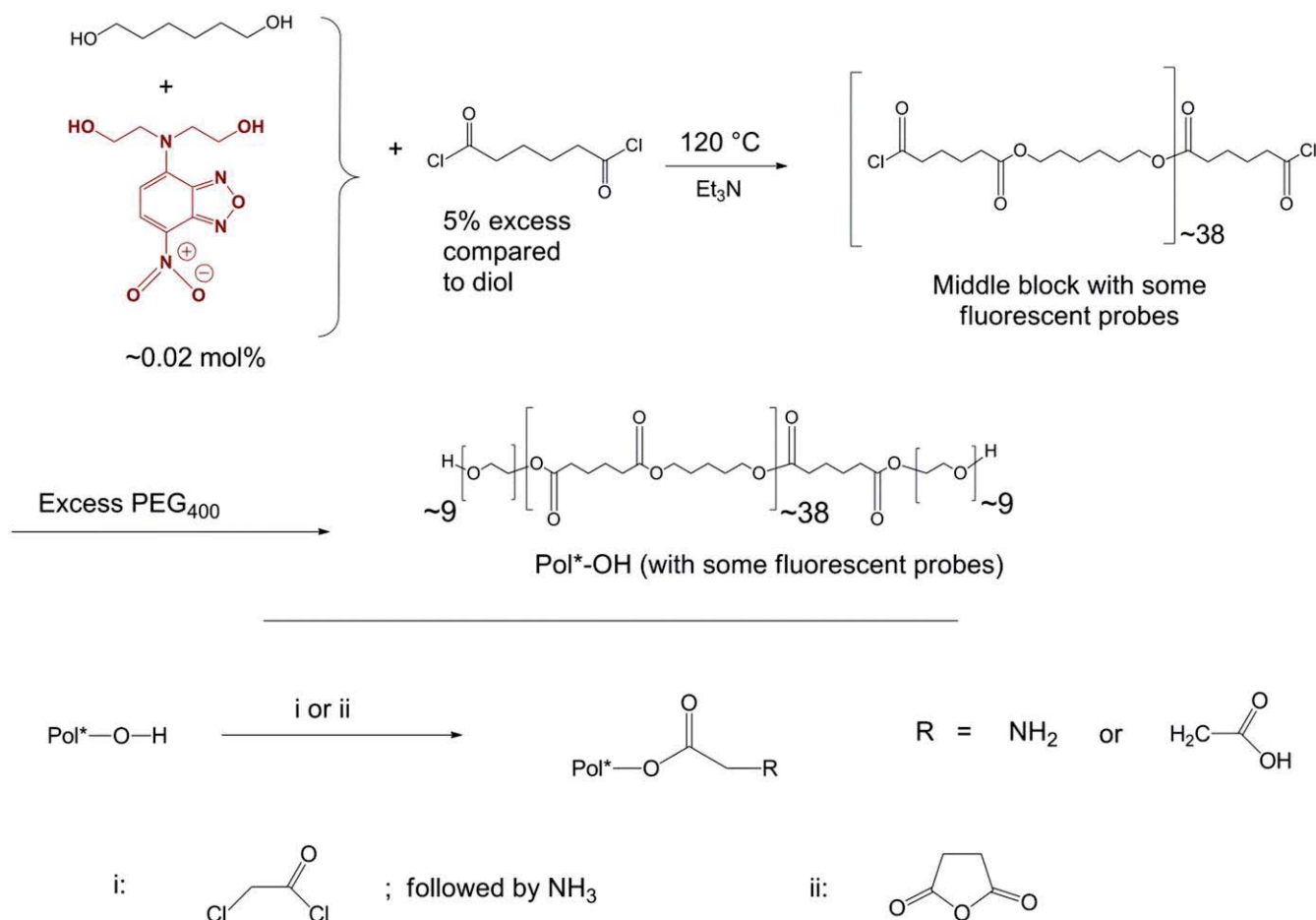
Figure 1: *Overview of the synthesis of PEG$_{400}$-PHA-PEG$_{400}$ (Pol$_{400}$) polymer with fluorescent probe and further conversion of the terminal hydroxyl groups to different functional end groups.*

Conversion of terminal hydroxyls to differently charged end groups

The terminal hydroxyl (-OH) groups of Pol$_{400}$ were converted into an amine by first reacting the polymer with chloroacetyl chloride and subsequently adding concentrated ammonia, which yielded Pol$_{400}$-NH$_2$. Reacting the polymers with succinic anhydride yielded Pol$_{400}$-COOH. In contact with water at neutral pH, this means that the terminal groups will be either positively charged (-NH$_3^+$) or negatively charged (COO$^-$) due to the pK$_a$ values of these groups. The degree of conversions of the terminal hydroxyl groups was assessed by reaction with trichloroacetyl isocyanate (TAIC).[26] Reaction of TAIC with terminal hydroxyl groups gives a characteristic peak in the ^{1}H NMR spectrum at δ = 4.43 ppm. Upon converting these -OH groups to amino or carboxylate moieties, this reaction with TAIC is not possible anymore, and this peak is thus smaller or even absent, depending on the conversion to -NH$_3^+$ or -COO$^-$. This analysis was used to quantify this conversion (Table 1 and *Appendix C*), which turned out to be almost quantitative for all polymers. The data on the characterization of Pol$_{400}$, including the conversions of the end hydroxyl groups to different functional groups (-NH$_2$ and -COOH) are

given in Table 1. The melting points of all polymers were determined by differential scanning calorimetry (DSC) and were found to be ~43 °C for all polymers. This indicates that the melting point is only determined by the middle block, which has the same length in all synthesized polymers.

Table 1: *Data of Pol$_{400}$ with its end group conversion rates.*

Polymer	Molecular weight (kDa)		Melting point (^{o}C)	PDI	Converted to	Conversion (%)
Pol$_{400}$	**^{1}H NMR** 9.0		43	1.47	Pol$_{400}$-NH$_2$	> 90
	SEC 9.0				Pol$_{400}$-COOH	> 90

Synthesis and characterization of different PNP

The different PNP$_{90}$ were prepared by nanoprecipitation, where a solution of Pol$_{400}$ polymer in tetrahydrofuran (THF) was injected into vigorously stirred water. Similarly, different PNP$_{45}$ were obtained from Pol$_{2000}$.[4] This resulted in a stable clear aqueous dispersion of PNP$_{90}$-X or PNP$_{45}$-X (X = NH$_2$, OH and COOH). The size of PNP$_{90}$ was 90 ± 5 nm as determined by scanning electron microscopy and supported by dynamic light scattering (DLS). Both DLS and scanning electron microscopy (Figure 2) data showed particles of comparable size and also revealed that their structural integrity is maintained, even upon drying. The scanning electron microscopy pictures of PNP$_{90}$-NH$_2$, PNP$_{90}$-OH and PNP$_{90}$-COOH are provided in *Appendix C*. The average ζ-potentials of these PNP$_{90}$ in aqueous dispersions (0.1 µg/ml) were found to be +22 mV for PNP$_{90}$-NH$_2$, -4 mV for PNP$_{90}$-OH and -19 mV for PNP$_{90}$-COOH. The hydrodynamic sizes of these PNP were also determined by DLS in F12-K and DMEM medium (0.1 µg/ml) that contained fetal calf serum (FCS). Upon addition of these PNP$_{90}$ into cell culture mediums, the sizes increased mainly due to surface adsorption of proteins although the polydispersity did not increase considerably. The DLS data of different PNP$_{90}$ are given in Table 2.

Table 2: *DLS data of PNP$_{90}$.*

| Type	Size in water (nm)	Size in F12-K (nm) (after 1 h)	Size in DMEM (nm) (after 1 h)
PNP$_{90}$-NH$_2$	*90 ± 5*	*145 ± 5*	*140 ± 5*
PNP$_{90}$-OH	*90 ± 5*	*115 ± 5*	*120 ± 5*
PNP$_{90}$-COOH	*90 ± 5*	*120 ± 5*	*130 ± 5*
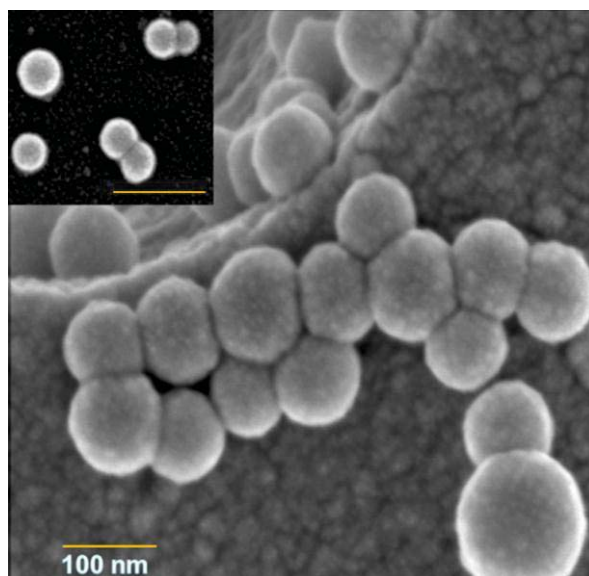
Figure 2: Scanning electron microscopy *image of monodisperse PNP$_{90}$ (90 ± 5 nm) and PNP$_{45}$ (45 ± 5 nm) (as insert). Scale bars show 100 nm.*

Evaluation of the cytotoxicity of nanoparticles

A. MTT assay. The cell viability of the different PNP$_{90}$ was determined in two different cell lines, i.e. NR8383 and Caco-2 cells. The PNP$_{90}$ were studied in the concentration range of 0-400 µg/ml after 24 h exposure and the results were compared with the data obtained previously for PNP$_{45}$.[4] These data are shown in Figure 3. Positively charged PNP$_{90}$-NH$_2$ were cytotoxic within the tested concentration range, whereas the negatively charged ones were not. The PNP$_{45}$-NH$_2$ were more cytotoxic than PNP$_{90}$-NH$_2$ as can be seen from the EC50 values (Table 3). Upon exposure to the positive control Triton-X (0.01 %), NR8383 and Caco-2 cells both showed a cell viability of ~1 % compared to their viability upon exposure to the negative control (0 µg/ml).
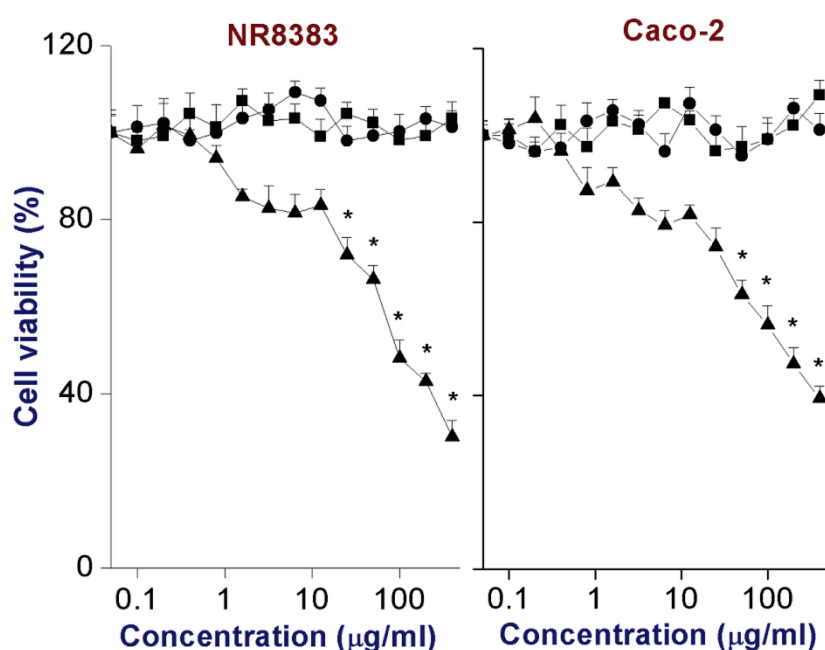
Figure 3: *Cytotoxicity of PNP$_{90}$-NH$_2$ (▲), PNP$_{90}$-OH (■) and PNP$_{90}$-COOH (●) on NR8383 and Caco-2 cells as measured by the MTT assay after 24 h exposure. The * sign signifies p < 0.05 compared*

B. Phagocytic Index (PI) measurement. The PI for macrophage NR8383 cells was determined by measuring the capability of the cells to phagocytose 1 μm fluorescent latex beads (see Figure 4). Like in the MTT assay, the positive PNP showed signs of cytotoxicity by causing a decrease of the PI upon increasing the concentration of PNP, whereas the negative PNP did not show any effect at all in the tested concentration range. The PNP_{45}-NH_2 was relatively more cytotoxic than PNP_{90}-NH_2, as can be derived from the EC50 values (Table 3). The NR8383 cells exposed to the positive control (100 μM $CuSO_4$) showed ~1 % PI compared to the NR8383 cells exposed to the negative control (0 μg/ml).
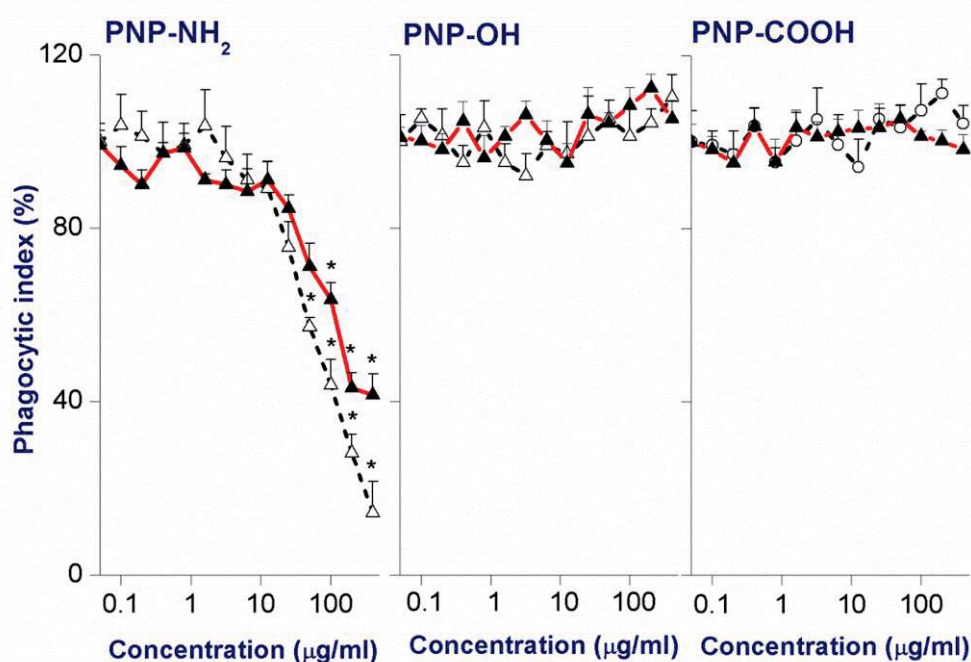
Figure 4: *Phagocytic Index (PI) in NR8383 cells after 24 h exposure to different PNP_{45} (Δ) and PNP_{90} (▲). The * sign signifies p < 0.05 compared to negative control (0 μg/ml).*

Assessment of intracellular reactive oxygen species (ROS) production by DCFH-DA assay

PNP with chemically reactive surfaces can interact with biological molecules resulting in production of radicals including reactive oxygen species (ROS), which in turn can cause toxicity. Production of ROS can be tested with the DCFH-DA assay, which measures the intracellular production of ROS. Positive PNP_{90}-NH_2 were able to induce intracellular ROS production in both NR8383 and Caco-2 cells, whereas negative PNP (both PNP_{90}-OH and PNP_{90}-COOH) did not (Figure 5). Furthermore, in both NR8383 and Caco-2 cells, the induction of intracellular ROS production with PNP_{45}-NH_2 was stronger than with PNP_{90}-NH_2 (see Table 3 for EC50 values). These results matched the results of the MTT assay and indicate a possible relation between oxidative stress and cell viability. Exposure of the NR8383 and Caco-2 cells to the positive control (10 mM H_2O_2) caused ~1000 % and ~900 % induction of ROS production, respectively, compared to the level of ROS production (100 %) in cells exposed to the negative control (0 μg/ml).
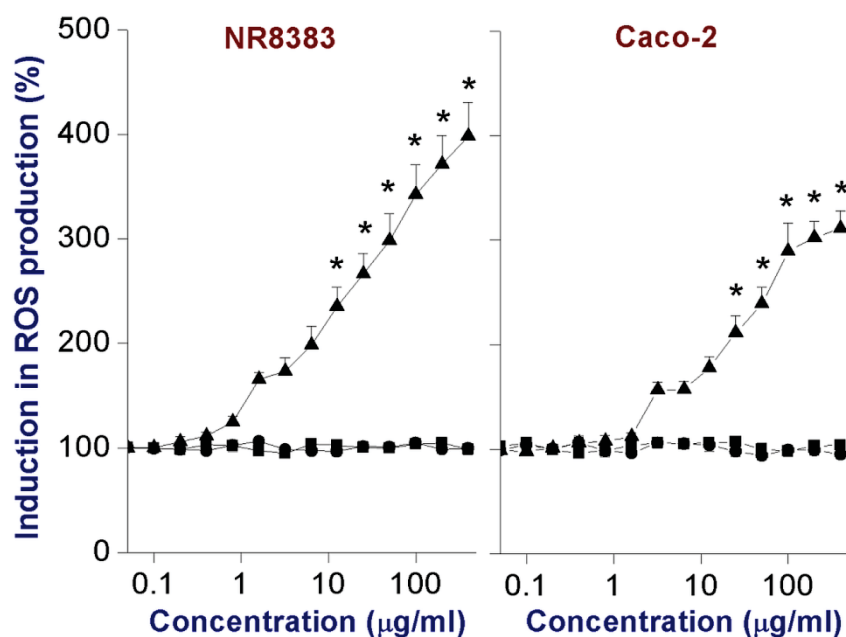
**Figure 5:** *Intracellular ROS induction in NR8383 and Caco-2 cells after 24 h exposure to PNP_{90}-NH_2 (▲), PNP_{90}-OH (■) and PNP_{90}-COOH (●). The * sign signifies $p < 0.05$ compared to negative control (0 µg/ml).*

Table 3: *EC50 values (µg/ml) obtained from different assays after 24 h exposure of NR8383 and Caco-2 cells to positively charged $PNP_{45}{}^4$ and PNP_{90}.*

Assay	Parameter	Reference figure	Cell line	PNP_{90}-NH_2 (90 ± 5 nm)	PNP_{45}-NH_2 (45 ± 5 nm)
MTT	Cell viability	3	NR8383	55	31
			Caco-2	68	54
PI	Phagocytosis	4	NR8383	80	64
DCFH-DA	Intracellular ROS production	5	NR8383	23	13
			Caco-2	33	21
Mitochondrial membrane potential ($\Delta\Psi_m$)	Mitochondrial membrane potential	6	NR8383	5	2
			Caco-2	6	3
ATP	Cellular ATP content	7	NR8383	26	14
			Caco-2	62	36
TNF-α	TNF-α release	8	NR8383	37	25
			Caco-2	63	32

Assessment of mitochondrial membrane potential ($\Delta\Psi_m$)

Figure 6 shows the results from assessment of the mitochondrial membrane potential ($\Delta\Psi_m$) in NR8383 and Caco-2 cells exposed to increasing concentrations of PNP_{45} or PNP_{90} with different charges. Only the cationic PNP ($-NH_2$ terminated) of both sizes, showed signs of decreasing the $\Delta\Psi_m$ for both the NR8383 and Caco-2 cells, whereas the anionic ones (-OH and -COOH terminated) did not show any effect. The EC50 values are given in Table 3. The smaller cationic PNP_{45} were more effective, reflected by lower EC50 values, compared to the bigger PNP_{90}. This reduction in mitochondrial membrane potential ($\Delta\Psi_m$) may affect ATP generation in the cells, thereby contributing to the mode of action for the cellular toxicity. Exposure of the cells to the positive control (100 μM ionomycin) caused a decrease of $\Delta\Psi_m$ to < 2 % of the $\Delta\Psi_m$ detected in cells exposed to the negative control (0 μg/ml).
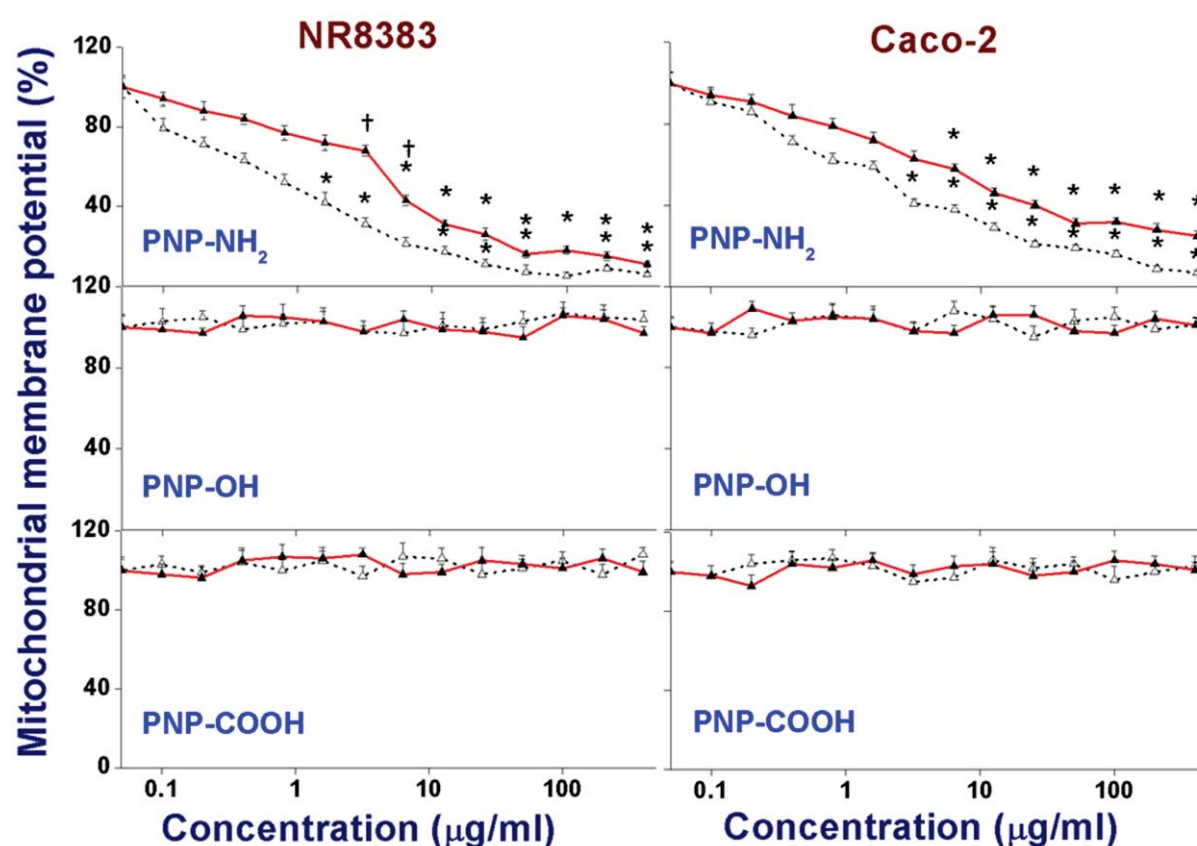
*Figure 6: Mitochondrial membrane potential ($\Delta\Psi_m$) of NR8383 and Caco-2 cells after 24 h exposure to different PNP_{45} (Δ) and PNP_{90} ($\blacktriangle$) as % of negative control (0 μg/l). The * sign signifies $p < 0.05$ compared to negative control (0 μg/ml). The "†" sign signifies $p < 0.05$ when compared between the PNP_{45} and PNP_{90}.*

Assessment of intracellular ATP content

As a consequence of interaction of charged NP with mitochondria, disruption of the electron transport chain reflected by a reduction of the mitochondrial membrane potential

($\Delta\Psi_m$) can occur. This may result in ROS production and in depletion of the cellular ATP content, the latter being an (additional) possible mechanism of cytotoxicity. Therefore, the intracellular ATP content of cells after exposure to PNP was determined. The intracellular ATP content after 24 h exposure to different PNP_{90} and PNP_{45} is shown in Figure 7 and the EC50 values are given in Table 3. Both NR8383 and Caco-2 cells showed a gradual dose-dependent decrease in intracellular ATP content only upon exposure to the positive PNP. This ATP depletion was more profound for PNP_{45} than for PNP_{90}. Exposure of the cells to the positive control (75 mM 2,4-dinitrophenol/DNP) caused a decrease of intracellular ATP to < 2 % of the levels in cells exposed to the negative control (0 µg/ml).
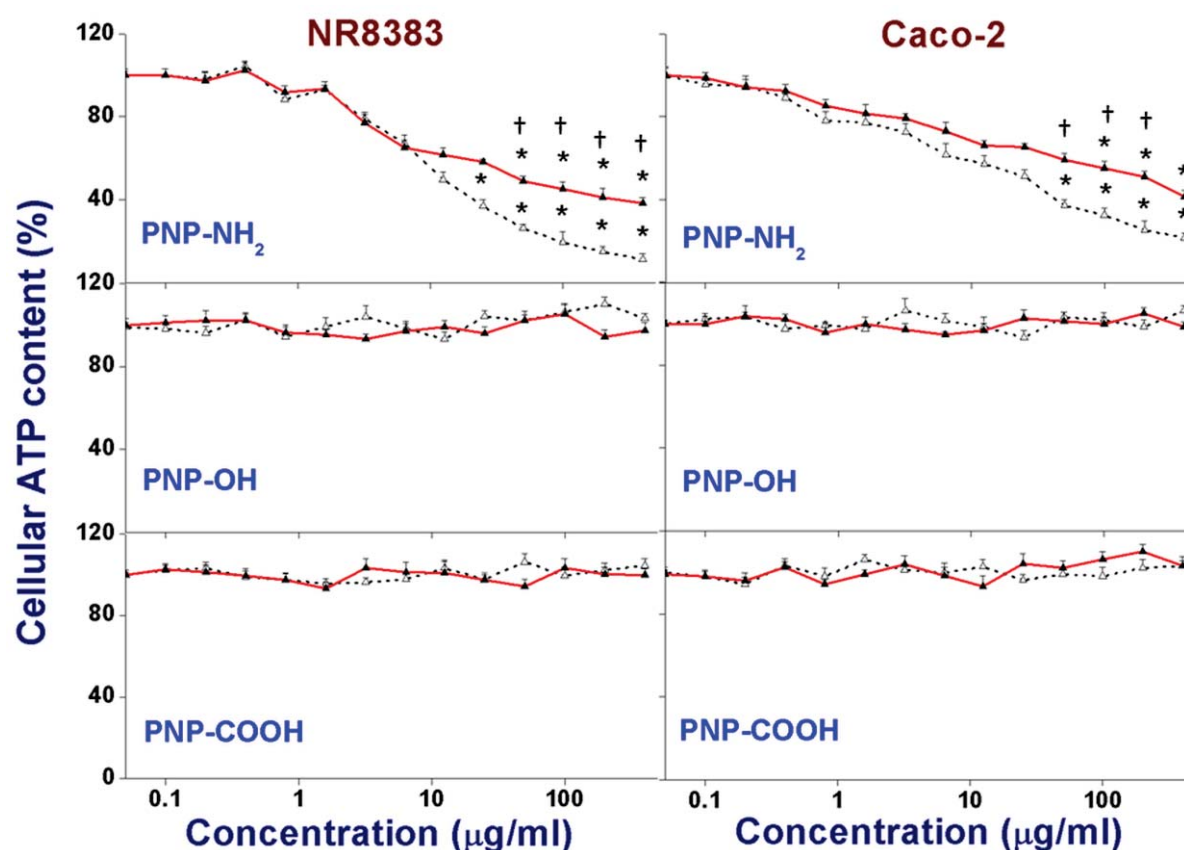
Figure 7: *Effect on cellular ATP content in NR8383 and Caco-2 after 24 h exposure to different PNP_{45} (Δ) and PNP_{90} (▲) as % of negative control (0 µg/l). The * sign signifies $p < 0.05$ compared to negative control (0 µg/ml). The "†" sign signifies $p < 0.05$ when compared between the PNP_{45} and PNP_{90}.*

Assessment of TNF-α production

TNF-α is a major biomarker cytokine for pro-inflammatory response. It can stimulate an acute phase reaction as well as apoptosis in living tissue.[35] Hence, a surge in the production of intracellular TNF-α indicates inflammation, which can also be a factor for the toxicity caused by PNP. The TNF-α production in NR8383 cells was measured for both sizes of PNP (45 and 90 nm) after 24 h exposure (see Figure 8). Only positive PNP of both sizes showed significant induction

of the TNF-α production. As found in the other cytotoxicity experiments, the results again indicate that the smaller positive PNP_{45} were more toxic than positive PNP_{90}. The corresponding EC50 values are listed in Table 3. Exposure of the cells to the positive control (lipopolysaccharide/LPS) caused an increase of TNF-α to > 900 pg/ml in both the NR8383 and Caco-2 cells.
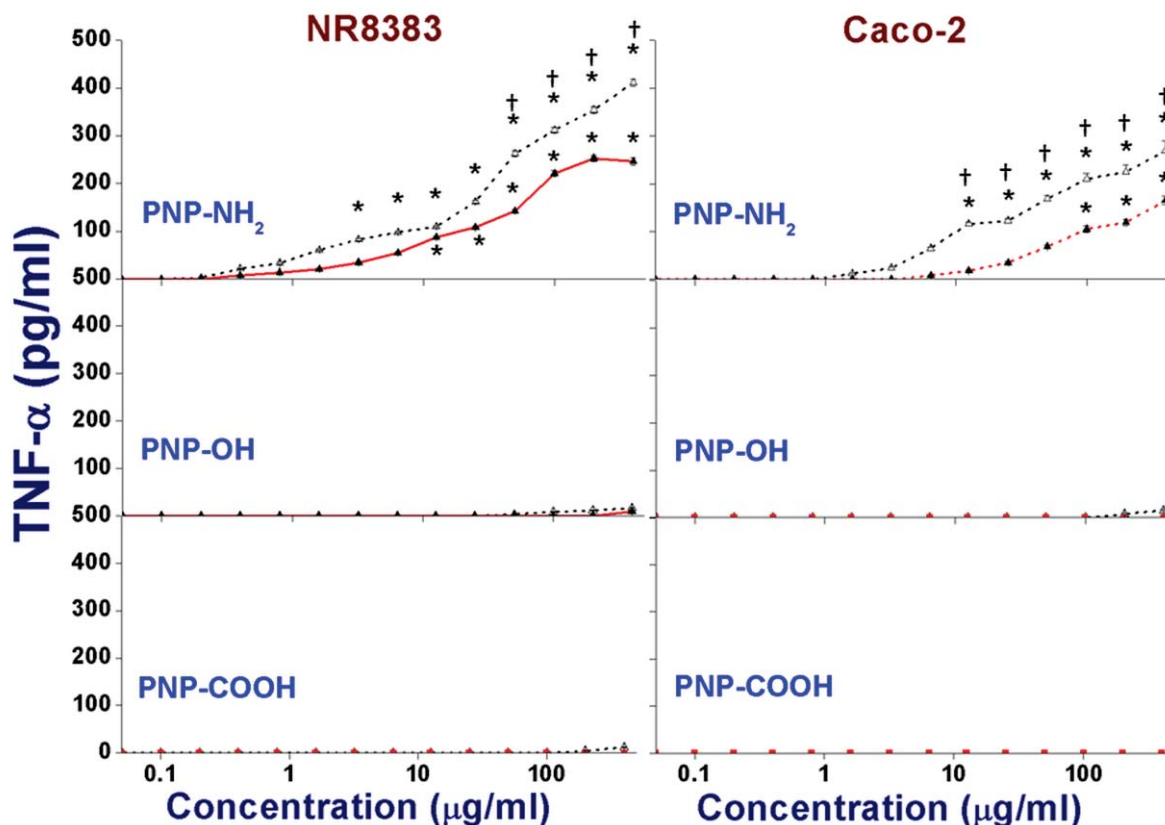

Figure 8: *Comparison of TNF-α release induced by PNP_{45} (Δ) and PNP_{90} (▲) in NR8383 and Caco-2 cells after 24 h exposure. The * sign signifies $p < 0.05$ compared to negative control (0 μg/ml). The "†" sign signifies $p < 0.05$ when compared between the PNP_{45} and PNP_{90}.*

Intracellular uptake of PNP_{90}

The intracellular uptake of different PNP_{90} could be monitored by CLSM (λ_{ex} = 488 nm and λ_{em}=543 nm) as these PNP carried a fluorescent probe. All the CLSM experiments were performed at a concentration of 1 μg/ml of PNP that was non-toxic, as determined by the MTT assay. In Figure 9 (Upper layer) representative CLSM images are given that show the relative intracellular uptake of these three different PNP. From the quantitative uptake results in Figure 9 (Lower layer) it follows that all PNP_{90} were taken up intracellularly, with PNP_{90}-NH_2 showing the highest and PNP_{90}-COOH the lowest cellular uptake. Interestingly, a surface charge-dependent intracellular distribution of these PNP is observed. Only the positive PNP_{90}-NH_2 showed stronger interactions with the cellular periphery, whereas the PNP_{90}-OH and PNP_{90}-COOH showed a more diffuse uptake in the cytoplasm. Upon exposure of the cells to equal

concentrations of the different PNP and integration of the fluorescence over several cells, a comparison between the uptake of the PNP_{90} and PNP_{45} particles with different surface charges could be made (see Figure 9 lower layer). The CLSM data were normalized for the uptake of $PNP_{45}-NH_2$. It is seen from this figure that the intracellular uptake of $PNP_{45}-NH_2$ was about three times (for NR8383) and two times (for Caco-2) higher than of $PNP_{90}-NH_2$. Similar size-dependent effects were found for both -OH and -COOH terminated PNP.
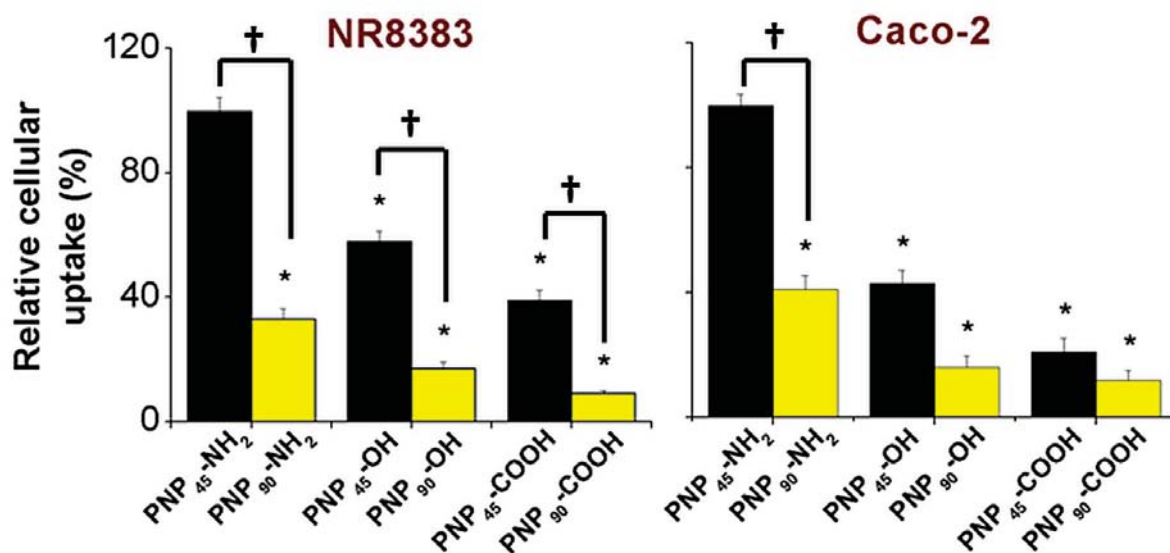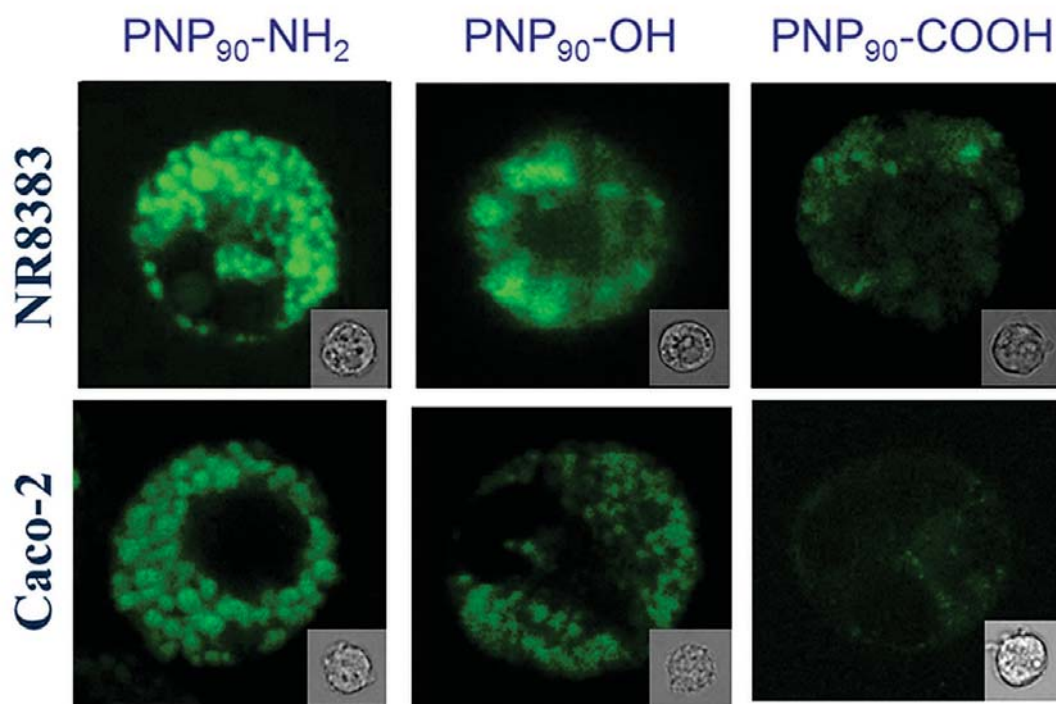
Figure 9: (Upper layer) *CLSM pictures of NR8383 and Caco-2 cells after 24 h exposure to non-toxic concentration of 1 µg/ml of different PNP_{90} (λ_{ex} = 488 nm and λ_{em} = 543 nm) with phase contrast figures given as inserts.* ***(Lower layer)*** *Relative cellular uptake of different PNP_{45}^4 and PNP_{90} in NR8383 and Caco-2 cells after 24 h exposure with the $PNP_{45}-NH_2$ (1 µg/ml) values taken as 100 % (n=5). The * sign signifies $p < 0.05$ when compared to the data for $PNP_{45}-NH_2$. The "†" sign signifies $p < 0.05$ when compared between the PNP_{45} and PNP_{90}.*

Effect of size and surface charge on endocytosis-based cellular uptake of PNP

The role of endocytosis in the cellular uptake of different PNP_{90} was tested by inhibiting endocytotic pathways either by lowering the experimental temperature to 4 °C or by exposing the cells to a mixture of 2-deoxyglucose (2-dOG) and sodium azide (NaN_3) (see Figure 10). The blocking of endocytosis by either procedure drastically reduced the cellular uptake of PNP_{90}, irrespective of the surface charge. However, the decrease was much stronger for PNP_{90}-OH and PNP_{90}-COOH (>80 %) than for PNP_{90}-NH_2 (~50 %). It was observed that the blockade of endocytosis had higher effect on the uptake of PNP_{90}-OH and PNP_{90}-COOH compared to the PNP_{90}-NH_2. To confirm that the PNP were inside the cells and not bound to the cell membrane, *z*-stack imaging was done. Such a *z*-stack imaging figure is provided in *Appendix C* and shows that PNP were inside the cells apart from being attached to the surface.
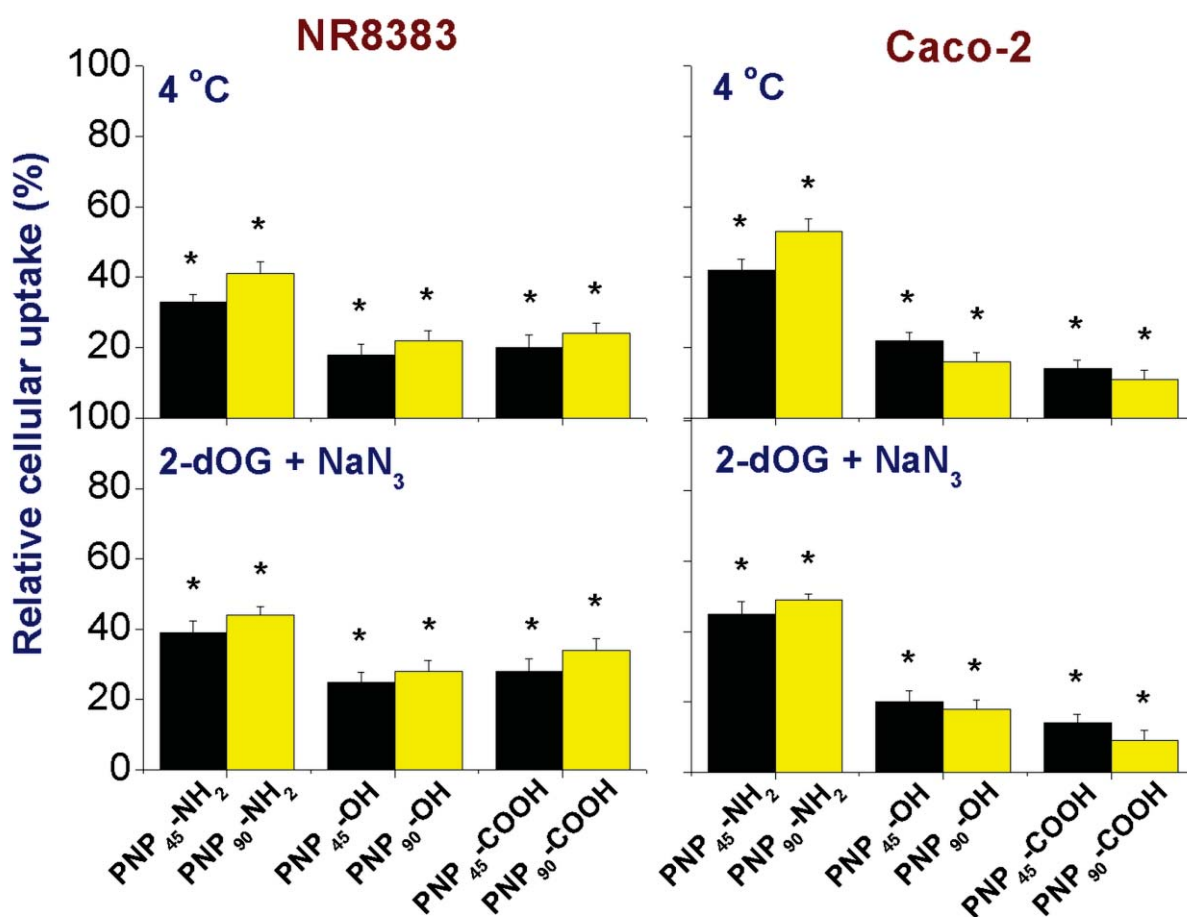
Figure 10: *Comparison of uptake of different PNP_{45}^4 and PNP_{90} in NR8383 and Caco-2 cells (1 µg/ml) as % of unperturbed uptake upon 24 h exposure after blocking the endocytotic uptake (n=5) at 4 °C or by a mixture of 2-deoxyglucose and sodium azide. The * sign signifies p < 0.05 compared to unperturbed uptake.*

Effect of size and surface charge on clathrin and caveolin mediated endocytosis

The size and charge-dependent involvement of clathrin and caveolin receptors in endocytosis of different PNP was tested by selectively blocking the clathrin and caveolin receptors and the results are shown in Figure 11. The clathrin receptors were inhibited by exposing the cells to a hypertonic 450 mM sucrose solution, as this causes polymerization and subsequent inactivation of clathrin receptors.[36] From the results (Figure 11A), it is clear that the positive PNP-NH$_2$ of both sizes showed a considerably reduced uptake upon blocking the clathrin receptors (effect: PNP$_{45}$ > PNP$_{90}$). In contrast, the uptake for both hydroxylated and acid terminated PNP was only affected to a milder extent (reduction to ~65 % and ~75 % of the original values for PNP-OH and PNP-COOH of both sizes, respectively). An opposite effect was seen when the caveolin receptors were blocked by exposing the cells to MβCD[16] as seen from Figure 11B. A profound decrease in the cellular uptake of both the negative PNP could be seen after blocking the caveolin receptors while uptake of PNP-NH$_2$ was only affected slightly. Here also a stronger decrease in uptake was found for the smaller PNP$_{45}$ than for the larger PNP$_{90}$.
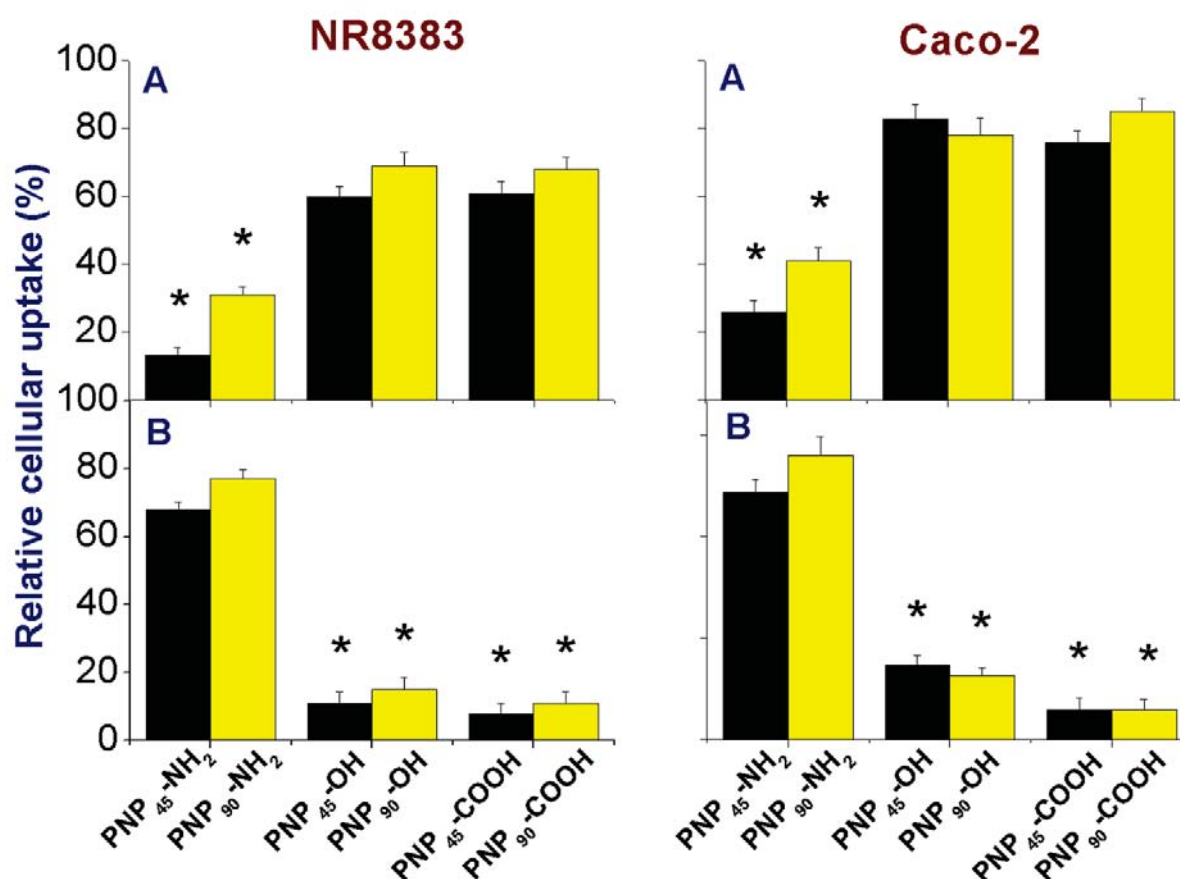

Figure 11: *Comparison of uptake of different PNP$_{45}$[4] and PNP$_{90}$ in NR8383 and Caco-2 cells (1 µg/ml) upon 24 h exposure after blocking the clathrin (A) and caveolin (B) receptors (n=5). The * sign signifies p < 0.05 when compared to unperturbed uptake.*

Effect of size and surface charge on mannose receptors

The role of mannose receptors in the intracellular uptake of different PNP was investigated by inhibiting the mannose receptors by exposing the cells to a high concentration of α-mannan (see Figure 12). It can be seen that inhibition of the mannose receptors decreased the intracellular uptake for all PNP, but the largest effects were seen for the negative PNP (PNP-OH > PNP-COOH), especially for the smaller ones (PNP_{45} > PNP_{90}).
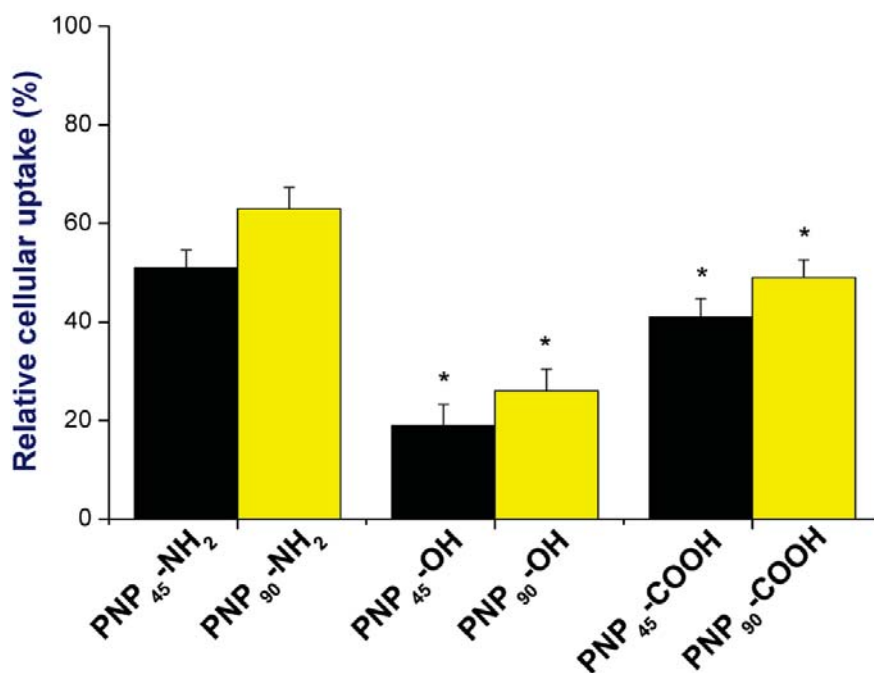

Figure 12: *Comparison of the uptake of different PNP_{45} and PNP_{90} in NR8383 cells (1 µg/ml) upon 24 h exposure after blocking the mannose receptors (n = 5). The * sign signifies p < 0.05 compared to unperturbed uptake.*

Discussion

Due to the nature of the tri-block copolymers synthesized and used in the present study, which have a hydrophobic middle block and hydrophilic terminal blocks, the PNP that were formed out of these polymers in water had a hydrophobic core and a hydrophilic corona. The size of the PNP depends largely on the size of the polymers and the ratio between their hydrophobic middle and hydrophilic terminal blocks.[37] The hydrophobic middle blocks (the polyhexylene adipate polyester) avoid contact with water, whereas the hydrophilic (PEG) blocks try to remain in contact with the water. This means that for the polymers with the larger hydrophilic blocks, the aggregate surface becomes crowded with PEG groups faster and the particles stop growing sooner than for the polymers with the smaller terminal groups. The polymers with the smaller PEG groups grow into larger particles, because in that case the surface does not get so easily crowded and more polymer molecules will add to the forming nanoparticle. The MTT assay data suggest that the positive PNP_{45} were more cytotoxic than the

positive PNP$_{90}$. Both the smaller and larger negative PNP did not induce any significant cytotoxic response at concentrations up to 12.5 µg/ml. Although some studies have been performed on the size-dependent cytotoxicity of NP, such studies on PNP are rare. In the present study the PNP$_{45}$ and PNP$_{90}$ that were used have very similar properties in surface charge density. To the best of our knowledge, this is the first report in which the effect of size on cytotoxicity of PNP is systematically investigated, while keeping the surface characteristics and PNP composition unchanged.

For inorganic NP, more is known on the effect of size on cytotoxicity. Recently, it was reported that smaller gold NP (1.4 nm) were much more cytotoxic than bigger (15 nm) ones.[38] In a similar experiment, silver NP of three different sizes (15, 30 and 55 nm) were tested on a rat alveolar macrophage cell line, which is comparable to the NR8383 cell line used in this study. The cytotoxicity of the smallest (15 nm) particles was highest and of the biggest ones (55 nm) the lowest.[39] The cytotoxicity of a wide size-range of silica NP (30, 48, 118 and 535 nm) was tested on a mouse keratinocyte HEL-30 cell line. A clear size-dependent cytotoxic pattern was reported. The smaller (30 and 48 nm) silica NP showed a much higher toxicity than the bigger (118, 535 nm) ones.[40] For copper NP, similar results were reported.[41] Some other reports also indicated an inverse relationship between size and toxicity of different NP including PNP.[13,42] Auffan et al. hypothesized that inorganic NP smaller than 30 nm are chemically very unstable due to the presence of many high energy surface states which makes them extremely reactive, which again results in an enhanced cytotoxicity.[43] However, many of the surface properties of inorganic NP are significantly different from the surface properties of organic PNP. Therefore, although our results match the findings for inorganic NP, a true comparison is difficult.

It should be noted that in all the cellular experiments reported in this article, cell culture media (DMEM and F12-K) contained FCS rich in proteins (like albumin). It has been observed before that the presence of FCS can cause an increase in the sizes of these PNP by surface adsorption of proteins although, the PNP, in this case, still remained highly monodisperse.[4] The presence of serum, by virtue of being high in protein content, has been reported to influence the toxicity and cellular uptake of NP.[3] This protein adsorption can be of influence on cellular uptake and toxicity, but it is expected that such protein effects will also occur in the gastrointestinal tract upon oral exposure to PNP. Thus, testing in the presence of serum reflects the physiological conditions better for PNP that may be developed with food-based applications in mind.

Two series of PNP were investigated that differed in size and within each series PNP with different surface charges (-NH$_2$, -OH and -COOH) were investigated. A distinct size-dependence was observed. For instance, although both amine-terminated PNP were toxic, the smaller PNP$_{45}$ were more cytotoxic than the larger PNP$_{90}$. Hence a size-dependent effect for PNP with comparable surface charge and surface functionalization was observed. In equivalent masses, the smaller PNP$_{45}$ (45 nm) presented eight times more surface area compared to the bigger PNP$_{90}$ (90 nm). Upon expressing the toxicity data based on surface area, it was found that the toxicity increased with an increase in PNP surface area.

Production of intracellular ROS after exposure to different NP has been amply reported.[44-48] It is thought that these ROS push the cellular physiology to the limits by inducing oxidative stress. Our data, obtained from the DCFH-DA assays, showed that only positive PNP induced intracellular ROS production with the smaller PNP showing a higher effect. These findings also matched the pattern of cytotoxicity (MTT assay) for these PNP. In literature, systematic studies on the effect of size on the intracellular ROS production are rare. Jiang et al.[49] investigated the

effect of size on intracellular ROS production by testing a wide range of titanium dioxide NP (4-195 nm) and reported the highest ROS induction for NP of 30 nm size. In a separate study, silver NP of 4, 20 and 70 nm were tested on macrophage U937 cells.[50] It was found that the 20 nm silver NP were the most capable of producing oxidative stress. A similar study by Choi et al.[51] showed that within a series of different sizes of silver NP tested, the smallest (5 nm) NP were the most capable of inhibiting the growth of nitrifying bacteria through production of ROS. Landsiedel et al.[52] also mentioned an inverse relationship between the size of NP and their induction of intracellular ROS in their comprehensive review on different metal oxide NP (like CeO_2, TiO_2, SiO_2, ZrO_2).

The decrease of the mitochondrial membrane potential ($\Delta\Psi_m$) by cationic PNP is an important finding. It shows that cationic PNP can indeed interact with intracellular mitochondria and compromise their integrity. The decrease in $\Delta\Psi_m$ after exposure to cationic PNP can have further consequences. This compromised state of the mitochondrial membrane can increase its permeability which may result in leaching of the mitochondrial calcium to the cytoplasm causing a cellular overload of calcium, release of cytochrome c and subsequently trigger apoptosis.[32] Similarly, a compromised mitochondrial membrane can also hamper the normal electron transport chain. This can result in decreased ATP production. The finding of ATP depletion of cells upon exposure to cationic PNP matched well with the observed effect on the mitochondrial membrane potential ($\Delta\Psi_m$). Previously, Bhattacharjee et al.[14] reported that positive silicon NP (1.6 ± 0.2 nm) were able to induce ROS production in isolated mitochondrial fractions from rat liver tissue. Similarly, Xia et al.[53] observed that cationic polystyrene nano-beads could interact with and subsequently harm intracellular mitochondria. Due to the continuous involvement of mitochondria in the respiratory cycle by virtue of the electron transport chain (ETC) processes occurring on the outer membrane, it was suggested that interaction of positive NP with mitochondrial membranes can disturb the mitochondrial membrane potential. This was shown in the present study to occur upon exposure of the cells to positive PNP. As a result, positive PNP might uncouple the cascade of reactions in the ETC and thus, not only hamper ATP production but also increase the intracellular ROS production.[14] A recent study reported that intracellular ATP depletion occurred upon exposure of human endothelial EAhy926 cells to differently sized polystyrene NP.[54] The data obtained in the present study are in line with the literature and this could shed some light on the poorly understood mechanism of intracellular ROS production induced by NP. In our opinion, reduction of the mitochondrial membrane potential ($\Delta\Psi_m$) followed by intracellular ATP depletion, as observed after exposure to cationic PNP, may also be a mechanism of cytotoxicity, related to or independent of intracellular ROS production and warrants further investigation.

It has been reported that several NP can induce production of pro-inflammatory cytokines, like TNF-α in different cell lines, including a primary rat brain microvessel cell line and human alveolar epithelial A549 cells.[35,55,56] However, a comparative study on the effect of NP size on TNF-α induction is rare, especially for PNP. Recently, size-dependent TNF-α induction was reported when titanium dioxide NP (5 and 200 nm) were intra-tracheally instilled in rats.[57] It was observed that 5 nm particles were much more effective in inducing TNF-α than 200 nm ones. A similar type of inverse relationship between size of NP and TNF-α production was reported by Hanley et al.[58] for silver oxide NP. Our data on TNF-α production matched these reported literature data and pointed towards an inverse relationship between size of PNP and TNF-α production.

Our data on the cellular uptake showed that smaller PNP$_{45}$ (45 nm) were taken up in appreciably larger amounts (as determined by CLSM) than the bigger PNP$_{90}$ (90 nm), irrespective of surface charge. Win et al.[59] reported a similar type of inverse relationship between size of PNP and cellular uptake in Caco-2 cells. Recently, fluorescent and carboxyl-terminated polystyrene NP of 20 and 200 nm sizes were tested on both rat and human primary hepatocyte cells[60] and it was found that the smaller 20 nm polystyrene NP showed a higher intracellular uptake than the bigger ones. Many other groups reported a higher intracellular uptake for smaller NP.[59,61-63] Zhang et al.[64] performed a molecular modelling and thermodynamics, study to understand this size dependence. From calculations and thermodynamics they predicted that NP of ~22 nm radius (i.e. ~44 nm in size) are more easily internalized by cells. Similarly, other computational models[65-67] also predicted an energetically favourable receptor-mediated intracellular uptake for NP of 30-50 nm sizes. These authors were also able to predict an upper threshold radius of ~60 nm (i.e. ~120 nm size), where receptor-based endocytosis will not be favourable anymore. These findings fit quite well with our data.

The inhibition of endocytosis (by performing the experiments at 4 °C or exposure to a mixture of 2-deoxyglucose and sodium azide) had a stronger effect on the uptake of PNP$_{45}$ than on the uptake of PNP$_{90}$. An explanation may be that smaller PNP enjoy a higher degree of binding with cell membrane receptors. Hence, inhibition of receptor-based endocytosis affects the cellular uptake of smaller particles more. An optimal size of 50 nm was proposed for uptake as well as saturation kinetics of NP uptake by Chithrani et al.[68] who investigated the uptake of gold NP of three different sizes (14, 50 and 74 nm) in HeLa cells.[2] Recently, Jiang et al.[69] also reported that receptor-based endocytosis was highest for 40-50 nm gold and silver NP tested on herceptic receptor ErbB2 expressed on macrophage cells. This preference for 40-50 nm NP also matches our data.

Like in the general receptor inhibition studies, our data showed that selective blocking of the clathrin, caveolin or mannose receptors had in all cases a stronger effect on the uptake of smaller PNP$_{45}$ particles than that of the larger PNP$_{90}$ particles. These results are independent of surface charge of the PNP, although the preference of clathrin receptors for positive PNP and caveolin receptors negative PNP is evident from the results. However, it should be also be noted that blockers lack absolute specificity and also, other endocytotic pathways for cellular PNP uptake remain available after blocking one receptor type. Furthermore, because different in vitro cellular systems have different physiologies and have different levels of expression of clathrin or caveolin receptors, results from different studies cannot always be easily compared.[70] Whether combined inhibition of the clathrin, caveolin and mannose receptors would completely abolish the cellular uptake of the PNP or that residual uptake would remain because also other uptake mechanisms are of importance remains to be investigated. There is only a limited amount of systematically performed size-dependent analyses on interactions of PNP with endocytosis receptors. Rejman et al.[71] performed a very extensive study on cellular uptake mechanisms of latex particles in murine melanoma B16-F10 cells and found a preference for clathrin receptors by smaller and caveolin receptors by bigger PNP. More recently, it was reported that carboxyl terminated polystyrene NP of 43 nm size got internalized by the cells through a clathrin-dependent pathway.[62] Oh et al.[72] also found that uptake of smaller metal hydroxide nanoparticles (50, 109, 200 nm), when tested on a human osteosarcoma (MNNG/HOS) cell line, showed a stronger clathrin receptor dependence of cellular uptake than the bigger ones (375 nm). So, although the effects are clearly different for the differently charged

PNP and the different receptors, our results seemed to be in line with the findings of the majority of these reports that smaller (or medium-sized) NP have stronger interactions with endocytosis receptors than larger NP.

Mannose receptors are a unique group of receptors that are often expressed on macrophage cell surfaces and recognize and endocytose a wide variety of carbohydrates. Though it is not clear yet how these receptors recognize such a huge variety of molecules, the orientation of the carbohydrate molecule is important. It is also known that hexoses with equatorially placed hydroxyl groups have a strong binding affinity towards these receptors.[73] Although our PNP did not contain carbohydrate groups, especially those that contain –OH groups on the surface, had some chemical resemblance with carbohydrates with -OH groups. The results of the inhibition studies matched with this since the maximum inhibition of intracellular uptake was observed for both hydroxyl- or acid-terminated PNP. This once again pointed towards a complex range of interactions between PNP and cell membranes and their receptors, leading to particle internalization. Although we are the first to actually show that inhibition of mannose receptors inhibits cellular uptake of PNP, there have been few reports already where these receptors have been targeted for facilitated drug delivery. Park et al.[74] used mannosylated polyethyleneimine coupled to silica NP to increase the transfection efficiency in macrophage cells by targeting the mannose receptors. Similar strategies have been employed by other groups to increase the delivery efficacy in biological systems.[75-77] Our results on mannose receptors are in line with data available in literature that point towards strong NP-receptor interactions. These results can further be developed for more sophisticated applications like drug delivery or food based delivery of functional ingredients.

Conclusion

Well-characterized, monodisperse and fluorescent PNP of different sizes (45 and 90 nm) and surface properties were synthesized. The PNP exhibited an inverse relationship between size and cytotoxicity as well as between size and cellular uptake. A size-dependent induction of intracellular ROS production identified oxidative stress as a possible mechanism of cytotoxicity with subsequent release of pro-inflammatory cytokines representing another mechanism for NP induced adverse effects. Reduction in the mitochondrial membrane potential, uncoupling of the electron transfer chain in mitochondria and resulting ATP depletion, induction of ROS and oxidative stress likely all play a role in the mode of action for the cytotoxicity of these PNP.

Although, at the concentrations tested, only positive PNP showed cytotoxic effects, all PNP were taken up by the cells. An involvement of clathrin, caveolin and mannose receptors could be seen in cell internalization of PNP with their relative importance depending on the surface properties of the PNP. Overall the results presented provide insight in size and surface charge-specific cellular uptake and cytotoxicity of PNP and possible modes of action underlying these effects. Typically, larger PNP and negatively charged PNP are less toxic in our tests than smaller and positively charged PNP. Translation of these results to recommendations for their preferential use in development of safer NP requires validation of their lower toxicity through in vivo studies.

References

1.   Lewinski N, Colvin V, Drezek R; *Small* 2008, 4:26-49.
2.   Chithrani BD, Ghazani AA, Chan WCW; *Nano Lett.* 2006, 6:662-668.
3.   Clift MJD, Bhattacharjee S, Brown DM, Stone V; *Toxicol. Lett.* 2010, 198:358-365.
4.   Bhattacharjee S, Ershov D, Gucht Jvd, Alink GM, Rietjens IMCM, Zuilhof H, et al.; *Nanotoxicology* 2011, Early Online:1-14.
5.   Gelperina S, Kisich K, Iseman MD, Heifets L; *Am. J. Resp. Crit. Care* 2005, 172:1487-1490.
6.   Irvine DJ; *Nat. Mater.* 2011, 10:342-343.
7.   Sozer N, Kokini JL; *Trends Biotechnol.* 2009, 27:82-89.
8.   Sinha R, Kim GJ, Nie S, Shin DM; *Mol. Cancer Ther.* 2006, 5:1909-1917.
9.   Donaldson K, Stone V, Borm PJA, Jimenez LA, Gilmour PS, Schins RPF, et al.; *Free Radical Bio. Med.* 2003, 34:1369-1382.
10.   Hussain S, Hess K, Gearhart J, Geiss K, Schlager J; *Toxicol. in Vitro* 2005, 19:975-983.
11.   Pisanic TR, Blackwell JD, Shubayev VI, Finones RR, Jin S; *Biomaterials* 2007, 28:2572-2581.
12.   Eom H-J, Choi J; *Environ. Sci. Technol.* 2010, 44:8337-8342.
13.   Nel A, Xia T, Madler L, Li N; *Science* 2006, 311:622-627.
14.   Bhattacharjee S, de Haan LHJ, Evers NM, Jiang X, Marcelis ATM, Zuilhof H, et al.; *Part. Fibre Toxicol.* 2010, 7:25.
15.   Ruizendaal L, Bhattacharjee S, Pournazari K, Rosso-Vasic M, de Haan LHJ, Alink GM, et al.; *Nanotoxicology* 2009, 3:339-347.
16.   Xia T, Kovochich M, Liong M, Zink JI, Nel AE; *ACS Nano* 2008, 2:85-96.
17.   Sayes CM, Reed KL, Warheit DB; *Toxicol. Sci.* 2007, 97:163-180.
18.   Brigger I, Dubernet C, Couvreur P; *Adv. Drug Deliver. Rev.* 2002, 54:631-651.
19.   Vasir JK, Labhasetwar V; *Biomaterials* 2008, 29:4244-4252.
20.   Chen LA, Mccrate JM, Lee JCM, Li H; *Nanotechnology* 2011, 22.
21.   Asati A, Santra S, Kaittanis C, Perez JM; *ACS Nano* 2010, 4:5321-5331.
22.   Huang M, Ma ZS, Khor E, Lim LY; *Pharm. Res.* 2002, 19:1488-1494.
23.   Spankuch B, Steinhauser I, Wartlick H, Kurunci-Csacsko E, Strebhardt KI, Langer K; *Neoplasia* 2008, 10:223-234.
24.   Lynch I, Dawson KA, Linse S; *Sci STKE* 2006, 2006:pe14.
25.   Gentili PL, Mugnai M, Bussotti L, Righini R, Foggi P, Cicchi S, et al.; *J. Photoch. Photobio. A* 2007, 187:209-221.
26.   Loccufier J, Vanbos M, Schacht E; *Polym. Bull.* 1991, 27:201-204.
27.   Khoee S, Hassanzadeh S, Goliaie B; *Nanotechnology* 2007, 18.
28.   van Berlo D, Haberzettl P, Gerloff K, Li H, Scherbart AM, Albrecht C, et al.; *Chem. Res. Toxicol.* 2009, 22:1548-1558.
29.   Howard KA, Paludan SR, Behlke MA, Besenbacher F, Deleuran B, Kjems J; *Mol. Ther.* 2009, 17:162-168.
30.   Hislop JN, Everest HM, Flynn A, Harding T, Uney JB, Troskie BE, et al.; *J. Biol. Chem.* 2001, 276:39685-39694.
31.   Srinivasan D, Fujino H, Regan JW; *J. Pharmacol. Exp. Ther.* 2002, 302:219-224.
32.   Xia T, Kovochich M, Liong M, Zink JI, Nel AE; *ACS Nano* 2007, 2:85-96.

33.   Stuart AD, Brown TDK; *J. Virol.* 2006, 80:7500-7509.

34.   Xu X, Xie Q, Shen Y, Lu G, Yao H, Chen Y, et al.; *Eur. J. Pharmacology* 2010, 641:229-237.

35.   Schrand AM, Rahman MF, Hussain SM, Schlager JJ, Smith DA, Syed AF; *Wiley Interdiscip. Rev. Nanomed. Nanobiotechnol.* 2010, 2:544-568.

36.   Suh HR, Jeong BM, Rathi R, Kim SW; *J. Biomed. Mater. Res.* 1998, 42:331-338.

37.   Zhang Y, Zhuo R; *Biomaterials* 2005, 26:6736-6742.

38.   Pan Y, Neuss S, Leifert A, Fischler M, Wen F, Simon U, et al.; *Small* 2007, 3:1941-1949.

39.   Carlson C, Hussain SM, Schrand AM, Braydich-Stolle LK, Hess KL, Jones RL, et al.; *J. Phys. Chem. B* 2008, 112:13608-13619.

40.   Yu KO, Grabinski CM, Schrand AM, Murdock RC, Wang W, Gu BH, et al.; *J. Nanopart. Res.* 2009, 11:15-24.

41.   Prabhu BM, Ali SF, Murdock RC, Hussain SM, Srivatsan M; *Nanotoxicology* 2010, 4:150-160.

42.   Oberdorster G, Oberdorster E, Oberdorster J; *Environ. Health Persp.* 2005, 113:823-839.

43.   Auffan M, Rose J, Bottero J-Y, Lowry GV, Jolivet J-P, Wiesner MR; *Nat. Nanotechnol.* 2009, 4:634-641.

44.   Horie M, Fukui H, Nishio K, Endoh S, Kato H, Fujita K, et al.; *J. Occup. Health* 2011, 53:64-74.

45.   Kim S, Choi JE, Choi J, Chung KH, Park K, Yi J, et al.; *Toxicol. in Vitro* 2009, 23:1076-1084.

46.   Pujalte I, Passagne I, Brouillaud B, Treguer M, Durand E, Ohayon-Courtes C, et al.; *Part. Fibre Toxicol.* 2011, 8(10).

47.   Stone V, Donaldson K; *Nat. Nanotechnol.* 2006, 1:23-24.

48.   Wang F, Gao F, Lan MB, Yuan HH, Huang YP, Liu JW; *Toxicol. in Vitro* 2009, 23:808-815.

49.   Jiang J, Oberdorster G, Elder A, Gelein R, Mercer P, Biswas P; *Nanotoxicology* 2008, 2:33-42.

50.   Park J, Lim DH, Lim HJ, Kwon T, Choi JS, Jeong S, et al.; *Chem. Commun.* 2011, 47:4382-4384.

51.   Choi O, Hu ZQ; *Environ. Sci. Technol.* 2008, 42:4583-4588.

52.   Landsiedel R, Ma-Hock L, Kroll A, Hahn D, Schnekenburger J, Wiench K, et al.; *Adv. Mater.* 2010, 22:2601-2627.

53.   Xia T, Kovochich M, Brant J, Hotze M, Sempf J, Oberley T, et al.; *Nano Lett.* 2006, 6:1794-1807.

54.   Frohlich E, Samberger C, Kueznik T, Absenger M, Roblegg E, Zimmer A, et al.; *J. Toxicol. Sci.* 2009, 34:363-375.

55.   Monteiller C, Tran L, MacNee W, Faux S, Jones A, Miller B, et al.; *Occup. Environ. Med.* 2007, 64:609-615.

56.   Trickler WJ, Lantz SM, Murdock RC, Schrand AM, Robinson BL, Newport GD, et al.; *Toxicol. Sci.* 2010, 118:160-170.

57.   Liu R, Zhang XY, Pu YP, Yin LH, Li YH, Zhang XQ, et al.; *J. Nanosci. Nanotechno.* 2010, 10:5161-5169.

58.   Hanley C, Thurber A, Hanna C, Punnoose A, Zhang JH, Wingett DG; *Nanoscale Res. Lett.* 2009, 4:1409-1420.

59.   Win KY, Feng SS; *Biomaterials* 2005, 26:2713-2722.

60.   Johnston HJ, Semmler-Behnke M, Brown DM, Kreyling W, Tran L, Stone V; *Toxicol. Appl. Pharmacol.* 2010, 242:66-78.

61. Oh W-K, Kim S, Choi M, Kim C, Jeong YS, Cho B-R, et al.; *ACS Nano* 2010, 4:5301-5313.

62. Lai SK, Hida K, Man ST, Chen C, Machamer C, Schroer TA, et al.; *Biomaterials* 2007, 28:2876-2884.

63. Foged C, Brodin B, Frokjaer S, Sundblad A; *Int. J. Pharm.* 2005, 298:315-322.

64. Zhang SL, Li J, Lykotrafitis G, Bao G, Suresh S; *Adv. Mater.* 2009, 21:419-424.

65. Bao G, Bao XR; *Proc. Natl. Acad. Sci.* 2005, 102:9997-9998.

66. Gao HJ, Shi WD, Freund LB; *Proc. Natl. Acad. Sci.* 2005, 102:9469-9474.

67. Tzlil S, Deserno M, Gelbert WM, Ben-Shaul A; *Biophys. J.* 2004, 86:2037-2048.

68. Chithrani BD, Chan WCW; *Nano Lett.* 2007, 7:1542-1550.

69. Jiang W, KimBetty YS, Rutka JT, Warren CWC; *Nat. Nanotechnol.* 2008, 3:145-150.

70. Thurn KT, Brown EMB, Wu A, Vogt S, Lai B, Maser J, et al.; *Nanoscale Res. Lett.* 2007, 2:430-441.

71. Rejman J, Oberle V, Zuhorn IS, Hoekstra D; *Biochem. J.* 2004, 377:159-169.

72. Oh JM, Choi SJ, Lee GE, Kim JE, Choy JH; *Chem-Asian. J.* 2009, 4:67-73.

73. Stahl PD, Ezekowitz RAB; *Curr. Opin. Immunol.* 1998, 10:50-55.

74. Park IY, Kim IY, Yoo MK, Choi YJ, Cho M-H, Cho CS; *Int. J. Pharm.* 2008, 359:280-287.

75. Cui ZR, Hsu CH, Mumper RJ; *Drug Dev. Ind. Pharm.* 2003, 29:689-700.

76. Kim TH, Jin H, Kim HW, Cho MH, Cho CS; *Mol. Cancer Ther.* 2006, 5:1723-1732.

77. Rieger J, Freichels H, Imberty A, Putaux JL, Delair T, Jerome C, et al.; *Biomacromolecules* 2009, 10:651-657.

Chapter 7

Surface charge-specific interactions between polymer nanoparticles and ABC transporters in Caco-2 cells

Abstract

The surface charge-dependent transport of polymeric nanoparticles (PNP) across Caco-2 monolayers grown in transwell culture systems as an in vitro model for intestinal transport was tested. The transports of well-characterized, monodisperse and fluorescent tri-block copolymer nanoparticles (size ~45 nm) and polystyrene nanoparticles (size ~50 nm), with different surface charges (positive and negative) were quantified. The positive PNP showed a higher intracellular uptake and flux across the Caco-2 monolayers than negative PNP. Multidrug resistance/P-glycoprotein (MDR1/P-gp), a specific ATP-binding cassette (ABC) transporter, was shown to play a major role in the cellular efflux of positive PNP, whereas the multidrug resistance protein 1 (MRP1) took part in the efflux of negative PNP from Caco-2 cells. The positive PNP also caused an increased cellular uptake and apical to basolateral transport of the carcinogen PhIP across the Caco-2 monolayer. The flavonoid quercetin, which is known to interact with ABC transporters, promoted the intracellular uptake of different PNP and interfered with the normal distribution patterns of PNP in the transwell system. These results indicate that PNP display surface charge-specific interactions with ABC transporters and can even affect the bioavailability of toxic food-borne compounds (like carcinogens).

Introduction

Over the last two decades, nanotechnology has become a flourishing field of science and the number of nanoparticle applications is increasing rapidly.[1] Besides applications in material science and medicine, new and interesting uses of nanotechnology are seen in food-based applications.[2] Although mankind has already been using nanoparticles (NP), like silver,[3] from antiquity to improve food conservation, the use of newly synthesized and chemically engineered NP in food formulations has recently increased. Unfortunately, the behavior and fate of different NP in human physiological systems, like the gastrointestinal (GI) system, is still poorly understood.[4] Although research on such topics has increased in recent years, knowledge on interactions between different NP and the GI system remains far from complete.

Besides inorganic NP, organic NP and especially polymeric NP (PNP) are interesting for a variety of reasons. Through chemical fine-tuning, these PNP can be provided with a large range of different and specific surface groups. Furthermore, these PNP do not contain inherently toxic elements, such as heavy metals,[5] which makes them interesting candidates for food applications.[6] As a result, PNP are gaining popularity, especially for delivery purposes[7] (e.g. delivery of probiotics[8, 9] or vitamins[10]). Some formulations are already commercially available and it can be expected that more products will reach the consumer market in the near future. Hence, research on the interactions of PNP with human intestinal cells is timely and justified. As such, it is important to scrutinize the factors that dominate the distinct cellular interactions of different PNP. The surface charge of the NP is considered to be important for nanoparticle-cell interactions,[11-13] although a clear mechanism of this interaction still remains to be elucidated. Interestingly, several reports indicated the importance of surface charge-dependent interactions of PNP with membrane-bound receptors.

Monolayers of human colonic adenocarcinoma-derived Caco-2 cells in a transwell cell culture system are a well-accepted in vitro model for assessing gastro-intestinal uptake of different materials.[14-16] These Caco-2 cells, once cultured under specific conditions, differentiate and mimic the enterocytes of the human small intestine.[17] Though being used widely for assessing the uptake of many orally administered substances, this model has up to now rarely been used for experiments with NP.[18] The presence of different ATP-binding cassette (ABC) transporters – like MDR1/P-gp, multiple drug resistance proteins MRP1, MRP2 and breast cancer resistance protein (BCRP) – in the apical and basolateral membranes of the Caco-2 cells[19] makes this model of significant interest to study transporter-based interactions of different NP (including PNP). The different efflux pumps expressed in the cultured Caco-2 monolayer in the transwell system are well documented.[20] ATP transporters preferentially promote the efflux of compounds from the intestinal cells. Transport from the intestinal cells promoted by transporters in the basolateral membrane of the cells, including MRP1, MRP3 and MRP5,[21] is a crucial step in the process leading to uptake in the blood. A more efficient transport from these intestinal cells thus increases the bioavailability. The reverse transport from the intestinal cells back to the intestinal lumen is promoted by transporters located in the apical membrane of the cells, including MDR1/P-gp and MRP2. This reverse transport opposes uptake and thereby decreases bioavailability.[21] It is, for example, well-documented that the apical ABC transporters efficiently export many pro-carcinogens, like PhIP (2-amino-1-methyl-6-phenylimidazo[4,5-*b*]pyridine), from gut cells to the gut lumen, thus facilitating excretion of toxic compounds from the human body and limiting their bioavailability.[22] Therefore, the role of ABC transporters is of

crucial importance and any interference with the normal function of these transporters will render the human body more susceptible to certain toxins that may cause adverse health effects.

The objectives of the present study were as follows: 1) To investigate the surface charge-dependent transport of PNP across the Caco-2 monolayer as an in vitro model for intestinal transport; 2) To study the interactions of the different PNP with membrane-bound active ABC transport proteins, with the aim to characterize their potential to influence the overall transport and thus the bioavailability of other substrates known to be transported by ABC transporters across the intestinal barrier; 3) Since, there are several different ABC transporters, the role of different ABC transporters in the translocation of the different PNP across the Caco-2 monolayer was characterized by using inhibitors that specifically block one or some of these; 4) To study whether exposure of the Caco-2 cells to PNP in the presence of quercetin affects their transport across the monolayer. This was done because it was previously demonstrated that this food-borne flavonoid (quercetin) increased the apical to basolateral transport of the flavonoid hesperitin across the Caco-2 monolayer and thus pointed at an increased bioavailability upon inhibition of the efflux by apical ABC transporters;[21] 5) To investigate whether PNP influence the transport of PhIP, an important food-borne carcinogen, across the intestinal barrier.

In this paper, the transport of differently charged PNP over monolayers of Caco-2 cells was investigated. For the first time, the surface charge-specific interactions between the PNP and ABC transporters were investigated, in which PNP were recognized as a substrate for the ABC transporters. In addition it was studied to which degree these PNP affect the bioavailability of toxic food-borne compounds, like carcinogens. This adds a new dimension to the hazard and risk assessment of the increasingly prevalent PNP.

Materials and methods

Polymeric nanoparticles (PNP)

The tri-block copolymer nanoparticles (TCNP) were synthesized and characterized as described before.[23] In short, these TCNP were prepared by a nanoprecipitation technique using tri-block copolymers PEG_{2000}–polyhexylene adipate–PEG_{2000} with different terminal groups (amine, hydroxyl and carboxylic acid). The polystyrene NP (PSNP) were purchased from Sigma Aldrich B.V. (product numbers L0780 and L5780 for amine- and carboxylic acid-terminated particles, respectively). The size and surface potentials of commercially available PSNP and of the synthetized TCNP were quantified by DLS and ζ-potential measurements (Table 2) as previously described.[23]

MTT assay in Caco-2 cells

Caco-2 cells were obtained from ATCC (Rockville, MD) and were cultured in DMEM medium (Gibco) (fortified with 10 % (v/v) heat inactivated fetal calf serum (FCS) and 50 mg/ml gentamicin) in a humidified atmosphere at 5 % CO_2 and 37 ºC. The cells were subcultured, after rinsing with phosphate buffered saline (PBS) using trypsin. Only cells from passage number 37-42 were used for the experiments. The cell suspension was made up to a concentration of 1×10^5 cells/ml in DMEM and 100 μl of the cell suspension was plated in each well of a 96-well plate

and incubated for 24 h. The cells were then exposed to different dilutions of PNP (in DMEM) and incubated again for 24 h. 5 μl of MTT solution in PBS (5 mg/ml) were added to each well followed by a 4 h incubation. The wells were then emptied and the violet crystals were dissolved in 100 μl of dimethysulfoxide (DMSO) per well before measuring absorption at 562 nm. The results were expressed as % of negative control. Plain DMEM medium and Triton-X (0.01 %) dissolved in DMEM medium, acted as negative and positive controls, respectively.

Transwell culture with Caco-2 cells

For experiments, 1×10^5 cells/cm^2 was seeded in Costar 12-well transwell inserts obtained from Corning (Corning, NY, product number 3401). The transwell inserts had a polycarbonate membrane with a pore size ~0.4 μm and a growth area of ~1.12 cm^2. The monolayers were maintained with replacement of old with fresh medium thrice per week and the integrity was regularly checked by TEER measurements using a Millicell ERS volt/ohmmeter from Millipore (Bedford, MA). Only monolayers showing initial TEER values >560 Ω were chosen for transport experiments. The integrity of the Caco-2 monolayers were further confirmed by measurement of the passage of the fluorescent dye lucifer yellow (λ_{ex} = 428 nm, λ_{em} = 540 nm).

Exposure of Caco-2 monolayers to different PNP

The different dilutions of TCNP and PSNP were made in phenol red-free DMEM medium. The Caco-2 monolayers were washed twice with PBS before exposure. The PNP dilutions, in phenol red-free DMEM medium (0.5 ml), were added to the apical compartments in the absence or presence of 5 μM PhIP, 10 μM quercetin, 100 μM verapamil,[14] 24 μM MK571 or 5 μM Ko143 as indicated, from 400 times concentrated stock solutions in DMSO. The concentration of the DMSO was always kept as 0.5 % in the apical compartments for all the transport experiments. At different time points (0.5, 1, 2, 4, 8, 12 and 24 h), aliquots of 150 μl were taken from both the apical and basolateral compartments (with immediate replenishment with fresh medium) for analysis by fluorescence (for TCNP λ_{ex} = 488 nm, λ_{em} = 543 nm; for PSNP λ_{ex} = 360 nm, λ_{em} = 420 nm). At 24 h, remaining medium from both the apical and basolateral parts were collected and the membrane was dissected with the help of a scissor. The membrane was then dissolved in 500 μl of 65 % methanol (v/v) in an Eppendorf tube before centrifuging it in order to lyse the cells and the supernatant thus obtained, was used for further analysis. Transwells with cells exposed to medium without PNP were used as negative control.

Confocal laser scanning microscopy (CLSM)

To confirm that the different PNP did enter the Caco-2 cells grown in monolayers after exposure, Caco-2 monolayers were trypsinized followed by CLSM for TCNP (λ_{ex} = 488 nm; λ_{em} = 543 nm).

Statistical analysis

Each experiment was repeated three times (n = 3) and the results are shown as mean ± standard error of mean (SEM) after analysis and plotting by Origin Pro (version 8.0) software.

Data points were taken as statistically significantly different if $p < 0.05$ compared to the negative control (unless stated otherwise) and marked with an asterisk (*) sign.

Results and Discussion

Motivation of choosing ABC transporters

The ABC transporters are located in human small intestinal cell membranes and influence the bioavailability of food-borne substrates, facilitating either absorption or excretion. A schematic representation depicting the location of these transporters and a short summary of substrates transported by some major ABC transporters are presented in Figure 1 (Top) and Table 1, respectively.[14,21]

Table 1*: Brief summary of different ABC transporters and their substrates.[21]*

Side expressed	ABC transporter	Physiological substrates
Apical	MDR1/P-gp (ABCB1)	Amphipathic drugs, positively charged hydrophobic compounds
	MRP2 (ABCC2)	Bile salts, xenobiotics, drug-conjugates, glutathione (GSH), GSSG, leukotriene-C4 (LT-C4)
	BCRP (ABCG2)	Amphipathic drugs, organic anions, hydrophilic anticancer agents, glutathione conjugates
Basolateral	MRP1 (ABCC1)	Anionic drug conjugates, GSH, LT-C4, sulphate conjugates
	MRP3 (ABCC3)	Bile salts, endogenous organic anions

Polymeric nanoparticles (PNP) and their characterization

Two types of PNP were tested in these experiments: tri-block copolymer nanoparticles (TCNP) and polystyrene nanoparticles (PSNP). The TCNP were synthesized and characterized as described before,[23] and were available with positive TCNP-NH$_3^+$ (amine-terminated), slightly negative TCNP-OH (hydroxyl-terminated) and negative TCNP-COO$^-$ (carboxylic acid-terminated) surface charges. The PSNP were commercially available with positive PSNP-NH$_3^+$ (amine-terminated) and negative PSNP-COO$^-$ (carboxylic acid-terminated) surface charges. The sizes and surface potentials of these PNP were measured by dynamic light scattering (DLS) and ζ-potential measurements, respectively. A summary of the different PNP used in the experiments and their major characteristics is given in Table 2. For the quantification of the transport of all PNP in the transwell experiments, fluorescence measurements were used.
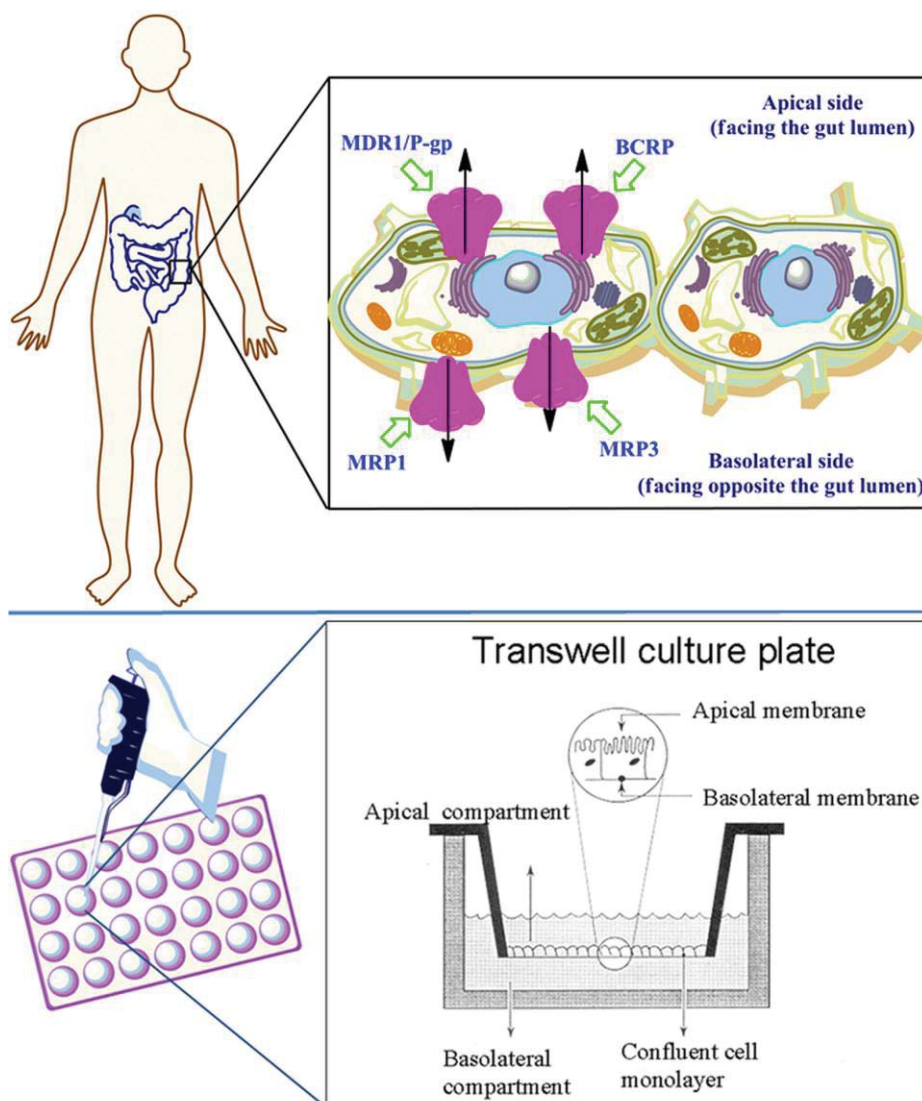
Figure 1*: Schematic representations of: (**Top**) different ABC transporters in human small intestinal cells located in apical or basolateral membranes of Caco-2 cells. (**Bottom**) The two-compartment (apical and basolateral) cell culture system consists of a permeable cell culture insert that is placed in a well of a cell culture plate. The Caco-2 cells are seeded on the filter inserts and when grown to confluence, the cell layer forms a densely packed cellular barrier between the two compartments.*

Table 2*: Brief summary of the different PNP used in the experiments.*

Polymer	PNP	Surface charge	ζ-potential (mV)	Size (nm)
Tri-block copolymer[23]	TCNP-NH$_3^+$	Positive	22 ± 5	45 ± 5
	TCNP-OH	Slightly negative	−8 ± 3	
	TCNP-COO$^-$	Negative	−23 ± 4	
Polystyrene	PSNP-NH$_3^+$	Positive	24 ± 5	50 ± 5
	PSNP-COO$^-$	Negative	−21 ± 5	

Cell viability measurements by MTT assay

The cell viability of Caco-2 cells was measured over a wide concentration-range of PNP (0-100 µg/ml) using the MTT assay. This was done in order to determine a non-toxic concentration for all the PNP to be used for transport experiments. The results are shown in Figure 2. For both TCNP and PSNP, only exposure of the cells to positive NP resulted in cytotoxicity. From the MTT data obtained, test concentrations of 0.5 and/or 1.0 µg/ml were chosen for further experiments, as these two concentrations did not show any cytotoxicity to Caco-2 cells for all different PNP.
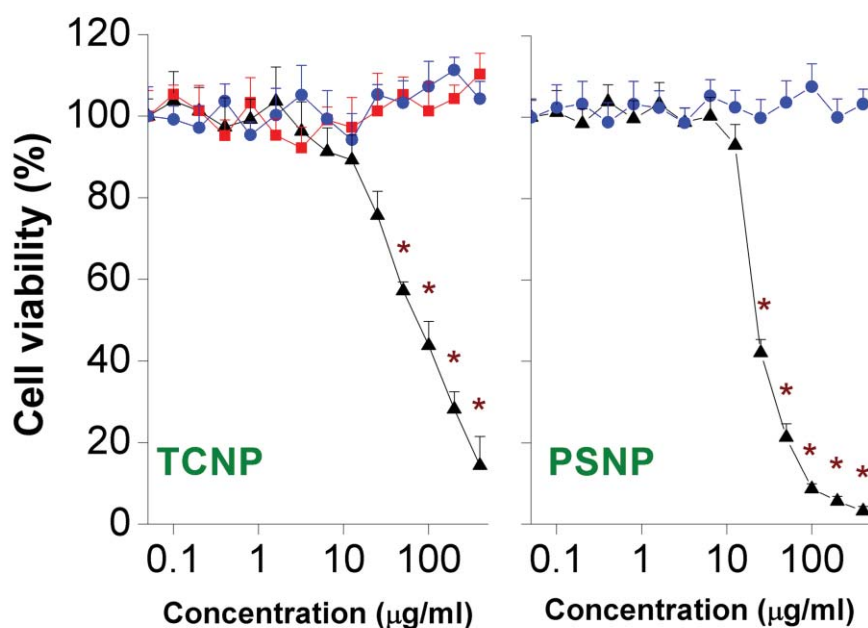
Figure 2: Cell viability of Caco-2 cells at different concentrations of positive amine (▲), slightly negative hydroxyl (■), and negative carboxylic acid (●) terminated tri-block copolymer NP (TCNP) and polystyrene NP (PSNP) after 24 h exposure as measured with the MTT assay. Results are shown as mean ± SEM (n = 3). The * signifies p < 0.05 compared to the negative control (0 µg/ml).

Transwell culture of Caco-2 cells and exposure to PNP

The TEER values of the Caco-2 monolayers were measured upon exposure to different PNP for different lengths of time (0.5, 1, 2, 4, 8, 12 and 24 h). For both TCNP and PSNP, only the positive NP showed a significant decrease in TEER measurements (Figure 3). Interestingly, the dip in TEER values after exposure to positive PNP, partially recovered to ~75 % of its original value within 12 h of exposure, although a complete recovery could not be seen even after 24 h. Our results are in line with literature reports where a decrease in TEER values of Caco-2 monolayers following exposure to positive PNP has been described,[23-26] while a partial recovery was also reported by Sadeghi et al.[24] in Caco-2 monolayers exposed to different cationic chitosan nanoparticles. The observation that only positively charged NP showed this effect might be explained by electrostatic attractions, via which positive NP interacted stronger with the overall negative cell membrane than negative NP. Several reports indicated stronger interactions of positively charged NP with biomembranes than negative ones.[27-30] To ascertain that the decrease

in TEER by the different PNP does not influence the integrity of the monolayer barrier, the trans-monolayer transport of lucifer yellow was tested. Lucifer yellow is a fluorescent dye (λ_{ex} = 428 nm, λ_{em} = 540 nm) that crosses the Caco-2 monolayer mainly through para-cellular transport. It was observed that the presence of even positively charged PNP did not significantly influence the passage of lucifer yellow (supplementary information, *Appendix D*). This showed that the integrity of the Caco-2 monolayers remained sufficient upon exposure to PNP of different surface charge, in spite of the somewhat reduced TEER values.
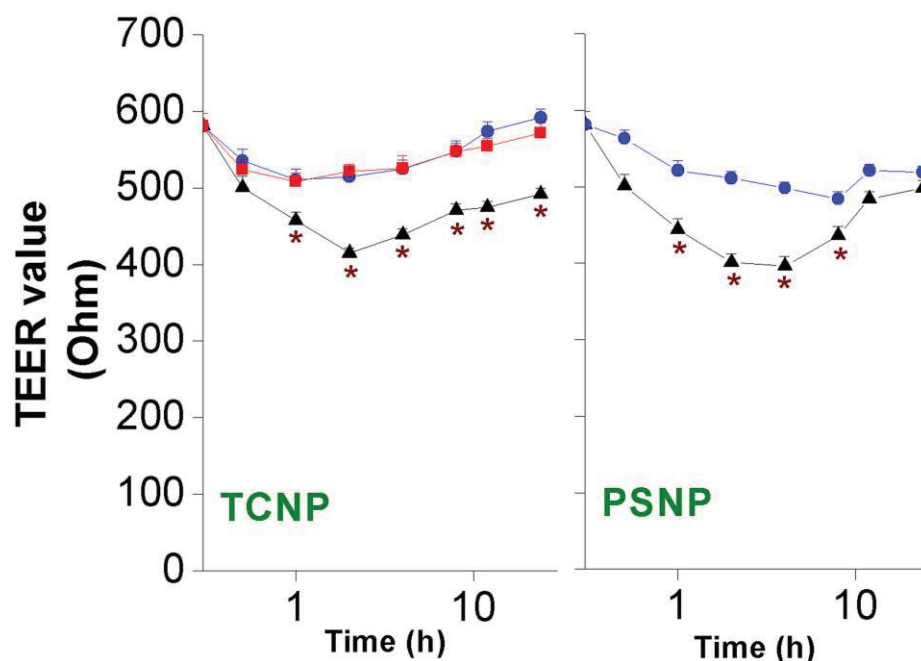
Figure 3: *Time-dependent TEER values of Caco-2 monolayers upon exposure to 1 μg/ml concentrations of positive amine (▲), slightly negative hydroxyl (■) and negative carboxylic acid (●) terminated tri-block copolymer NP (TCNP) and polystyrene NP (PSNP). Results are shown as mean ± SEM (n = 3). The * signifies p < 0.05 compared to starting values (t = 0).*

Transport of different TCNP and PSNP across Caco-2 monolayers

In Figure 4, the time-dependent TCNP and PSNP transport from the apical to the basolateral sides across Caco-2 monolayers (at a dose of 1 μg/ml) is presented. At 24 h, ~40 % and ~35 % of the amount administered at the apical compartment was transported to the basolateral sides for the positive TCNP-NH$_3^+$ and PSNP-NH$_3^+$, respectively. In contrast, the transport rates for negative TCNP (TCNP-OH and TCNP-COO$^-$) and PSNP (PSNP-COO$^-$) were lower (transport rate: TCNP-NH$_3^+$ > TCNP-OH > TCNP-COO$^-$ and PSNP-NH$_3^+$ > PSNP-COO$^-$). Similar findings of cationic NP showing higher transport than the anionic ones is also reported for monolayers of MDCK-II,[31] rat alveolar epithelial RAECM,[32] buccal mucosal[33] and co-cultures of Caco-2 and RajiB cells.[34] In the present study both the positive TCNP-NH$_3^+$ and PSNP-NH$_3^+$ showed higher transport from the apical to the basolateral compartment than the negatively-charged TCNP and PSNP. The intracellular content of these positive PNP was also higher than that of negative PNP. Several groups also found a comparatively higher intracellular uptake of positive NP than of negative ones.[35-37] While it is not fully clear how surface charge influences

the transport of different PNP across cell monolayers, the electrostatic interaction mentioned before may facilitate the interaction between positive PNP and the negatively charged cell membrane. This may enhance cellular traffic of positive PNP across the cells. Another explanation may be found in possible differential interactions of the differently charged PNP with the various cell membrane-bound transporters such as the ABC transporters, which is studied in the next section.
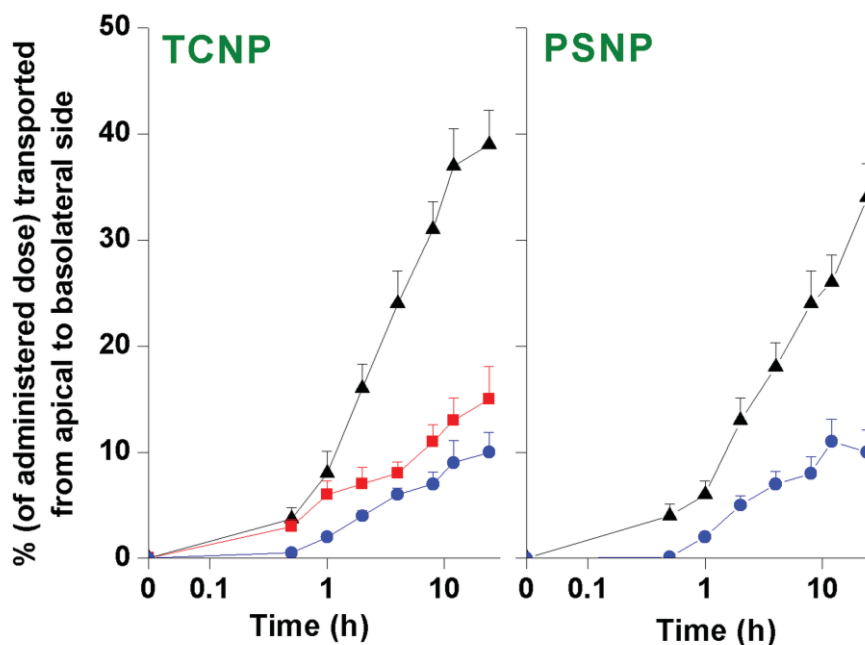

Figure 4: *Time dependent transport of tri-block copolymer NP (TCNP) and polystyrene NP (PSNP) (1 μg/ml) with positive amine (▲), slightly negative hydroxyl (■) and negative carboxylic acid (●) terminated surface charges across Caco-2 monolayers. Results are shown as mean ± SEM (n=3).*

Effect of specific ABC transporter inhibitors on TCNP and PSNP transport across Caco-2 monolayer

For a better understanding on the possible role of different ABC transporters in the transport of PNP with different surface charges, the transwell experiments were repeated in the presence of specific ABC transporter inhibitors (100 μM verapamil[14] for MDR1/P-gp, which is located in the apical membrane; 24 μM MK571[14] for MRP1, which is located in the basolateral membrane and 5 μM Ko143[14] for BCRP, which is located in the apical membrane). The results are shown in Figure 5. Verapamil significantly reduced the apical compartment concentration of both positive PNP but had no significant effect on the transport of the negative PNP across the Caco-2 monolayer. The decreased amounts of positive PNP in the apical compartment was accompanied by a significant increase in the intracellular amounts of these PNP. This intracellular uptake of positive PNP in Caco-2 cells was confirmed by confocal laser scanning microscopy (CLSM) (supplementary information, *Appendix D*). With MK571, the concentrations of negative PNP in the basolateral compartment were significantly reduced, reflecting a decreased transport across the Caco-2 monolayer. Blocking BCRP with Ko143 did not show any effect on the trans-monolayer transport of any PNP. Based on these results, obtained upon

inhibition of specific ABC transporters, it can be concluded that MDR1/P-gp plays a role in the cellular efflux of positive PNP and that MRP1 affects the cellular efflux of negative PNP. Although an interaction between cationic PNP and MDR1/P-gp has been claimed before,[38] to the best of our knowledge, this is the first time that it was shown that positive PNP are a substrate for MDR1/P-gp mediated transport.
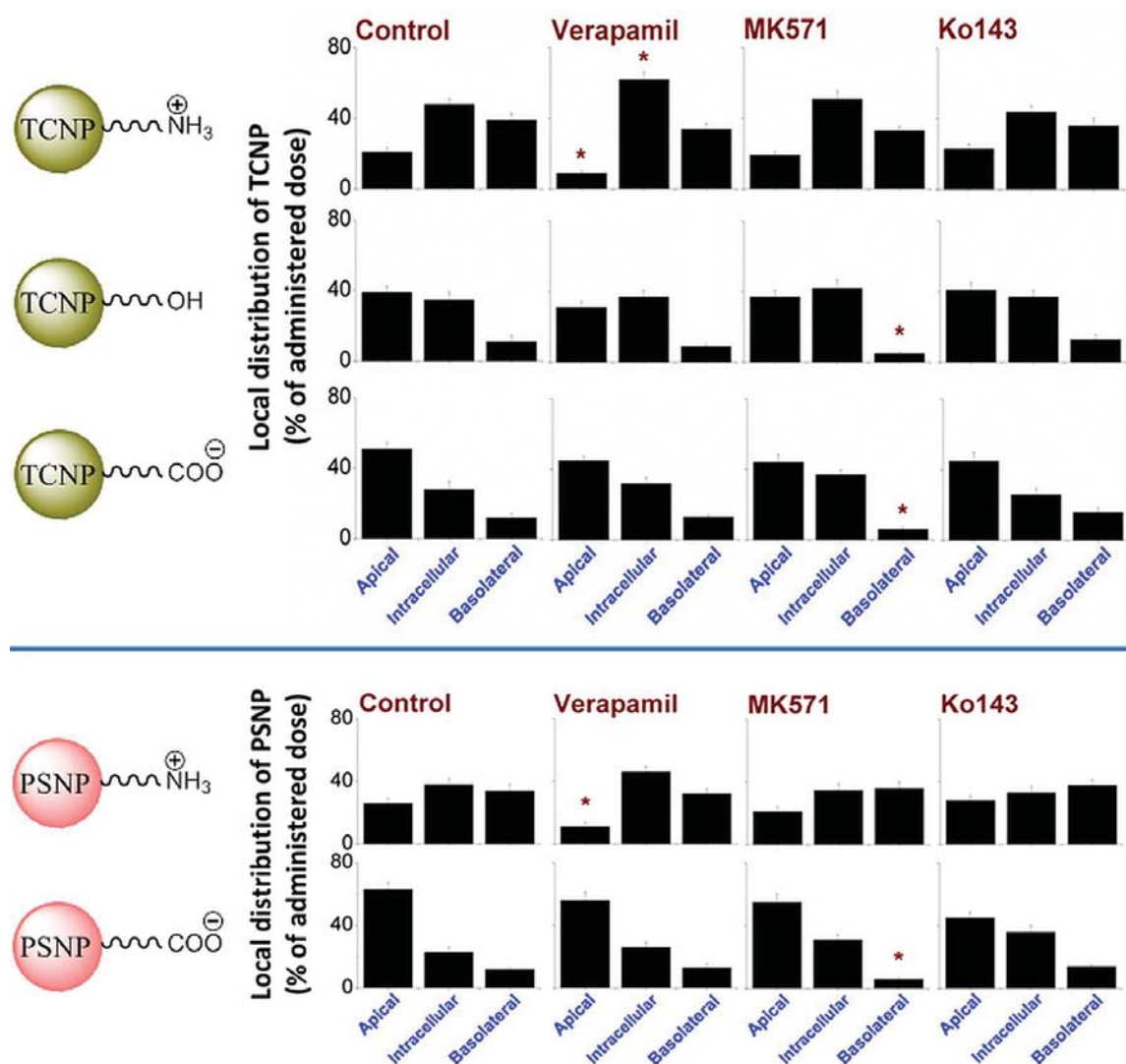

Figure 5: *Effect of specific ABC transporter inhibitors on the tri-compartmental distribution of different tri-block copolymer NP (TCNP) and polystyrene NP (PSNP) across Caco-2 monolayers after 24 h at 1 μg/ml. Results are shown as mean ± SEM (n=3). The * signifies p < 0.05 compared to negative control (0 μg/ml).*

Several experimental and computational studies indicated that the presence of hydrogen bond donor moieties makes a molecule a good substrate for MDR1/P-gp.[39,40] Similarly, MRP1 seems to play an important role in the transport of negatively charged PNP. A brief scrutiny of the chemical structures of the known substrates of MRP1 (Table 1) reveals an inclination for negatively charged molecules. So, our results on the surface charge-specific interaction between ABC transporters and PNP are in line with current knowledge on the substrate characteristics for the different ABC transporters.

Effect of ABC transporter inhibition by quercetin on TCNP transport across Caco-2 monolayers

To investigate whether the observed interaction of PNP with the different ABC transporters is affected by food-borne compounds, trans-monolayer transport of PNP was investigated in the presence of the flavonoid quercetin. Quercetin is known to interact with most ABC transporters expressed in Caco-2 cells (MDR1/P-gp, MRP2, MRP4 MRP5, BCRP), usually with an inhibitory effect.[40] Figure 6 shows the tri-compartmental (apical, intracellular and basolateral) distribution of PNP upon 24 h exposure of the Caco-2 monolayers to PNP added to the apical side, in either absence (control) or presence of 10 µM quercetin. Exposure of Caco-2 monolayers to positive PNP, in the presence of quercetin, showed a significant decrease of the positive PNP in the apical compartment and a concomitant increase in the intracellular as well as basolateral levels. For the negative TCNP-COO-, the co-exposure with quercetin resulted in an overall increase in the intracellular levels. This indicated that quercetin influences the transport of especially positive PNP by an interaction with the ABC transporters. The obtained data showed that the bioavailability of positive PNP is increased by the presence of quercetin as a flavonoid component often present in food.
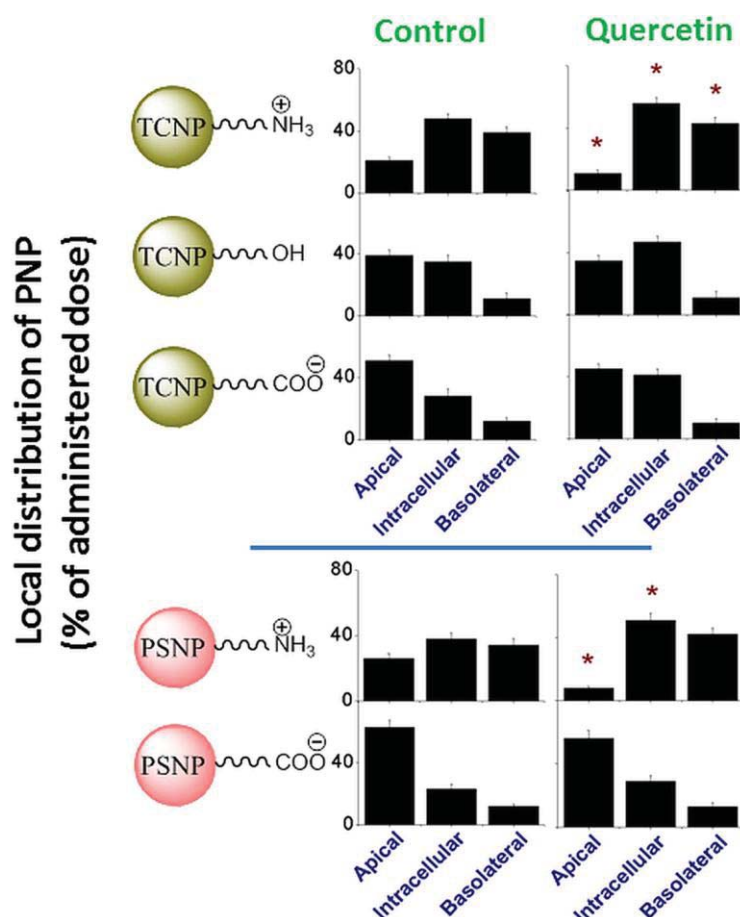
Figure 6: *Tri-compartmental distribution of different surface charge-bearing tri-block copolymer NP (TCNP) and polystyrene NP (PSNP) upon incubation of Caco-2 monolayers for 24 h to the different PNP (1 µg/ml) in the absence (control) or presence of 10 µM quercetin. Results are shown as mean ± SEM (n=3). The * signifies p < 0.05 compared to control.*

PhIP transport across Caco-2 monolayers upon co-exposure with different PNP

ABC transporters are quite important in protecting the human body from pro-carcinogens, like PhIP, as the transporters present on the apical (luminal) side of enterocytes pump the PhIP back to the intestinal lumen, thereby reducing its bioavailability. PhIP is a pro-carcinogenic heterocyclic amine that is abundantly present in the crust of fried meat[22,41] and is reported to cause lymphomas in mice and mammary and colon carcinomas in rats.[42,43] Figure 7 shows the time-dependent transport of PhIP across Caco-2 monolayers, where 5 µM PhIP was added to the apical compartment in the absence or presence of different PNP.
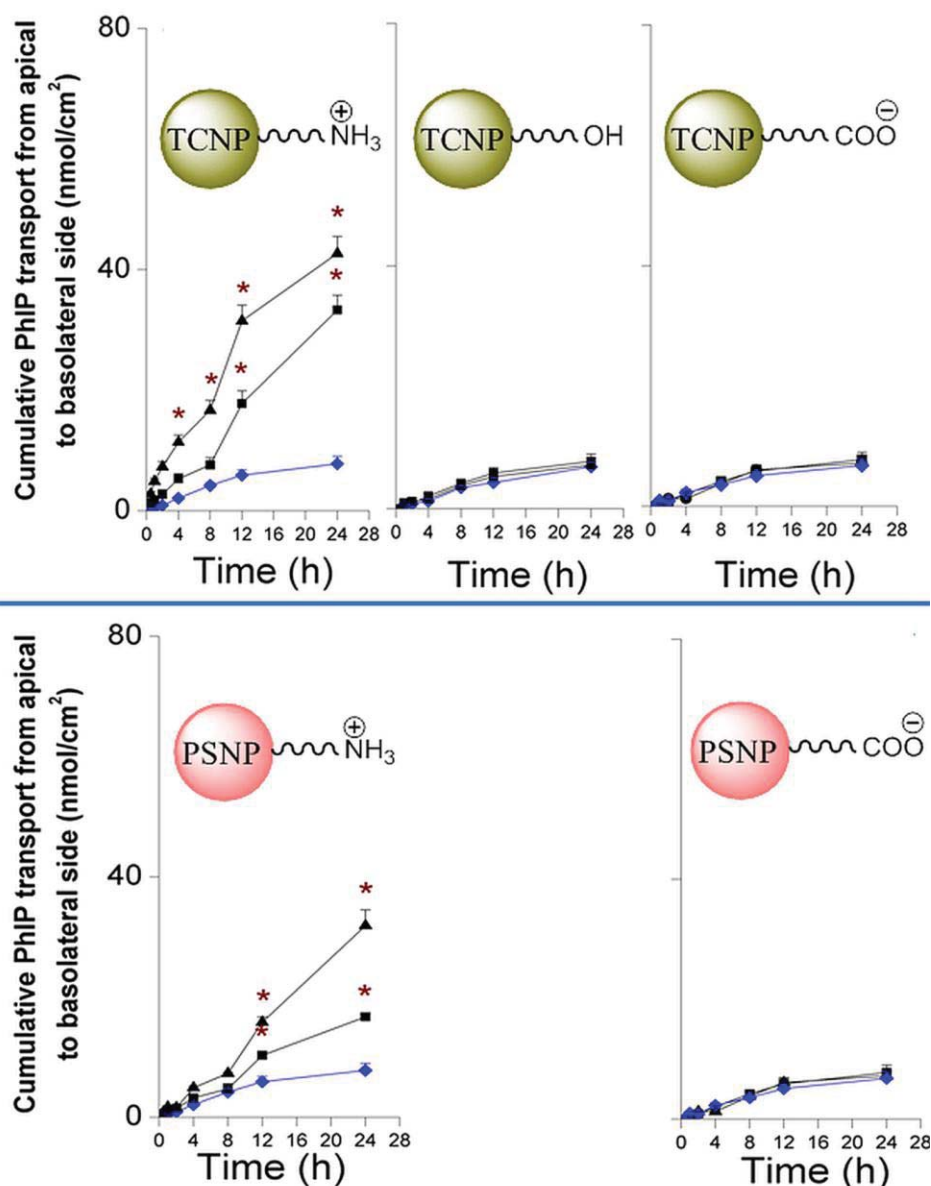
Figure 7: *Time-dependent transport of PhIP across Caco-2 monolayers upon apical exposure of the cells to PhIP in the absence (♦) or presence of 0.5 µg/ml (■) or 1.0 µg/ml (▲) of: (**Upper layer**) different tri-block copolymer NP (TCNP) and (**Lower layer**) polystyrene NP (PSNP). The * signifies p < 0.05 compared to negative control (0 µg/ml polymeric NP). Results are shown as mean ± SEM (n=3).*

For both TCNP and PSNP, only the positive NP showed an increase in the transport of PhIP across the Caco-2 monolayer from the apical to the basolateral compartments with the effect being more pronounced at PNP concentrations of 1 µg/ml than of 0.5 µg/ml. The distribution of PhIP over different compartments (apical, intracellular, basolateral) after 24 h exposure to PhIP in the presence of various PNP are shown in Figure 8. Interestingly, for both TCNP (Figure 8; upper layer) and PSNP (Figure 8; lower layer), the presence of positive PNP decreased the amount of PhIP in the apical compartment significantly, whereas the basolateral compartments showed a considerable increase in PhIP content. This agrees with the findings that the positive PNP interfered with the P-gp transporters. When control experiments were done with measuring the tri-compartmental distribution of PhIP in an identical experimental set-up, in which P-gp was selectively blocked by verapamil, a similar distribution pattern of PhIP was observed. This indicates that a higher bioavailability of compounds, like PhIP, can be achieved by inhibition of an apical ABC transporter. For the negative PNP, no significant effect on inter-compartmental distribution of PhIP could be observed for both TCNP and PSNP. Zhang et al.[44] reported about interactions of poly(ethylene glycol)–polylactide polymer (PEG-PLA) NP (size ~155 nm) with ABC transporters using a monolayer of HepG2 cells.
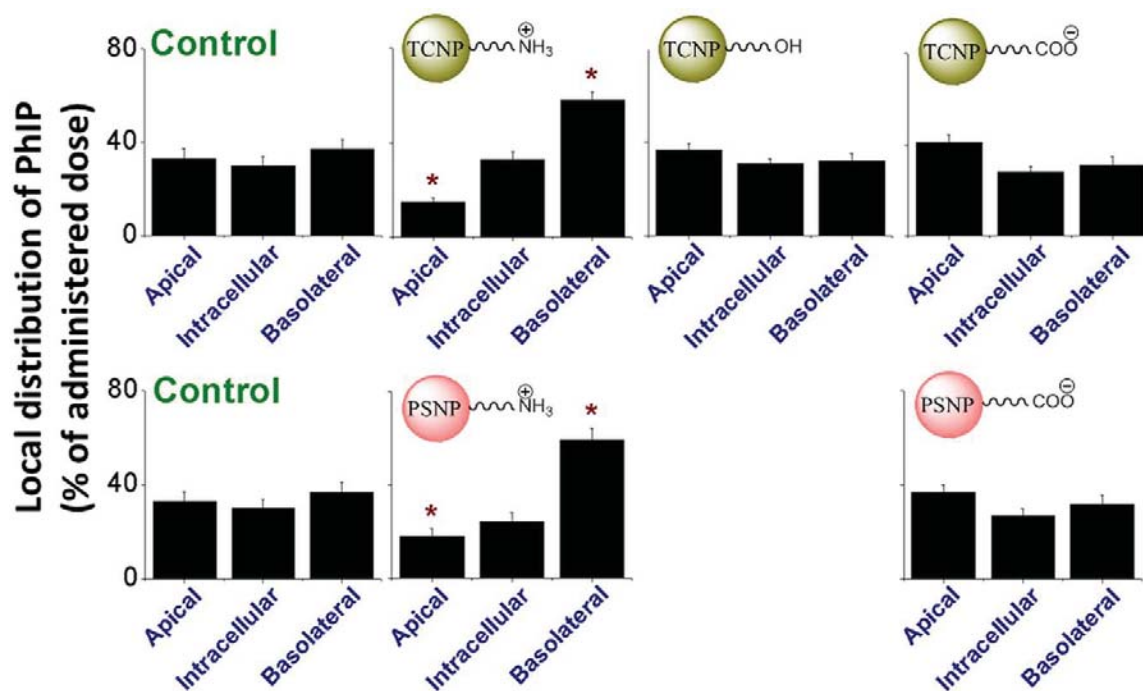

*Figure 8: Tri-compartmental distribution of PhIP across Caco-2 monolayers after 24 h exposure to 5 µM PhIP, in the absence (control) or presence of 1 µg/ml of: (**Upper layer**) different tri-block copolymer NP (TCNP) and (**lower layer**) polystyrene NP (PSNP). The * signifies p < 0.05 compared to negative control (0 µg/ml). Results are shown as mean ± SEM (n=3).*

Similarly, it was recently claimed that blocking of P-gp by iron nanoparticles can be used to enhance intracellular delivery of anti-cancer drugs (like doxorubicin) in rat glioma C6 cells.[45] These findings can have important implications for orally administered cancer therapeutics. ABC transporters are notorious for causing resistance towards multiple anti-cancer drugs as they effectively promote cellular efflux of the drugs.[46] With the growing use of PNP in different (like

anti-cancer) therapies, our finding can be useful in formulating an effective way of drug delivery and reducing multidrug resistance. Positively charged PNP inhibited MDR1/P-gp and can thus possibly be used to (partly) overcome multidrug resistance towards certain drugs that are otherwise transported out of the cells by MDR1/P-gp.

Taken together, the results reported here, characterized for the first time the transport of differently charged PNP over a monolayer of Caco-2 human colon cells. They showed that PNP display a significant interaction with cellular ABC transporters and thereby can strongly influence the overall transport achieved by these transporter proteins. This effect is typically (much) larger for positively charged PNP than for negatively charged PNP, i.e. charge matters. This influence of PNP on ABC transporters will strongly affect the bioavailability of materials that enter the wall of the intestines and therefore their uptake into the blood stream. These conclusions thus add a new dimension to the hazard and risk assessment of PNP.

References

1. Das M, Ansari KM, Tripathi A, Dwivedi PD; *J. Biomed. Nanotechnol.* 2011, 7:13-14.
2. Garcia M, Forbe T, Gonzalez E; *Ciencia. Tecnol. Alime.* 2010, 30:573-581.
3. Ahamed M, AlSalhi MS, Siddiqui MKJ; *Clinica. Chimica. Acta.* 2010, 411:1841-1848.
4. Araujo L, Sheppard M, Löbenberg R, Kreuter J; *Int. J. Pharm.* 1999, 176:209-224.
5. Paul DR, Robeson LM; *Polymer* 2008, 49:3187-3204.
6. Otman O, Boullanger P, Drockenmuller E, Hamaide T; *Beilstein J. Org. Chem.* 2010, 6.
7. Zambrano-Zaragoza ML, Mercado-Silva E, Gutiérrez-Cortez E, Castaño-Tostado E, Quintanar-Guerrero D; *LWT - Food Sci.Technol.* 2011, 44:1362-1368.
8. Soppimath KS, Aminabhavi TM, Kulkarni AR, Rudzinski WE; *J. Control. Release* 2001, 70:1-20.
9. Pridgen EM, Langer R, Farokhzad OC; *Nanomedicine* 2007, 2:669-680.
10. Stevanovic M, Uskokovic D; *Curr. Nanosci.* 2009, 5:1-14.
11. Ruizendaal L, Bhattacharjee S, Pournazari K, Rosso-Vasic M, de Haan LHJ, Alink GM, et al.; *Nanotoxicology* 2009, 3:339-347.
12. Bhattacharjee S, de Haan LHJ, Evers NM, Jiang X, Marcelis ATM, Zuilhof H, et al.; *Part. Fibre Toxicol.* 2010, 7(25).
13. Liong M, Lu J, Kovochich M, Xia T, Ruehm SG, Nel AE, et al.; *ACS Nano* 2008, 2:889-896.
14. Brand W, van der Wel PAI, Rein MJ, Barron D, Williamson G, van Bladeren PJ, et al.; *Drug Metab. Dispos.* 2008, 36:1794-1802.
15. Schutte ME, Boersma MG, Verhallen DAM, Groten JP, Rietjens IMCM; *Food Chem. Toxicol.* 2008, 46:557-566.
16. Dihal AA, Woutersen RA, Ommen Bv, Rietjens IMCM, Stierum RH; *Cancer Lett.* 2006, 238:248-259.
17. Lo D, Tynan W, Dickerson J, Scharf M, Cooper J, Byrne D, et al.; *Int. Immunol.* 2004, 16:91-99.
18. Mahler GJ, Esch MB, Tako E, Southard TL, Archer SD, Glahn RP, et al.; *Nat. Nanotechnol.* 2012, *Advance Online Publication* (DOI: 10.1038/nnano.2012.3).
19. Naruhashi K, Kurahashi Y, Fujita Y, Kawakita E, Yamasaki Y, Hattori K, et al.; *Drug Metab. Pharmacok.* 2011, 26:145-153.
20. Wang XD, Meng MX, Gao LB, Liu T, Xu Q, Zeng S; *Int. J. Pharm.* 2009, 378:1-8.
21. Brand W, Schutte ME, Williamson G, van Zanden JJ, Cnubben NHP, Groten JP, et al.; *Biomed. Pharmacother.* 2006, 60:508-519.
22. Schutte ME, van de Sandt JJM, Alink GM, Groten JP, Rietjens IMCM; *Cancer Lett.* 2006, 231:36-42.
23. Bhattacharjee S, Ershov D, Gucht Jvd, Alink GM, Rietjens IMCM, Zuilhof H, et al.; *Nanotoxicology* 2011, *Early Online* (DOI: 10.3109/17435390.2011.633714) :1-14.
24. Lin IC, Liang M, Liu T-Y, Ziora ZM, Monteiro MJ, Toth I; *Biomacromolecules* 2011, 12:1339-1348.
25. Sadeghi AMM, Dorkoosh FA, Avadi MR, Weinhold M, Bayat A, Delie F, et al.; *Eur. J. Pharm. Biopharm.* 2008, 70:270-278.
26. McClean S, Prosser E, Meehan E, O'Malley D, Clarke N, Ramtoola Z, et al.; *Eur. J. Pharm. Sci.* 1998, 6:153-163.
27. Chen F, Zhang Z-R, Yuan F, Qin X, Wang M, Huang Y; *Int. J. Pharm.* 2008, 349:226-233.
28. Ambike A, Rosilio Vr, Stella B, Lepêtre-Mouelhi S, Couvreur P; *Langmuir* 2011, 27:4891-4899.

29. Zhang J, Fan H, Levorse DA, Crocker LS; *Langmuir* 2011, 27:9473–9483.

30. Ventura CA, Tommasini S, Crupi E, Giannone I, Cardile V, Musumeci T, et al.; *Eur. J. Pharm. Biopharm.* 2008, 68:235-244.

31. Bhattacharjee S, Ershov D, Islam MA, Kaempfer AM, Gucht Jvd, Alink GM, et al.; 2012, *Submitted*.

32. Fazlollahi F, Angelow S, Yacobi NR, Marchelletta R, Yu ASL, Hamm-Alvarez SF, et al.; *Nanomed-Nanotechnol.* 2011, 7:588-594.

33. Yacobi NR, DeMaio L, Xie J, Hamm-Alvarez SF, Borok Z, Kim K-J, et al.; *Nanomed-Nanotechnol.* 2008, 4:139-145.

34. Roblegg E, Fröhlich E, Meindl C, Teubl B, Zaversky M, Zimmer A; *Nanotoxicology* 2011, Early Online:1-15.

35. des Rieux A, Ragnarsson EGE, Gullberg E, Preat V, Schneider YJ, Artursson P; *Eur. J. Pharm. Sci.* 2005, 25:455-465.

36. Chen LA, Mccrate JM, Lee JCM, Li H; *Nanotechnology* 2011, 22.

37. Hung Y, Chung TH, Wu SH, Yao M, Lu CW, Lin YS, et al.; *Biomaterials* 2007, 28:2959-2966.

38. Yue Z-G, Wei W, Lv P-P, Yue H, Wang L-Y, Su Z-G, et al.; *Biomacromolecules* 2011, 12:2440-2446.

39. Niu G, Castro CH, Nguyen N, Sullivan SM, Hughes JA; *J. Drug Target.* 2010, 18:468-476.

40. van Bladeren PJ, Brand W, Schutte ME, Williamson G, van Zanden JJ, Cnubben NHP, et al.; *Biomed. Pharmacother.* 2006, 60:508-519.

41. Frandsen H, Alexander J; *Carcinogenesis* 2000, 21:1197-1203.

42. Esumi H, Ohgaki H, Kohzen E, Takayama S, Sugimura T; *Jpn. J. Cancer Res.* 1989, 80:1176-1178.

43. Ito N, Hasegawa R, Imaida K, Tamano S, Hagiwara A, Hirose M, et al.; *Mutat. Res-Fund. Mol. M.* 1997, 376:107-114.

44. Zhang Y, Hu Z, Ye M, Pan Y, Chen J, Luo Y, et al.; *Eur. J. Pharm. Biopharm.* 2007, 66:268-280.

45. Kievit FM, Wang FY, Fang C, Mok H, Wang K, Silber JR, et al.; *J. Control. Release* 2011, 152:76-83.

46. Dean M; *J. Mammary Gland Biol.* 2009, 14:3-9.

Chapter 8

Role of surface charge in bioavailability and biodistribution of tri-block copolymer nanoparticles in rats after oral exposure

Abstract

Background: Tri-block copolymer nanoparticles (TCNP) are increasingly utilized, especially in drug delivery and diagnostics platforms. From in vitro studies, surface charge was observed to influence the transport of TCNP across Caco-2 monolayers grown on transwell inserts. **Objectives**: To investigate the influence of surface charge on bioavailability and biodistribution of TCNP after oral exposure in vivo and compare the results obtained with those from the in vitro Caco-2 transwell model. **Methods**: Monodisperse (45 ± 5 nm), fluorescent and differently charged (positive and negative) TCNP were orally administered to inbred Fischer 344 rats. Blood samples were collected at $t = 0$, ½, 1, 2, 4 and 6 h followed by sacrifice of the animals and collection of the major organs (lungs, liver, kidney, spleen, brain, intestine) and the tibia. The quantitative assessments for TCNP in blood, organs and tibia were performed by fluorescence measurements. **Results**: TCNP of both surface charges were absorbed from the gut and appeared in the blood within ½ h of oral administration. No significant difference in bioavailability and biodistribution could be found between positive and negative TCNP. Both TCNP, irrespective of charge, showed accumulation in especially the liver, kidneys and spleen while they were also detected in cerebral tissue. TCNP exposure was not accompanied by a significant increase in the serum alkaline phosphatase levels, pointing at absence of severe hepatotoxicity at the dose levels applied. **Conclusion**: In contrast to the data obtained in vitro, surface charge was not found to influence the in vivo bioavailability of TCNP after oral exposure, which may be ascribed to structural modifications induced during passage through the gastrointestinal tract. Liver and kidneys were the major sites of bioaccumulation for the TCNP. The obtained results encourage further elucidation of factors determining in vivo bioavailability which apparently cannot be adequately characterized in the currently often applied in vitro Caco-2 transwell model.

Introduction

With the growing use of nanotechnology-based products, it is necessary to characterize their toxic potentials as well as their interactions with living organisms.[1] Unfortunately, most of the investigations performed so far were based on in vitro experimental platforms comprising of a diverse range of nanoparticles (NP). As a result, there is a shortage of in vivo data enabling validation of the in vitro results and understanding the bioavailability and biodistribution of NP after introduction into the body. Recently, we reported the synthesis of fluorescent, monodisperse, well characterized tri-block copolymer [PEG_{2000}-polyhexylene adipate-PEG_{2000}] nanoparticles (TCNP) with different surface charges (amine modified positive/TCNP-NH_2 and acid modified negative/TCNP-COOH) and sizes (45 ± 5 nm and 90 ± 5 nm).[2] These TCNP had a hydrophobic polyester core protected from the outer aqueous environment by hydrophilic PEG tails. Interestingly, by incorporating a fluorescent probe in the polyester middle-block, it is possible to render these TCNP[3] fluorescent and hence detectable in vivo by fluorescence. The availability of these TCNP with different surface charges (positive and negative) allows the investigation of how surface charge influences the bioavailability and biodistribution of these TCNP after oral exposure. Many of the newly developed NP, including TCNP, were developed keeping in mind their potential use in food[4] and medicinal applications, like targeted drug delivery.[5,6] This further increases the possibility of human exposure to comparatively larger amounts of different TCNP, especially via oral route, highlighting the need for more in vivo studies.

In a previous study, surface charge was identified as an important factor in transport of TCNP across Caco-2 monolayers, which is a widely accepted in vitro model for human gut enterocytes.[7] Compared to the anionic NP, the cationic NP demonstrated significantly higher transport as well as greater cellular uptake across such transwell Caco-2 monolayer systems. Hence, the in vitro data suggested a higher bioavailability for cationic TCNP in vivo after oral administration compared to the anionic ones. It is important to investigate this effect of surface charge in vivo, as a better understanding on the influence of surface charge on bioavailability of TCNP after oral exposure can improve the development of tailor-made TCNP. In vivo data on NP described so far are mostly derived from studies with parenteral routes of exposure (like iv, sc)[8,9] and these cannot be compared to oral exposure scenarios as such. The intrinsic complexity of the gastrointestinal (GI) tract (like mucosal barrier, pH, presence of food matrix) can have an effect on the absorption of the TCNP. With very little amount of such in vivo data after oral exposure of NP available, a need for such an experiment was felt to be justified and timely.

The aim of this study was to investigate the role of surface charge in bioavailability and biodistribution of TCNP in rats after oral exposure and compare the findings with the available in vitro data. In the present study, inbred Fischer 344 rats were chosen due to the abundance of bioavailability studies performed on them after oral exposure.[10,11] TCNP with intrinsic fluorescent labelling and positive or negative charges were used for quantitative assessment of bioavailability and tissue distribution upon oral dosing.

Keeping in mind the probable uses of these TCNP in food-based formulations and drug delivery systems in future, the obtained data on bioavailability and biodistribution can be helpful in evaluating the potential of the TCNP for such applications.

Materials and methods

TCNP synthesis and characterization

The positive TCNP-NH$_2$ and negative TCNP-COOH of 45 ± 5 nm sizes, were synthesized and characterized as described before.[2] For the in vivo study, aqueous suspensions of TCNP (3.75, 7.5 and 30 mg/kg) were used.

Animal experiment

The animal experiment was approved by the ethical committee on animal experimentation in Wageningen University, the Netherlands and complied with the Dutch law on animal experimentation (Stb. 1977, 67; Stb. 1996, 565), revised February 5, 1997. Eight weeks old male Fischer 344 rats, with an average body weight of ∼200 g were obtained from Harlan (Horst, the Netherlands). The rats were divided into groups and housed together under standard conditions (22 ^{o}C, relative humidity 30-70 %, 12 h light/dark cycle) with *ad libitum* access to food and water. Prior to the oral gavage, rats were fasted for 4 h.

First, a pilot experiment was done with 4 rats (2 rats for both positive or negative TCNP) for each concentration (3.75, 7.5 and 30 mg/kg) of TCNP (total 12 rats). A single dose of 1.5 ml aqueous suspension of TCNP was administered through oral gavage. Blood was collected (150 µl) from tail veins of the rats in heparinized tubes at t = 0, ½, 1, 2, 4 and 6 h. After 6 h, rats were sacrificed under isoflurane anaesthesia and the blood from the aorta (∼7 ml) was collected. The following organs and tissues were collected: lungs, liver, kidneys, brain, spleen, stomach, small intestine, caecum and tibia. The organs and tissues were weighed and preserved in 10 % formalin solution before analysis with fluorescence.

The pilot experiment was followed by a main experiment of 14 rats: 2 rats as control where only 1.5 ml water was administered and 6 rats for both positive and negative TCNP each and were given 1.5 ml oral dose of only 30 mg/kg of TCNP. Blood and organs were collected and analysed in the same way as described above for the pilot phase.

Quantitative assessment of TCNP by fluorescence measurements

The blood samples (150 µl), collected from the tail veins at different time points as well as the aorta after sacrifice, were analysed by fluorescence (λ_{ex} = 488 nm ; λ_{em} = 543 nm). The amount of TCNP was estimated by a pre-determined calibration curve obtained by mixing Fischer 344 rat blood with serial dilutions of TCNP. The data obtained were adjusted to the total volume of blood present in the rat (∼8 ml) and the bioavailability was quantified after comparison to the administered dose. The preserved pieces of the organs were homogenized and a 150 µl aliquot of the homogenized tissue sample was diluted in ice cold nanopure water to one ml, before analysing it by fluorescence. The blood contents of the organs were determined as described before.[12] Calibration curves for each tissue was prepared by mixing known amounts of TCNP with homogenized tissue samples.

Estimation of serum ALP levels

The levels of serum ALP were measured by a commercial kit available from the Sigma Aldrich Chemie BV (Catalogue No: APF) and measured with fluorescence (λ_{ex} = 360 nm; λ_{em} = 440 nm).

Statistical analysis

The data were plotted using Origin Pro (version 8.0) software. Results were shown as mean ± standard error of the mean (SEM). Student's *t*-test was performed and data points were notified with an asterisk (*) when the readings for positive and negative TCNP were significantly different ($p < 0.05$) from each other.

Results

Bioavailability and blood clearance of TCNP

The quantitative assessment of TCNP in rat blood at t = 0, ½, 1, 2, 4 and 6 h was done by fluorescence and the results are shown in Figure 1. Both the positive and negative TCNP could be detected in the blood at t = ½ h. The amount of TCNP in blood increased in a dose-dependent way for 2-4 h and then started declining which was slightly more visible for the negative TCNP-COOH compared to the positive TCNP-NH2.
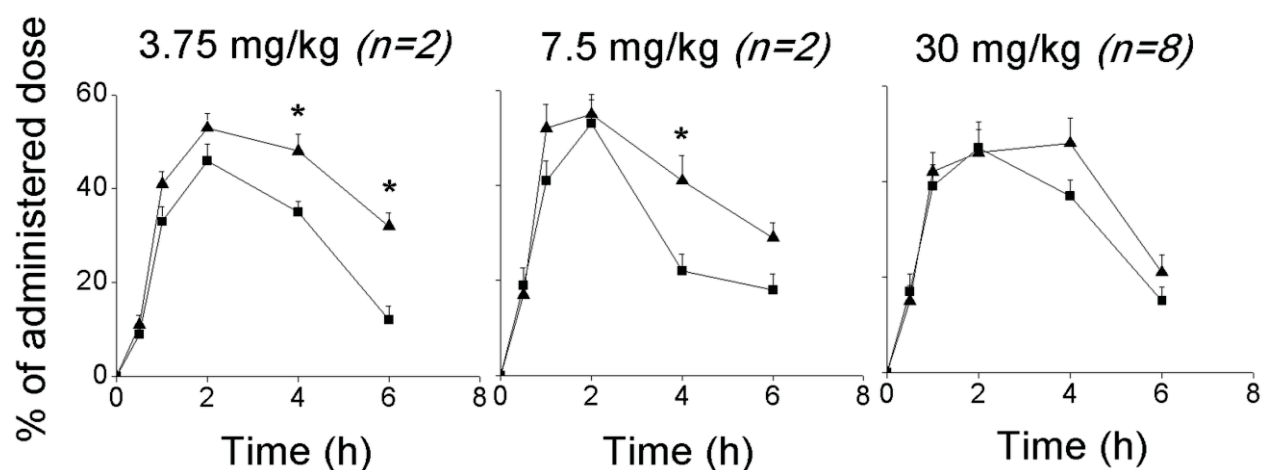
Figure 1: *Time dependent blood levels of positive TCNP-NH₂ (▲) and negative TCNP-COOH (■), expressed as % of the administered oral dose in rat at t = 0, ½, 1, 2, 4 and 6 h upon administration of three different dose levels (3.75, 7.5 and 30 mg/kg b.w.). Results are shown as mean ± SEM. The asterisk (*) denotes a statistically significant difference (p < 0.05) between the data for TCNP-NH₂ and TCNP-COOH.*

Qualitative organ distribution of TCNP

As the TCNP contained a fluorescent and UV-active probe, the organs were illuminated under UV light to visualise the possible presence of TCNP. The results are shown in Figure 2. Both TCNP were mainly deposited in liver and kidneys. Interestingly, some fluorescence could also be detected in the brain. The detection of TCNP in the whole caecum indicates that the TCNP were displaced from stomach with peristalsis.
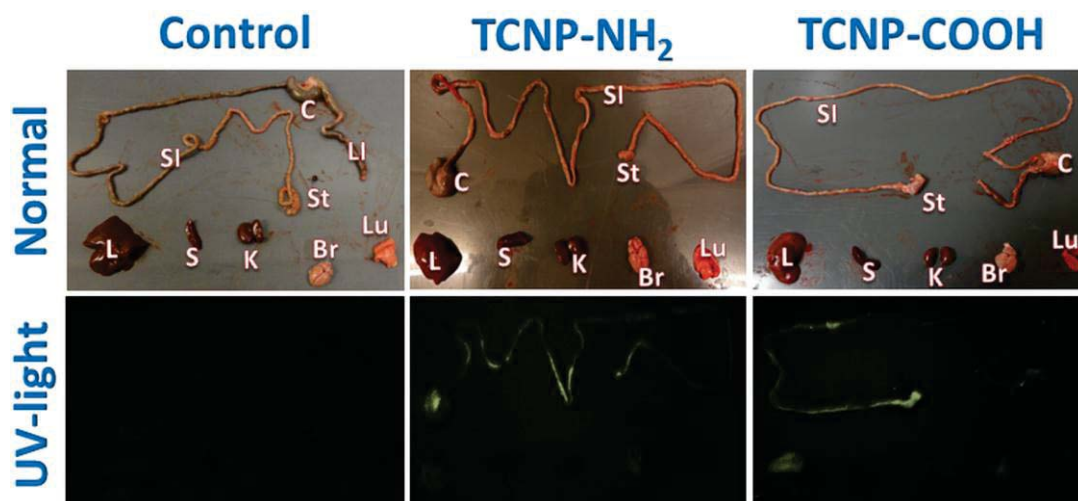

Figure 2: *Different organs (L = liver, K = kidney, S = spleen, Br = brain, Lu = lungs, St = stomach, SI = small intestine, C = caecum, LI = large intestine) collected from the rats treated with only water (control), positive TCNP-NH₂ and negative TCNP-COOH under UV-light illumination showing both the TCNP to be present mostly in the liver followed by kidneys and brain. Both the positive and negative TCNP were detected in the large intestine as well.*

Quantitative assessment of organ distribution of TCNP

The results from the quantitative assessment of the TCNP in different collected organs are shown in Figure 3. It was confirmed that the fluorescence spectrum detected in the various tissues (λ_{ex}=488 nm; λ_{em}=543 nm) were similar of the fluorescence characteristics of the dye when part of the TCNP and different from those of the free dye molecule (λ_{ex}=488 nm; λ_{em}=566 nm). The highest amounts of TCNP, irrespective of surface charge, were detected in the liver followed by the kidneys and spleen. Some TCNP could also be detected in the lungs, although the amounts were much lower compared to those detected in hepatic or renal tissues. Interestingly, both TCNP were detected to some extent in the brain. The % of the dose accumulating in the various organs were the same for all three dose levels indicating an increase in the accumulated contents in the organs with a clear dose-response behaviour.

To understand the efficiency of different organs in accumulating the TCNP from the blood circulation, the contents of the TCNP in the organs were re-plotted as amount of TCNP per g of tissues. The results are shown in Figure 4. It could be seen that when the amount of TCNP was expressed per unit mass of tissue, the amounts in spleen and liver were almost the same with small but detectable amounts in brain. The rest of the organs also contained TCNP although, the levels of accumulation were much lower.
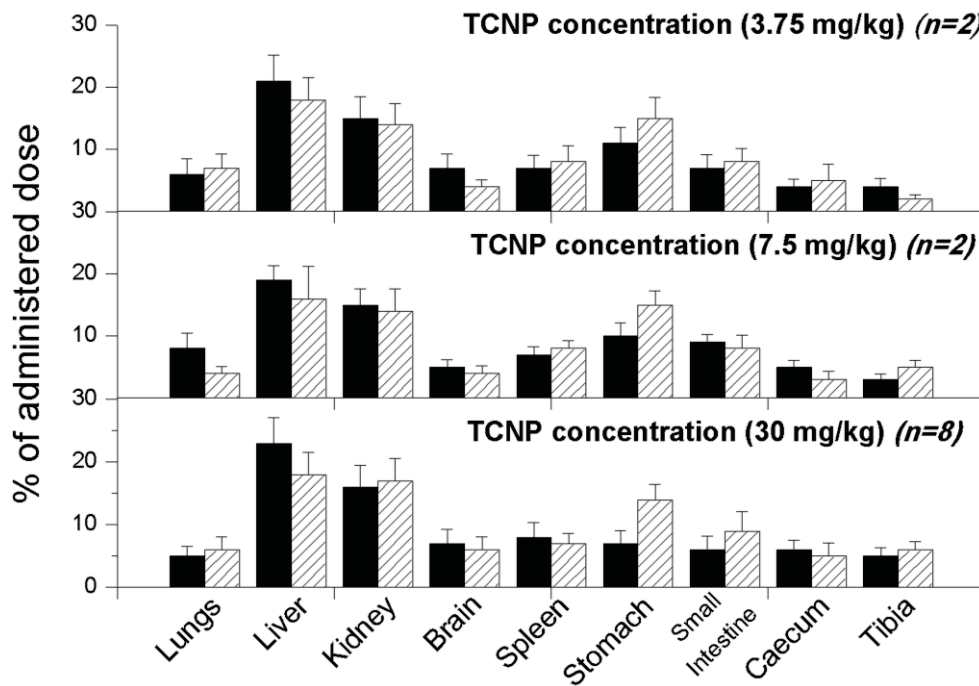
*Figure 3: Organ distribution of positive TCNP-NH$_2$ (black columns) and negative TCNP-COOH (shaded columns) in Fischer 344 rats at 6 h following oral administration. Three doses of TCNP were applied: 3.75 mg/kg (**top histogram**), 7.5 mg/kg (**middle histogram**) and 30 mg/kg (**bottom histogram**) b.w. Results are shown as mean % of administered dose ± SEM.*
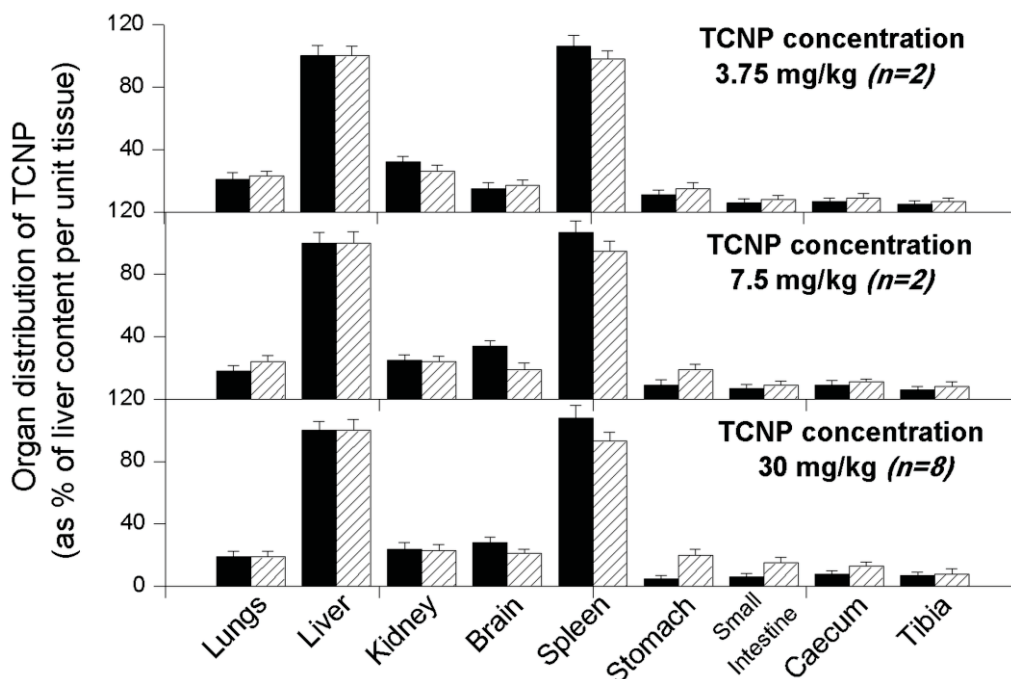

*Figure 4: Organ distribution of TCNP expressed in Fischer 344 rats at per g of tissue and as % of liver content (set at 100 %) at 6 h following oral administration to: 3.75 mg/kg (**top histogram**), 7.5 mg/kg (**middle histogram**) and 30 mg/kg (**bottom histogram**) b.w. of positive TCNP-NH$_2$ (black columns) and negative TCNP-COOH (shaded columns). Results are shown as mean ± SEM.*

Measurement of alkaline phosphatase enzyme activity

To detect possible hepatotoxicity of the TCNP, serum alkaline phosphatase (ALP) levels were measured in the blood samples and the results are shown in Figure 5. Compared to the negative TCNP-COOH, the positive TCNP-NH$_2$ caused some increase in serum ALP, only at the highest concentration (30 mg/kg) and after 6 h exposure. For other concentrations and time points, no effect on serum ALP levels was observed.
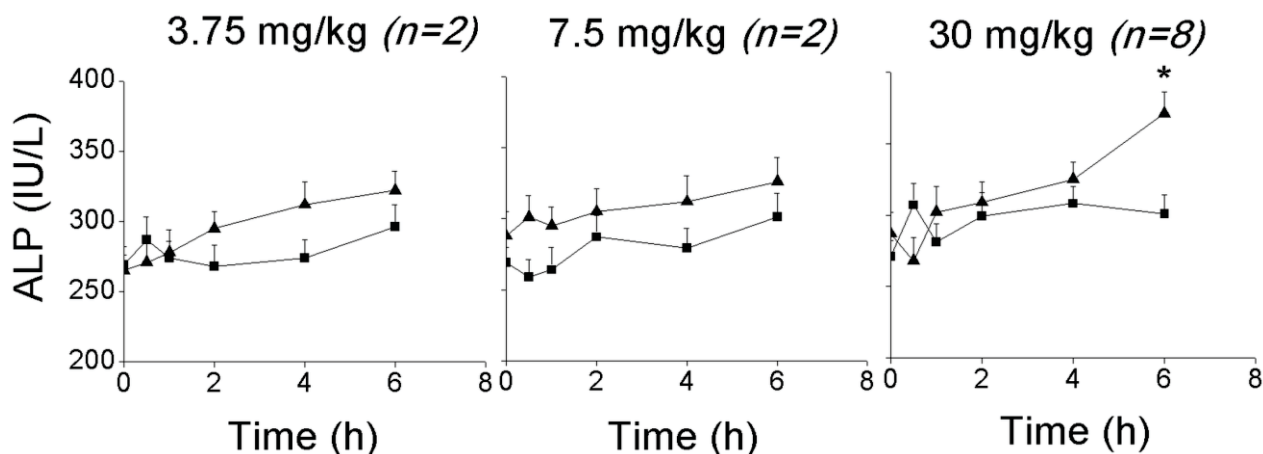

Figure 5: Serum ALP levels in Fischer 344 rats at t = 0, ½, 1, 2, 4 and 6 h following oral administration to positive TCNP-NH$_2$ (▲) and negative TCNP-COOH (■) TCNP of 3.75 mg/kg, 7.5 mg/kg and 30 mg/kg dose-levels. Results are shown as mean ± SEM. The asterisk (*) denotes significant difference (p < 0.05) between the TCNP-NH$_2$ and TCNP-COOH.

Discussion

The aim of this study was to check whether surface charge has an effect on the bioavailability and biodistribution of TCNP after oral administration in rats and compare the data with erstwhile in vitro data compiled from Caco-2 monolayer systems grown on transwell inserts. Although pivotal in transport of TCNP in vitro, surface charge was not found to influence the bioavailability and biodistribution of TCNP in vivo following oral exposure. Hence, the in vitro data based on Caco-2 transwell monolayer systems seemed inadequate in characterizing the overall in vivo behaviour of TCNP, including their passage through the GI tract.

The stabilities of the various TCNP at different pH (3-11) were confirmed by dynamic light scattering (DLS). Control experiments in which Caco-2 cells were exposed in vitro to only the fluorescent dye molecules, not being a part of the TCNP, revealed that the dye molecules alone did not pass through the cell layer, whereas when part of TCNP they were readily transported over the Caco-2 monolayer albeit at a different rate for positive and negatively charged TCNP respectively.[2] Furthermore, as the dye molecules were covalently attached to the polymer molecule, they cannot leak out freely from the polymer molecule. Additionally, the fluorescence characteristics of the dye molecule changes when it becomes part of the polymer, which may be due to the changes in the electronic environment. Taken together, these clues were used to

confirm the stability of the TCNP and exclude loss of the fluorescent dye from the TCNP during the in vivo study.

The mechanism of absorbance of the TCNP from the gut is still unclear. Few groups have proposed the role of intercellular juncture and fenestrations of the endothelia[13] apart from the role of dendritic cells[14] in absorption of NP. An another explanation may be the role of M-cells located in the Peyer's patches.[15-17] After being absorbed and thus detectable in blood, both the positive and negative TCNP showed an initial increase in amounts present in blood followed by a decline. This decline could be due to excretion of TCNP from the body or accumulation in different organs. In contrary to the in vitro data – where surface charge played an important role in toxicity, cellular uptake and transport across Caco-2 monolayers – there was no differential effect of surface charge on bioavailability of TCNP in vivo. One possible explanation for this discrepancy between the in vitro and in vivo results may be the other factors (like mucous coating over TCNP, pH, food matrix), which are present only in vivo. Although few reports tried to shed some light on the role of specific conditions of the GI tract in absorbance of NP,[18,19] a true understanding of this issue is yet to be achieved. The pH of the gut can also play a role in protecting or neutralizing the surface charge depending on the gut physiology. An important factor can be the mucous layer present in the GI tract, which is reported to form adsorbed layers over the NP and thus to alleviate the surface charge-effect that is otherwise visible in vitro. This interference from a mucous layer can be a hindrance to nanoparticle-based drug delivery platforms via oral exposure and had already initiated research in finding ways to overcome this mucous barrier for orally administered NP.[20] Very recently, an experiment with oral exposure with positive and negatively charged gold NP of different sizes was reported.[21] Interestingly, in line with our data, no significant surface charge-dependence in bioavailability or biodistribution of gold NP was observed. Similarly, no significant effect of surface charge was found in a report by Yamamoto et al.,[22] when neutral tyrosine and negative tyrosine-glutamine coated PEG/PDLLA nano-micelles were investigated for bioavailability in mice after iv infusion. However, a 100 % bioavailability is reached after iv infusion, which is incomparable to the oral exposure and makes our study distinct.

An interesting observation was the relatively rapid clearance of negative TCNP-COOH from the blood compared to the positive TCNP-NH$_2$. Bhattacharjee et al.[23] showed that acid terminated anionic silicon NP (1.6 ± 0.2 nm) induced phagocytosis in rat alveolar macrophage NR8383 cells compared to the positive amine terminated ones. It is often hypothesized that the negative NP easily acquire a coating of *opsonin* proteins in the blood, which induces phagocytosis by macrophage cells. Another explanation may be that after reaching the blood, the NP get coated with serum proteins, which render the NP to acquire a protein corona[24-26] that triggers phagocytosis by the macrophages.[27-29]

The high hepatic accumulation of TCNP of both surface charges was expected due to the high blood perfusion of the liver. It is suggested that, due to macrophage cells, like the Browicz-Kupffer cells in the liver,[30] the reticulo-endothelial system (RES) has a high capability of phagocytosing the TCNP from the blood circulation. Hence, organs like spleen also showed good accumulation of TCNP. Previously, Bhattacharjee et al.[23] showed that these TCNP can actively enter rat macrophage NR8383 cells in vitro. From this, it can be expected that the macrophage cells present in the RES can phagocytose the TCNP, thereby eliminating them from the blood circulation and causing a deposition of the TCNP in the relevant tissues. Similar accumulation of different NP in RES organs, like liver and spleen, has also been reported before. Choi et al.[31]

reported high accumulation of CdSe/ZnS quantum dots in liver and spleen of CD-1 mice after iv exposure. Similar involvement of macrophage cells in clearance of NP from the blood circulation has been reported before for other cells, like the hepatic macrophages[32] and hepatic endothelial cells.[33,34] For splenic tissue, a role for macrophage cells (dendritic cells) in phagocytosing the NP has also been proposed.[35] Interestingly, osseous tissue was often omitted in previous in vivo studies with NP. In our case, we chose the tibial bone and noticed some bio-accumulation. A possible explanation for this may be that bone marrow is also rich in macrophage cells.

The quick filtering of the TCNP from the blood stream by the macrophage cells of the RES can pose a challenge for targeted drug delivery by decreasing the concentrations of nanoparticulate drug formulations in blood. A detailed discussion of the on-going research on preventing this problem is beyond the scope of this article. However, it can be said that reduction of the phagocytosis of NP via surface modifications, like attaching hydrophilic PEG,[36] looks a promising option. The organ distribution of both types of TCNP showed an overall dose-dependence with bioaccumulation of the TCNP in each organ increasing with higher concentrations.

Interestingly, both the TCNP could also be detected in the brain. In the only comparable study with oral exposure of NP,[21] in contrast to the negative ones, positive gold NP (2.8 nm) reached brain. Especially for NP-based drug delivery in brain, where crossing the blood brain barrier is crucial, this finding can be of importance. Surface charge seemed not to influence the penetration of TCNP across the blood brain barrier.

Although TCNP-NH$_2$ showed some increase in serum ALP levels compared to the TCNP-COOH, the results were inconclusive to indicate hepatic stress for TCNP-NH$_2$. Polystyrene NP were reported to be toxic for HepG2 cell lines in vitro.[37] However, in vivo data on such hepatic stress induced by NP is rare. In an oral 13 weeks exposure study in F344 rats with 56 nm silver NP, a mild increase in serum ALP was observed,[38] which showed an overall match with our data.

Conclusion

In contrast to the in vitro data obtained via transwell Caco-2 cell experiments – surface charge does not influence the bioavailability and biodistribution of TCNP after oral exposure in vivo. The interaction of TCNP with the GI tract (for example, leading to surface adsorption of mucous) can be an explanation for this discrepancy. With high accumulation of TCNP occurring in liver and spleen, the RES seems to play an important role in deposition of the TCNP. Other organs and tissues (like kidney, lungs, tibia) also showed bio-accumulation of TCNP. The TCNP, irrespective of surface charges, crossed the blood brain barrier, which encourages their further development as drug delivery vehicles for cerebral tissues. The obtained data pointed the need of further in vivo characterizations on the behaviour of orally administered NP, which seemed to differ from in vitro Caco-2 transwell systems, possibly due to surface adsorption of mucous.

References

1. Karakoti AS, Hench LL, Seal S; *Jom.* 2006, 58:77-82.
2. Bhattacharjee S, Ershov D, Gucht JV, Alink GM, Rietjens IM, Zuilhof H, et al.; *Nanotoxicology* 2011, *Advanced Online Publication*, 1-14.
3. Khoee S, Hassanzadeh S, Goliaie B; *Nanotechnology* 2007, 18.
4. Das M, Saxena N, Dwivedi PD; *Nanotoxicology* 2009, 3:10-18.
5. Lamprecht A, Ubrich N, Yamamoto H, Schäfer U, Takeuchi H, Maincent P, et al.; *J. Pharmacol. Exp. Ther.* 2001, 299:775-781.
6. Liong M, Lu J, Kovochich M, Xia T, Ruehm SG, Nel AE, et al.; *ACS Nano* 2008, 2:889-896.
7. Lin IC, Liang M, Liu T-Y, Monteiro MJ, Toth I; *Nanomed-Nanotechnol.* 2012, 8:8-11.
8. Farokhzad OC, Cheng J, Teply BA, Sherifi I, Jon S, Kantoff PW, et al.; *Proc. Natl. Acad. Sci.* 2006, 103:6315-6320.
9. Park J-H, Gu L, von Maltzahn G, Ruoslahti E, Bhatia SN, Sailor MJ; *Nat. Mater.* 2009, 8:331-336.
10. Heim KE, Bates HK, Rush RE, Oller AR; *Toxicol. Appl. Pharmacol.* 2007, 224:126-137.
11. Arts JHE, Muijser H, Appel MJ, Frieke Kuper C, Bessems JGM, Woutersen RA; *Food Chem. Toxicol.* 2004, 42:1389-1399.
12. Oeff K, Konig A; *Naunyn-Schmiedebergs Archiv Fur Experimentelle Pathologie Und Pharmakologi* 1955, 226:98-102.
13. Ruenraroengsak P, Cook JM, Florence AT; *J. Control. Release* 2010, 141:265-276.
14. Rimoldi M, Rescigno M; *Vaccine* 2005, 23:1793-1796.
15. Seifert J, Haraszti B, Sass W; *J. Anatomy* 1996, 189:483-486.
16. Seifert J, Sass W; *Digestive Diseases* 1990, 8:169-178.
17. Sass W, Ganser R, Enders G, Seifert J; *Zeitschrift Fur Gastroenterologie* 1987, 25:645-645.
18. Hillery AM, Jani PU, Florence AT; *J. Drug Target.* 1994, 2:151-156.
19. Smyth SH, Feldhaus S, Schumacher U, Carr KE; *Int. J. Pharm.* 2008, 346:109-118.
20. Lai SK, Wang Y-Y, Hanes J; *Adv. Drug Deliv. Rev.* 2009, 61:158-171.
21. Schleh C, Semmler-Behnke M, Lipka J, Wenk A, Hirn S, Schäffler M, et al.; *Nanotoxicology* 2012, 6:36-46.
22. Yamamoto Y, Nagasaki Y, Kato Y, Sugiyama Y, Kataoka K; *J. Control. Release* 2001, 77:27-38.
23. Bhattacharjee S, de Haan LHJ, Evers NM, Jiang X, Marcelis ATM, Zuilhof H, et al.; *Part. Fibre Toxicol.* 2010, 7(25).
24. Lundqvist M, Stigler J, Elia G, Lynch I, Cedervall T, Dawson KA; *Proc. Natl. Acad. Sci.* 2008, 105:14265-14270.
25. Dobrovolskaia MA, Patri AK, Zheng JW, Clogston JD, Ayub N, Aggarwal P, et al.; *Nanomed-Nanotechnol.* 2009, 5:106-117.
26. Lacerda SHD, Park JJ, Meuse C, Pristinski D, Becker ML, Karim A, et al.; *ACS Nano* 2010, 4:365-379.
27. Aggarwal P, Hall JB, McLeland CB, Dobrovolskaia MA, McNeil SE; *Adv. Drug Deliv. Rev.* 2009, 61:428-437.
28. Dobrovolskaia MA, Aggarwal P, Hall JB, McNeil SE; *Mol. Pharm.* 2008, 5:487-495.

29. Rothen-Rutishauser BM, Schurch S, Haenni B, Kapp N, Gehr P; *Environ. Sci. Technol.* 2006, 40:4353-4359.

30. Sadauskas E, Wallin H, Stoltenberg M, Vogel U, Doering P, Larsen A, et al.; *Part. Fibre Toxicol.* 2007, 4:10.

31. Soo Choi H, Liu W, Misra P, Tanaka E, Zimmer JP, Itty Ipe B, et al.; *Nat. Biotechnol.* 2007, 25:1165-1170.

32. Cho CS, Kobayashi A, Takei R, Ishihara T, Maruyama A, Akaike T; *Biomaterials* 2001, 22:45-51.

33. Chiannilkulachai N, Ammoury N, Caillou B, Devissaguet JP, Couvreur P; *Cancer Chemoth. Pharm.* 1990, 26:122-126.

34. Gentile F, Ferrari M, Decuzzi P; *Ann. Biomed. Eng.* 2008, 36:254-261.

35. Demoy M, Gibaud S, Andreux JP, Weingarten C, Gouritin B, Couvreur P; *Future Strategies for Drug Delivery with Particulate Systems* 1998**:**17-22.

36. Otsuka H, Nagasaki Y, Kataoka K; *Adv. Drug Deliv. Rev.* 2003, 55:403-419.

37. Johnston HJ, Semmler-Behnke M, Brown DM, Kreyling W, Tran L, Stone V; *Toxicol. Appl. Pharmacol.* 2010, 242:66-78.

38. Kim YS, Song MY, Park JD, Song KS, Ryu HR, Chung YH, et al.; *Part. Fibre Toxicol.* 2010, 7.

Chapter 9

Oxidative stress is a secondary mode of action in the cytotoxicity of polystyrene nanoparticles

Abstract

The present paper probes the importance of the production of reactive oxygen species (ROS) and oxidative stress in the mode of action underlying the cytotoxicity of positively charged polystyrene nanoparticles (PSNP). Monodisperse, amine-terminated cationic polystyrene nanoparticles (PSNP-NH$_2$) were tested for cytotoxicity in macrophage NR8383 cells. ROS formation, protection by vitamin E and C, as well as the effect of increased or decreased levels of intracellular glutathione on the cytotoxicity were quantified. Results were compared to those from similar experiments with the mitochondrial electron transport chain (ETC) disrupting agent 2,4-dinitrophenol (DNP), or with the model inducer of oxidative stress hydrogen peroxide (H$_2$O$_2$). The induction of ROS and the protection by the various antioxidants against the cytotoxicity induced by PSNP-NH$_2$ resembled the results obtained for DNP and not those obtained for H$_2$O$_2$. Taken together, the results pointed at a secondary role for oxidative stress in the mode of action underlying the cytotoxicity of PSNP-NH$_2$. It is concluded that ETC disruption in the mitochondria is the primary cause for cytotoxicity of PSNP-NH$_2$, which subsequently leads to ROS production and oxidative stress as a secondary effect.

Introduction

With significant growth in the number of nanotechnology-based products entering the consumer market, exposure to nanomaterials is inevitable. In response to this exposure scenario coupled with the health hazards posed by the nanomaterials due to exceptional physico-chemical properties,[1] toxicity investigations on nanomaterials are justified and timely. Unfortunately, the knowledge on the mode of action underlying the cytotoxicity of nanoparticles (NP) remains far from complete.

Oxidative stress has often been hypothesized to be the primary mechanism of cytotoxicity of NP.[2] A surface chemistry-driven rapid induction in intracellular ROS after exposure to different NP was reported.[3] However, the source of cellular ROS still remains unclear. It is feasible that NP can react with a wide variety of biomolecules producing radicals, like ROS. Simultaneously, few recent reports identified intracellular mitochondria as target organs for different NP.[4] Charged NP can interact with intracellular mitochondria and dissipate the mitochondrial membrane potential ($\Delta\Psi_m$). A disturbance in mitochondrial membrane physiology can also disrupt the electron transport chain (ETC) and induce the production of ROS in addition to causing cellular ATP depletion. Then the question may be raised whether the ROS production is the cause of the cytotoxicity or rather a secondary effect occurring after ATP depletion or other effects following disruption of the mitochondrial membrane.

The aim of the present paper is to investigate the importance of ROS production and resulting oxidative stress as a mechanism of cytotoxicity of a selected toxic type of NP. To this end well-characterized, monodisperse (50 nm) polystyrene nanoparticles (PSNP) of positive charge (as negative PSNP did not show any cytotoxicity) were tested for ROS production and cytotoxicity in macrophage NR8383 cells in which antioxidant levels were artificially modified. We aimed to elucidate whether the PSNP-NH$_2$ act more as an oxidant causing oxidative stress, or rather cause cytotoxicity by disrupting the mitochondrial membrane, disturbing the electron transport chain (ETC). Therefore, similar experiments, as done with the PSNP were performed using the mitochondrial ETC disrupting agent, 2,4-dinitrophenol (DNP) and with the model inducer of oxidative stress, hydrogen peroxide (H_2O_2). The combined data clarify the degree of importance of oxidative stress in the mode of action underlying the cytotoxicity inflicted by cationic PSNP-NH$_2$.

Materials and methods

Polystyrene nanoparticles (PSNP)

Monodisperse (50 ± 5 nm) amine-terminated positive PSNP (PSNP-NH$_2$) were bought from Sigma Aldrich Chemie BV, and characterized as described before.[5]

NR8383 cells

The rat alveolar macrophage NR8383 cells were obtained from ATCC (Manassas, VA) and were cultured in 150 cm^2 flasks in F12-K medium supplemented with 10 % (v/v) FCS.[6] The cells were maintained under 37 °C and 5 % CO$_2$ atmosphere.

Measurement of intracellular ROS production by DCFH-DA assay

50 µl of an NR8383 cell suspension (2×10^5 cells/ml) in F12-K medium, containing 100 µM vitamin E or 1 mM vitamin C, or no added antioxidants (negative control), was seeded in each well of a 96-well plate and incubated for 24.[6] The vitamin C was added after 22 h of incubation, making the pre-incubation time for vitamin E and vitamin C, 24 h and 2 h, respectively. Different DNP, PSNP-NH$_2$ and H$_2$O$_2$ dilutions were then added to obtain the test dilutions (0-75 mM for DNP, 0-100 µg/ml for PSNP-NH$_2$ and 0-1 mM for H$_2$O$_2$). 5 µl of a 20 mM DCFH-DA solution in DMSO was added to each well after 4 h and incubated for further 4 h (total exposure time of 8 h). The fluorescence was measured (λ_{ex} = 485 nm, λ_{em} = 538 nm) and the induction factors for each concentration of PSNP were obtained by expressing the readings of the wells as % of the negative control. Control experiments were performed by incubating the DNP, PSNP-NH$_2$ and H$_2$O$_2$ at their test concentrations with DCFH-DA to exclude any interference with the fluorescence.

MTT assay to investigate protective effects of vitamins E and C against the cytotoxicity of DNP, PSNP-NH$_2$ and H$_2$O$_2$

The NR8383 cells were pre-incubated with vitamins E or C and then exposed to DNP, PSNP-NH$_2$ and H$_2$O$_2$ as described above. After 4 h, 5 µl of MTT solution in PBS (5 mg/ml) was added to each well and the plate was incubated for another 4 h. The purple formazan crystals were then dissolved in 100 µl/well DMSO and measured at 562 nm and 612 nm (as background). The reading of each well was expressed as % of the negative control (0 µg/ml).

MTT assay with pre-exposure to BSO or N-acetyl cysteine (NAC) to investigate the protective role of cellular GSH

The NR8383 cells were plated with medium containing BSO (100 µM/well) to reduce cellular GSH levels[7] or NAC (10 mM/well) to increase cellular GSH levels[8] for 24 h and 1 h, respectively, before being exposed to DNP, PSNP-NH$_2$ and H$_2$O$_2$ and performing the MTT assay as before.

Statistical analysis

Each experiment was repeated three times (n = 3) and data are presented as mean ± standard error of mean (SEM) before analysing with OriginPro software (version 8.0). Results significantly different ($p < 0.05$) from the negative control (for Figure 1) and from the data for DNP, PSNP-NH$_2$ or H$_2$O$_2$ (for Figures 2, 3) were marked with an asterisk (*) sign.

Results

Induction of intracellular ROS measured by the DCFH-DA assay

Figure 1 shows the induction of ROS in NR8383 cells after 4 h exposure to serial dilutions of DNP, PSNP-NH$_2$ and H$_2$O$_2$. In the absence of vitamins E or C, H$_2$O$_2$ showed maximal induction of ROS production (> 1100 %) followed by the PSNP-NH$_2$ (~563 %) and DNP (~500 %), all compared to the negative control. Vitamins E and C suppressed the inductions of ROS for all three exposure agents markedly, to a level hardly above control values. The corresponding EC50 values are given in Table 1. The pattern of ROS production induced by PSNP-NH$_2$ resembled that of the ETC uncoupler DNP more than that of the oxidative stress model compound H$_2$O$_2$.
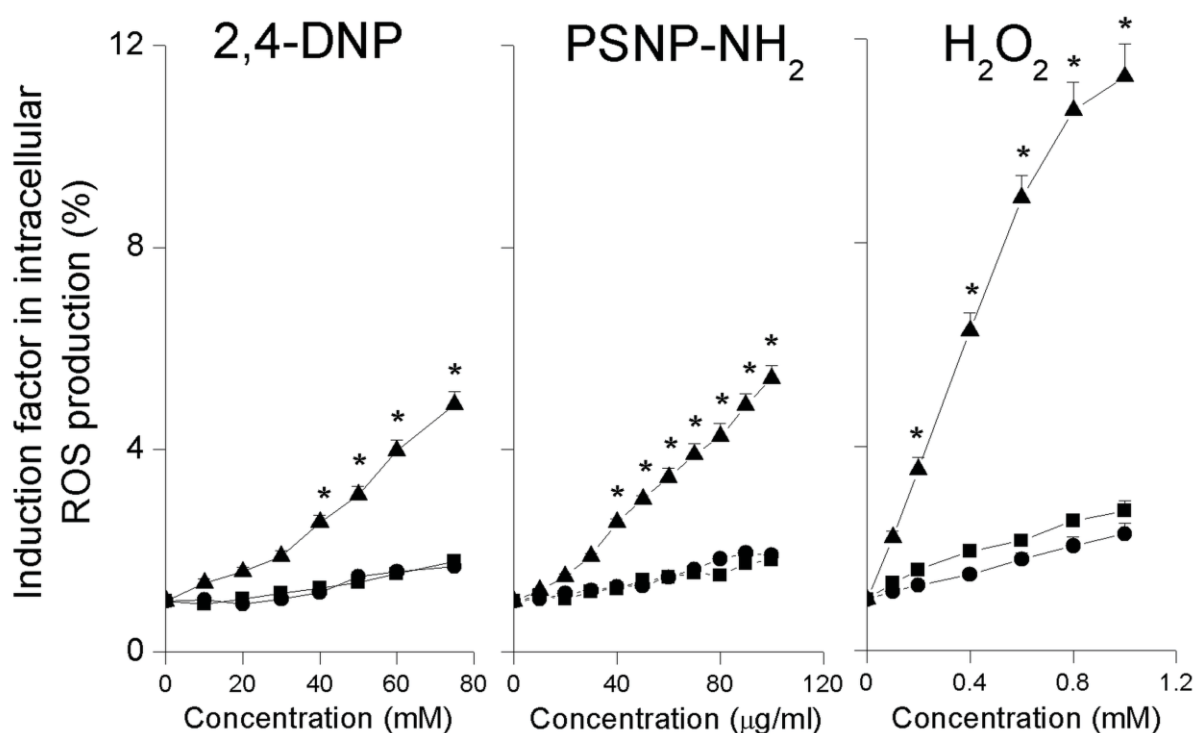
Figure 1: *Effects of vitamins E (■) and C (●) on the intracellular ROS induction in NR8383 cells after 4 h exposure to serial dilutions of DNP (0-75 mM), PSNP-NH$_2$ (0-100 µg/ml) or H$_2$O$_2$ (0-1 µM) (▲) as measured by the DCFH-DA assay (n = 3). The asterisk (*) sign marks significant differences (p < 0.05) compared to the negative control (0 µg/ml).*

MTT assay to investigate protective effects of vitamins E and C against the cytotoxicity of DNP, PSNP-NH$_2$ and H$_2$O$_2$

The NR8383 cells were pre-incubated with vitamins E or C and then exposed to DNP, PSNP-NH$_2$ and H$_2$O$_2$ as described above. After 4 h, 5 µl of MTT solution in PBS (5 mg/ml) was added to each well and the plate was incubated for another 4 h. The purple formazan crystals were then dissolved in 100 µl/well DMSO and measured at 562 nm and 612 nm (as background). The reading of each well was expressed as % of the negative control.
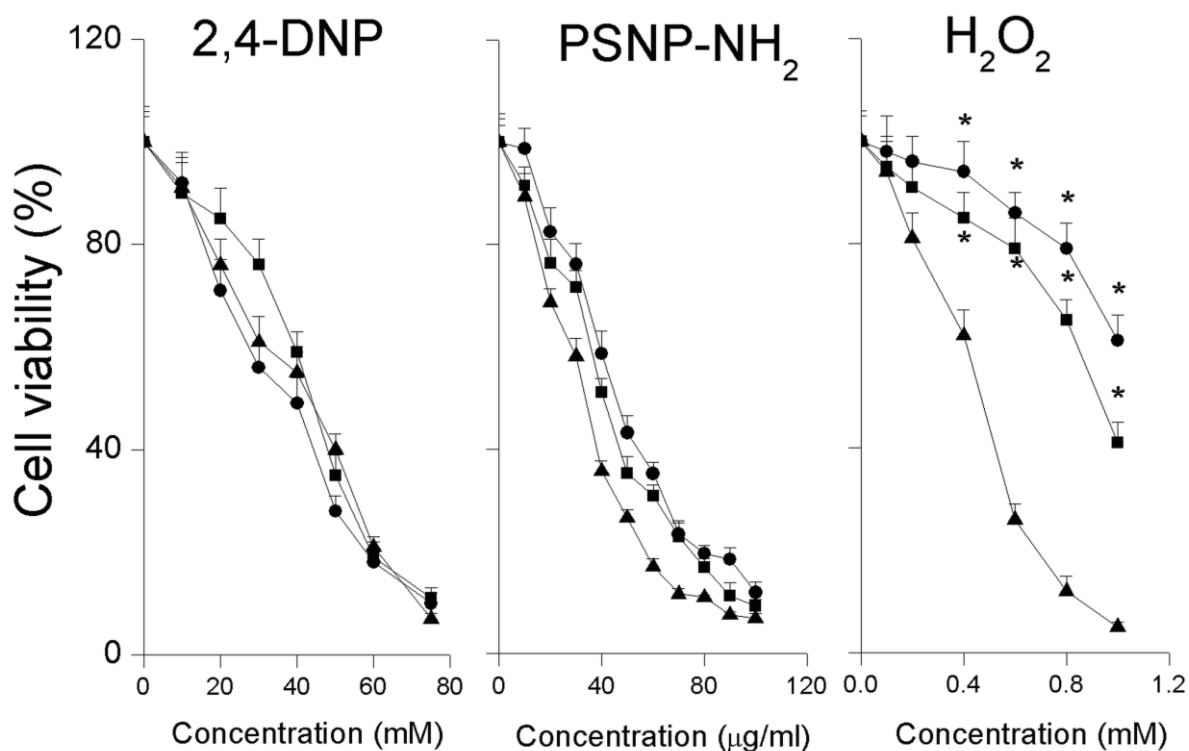
Figure 2: *Effects of vitamins E (■) and C (●) on cell viability in NR8383 cells after 4 h exposure to serial dilutions of DNP (0-75 mM), PSNP-NH₂ (0-100 µg/ml) or H₂O₂ (0-1 µM) (▲) as measured by the MTT assay (n = 3). The asterisk (*) sign marks significant differences (p < 0.05) compared to the corresponding values without vitamin E or C.*

Effect of exposure to BSO or NAC on the cytotoxicity caused by DNP, PSNP-NH₂ and H₂O₂

The effect of co-exposure to BSO or NAC on the cytotoxicity caused by DNP, PSNP-NH$_2$ and H$_2$O$_2$ are shown in Figure 3 with the EC50 values given in Table 1. Both decreasing the intracellular glutathione levels by incubation with BSO and increasing these levels by incubation with NAC, did not result in respectively a significant ($p < 0.05$) increase or decrease in cytotoxicity in case of DNP and PSNP-NH$_2$. However, for H$_2$O$_2$ the exposure to BSO and NAC significantly increased and decreased the cytotoxicity, respectively. Also, in these experiments the pattern of cytotoxicity and cellular protection observed for PSNP-NH$_2$ resembled that of the ETC uncoupler DNP more than that of the oxidative stress model compound H$_2$O$_2$.
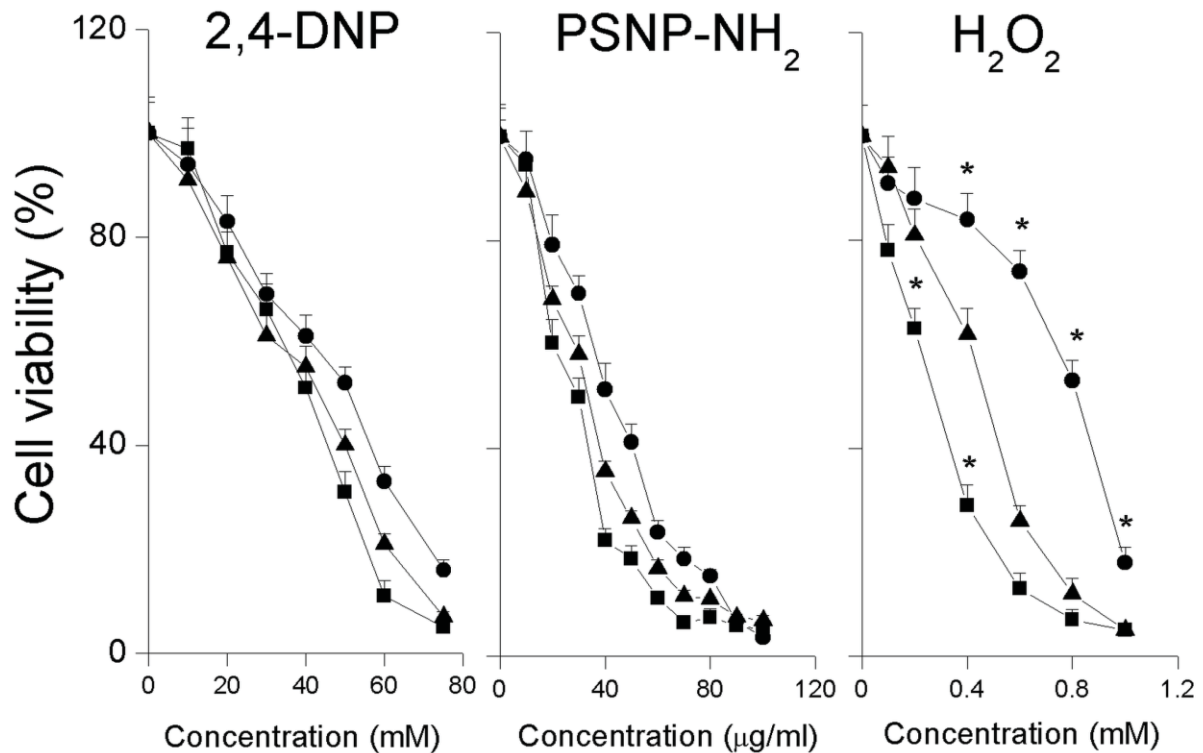
Figure 3: *Effects of BSO (■) and NAC (●) on cell viability in NR8383 cells after 4 h exposure to serial dilutions of DNP (0-75 mM), PSNP-NH₂ (0-100 μg/ml) or H₂O₂ (0-1 μM) (▲) as measured by the MTT assay (n = 3). The asterisk (*) sign marks significant differences (p < 0.05) compared to the corresponding values without BSO or NAC.*

Table 1: *The EC50 values obtained from different end-points reported in this article.*

End point	Agent	Figure	Without agent	Vitamin E	Vitamin C	BSO	NAC
ROS induction	DNP	1	33 mM	43 mM	48 mM		
	PSNP-NH₂		41 μg/ml	57 μg/ml	61 μg/ml		
	H₂O₂		0.4 mM	1.7 mM	2.2 mM		
Cell viability	DNP	2	28 mM	34 mM	26 mM		
	PSNP-NH₂		33 μg/ml	37 μg/ml	41 μg/ml		
	H₂O₂		0.2 mM	0.7 mM	0.8 mM		
Protection by changing cellular anti-oxidant levels	DNP	3	28 mM			22 mM	37 mM
	PSNP-NH₂		33 μg/ml			28 μg/ml	39 μg/ml
	H₂O₂		0.2 mM			0.05 mM	1.2 mM

Discussion

The results presented in this paper indicated that the pattern of ROS production, cytotoxicity and cellular protection against the cytotoxicity by antioxidants observed for PSNP-NH$_2$ resembled the pattern observed for the ETC uncoupler DNP more than that observed for the oxidative stress model compound H$_2$O$_2$. Based on these results, it is concluded that for cationic PSNP-NH$_2$, instead of being the primary mode of toxic action, ROS production and oxidative stress rather emerge as an aftermath of direct or indirect mitochondrial interaction with cationic PSNP-NH$_2$. Hence, oxidative stress is a consequence rather than the major cause of cytotoxicity for cationic PSNP.

With reference to several recent reports, a surface charge-driven interaction between PSNP-NH$_2$ and the mitochondrial membrane may be suggested as the major mode of action underlying the cytotoxicity of cationic PSNP-NH$_2$.[3,4] Simultaneously, it was also mentioned that oxidative stress failed to explain several findings (like the NF-κB expression) related to the primary mechanism of cytotoxicity for NP.[9] The experiments with DNP and H$_2$O$_2$ were therefore intentionally chosen in order to delineate the role of intracellular ROS and oxidative stress. It was observed that the damage done by H$_2$O$_2$, which is a known inducer of oxidative stress, can be mitigated effectively by both the vitamins E and C. In contrast, these vitamins failed to significantly ($p < 0.05$) reduce cytotoxicity caused by DNP or PSNP-NH$_2$. In fact, the protection patterns exhibited by the vitamins E and C against the cytotoxicity of DNP and PSNP-NH$_2$ showed an overall resemblance with each other and were clearly different from those obtained for H$_2$O$_2$.

The data obtained by decreasing or augmenting the cellular glutathione levels further supported the notion. It is reported that cationic PSNP-NH$_2$ caused a depletion of cellular GSH levels.[10] Hence, external application of NAC should have largely curbed the cytotoxicity of PSNP-NH$_2$ if oxidative stress was the main driving event behind cytotoxicity. In literature, although there are reports available on protective effects of externally applied anti-oxidants against cytotoxicity of NP, the results are often confusing and not consistent for the different end points measured.

Our data showed for the first time, through systematic investigations, that for cationic PSNP-NH$_2$, it is not oxidative stress but the mitochondrial dysfunction with cationic PSNP-NH$_2$ (with possible ETC disruption) that propels the cytotoxicity pathway, including the induction of ROS. PSNP-NH$_2$ had been shown to produce other toxic manifestations, like genotoxicity or production of cytokines (like interleukins) through involvement of transcription factors (like NF-κB).[11] Oxidative stress can be pivotal in such cellular events, as reflected in the protection by antioxidants against these different cellular events. Given the interplay between these various biological processes, it is clear that further data are desirable to understand in more detail the role of ROS in such manifestations.

Taken together, the results of the present paper point to ETC disruption in the mitochondria by the interaction between PSNP-NH$_2$ and mitochondria as the primary cause for the cytotoxicity of PSNP-NH$_2$. This disruption of the ETC then leads to ROS production, with oxidative stress as a secondary effect. Given the complexity, this does not present an estimate of the relative importance of the various effects, but clarifies the order of toxicity-inducing events for these cationic PSNP.

References

1. Clift MJD, Bhattacharjee S, Brown DM, Stone V; *Toxicol. Lett.* 2010, 198:358-365.
2. Stone V, Donaldson K; *Nat. Nanotechnol.* 2006, 1:23-24.
3. Xia T, Kovochich M, Brant J, Hotze M, Sempf J, Oberley T, et al.; *Nano Lett.* 2006, 6:1794-1807.
4. Xia T, Kovochich M, Liong M, Zink JI, Nel AE; *ACS Nano* 2007, 2:85-96.
5. Bhattacharjee S, Ershov D, Arif MI, Kämpfer AM, Maslowska AM, Gucht Jvd, et al.; *Submitted* 2012.
6. Bhattacharjee S, de Haan LHJ, Evers NM, Jiang X, Marcelis ATM, Zuilhof H, et al.; *Part. Fibre Toxicol.* 2010, 7(25).
7. van Berlo D, Knaapen AM, van Schooten FJ, Schins RPF, Albrecht C; *Part. Fibre Toxicol.* 2010, 7.
8. Shi MM, Chong IW, Godleski JJ, Paulauskis JD; *Immunology* 1999, 97:309-315.
9. Romoser AA, Figueroa DE, Sooresh A, Scribner K, Chen PL, Porter W, et al.; *Toxicol. Lett.* 2012, 210:293-301.
10. Hoet PH, Bruske-Hohlfeld I, Salata OV; *J. Nanobiotechnol.* 2004, 2:12.
11. Xia T, Li N, Nel AE; *Ann. Rev. Pub. Heal.* 2009, 30:137-150.

Chapter 10

Surface charge and size-dependent cytotoxicity and cell membrane interaction of polystyrene nanoparticles

Abstract

To assess the role of surface charge and particle size on the cytotoxicity and cellular uptake, monodisperse, fluorescent, positive and negative polystyrene nanoparticles (PSNP) of 50 and 100 nm sizes were tested in macrophage NR8383 cells. Only cationic PSNP showed cytotoxicity and a reduction in phagocytic index. Exposure to cationic PSNP also resulted in inductions of intracellular ROS production, cytoplasmic free Ca^{2+}, TNF-α, caspase-3 and NF-κB levels while decreasing the mitochondrial membrane potential ($\Delta\Psi_m$) as well as intracellular ATP content; with 50 nm PSNP showing larger effects. By confocal laser scanning microscopy (CLSM), higher cellular uptake for cationic PSNP was found. By atomic force microscopy (AFM), the cationic PSNP were found to increase the roughness of the cell membrane more, compared to the anionic PSNP. The results showed the importance of surface charge in determining the cytotoxicity and cellular uptake of PSNP, while identifying mitochondria and cellular membranes as important targets.

Introduction

In recent years nanotechnology has experienced unprecedented growth with its applications ranging from energy production to food and medicine. The increase in nanotechnology-based products also raises concerns for health-related aspects[1,2] with regard to the inevitable human exposure. Among the less understood topics related to nanotoxicological research are the factor(s) that influence the interaction between nanoparticles (NP) and cells. Surface charge and particle size are often hypothesized as important factors in such interactions.[3] Although several studies reported the influence of surface charge[4-6] and particle size[7,8] on cellular interactions of NP, concrete and systematic investigations on this issue are scarce. Recently, several reports have been published on the interactions of different NP with cell membrane-bound receptors,[9-11] although most of the reports focused on inorganic NP with very little data available on polymeric nanoparticles (PNP).

With polymer chemistry and engineering, different PNP with diverse physico-chemical properties (like surface properties, size, biodegradability, fluorescence, etc.) can be synthesized. This provides a unique tool to investigate how surface charge and particle size influence cellular interactions and toxicity of PNP. Such studies are also important considering the growing use of PNP in bioimaging and drug delivery.[12,13] Hence, an investigation into the role of surface charge and size on the cellular interactions of PNP is timely and justified. The aim of the present paper is to present such a systematic investigation on the role of surface charge and size of PNP on several related endpoints for cellular interaction and toxicity. Such a systematic in vitro study provides further insight in the possible mode of action underlying the cellular toxicity of these PNP.

The model PNP used in the present study were polystyrene nanoparticles (PSNP) which are available commercially in different sizes and surface properties. These PSNP are highly monodisperse and due to an embedded fluorescent probe, can be traced in biological environments through confocal laser scanning microscopy (CLSM). The model in vitro system used was the rat lung alveolar macrophage NR8383 cell line. This cell line is an adequate and widely accepted in vitro model. As these NR8383 cells are macrophage cells, a toxic effect exerted on them by the PSNP could also give some prediction towards toxicity that might be caused by PSNP on the innate immune system.

Oxidative stress caused by the induction of intracellular reactive oxygen species (ROS) production by different NP is a popular model to explain the cytotoxicity.[14-16] However, controversy exists whether ROS production is the cause or just a secondary consequence of the mode of action for cytotoxicity. Recently, some groups have claimed that especially for cationic NP, intracellular mitochondria are a target organelle.[17,18] It is possible that this interaction of PSNP with mitochondria, with possible disruption of its membrane permeability can decrease the cellular ATP content as well as increase the ROS production by uncoupling the electron transfer chain (ETC). To investigate the inflammatory response, at least partially caused by the ROS, tumor necrosis factor–alpha (TNF-α) can be a useful pro-inflammatory biomarker. The nuclear factor kappa-light-chain-enhancer of activated B cells (NF-κB) is often associated with such stress responses[19] and hence, can be monitored while investigating the implications of oxidative stress.

Furthermore, as intracellular mitochondria are an important storage site for calcium, it can be expected that upon exposure to charged PSNP and subsequent deterioration of the

mitochondrial membranes, the mitochondrial calcium can get access to the cellular cytoplasm causing a cytoplasmic free calcium overload, which can subsequently trigger apoptotic pathways.[20] Previously, some groups have reported such an increase in intracellular free calcium after exposure to cationic NP.[21,22] Regarding activation of the apoptosis, caspase-3 can be an important biomarker.

With CLSM, a detailed investigation of the interactions of the different PSNP with the cellular system as well as cellular uptake is possible. This is of interest given the growing evidence that different NP show interactions with various cell membrane-bound receptors (like clathrin, caveolin, mannose and other receptors).[23] A common hypothesis put forward to describe cell-NP interactions states that the positive NP get electrostatically attracted towards the cell membranes because at normal physiological pH, cell membranes are overall negatively charged.[24,25] It has been shown by different groups that positive NP and not negative NP, cause holes or pores in suspended lipid bilayers (as an in vitro mimic of the lipid bilayer biomembranes of cells or mitochondria).[26,27] Recently, Verma et al.[28] showed that cationic gold NP can create transient pores in the cell membrane. This is an important finding as formation of such pores in biomembranes could actually contribute to the cytotoxicity of NP. However, so far the creation of holes in the cell membranes of living cells upon exposure to positive NP was not reported.

In the current paper, we present a systematic investigation of the surface charge and size-dependence of the cytotoxicity of PSNP using an extensive series of cellular end points (MTT, phagocytic index, mitochondrial membrane potential measurement ($\Delta\Psi_m$), intracellular ATP concentration, DCFH-DA assay, cytoplasmic free Ca^{2+} levels, TNF-α, caspase-3 and NF-κB expressions) in rat alveolar macrophage NR8383 cells. These experiments were complemented by AFM and CLSM techniques that - for the first time - allowed direct imaging of the cell membrane topography of live cells and the disruption thereof upon exposure to differently charged PSNP. By combining these experiments we further extended the understanding of the effects of surface charge of PSNP with cellular membranes.

Materials and methods

Polystyrene nanoparticles (PSNP)

Fluorescent PSNP of two different surface charges (positive and negative) and sizes (50 and 100 nm) were purchased from Sigma Aldrich Chemie BV. The positive and negative PSNP were amine and carboxylic acid modified, respectively. The PSNP were characterized in three ways: 1) the size and polydispersity index (PDI) were obtained by dynamic light scattering (DLS) followed by analysis using the CONTIN algorithm; 2) the surface potential (as an indicator for surface charge) was determined by ζ-potential measurements; and 3) imaging was performed by scanning electron microscopy.

NR8383 cells

Rat alveolar macrophage (NR8383) cells were obtained from ATCC (Manassas, VA). The NR8383 cells were cultured in 150 cm^2 cell culture flasks with 25 ml F12–K culture medium

(Gibco 21127) supplemented with 10 % (v/v) heat inactivated fetal calf serum (FCS) in a humidified atmosphere containing 5 % CO_2 at 37 °C.

MTT assay

An NR8383 cell suspension was centrifuged at 140 *g* for 5 min before resuspending the cell pellet in F12-K medium followed by counting and adjusting the cellular concentration to 2×10^5 cells/ml.[29] The cells were then seeded in a 96-well plate (50 μl/well) and the plate was kept in a 5 % CO_2 incubator at 37 °C for 24 h.[29] Subsequently, 50 μl of serial dilutions of different PSNP in F12-K medium were added to the wells to obtain the required final concentrations (0-100 μg/ml) on the time of incubation. This was followed by incubation for another 4 h after which 5 μl of MTT solution in PBS (5 mg/ml) was added to each well and the plate was incubated for another 4 h. Then, 100 μl of pure dimethysulfoxide (DMSO) was added to each well to dissolve the formazan crystals. The absorption reading of each well was measured at 562 nm in a 96-well plate reader and the background absorption reading at 612 nm was subtracted. Mitochondrial metabolic activity for each concentration of PSNP was expressed as % of the negative control (0 μg/ml) reading. Medium without PSNP and medium with Triton-X (0.01 %) were used as negative and positive controls, respectively.

Phagocytic index (PI) measurement

An NR8383 cell suspension (2×10^5 cells/ml) was seeded in a 96-well plate (50 μl/well) in F12-K medium, followed by addition of 50 μl/well of serial dilutions of different PSNP in F12-K medium to obtain the required final test concentrations of PSNP (0-100 μg/ml) on the time of incubation as reported before.[17] Plain F12-K medium without PSNP and medium containing 100 μM $CuSO_4$ were used as negative and positive controls, respectively. After 4 h, the cells were exposed to yellow green fluorescent latex beads (1 μm size) at a ratio of beads to cells in each well of 50:1. After 4 h of incubation (total exposure time 8 h), counting samples were taken from the wells and viewed first under a fluorescent microscope to visualize the fluorescent beads, followed by bright field view to visualize the cells. Samples were also taken out of each well to assess the cell viability by trypan blue exclusion test. The trypan blue exclusion test was performed by adding trypan blue dye with cell suspension (1:1) before measuring the amount of viable cells under light microscope. The phagocytic index was determined by calculating the average number of fluorescent beads phagocytosed per viable cell and expressed as % of the negative control (0 μg/ml).

Measurement of mitochondrial membrane potential (ΔΨ$_m$)

The NR8383 cell suspension was adjusted to 2×10^5 cells/ml and seeded in a 96-well plate (50 μl/well) in F12-K medium. A 50 μl/well of serial dilutions of different PSNP in F12-K medium were added to obtain the required final test concentrations of PSNP (0-100 μg/ml). After 4 h incubation, the mitochondrial membrane potential (ΔΨ$_m$) was measured by a commercially available kit from Invitrogen (MitoProbe™ Transition Pore Assay Kit; Catalogue No. M34153) and expressed as % of the negative control (0 μg/ml). A 100 μM solution of ionomycin in DMSO (supplied with the kit) and F12-K medium without PSNP were used as positive and negative controls, respectively.

Measurement of cellular ATP content

The NR8383 cell suspension was adjusted to 2×10^5 cells/ml and seeded in a 96-well plate (50 µl/well) in F12-K medium. A 50 µl/well of serial dilutions of different PSNP in F12-K medium were added to obtain the required final test concentrations of PSNP (0–100 µg/ml). After 4 h incubation, the cellular ATP was then measured by a commercially available kit from Invitrogen (Catalogue No. FLASC) and expressed as % of negative control (0 µg/ml). A 75 mM solution of 2,4-dinitrophenol (in DMSO) and F12-K medium without PSNP were used as positive and negative controls, respectively.

Measurement of intracellular ROS by the DCFH-DA assay

The NR8383 cell suspension was adjusted to 2×10^5 cells/ml and seeded in a 96-well plate (50 µl/well) in F12-K.[2] 50 µl/well of serial dilutions of different PSNP in F12-K medium were added to obtain the required final test concentrations of PSNP (0–100 µg/ml). A concentration of 10 mM H_2O_2 was used as positive control and F12-K medium without PSNP as negative control. Immediately after exposure to the PSNP, 5 µl of a 20 mM solution of DCFH-DA (in DMSO) was added to each well and the plates were incubated for 4 h in a 5 % CO_2 atmosphere at 37 °C making the total exposure time of 8 h. The fluorescence was then measured on a spectrofluorometer at $\lambda_{ex} = 485$ nm and $\lambda_{em} = 538$ nm. The fluorescence induction factor for each concentration of PSNP was calculated by dividing the reading of each well by the average reading of the negative control (0 µg/ml) and expressed as % of the control. Control experiments were performed by incubating the PSNP at their test concentrations with DCFH-DA in the absence of cells to check the possibility of a positive fluorescence reading caused by reaction of DCFH-DA with PSNP alone.

Measurement of cytoplasmic calcium

The NR8383 cell suspension was adjusted to 2×10^5 cells/ml and seeded in a 96-well plate (50 µl/well) in F12-K medium. A 50 µl/well of serial dilutions of different PSNP in F12-K medium were added to obtain the required final test concentrations of PSNP (0–100 µg/ml). After 4 h incubation, the cytoplasmic free calcium was then measured by a commercially available kit from Invitrogen (Fluo-4 Direct™ Calcium Assay Kit; Catalogue No. F10472) and expressed as % of negative control (0 µg/ml). F12-K medium without PSNP was used as negative control.

Measurement of TNF-α

The NR8383 cell suspension was adjusted to 2×10^5 cells/ml and seeded in a 96-well plate (50 µl/well) in F12-K medium. A 50 µl/well of serial dilutions of different PSNP in F12-K medium were added to obtain the required final test concentrations of PSNP (0–100 µg/ml). After 4 h incubation, the TNF-α was then measured by a commercially available kit from Invitrogen (Catalogue No. KRC3011) and expressed as % of negative control (0 µg/ml). A concentration of 10 mM H_2O_2 and F12-K medium without PSNP were used as positive and negative controls, respectively.

Measurement of caspase-3 activity

After plating the NR8383 cells and exposing them to serial dilutions of PSNP for 4 h as described above, the cellular caspase-3 activities were measured by a commercially available kit (Catalogue No. CASP3C) from Sigma Aldrich Chemie BV. The results were expressed as % of the negative control (0 μg/ml).

Measurement of NF-κB

The NR8383 cells were plated and exposed to serial dilutions of different PSNP for 4 h as described above. Following exposure, the NF-κB levels were measured by a kit from Invitrogen (KHO 0371) and the results were expressed as % of the negative control (0 μg/ml).

Confocal laser scanning microscopy (CLSM)

The NR8383 cell suspension was adjusted to 2×10^5 cells/ml and seeded in a 96-well plate (50 μl/well) in F12-K medium. A 50 μl/well of serial dilutions of different PSNP in F12-K medium were added to obtain a required non-toxic concentration of PSNP (1 μg/ml). After 4 h of exposure, samples were taken out and put on a glass slide before examining them under oil immersion microscope (100×) and then visualizing the cells under a Zeiss confocal laser scanning microscope (λ_{ex} = 543 nm; λ_{em} = 620 nm). Different samples were measured with the same resolution, laser and detector settings, aperture width and image gain. The relative cellular uptake of 100 nm cationic and anionic PSNP were expressed as an arithmetic mean of data obtained from 20 individual cells from at least five different experiments (n = 5). Cells exposed to only F12-K medium were used as control.

Calcein assay

The NR8383 cell suspension was adjusted to 2×10^5 cells/ml and exposed to 1 μM concentration of calcein-AM (calcein-acetomethoxy) for 1 h. The cells were then washed with PBS by repeated centrifugation and then exposed to non-toxic concentration of PSNP (1 μg/ml). After 4 h of exposure, samples were taken out and put on a glass slide before examining it under oil immersion microscope (100×) and then visualizing the cells under a Zeiss confocal laser scanning microscope (λ_{ex} = 488 nm; λ_{em} = 538 nm). Different samples were measured with the same set up of similar resolution, aperture width and image gain. Cells exposed to only calcein were used as control.

Atomic force microscopy (AFM)

After exposure to PSNP (1 μg/ml) for 4 h, samples were taken from a NR8383 cell suspension (2×10^5 cells/ml) before placing it on mica slides. The samples were then checked by AFM in contact tapping mode with a silicon nitride tip and an average diameter of 30 nm. Each time an area of 2×2 μm was scanned and height tracings and three dimensional images of the surfaces were made. The roughness (r) was calculated for the area scanned by the IgorPro 3.0 computer software.

Statistical analysis

Each experiment was repeated three times (n = 3) and the results are shown as mean ± standard error of mean after analysis and plotting by Origin Pro (version 8.0) software. Data

points were taken as statistically significantly different if $p < 0.05$ compared to the negative control (unless stated otherwise) and marked with a * sign. Results are shown as mean ± standard error of mean (SEM).

Results

Characterization of PSNP

The PSNP were terminated with amine (PSNP-NH$_2$) or carboxylic acid (PSNP-COOH) moieties, rendering them positively (PSNP-NH$_3^+$) or negatively (PSNP-COO$^-$) charged in aqueous dispersions. The characterization results are provided as Table 1. The PSNP can clearly be visualized, and were found to be overall monodisperse. The monodispersity of the PSNP was also confirmed by DLS and the PDI of the PSNP in aqueous dispersions were determined to be < 0.1 for all for samples.

Table 1: *Physico-chemical characterization of the different PSNP.*

Polymer	PSNP	Surface charge	ζ-potential (mV)	Hydrodynamic size (nm)
Polystyrene	PSNP-NH$_2$	Positive	24 ± 5	50 ± 5
			23 ± 5	100 ± 5
	PSNP-COOH	Negative	–21 ± 5	50 ± 5
			–24 ± 5	100 ± 5

Cytotoxicity measurement by MTT and phagocytic index (PI) assay

The cytotoxicity of the PSNP was measured by both the MTT (Figure 1) and the PI (Figure 2) assay. In the MTT and PI assay, the mitochondrial metabolic activity and phagocytic capabilities were measured upon exposure of the cells to the PSNP in the concentration range of 0 – 100 µg/ml. At the concentrations tested, only the cationic PSNP showed signs of cytotoxicity for both these assays (see Figures 1 and 2, for MTT and PI assays, respectively). For the anionic PSNP, no cytotoxicity could be observed in the tested concentration range. The EC50 values obtained from the MTT and PI assays are presented in Table 2. Although not always statistically significant ($p < 0.05$), a size-dependent effect on the cytotoxicity of PSNP could be observed. In this case, the smaller cationic PSNP (50 nm) were relatively more cytotoxic than the larger ones (100 nm).
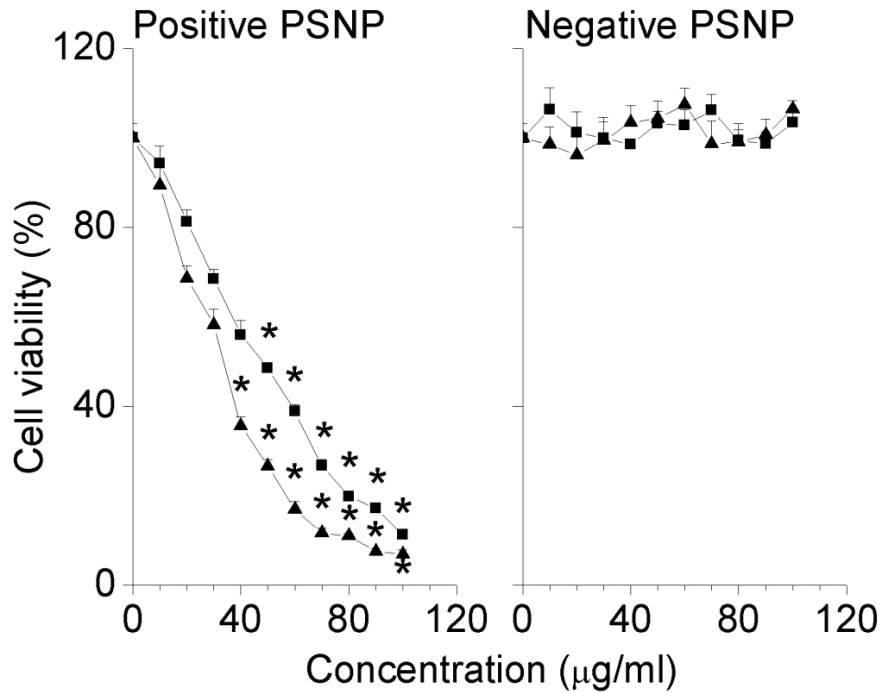
Figure 1: *Cell viability measured by the MTT assay and expressed as % of negative control (0 μg/ml) after 4 h exposure of NR8383 cells to positive and negative PSNP of 50 (▲) and 100 (■) nm sizes. The * sign signifies statistical difference from the negative control at p < 0.05. Results are shown as mean ± SEM (n = 3).*
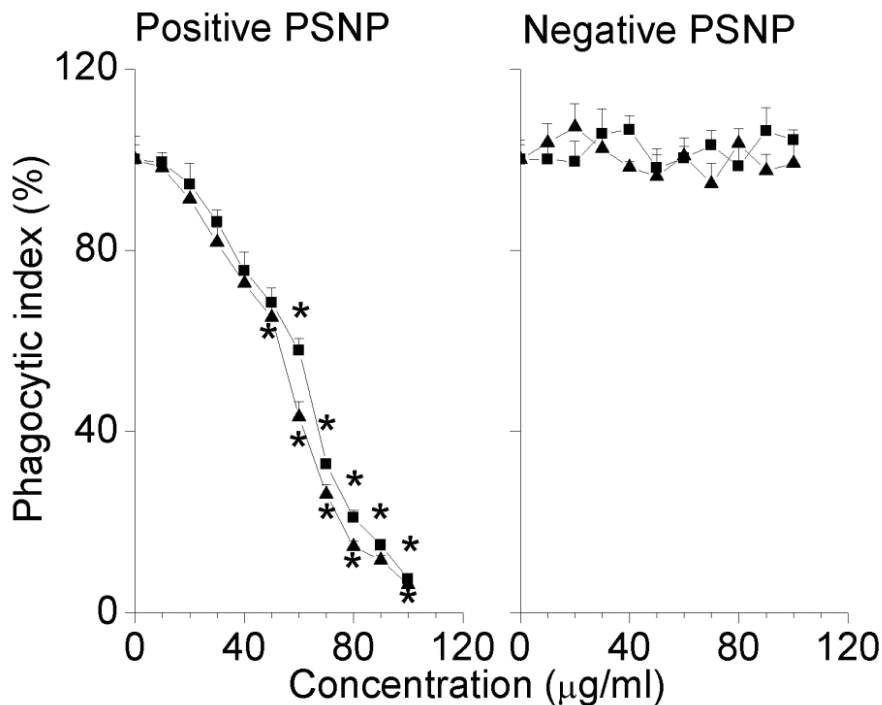

Figure 2: *Phagocytic index (PI) expressed as % of negative control (0 μg/ml) after 4 h exposure of NR8383 cells to positive and negative PSNP of 50 (▲) and 100 (■) nm sizes. The * sign signifies statistical difference from the negative control at p < 0.05. Results are shown as mean ± SEM (n = 3)*

Mitochondrial membrane potential (ΔΨₘ) assessment

In order to investigate the possible effect of different PSNP on intracellular mitochondria, the change in mitochondrial membrane potential ($\Delta\Psi_m$) was measured by a commercially available kit. The obtained results are shown in Figure 3. The cationic PSNP of both sizes (with 50 nm NP being more effective than 100 nm NP) caused a reduction in the $\Delta\Psi_m$ within the tested concentration range (0 - 100 µg/ml) in contrast to the anionic ones, which did not show any effect on the $\Delta\Psi_m$. The EC50 values are given in Table 2.
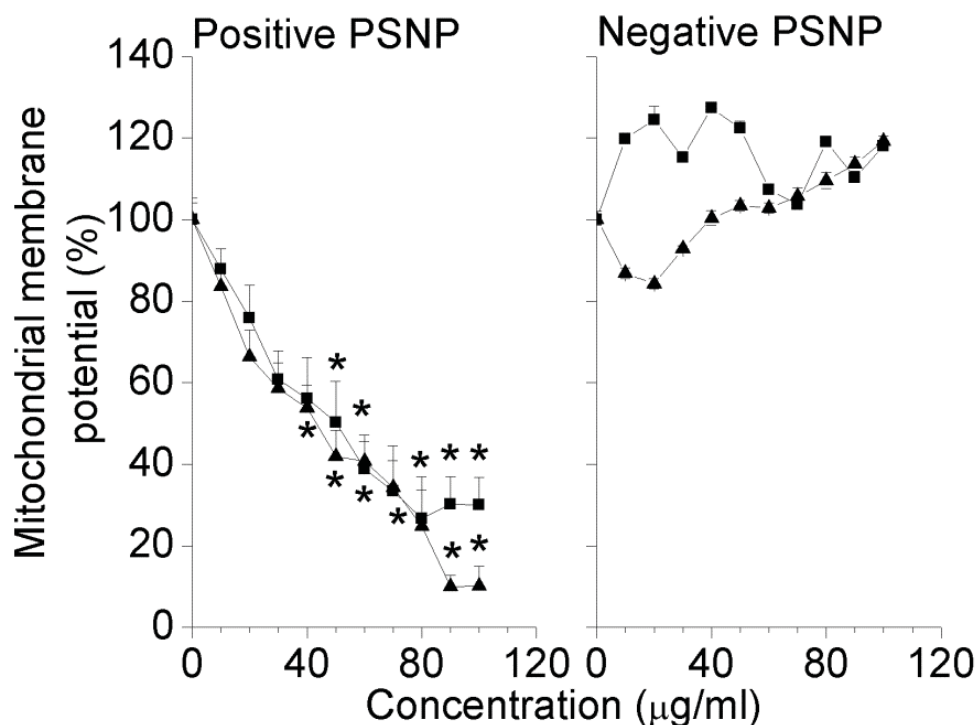
Figure 3: *Change in mitochondrial membrane potential ($\Delta\Psi_m$), expressed as % of negative control (0 µg/ml) after 4 h exposure of NR8383 cells to positive and negative PSNP of 50 (▲) and 100 (■) nm sizes. The * sign signifies statistical difference from the negative control at p < 0.05. Results are shown as mean ± SEM (n = 3).*

Measurement of intracellular ATP content

The intracellular ATP was measured in NR8383 cells after 4 h exposure to different PSNP in order to further extend the scope of ongoing investigations on the interaction of different surface charge-bearing PSNP with intracellular mitochondria. The results are shown in Figure 4 with the corresponding EC50 values being presented in Table 2. For the cationic PSNP, a dose-dependent decrease in the cellular ATP content was observed, with the 50 nm PSNP being more effective than the 100 nm particles. In contrast, the anionic PSNP failed to induce any such decrease in cellular ATP content at the concentrations tested.
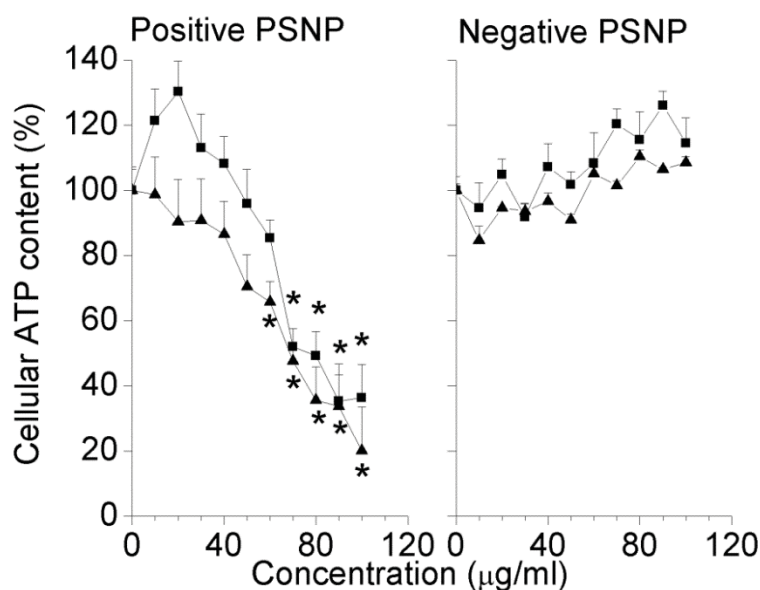
Figure 4: *Cellular ATP content expressed as % of negative control (0 μg/ml) after 4 h exposure of NR8383 cells to positive and negative PSNP of 50 (▲) and 100 (■) nm sizes. The * sign signifies statistical difference from the negative control at p < 0.05. Results are shown as mean ± SEM(n = 3).*

Measurement of intracellular ROS

The DCFH-DA assay was used to assess any induction in intracellular ROS production by different PSNP. The results of the DCFH-DA assay are shown in Figure 5. In contrast to the anionic PSNP, which showed no response, the cationic PSNP of both sizes showed induction in ROS production, with the 50 nm PSNP being more active than the 100 nm. The corresponding EC50 values are given in Table 2.
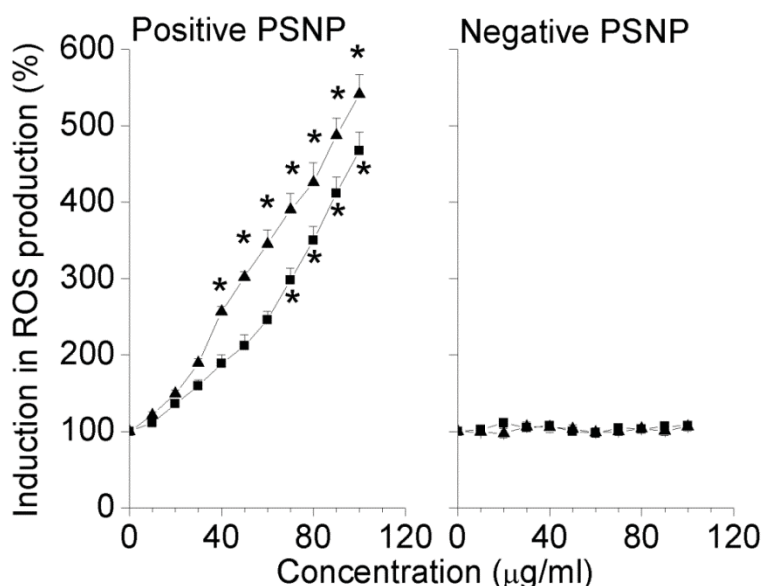
Figure 5: *Induction of intracellular ROS production expressed as % of negative control (0 μg/ml) after 4 h exposure of NR8383 cells to positive and negative PSNP of 50 (▲) and 100 (■) nm sizes. The * sign signifies statistical difference from the negative control at p < 0.05. Results are shown as mean ± SEM (n = 3).*

Measurement of intracellular calcium

The results are shown in Figure 6 and the corresponding EC50 values are given in Table 2. As expected, only the cationic PSNP, with 50 nm PSNP showing a higher effect than 100 nm PSNP, caused a dose-dependent increase in the cytoplasmic free calcium levels, whereas no such effects were observed for anionic PSNP.
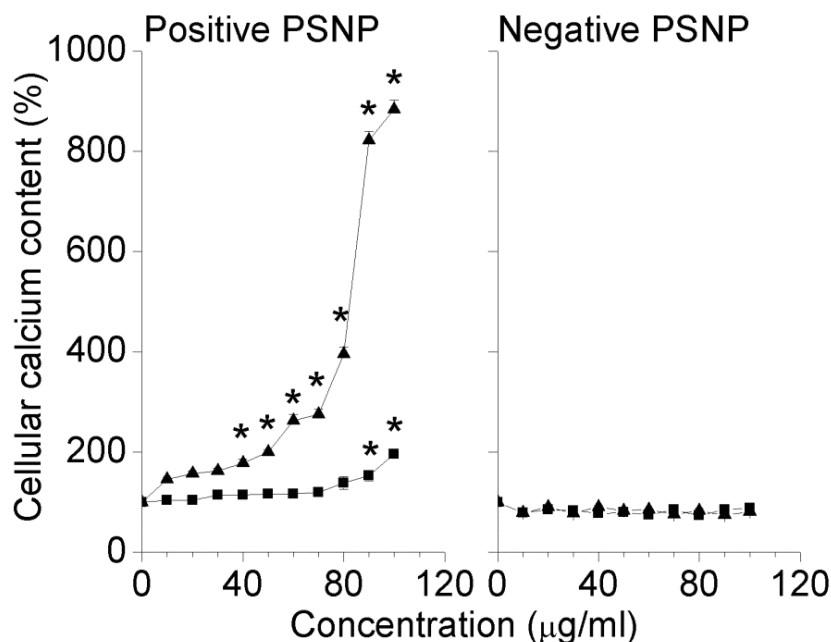

Figure 6: *Cytoplasmic free calcium content expressed as % of negative control (0 µg/ml) after 4 h exposure of NR8383 cells to positive and negative PSNP of 50 (▲) and 100 (■) nm sizes. The * sign signifies statistical difference from the negative control at p < 0.05. Results are shown as mean ± SEM (n = 3).*

Measurement of cellular TNF-α

The probability of inflammation following such a compromised state of normal cellular physiology including oxidative stress cannot be ruled out. Hence, as a biomarker of inflammatory response, cellular TNF-α production by the cells exposed to PSNP was measured. The results are shown in Figure 7 and the corresponding EC50 values are given in Table 2. An increase in the cellular TNF-α production could be seen only upon exposure to cationic PSNP. The anionic PSNP did not show any induction of TNF-α production. For the cationic PSNP, the 50 nm PSNP induced a higher TNF-α production compared to the 100 nm PSNP.

Effect on caspase-3 activity

The effects on the activity of caspase-3 after 4 h exposure of NR8383 cells to the positive PSNP are shown in Figure 8 with the EC50 values enlisted in Table 2. From the results obtained, it can be seen that exposure of the cells to cationic PSNP increased the caspase-3 activity compared to the negative control (0 µg/ml) with smaller 50 nm PSNP showing a higher effect compared to the bigger 100 nm PSNP. For cells exposed to anionic PSNP, in comparison to the control values no significant changes could be seen with the test concentrations.
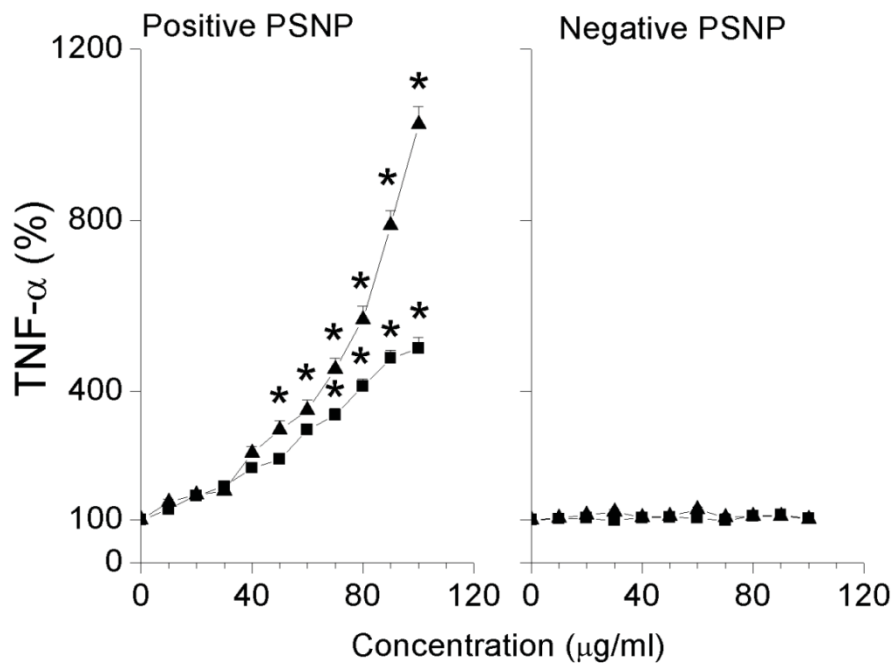
*Figure 7: Cellular TNF-α expressed as % of negative control (0 µg/ml) after 4 h exposure of NR8383 cells to positive and negative PSNP of 50 (▲) and 100 (■) nm sizes. The * sign signifies statistical difference from the negative control at p < 0.05. Results are shown as mean ± SEM(n = 3).*
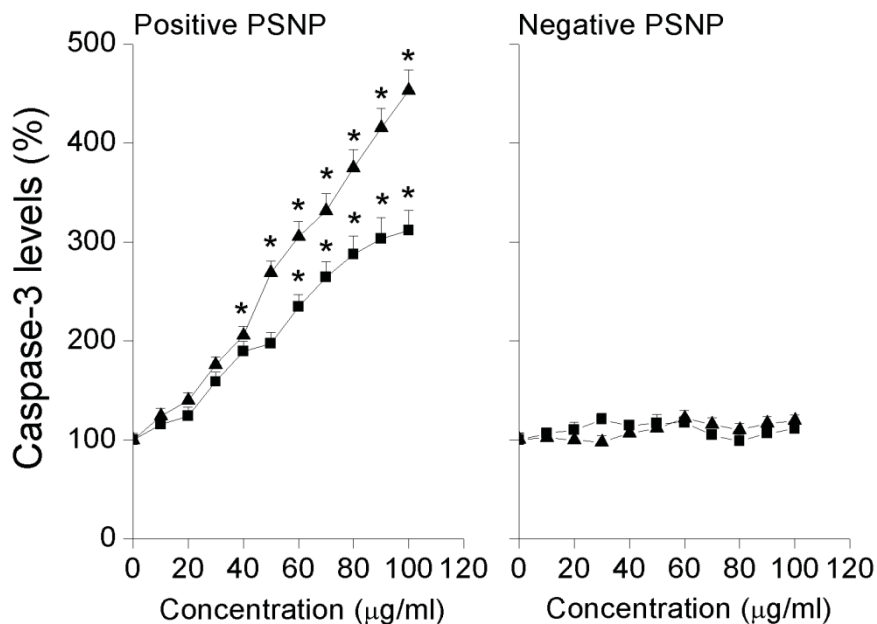

*Figure 8: Cellular caspase-3 activity expressed as % of negative control (0 µg/ml) after 4 h exposure of NR8383 cells to positive and negative PSNP of 50 (▲) and 100 (■) nm sizes. The * sign signifies statistical difference from the negative control at p < 0.05. Results are shown as mean ± SEM (n = 3).*

Effect on NF-κB levels

The effect on NF-κB levels are shown in Figure 9 with the EC50 values given in Table 2. The cationic PSNP caused an increase in the levels of NF-κB whereas the anionic PSNP did not show any such effects compared to the negative control (0 μg/ml) after 4 h exposure. The smaller 50 nm cationic PSNP showed higher effects compared to the larger 100 nm cationic PSNP.
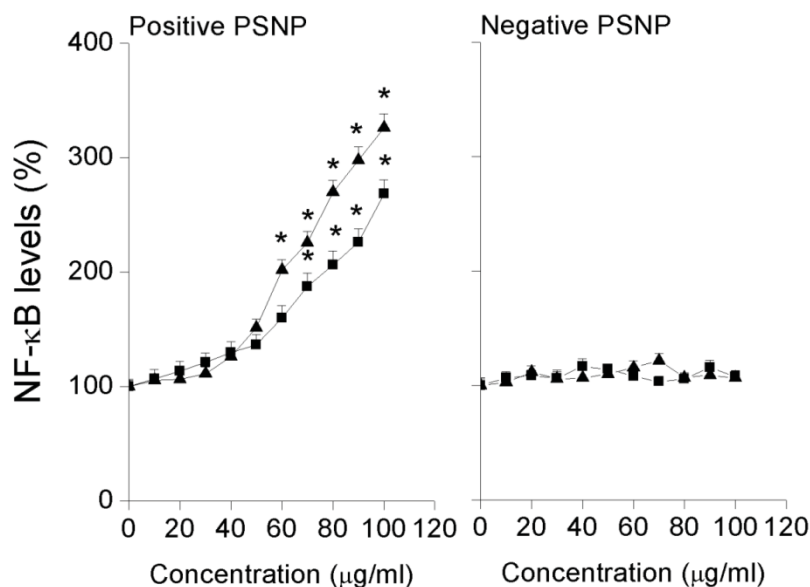

*Figure 9: Cellular NF-κB expressed as % of negative control (0 μg/ml) after 4 h exposure of NR8383 cells to positive and negative PSNP of 50 (▲) and 100 (■) nm sizes. The * sign signifies statistical difference from the negative control at p < 0.05. Results are shown as mean ± SEM(n = 3).*

Table 2: The EC50 values (μg/ml) *obtained from different experiments on NR8383 cells after 4 h exposure to the test concentrations (0–100 μg/ml) of cationic PSNP. No EC50 values are given for anionic PSNP due to their non-toxicity in the tested concentration range.*

Assay	Figure	EC50 (μg/ml)	
		50 nm	100 nm
MTT	1	33	35
PI	2	56	62
$\Delta\Psi_m$	3	34	38
ATP	4	63	65
DCFH-DA	5	54	68
Calcium	6	62	88
TNF-α	7	66	96
Caspase-3	8	69	74
NF-κB	9	65	77

Investigation of the role of surface charge on cellular uptake and cellular distribution of PSNP by CLSM

The NR8383 cells were exposed to a non-toxic concentration (1 μg/ml) of both cationic and anionic 100 nm PSNP for 4 h before checking the cellular uptake and cellular distribution of the PSNP. The CLSM technique was employed in order to investigate the uptake patterns as well as to perform quantitative uptake analyses of the PSNP of different surface charges. The results are shown in Figure 10A, in which the nucleus is observed as a dark space inside the cells. The results from at least 20 individual cells from three separate experiments were counted. The uptake of cationic PSNP was almost twice the uptake of anionic PSNP (Figure 10B). It was found that cationic PSNP showed mainly interaction with the cellular periphery with the fluorescence halo visible from the cell membrane. For anionic PSNP, no such enhanced interaction between the PSNP and the cell membrane was observed. Differences could also be seen in the intracellular distribution patterns of the two different surface charge-bearing PSNP. For anionic PSNP, small vesicular structures could be seen inside the cells; this was not the case for the cationic PSNP. For the cationic PSNP, the NP were found to be diffusely spread across the cytoplasm and also in the peri–nuclear regions.
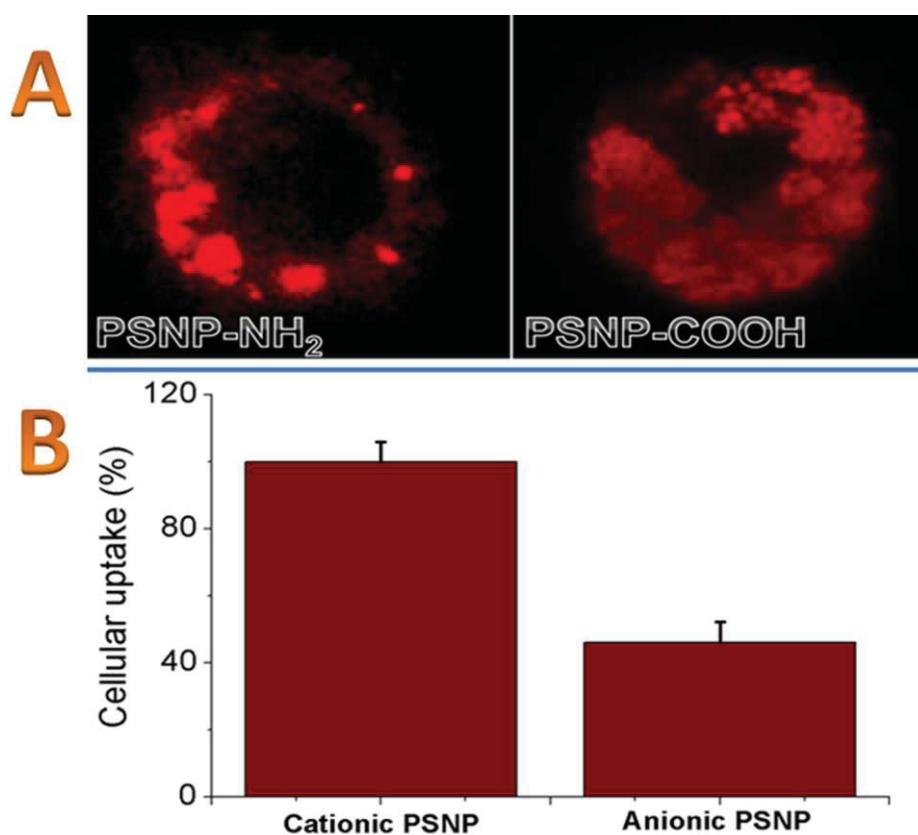

Figure 10: *(A) CLSM images of NR8383 cells (λ_{ex} = 543 nm, λ_{em}=620 nm) after 4 h exposure to positive (amine-terminated/PSNP-NH$_2$) and negative (acid-terminated/PSNP-COOH) 100 nm PSNP. (B) Relative cellular uptake of 100 nm cationic and anionic PSNP in NR8383 cells after 4 h exposure to non-toxic 1 μg/ml concentrations. Results are shown as mean ± SEM. The uptake of the cationic PSNP was taken as 100 %. The results were expressed as an arithmetic mean of the CLSM data obtained from 20 individual cells from five separate experiments (n = 5).*

Integrity of cell membrane after exposure to PSNP

Calcein assay

The results are shown in Figure 11 and reveal that the cationic PSNP (at a non-toxic concentration of 1 μg/ml) created membrane-bound pouches of calcein leaking out of the cell membrane, suggesting a compromised structure of the cell membrane. In contrast, for the anionic PSNP (also at 1 μg/ml), the integrity of the cell membrane was maintained, and comparable to that of a normal NR8383 cell (control).
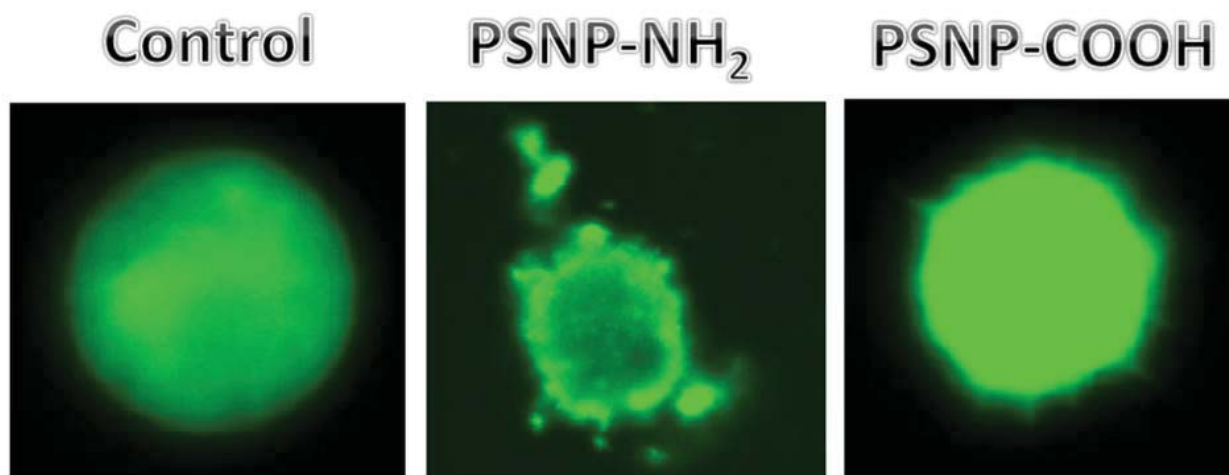

Figure 11: *Calcein assay (λ_{ex} = 488 nm, λ_{em} = 538 nm) of NR8383 cells after 4 h exposure to non-toxic (1 μg/ml) concentrations of positive (amine-terminated/PSNP-NH$_2$) and negative (acid-terminated/PSNP-COOH) 100 nm PSNP.*

Atomic force microscopy (AFM)

The results of the AFM investigation are shown in Figure 12. The cationic PSNP-NH$_2$ caused a higher disruption of cell surface topography and increased the overall roughness of the surface. The normal mean roughness of NR8383 cells was found to be ~5.3 nm, whereas after exposure to the cationic PSNP the mean roughness showed an almost five-fold increase (~24.7 nm). Additionally, pores or holes of different sizes (at least ~150 nm in size) could be observed on the surface. In contrast, anionic PSNP-COOH caused a much smaller increase in roughness of the NR8383 cell surface (~10.2 nm) and no hole formation could be observed.

Discussion

The aim of this study was to systematically probe the influence of surface characteristics (like surface charge) and physical properties (like particle size) of PSNP in the cytotoxicity inflicted towards macrophage NR8383 cells. To this point, various cellular endpoints were identified in order to better understand the mechanism of such toxicity. The major observations were: 1) the cationic PSNP showed higher cytotoxicity as well as cellular uptake compared to the anionic PSNP showing an effect of surface charge; 2) a size-effect was also found since smaller

50 nm cationic PSNP were found to be more toxic compared to the bigger 100 nm cationic PSNP; 3) especially positive PSNP caused a disruption of the membrane integrity and pore formation could be visualized; 4) intracellular mitochondria were identified as a major target organelle in the cytotoxicity causing pathway; 5) based on these investigations, a pathway resulting in cytotoxicity of cationic PSNP can be proposed.
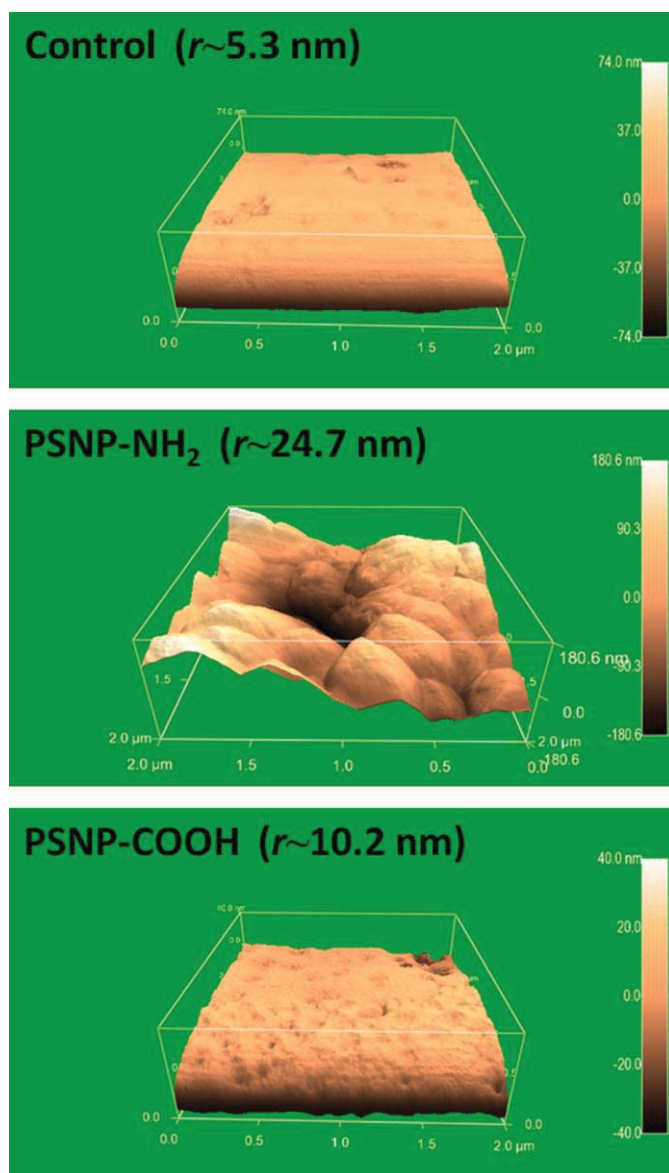

Figure 12: AFM (contact tapping mode) images of NR8383 cells placed on mica surface after 4 h exposure to non-toxic (1 µg/ml) concentrations of positive (amine-terminated) and negative (acid-terminated) 100 nm PSNP. The controls were cells that were not exposed to PSNP. The average roughness was calculated by the IgorPro 3.0 software and denoted as "r".

Our cytotoxicity data, based on the MTT and phagocytic index measurements, were in line with the literature, where cationic NP showed greater cytotoxicity compared to the anionic ones, both for polymer[30] and inorganic NP.[31] It is still not clear on mechanistic grounds, why cationic NP, in general, are more cytotoxic than the anionic ones. A hypothesis that has been put forward is that the cationic NP experience electrostatic attraction towards the (overall) anionic cell membrane and other lipid-based biomembranes, which makes their interactions with biomembranes much easier compared to that of the anionic ones.[32-34] A similar size-dependent cytotoxicity of different NP (with cytotoxicity inversely related to the sizes of NP) was also reported for other types of NP. A clear understanding of the mode of action underlying this size

effect on the cytotoxicity of NP is lacking, although a hypothesis has been put forward that with decreasing size, NP are more reactive, and hence can react with a wider variety of biomolecules causing toxicity.[35] It is also possible that with decreasing size, a higher percentage of the molecules in the NP get expressed on the surface, making smaller NP more reactive per gram of material than the larger ones.[36] Alternatively, one may suggest that for the smaller NP with higher reactivity, the interaction between the membrane phospholipids and the NP becomes more favorable.

The induction of the intracellular ROS production in NR8383 cells only after exposure to cationic PSNP, can cause oxidative stress. It has been hypothesized that oxidative stress is the mechanism of cytotoxicity of different NP including PSNP.[37-39] Our results are therefore in line with reported literature. However, there is still controversy about what may be the source of the production of intracellular ROS. Some groups have reported that intracellular mitochondria can be a target organ for NP.[40,41] The size-dependence that we observed (smaller PSNP causing more induction of intracellular ROS production than the larger PSNP) also matches with literature.[42,43]

The finding of cellular ATP depletion in NR8383 cells after 4 h exposure to only cationic PSNP (and not anionic ones) is interesting for various reasons. It showed that PSNP can interact with intracellular mitochondria, hampering their normal membrane physiology. ATP gets produced as a result of the ongoing ETC cycle in the mitochondrial membrane, and thus a reduction in the ATP production points towards a compromised ETC. These results fit well with the data on the effects of the PSNP on the mitochondrial membrane potential and strengthen the idea that cationic PSNP hamper the integrity of the mitochondrial membrane and disrupt the ETC. This can also lead to increased ROS production inside the cells.[44,45] In a recent study by Xia et al.,[17] a reduction in cellular ATP was also reported in RAW 264.7 murine macrophage cells after exposure to cationic 60 nm PSNP. This decrease in cellular ATP content after exposure to cationic PSNP matched well with our data.

With evidence pointing towards cationic PSNP causing a deteriorating effect on the mitochondrial membrane, it is possible that mitochondrial calcium can leak out into the cytoplasm.[46] To investigate this to a further extent, the cellular calcium content was measured and the results matched our expectations and corroborated with our findings on mitochondrial membrane potential ($\Delta\Psi_m$) which decreased after exposure to cationic and not anionic PSNP. Xia et al.[17] reported such an increase in cytoplasmic calcium levels in RAW 264.7 cells upon exposure to cationic PSNP of 60 nm sizes which matched well with our results. This effect on cytoplasmic calcium caused by cationic PSNP, pointed towards an interaction between the mitochondria and PSNP further confirming that mitochondria are a target cellular organelle. The increased levels of cytoplasmic calcium can subsequently trigger apoptotic pathways and this is corroborated by our data showing an increased caspase-3 activity, as caused only by the cationic PSNP.

Previously, several groups reported that cationic NP caused an induction of TNF-α production whereas anionic NP did not.[18,47,48] Similarly, it was also reported that smaller NP can display a higher cytotoxicity compared to larger NP. Hence, our data match well with literature. An increase in the production of TNF-α pointed towards an inflammatory response that may be caused by the ROS, although taking the compromised state of the mitochondria into account, the cause of this oxidative stress can be attributed to a variety of reasons and may not be exclusively due to ROS production.

The induced ROS in the cytoplasm can send signals to the nucleus via up-regulation of different transcription factors to produce various pro-inflammatory and inflammatory cytokines, including TNF-α. Our data on NF-κB support this mechanism where an increase in the transcription factor NF-κB can be seen as a predecessor to the acceleration of TNF-α. The increase in such transcription factors by cationic NP is rarely reported before.[49] Similar reports exist[50] where up-regulation of transcription factors were noted in case of exposure to the NP. It had also been shown before that the fluctuation of cytoplasmic contents including the ROS and free calcium can also influence the signaling to the nucleus at post-translational level,[51] although more data are required before drawing firm conclusions.

The findings on the role of surface charge in the intracellular distribution patterns can have further implications. In a recently published study, Bhattacharjee et al.[52] showed that surface charge played an important role in cellular interactions as well as cellular uptake of tri-block copolymer NP in NR8383 cells.[29] These cationic NP interacted strongly with the cellular periphery (cell membrane) and were even found to enter the cellular nucleus, whereas the anionic NP were preferably located inside vesicular structures within the cells. It was also shown by Bhattacharjee et al,[52] a surface charge-specific activation of clathrin (for cationic NP) and caveolin (for anionic NP) receptors occurred, which played a significant role in the cellular uptake of NP. Similar surface charge-dependent involvement of clathrin and caveolin receptors was already reported before.[52]

It was reported before that cationic NP can cause holes in lipid bilayers and structured biomembranes,[33,34,36] although no reports are available that this is also true for cationic PSNP and living cells. To investigate this to a further extent, a calcein assay was employed in which a non-fluorescent calcein–AM (acetomethoxy) salt was administered that after entering cells is converted into calcein by intracellular esterases and thus becomes fluorescent. The calcein content inside the cells could then be visualized with CLSM. This is a standard technique for testing the integrity of the cell membrane.[28] This once again showed that cationic PSNP harm the structural integrity of the cell membrane.

Although the calcein assay only gives an indirect assessment of the compromised cell membrane integrity after exposure to especially cationic PSNP, more direct evidence for disturbance of the membrane structure could be obtained by AFM. Some groups have already advocated the use of AFM in imaging the surface topography of biological samples, including cells.[53,54] An advantage of AFM is that it can be performed under water-rich biological conditions, making the technique suitable for imaging the surface characteristics of cells. This is preferable over conventional electron microscopy measurements that require ultra high vacuum conditions and low temperatures during sample preparation, which may deform cell membranes.

To the best of our knowledge, this is the first time the effect is imaged of the interaction of NP with different surface charges on the topography of the cell membrane surface of living cells. It also gave direct evidence for pore creation caused by the interaction of cationic NP with the cell membranes. The observation that hole-like structures are created in the cell membrane by cationic PSNP can add to the mechanistic understanding of the cytotoxicity of cationic PSNP. The concentrations applied were non-toxic (1 μg/ml) and hence this deterioration of the cell membrane is not due to necrosis. By creating holes in the cell membrane, the cationic PSNP can cause an increase in the cell membrane permeability and thereby disturb the normal transport of molecules in and out of the cells and thus eventually lead to cytotoxicity at higher concentrations. Why cationic PSNP caused punctures in the cell membrane is not well

understood. Based on computational studies, it was argued that due to the electrostatic attraction between the cationic PSNP and the (overall) anionic cell membrane, a part of the cell membrane protrudes to first cover the PSNP and then gradually incorporates the PSNP into the lipid bilayer structure of the cell membrane. Then, this membrane-bound pouch containing the cationic PSNP enters the cell. In this process membrane molecules are apparently bound stronger to positively charged PSNP than – via van der Waals forces – to each other, which leads to a disruption of the cell membrane, i.e. the formation of the hole-like structures. In contrast, it was reported in literature that anionic PSNP got embedded within the membrane lipid bilayer and did not form holes like the cationic ones.[55,56] Although such explanations for the formation of the holes in the cell membrane by cationic PSNP need further evidence, the current data point at pore formation as a possible mode of action for the adverse effects of cationic PSNP on cell membrane integrity.

Based on these obtained data, a pathway of the toxicity caused by the cationic PSNP in NR8383 cells after 4 h exposure is proposed (Figure 13). The proposal classifies the pathway into three broad phases: 1) *Pre-mitochondrial phase*, where the cationic PSNP interacts with the cell membrane with activation of cell membrane-bound receptors (facilitating cellular uptake) and compromised cell membrane integrity. 2) *Mitochondrial phase*, where a surface charge-driven interaction between the mitochondrial membrane and cationic PSNP occurs. This interaction results in dissipation of the mitochondrial membrane potential indicating deterioration of the mitochondrial membrane, disruption of mitochondrial ETC causing cellular ATP depletion, induction of ROS production and increase in cellular free calcium levels. 3) *Post-mitochondrial phase*, where the increased free calcium and high ROS in cellular cytoplasm impart stress on the cells including oxidative stress. Due to these stress conditions and (probably) with involvement of transcription factors (like NF-κB), the expression of pro-inflammatory markers, like TNF-α, is enhanced. On the other hand, the increased free calcium in cellular cytoplasm can activate the caspase-dependent apoptotic pathways. Altogether the results showed the importance of surface charge in determining the cytotoxicity and cellular uptake of PSNP, while identifying mitochondria and cellular membranes as important targets.
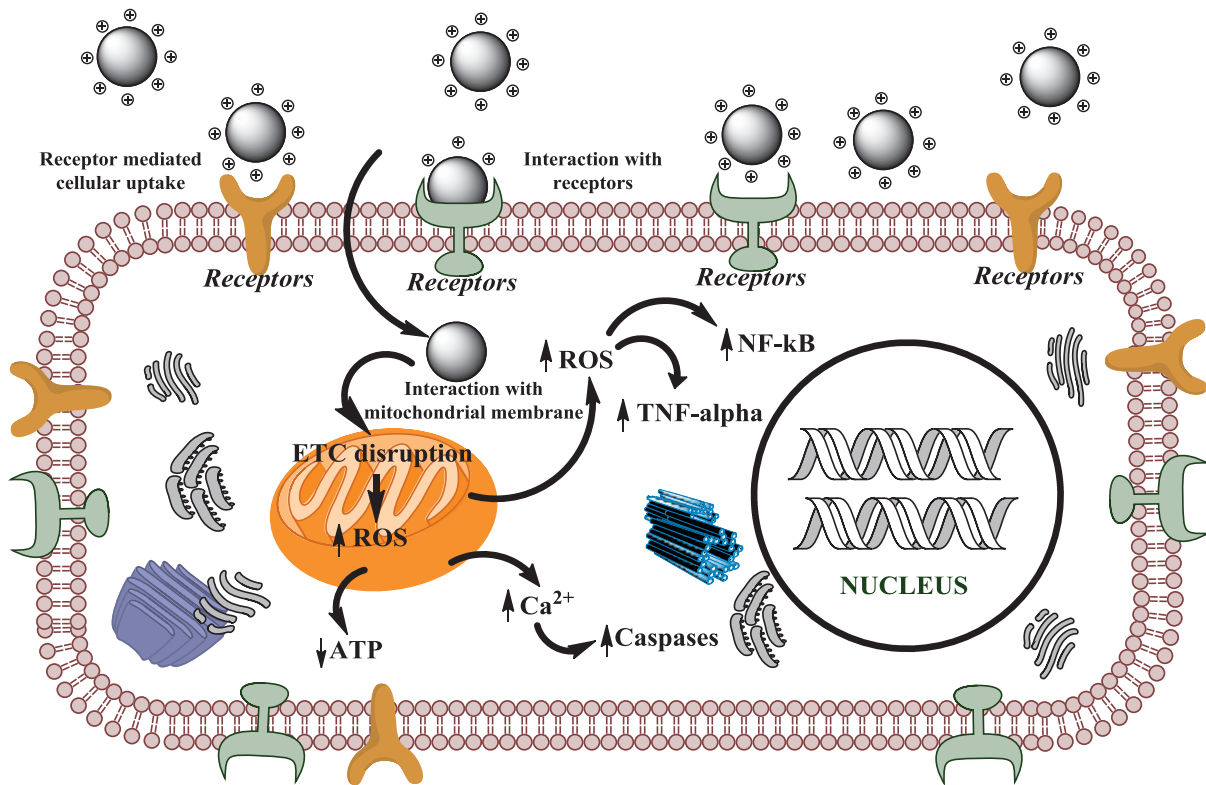
Figure 13: *Schematic representation of the proposed pathway of cytotoxicity caused by cationic PSNP in NR8383 cells after 4 h exposure.*

References

1. Clift MJD, Bhattacharjee S, Brown DM, Stone V; *Toxicol. Lett.* 2010, 198:358-65.
2. Donaldson K, Stone V; *Royal Soc. Chem.* (Chapter) 5 2007.
3. Bhattacharjee S, de Haan LHJ, Evers NM, Jiang X, Marcelis ATM, Zuilhof H, et al.; *Part. Fibre Toxicol.* 2010, 7(25).
4. Asati A, Santra S, Kaittanis C, Perez JM; *ACS Nano* 2010, 4:5321-5331.
5. El Badawy AM, Silva RG, Morris B, Scheckel KG, Suidan MT, Tolaymat TM; *Environ. Sci. Technol.* 2010, 45:283-287.
6. Jiang J, Oberdörster G, Biswas P; *J. Nanopart. Res.* 2009, 11:77-89.
7. Asharani PV, Lian Wu Y, Gong Z, Valiyaveettil S; *Nanotechnology* 2008, 19:255102.
8. Keelan JA; *Nat. Nanotehnol.* 2011, 6:263-264.
9. Davis ME, Chen Z, Shin DM; *Nat. Rev. Drug Discov.* 2008, 7:771-782.
10. Verma A, Rotello VM; *Chem. Commun.* 2005, 303-312.
11. Yang Y-H, Nam J-M; *Analyt. Chem.* 2009, 81:2564-2568.
12. Bisht S, Feldmann G, Soni S, Ravi R, Karikar C, Maitra A, et al.; *J. Nanobiotechnol.* 2007, 5:3.
13. Feng X, Lv F, Liu L, Tang H, Xing C, Yang Q, et al.; *ACS Appl. Mater. Interf.* 2010, 2:2429-2435.
14. Hussain SM, Hess KL, Gearhart JM, Geiss KT, Schlager JJ; *Toxicol. in Vitro* 2005, 19:975-983.
15. Monteiller C, Tran L, MacNee W, Faux S, Jones A, Miller B, et al.; *Occup. Environ. Med.* 2007, 64:609-615.
16. Yu K, Grabinski C, Schrand A, Murdock R, Wang W, Gu B, et al.; *J. Nanopart. Res.* 2009, 11:15-24.
17. Xia T, Kovochich M, Liong M, Zink JI, Nel AE; *ACS Nano* 2007, 2:85-96.
18. Xia T, Kovochich M, Brant J, Hotze M, Sempf J, Oberley T, et al.; *Nano Lett.* 2006, 6:1794-1807.
19. Lewinski N, Colvin V, Drezek R; *Small* 2008, 4:26-49.
20. Bexiga MG, Varela JA, Wang F, Fenaroli F, Salvati A, Lynch I, et al.; *Nanotoxicology* 2011, 5:557-567.
21. Wani MY, Hashim MA, Nabi F, Malik MA; *Adv. Phys. Chem.* 2011.
22. Zhang H, Xia T, Meng H, Xue M, George S, Ji Z, et al.; *ACS Nano* 2011, 5:2756-2769.
23. Spankuch B, Steinhauser I, Wartlick H, Kurunci-Csacsko E, Strebhardt KI, Langer K; *Neoplasia* 2008, 10:223-234.
24. Kim WJ, Bonoiu AC, Hayakawa T, Xia C, Kakimoto M-a, Pudavar HE, et al.; *Int. J. Pharm.* 2009, 376:141-152.
25. Malhotra M, Lane C, Tomaro-Duchesneau C, Saha S, Prakash S; *Int. J. Nanomed.* 2011, 6:485-494.
26. Leroueil PR, Berry SA, Duthie K, Han G, Rotello VM, McNerny DQ, et al.; *Nano Lett.* 2008, 8:420-424.
27. Lin J-Q, Zheng Y-G, Zhang H-W, Chen Z; *Langmuir* 2011.
28. Verma A, Uzun O, Hu Y, Hu Y, Han H-S, Watson N, et al.; *Nat. Mater.* 2008, 7:588-595.
29. Bhattacharjee S, Ershov D, Gucht Jvd, Alink GM, Rietjens IMCM, Zuilhof H, et al.; *Nanotoxicology* 2011, Early Online:1-14.

30. Wagner AJ, Bleckmann CA, Murdock RC, Schrand AM, Schlager JJ, Hussain SM; *J. Phys. Chem. B* 2007, 111:7353-7359.

31. De Jong WH, Borm PJA; *Int. J. Nanomed.* 2008, 3:133-149.

32. Arvizo RR, Miranda OR, Thompson MA, Pabelick CM, Bhattacharya R, Robertson JD, et al.; *Nano Lett.* 2010, 10:2543-2548.

33. Liu L, Xu K, Wang H, Jeremy Tan PK, Fan W, Venkatraman SS, et al.; *Nat. Nanotechnol.* 2009, 4:457-463.

34. Verma A, Stellacci F; *Small* 2010, 6:12-21.

35. Kim S, Qadir K, Jin S, Satyanarayana Reddy A, Seo B, Mun BS, et al.; *Catalysis Today*.

36. Auffan M, Rose J, Bottero JY, Lowry GV, Jolivet JP, Wiesner MR; *Nat. Nanotechnol.* 2009, 4:634-641.

37. Choi JE, Kim S, Ahn JH, Youn P, Kang JS, Park K, et al.; *Aquat. Toxicol.* 2010, 100:151-159.

38. Foucaud L, Goulaouic S, Bennasroune A, Laval-Gilly P, Brown D, Stone V, et al.; *Toxicol. in Vitro* 2010, 24:1512-1520.

39. Mocan T, Clichici S, Agoşton-Coldea L, Mocan L, Şimon Ş, Ilie I, et al.; *Acta Physiol. Hung.* 2010, 97:247-255.

40. Nadia B, Wided K, Kheira B, Hassiba R, Lamia B, Rhouati S, et al.; *Acta Biol. Hung.* 2009, 60:385-398.

41. Salnikov V, Lukyánenko YO, Frederick CA, Lederer WJ, Lukyánenko V; *Biophys. J.* 2007, 92:1058-1071.

42. Jiang J, Oberdörster G, Elder A, Gelein R, Mercer P, Biswas P; *Nanotoxicology* 2008, 2:33-42.

43. Carlson C, Hussain SM, Schrand AM, K. Braydich-Stolle L, Hess KL, Jones RL, et al.; *J. Phys. Chem. B* 2008, 112:13608-13619.

44. Liu Y, Fiskum G, Schubert D; *J. Neurochem.* 2002, 80:780-787.

45. Zimmerman MC, Zucker IH; *Hypertension* 2009, 53:112-114.

46. Duchen MR; *J. Physiol.* 2000, 529:57-68.

47. Lee H-M, Shin D-M, Song H-M, Yuk J-M, Lee Z-W, Lee S-H, et al.; *Toxicol. Appl. Pharmacol.* 2009, 238:160-169.

48. Liu R, Zhang X, Pu Y, Yin L, Li Y, Liang G, et al.; *J. Nanosci. Nanotechnol.* 2010, 10:5161-5169.

49. Bhattacharjee S, Ershov D, Islam MA, Kämpfer A, Gucht Jvd, Alink GM, et al.; *Submitted* 2012.

50. Brown DM, Donaldson K, Borm PJ, Schins RP, Dehnhardt M, Gilmour P, et al.; *Am. J. Physiol-Lung C* 2004, 286:L344-L353.

51. Kitahara-Tanabe N, Tanabe Y, Morikawa A, Mizundo DI, Soma GI; *Chem. Pharm. Bull.* 1991, 39:417-420.

52. Bhattacharjee S, Ershov D, Gucht Jvd, Alink GM, Rietjens IMCM, Zuilhof H, et al.; *Nanotoxicology* 2011, Early Online (DOI: 10.3109/17435390.2011.633714):1-14.

53. Muys JJ, Alkaisi MM, Melville DO, Nagase J, Sykes P, Parguez GM, et al.; *J. Nanobiotechnol.* 2006, 4:1.

54. Le Grimellec C, Lesniewska E, Giocondi MC, Finot E, Vie V, Goudonnet JP; *Biophys. J.* 1998;75:695-703.

55. Li Y, Chen X, Gu N; *J. Phys. Chem B* 2008, 112:16647-16653.

56. Lee H, Larson RG; J. Phys. Chem. B 2008, 112:12279-12285.

Chapter 11

Summary,

General Discussion

and

Future Perspectives

In this thesis, investigations are described that probe the interactions of nanoparticles (NP) with biological systems at multiple levels. The ultimate aim of the thesis was to investigate the role of surface properties (like surface charge) and physical properties (like size) in cytotoxicity and cellular uptake of NP in vitro before extending the scope of the research to in vivo conditions. In Chapter 1 of the thesis, the aim is introduced and background information with respect to the NP and the in vitro and in vivo models used in the present thesis was presented. In line with the order of the chapters, the research done with inorganic silicon nanoparticles (Si NP) and germanium nanoparticles (Ge NP) will be discussed first (Chapters 2-4), followed by research done with different polymer nanoparticles (PNP), including tri-block copolymer NP (Chapters 5-8) and polystyrene NP (Chapters 7, 9 and 10).

The Si NP and Ge NP were obtained via a variety of synthetic routes and their surfaces were densely packed with a monolayer of alkyl chains ending in different terminal functional groups as described in Chapters 2-4.[1-3] As a result, these Si NP and Ge NP had different surface charges in aqueous suspensions at physiological pH. Being semiconductor quantum dots, these Si NP are fluorescent and emit in the blue region when excited with UV-light. It is because of their inherent and non-bleaching[4] fluorescent properties that these Si NP and Ge NP hold good promise to be developed as bioimaging agents in the future. To further increase the scope of these semiconductor NP for medical applications and other multimodal imaging experiments, the Si core of some batches of the Si NP were doped with paramagnetic atoms, like manganese (Mn) or iron (Fe), making these Si NP detectable by magnetic resonance imaging (MRI).[5, 6] Taken together, these Si NP and Ge NP presented a unique set of well-characterized NP that have good potential to be developed as bioimaging tools. A toxicological assessment of these NP thus increases the validity of further research in the medical development of these NP.

As mentioned in the introductory Chapter 1, surface charge is often proclaimed to be one of the major factors in the cellular interactions of NP.[7-9] The present range of available Si NP and Ge NP presented us with an exciting opportunity to investigate the role of surface charge in cytotoxicity. The cytotoxicity of these Si NP was tested on both human colonic adenocarcinoma Caco-2 and rat alveolar macrophage NR8383 cells and the results were reported in Chapters 2 and 3.

Only the cationic Si NP-NH_2 showed evidence of cytotoxicity in both Caco-2 and NR8383 cells, whereas the Si NP-N_3 showed cytotoxicity only at much higher concentrations (> 2 µg/ml).[7, 8] In contrast, the Si NP-COOH did not show any signs of toxicity within the tested concentration range (0-3 µg/ml). Although neutral NP are mostly reported to be non-toxic, the Si NP-N_3 did show some signs of toxicity, albeit at higher concentrations than the cationic Si NP-NH_2. This is a first indication of the importance of charge on the toxicity of NP. In this case it is additionally possible that with time, or under the influence of enzymes, a fraction of the azide moieties got reduced to amines. Therefore the observed toxicity of azide-terminated Si NP could in fact have appeared as a result of the presence of these terminal amine groups.

The DCFH-DA assay showed that only cationic Si NP-NH_2 and overall neutral Si NP-N_3 (at much higher concentrations) induced intracellular reactive oxygen species (ROS) production in both Caco-2 and NR8383 cells. The anionic Si NP-COOH failed to induce intracellular ROS production in both cell lines. Oxidative stress has been regarded as one of the primary causes of cytotoxicity for NP.[10-12] Although our data from the DCFH-DA assay supported the formation of ROS, this does not necessarily mean that oxidative stress is the principal mechanism of

cytotoxicity. Various groups have reported that cationic NP can cause cytotoxicity with induction of intracellular ROS production and our data seem to strengthen the reported findings.[13, 14]

Why intracellular ROS production is induced after exposure to especially cationic NP was still unclear. From a detailed survey of the literature, it was found that intracellular mitochondria are a major target organelle for the NP.[15, 16] It was postulated that cationic NP, by virtue of their positive charge, can interfere with the mitochondrial membrane. This could affect the mitochondrial membrane potential ($\Delta\Psi_m$) and increase the permeability of the mitochondrial membrane.[17] However, investigations on such interference with intracellular mitochondrial homeostasis by inorganic NP (like silicon, germanium) are scarce. Hence, a mitochondrial fraction from male Wistar rat liver was isolated and exposed to Si NP-NH$_2$, Si NP-N$_3$ and Si NP-COOH (Chapter 3). It was observed that only cationic Si NP-NH$_2$ and neutral Si NP-N$_3$ (at much higher concentrations) could induce ROS production from such isolated mitochondrial fractions. This showed that cationic NP could possibly interfere with the electron transport chain (ETC) of intracellular mitochondria. The compromised ETC in mitochondria can release an array of different ROS into the cytoplasm causing oxidative stress. The affected mitochondrial membrane integrity and the ETC can also include a cascade of events causing cytotoxicity in other ways. Due to the reduced mitochondrial membrane integrity, the cellular calcium supply – which is stored to a significant degree within the mitochondria – can leach out of the mitochondria into the cytoplasm, causing a free calcium overload. This increased calcium level in the cytoplasm can initiate apoptotic pathways by way of cell signaling. The damaged ETC can also cause a serious depletion of cellular ATP and the cellular viability can then get compromised due to ATP depletion. Hence, investigation of the interactions of especially cationic NP with intracellular mitochondria is crucial in understanding the cascade of reactions resulting ultimately in cytotoxicity.

It became evident from the afore-mentioned experiments that the surface characteristics of NP play a salient role in the cytotoxic effects of NP, although a clear mechanistic view on the order of events was missing. Hence, in order to broaden the scope of our investigations, a series of monodisperse and well-characterized Si NP and Ge NP (obtained from collaborating laboratories in the USA and Canada) were included in an even more extensive set of toxicological experiments, as described in Chapter 4. Due to their variety of surface functionalizations, these Si NP and Ge NP carried different surface groups and surface charges. Hence, the effect of these different surface functionalities on the cytotoxicity of Si NP and Ge NP could be investigated to obtain information on mechanistic implications as well as their biocompatibility.

Only the cationic NP showed cytotoxicity and induction of ROS production, which matched with the previously obtained results. The cationic NP also induced a decrease in the cellular ATP content. This further strengthens the earlier findings that cationic Si NP interact with isolated mitochondrial fractions and also showed that cationic Si NP disrupt the ETC, possibly resulting in ATP depletion. It has been reported that cellular ATP depletion occurs upon exposure to cationic NP,[17,18] although a systematic investigation that probed the cascade of events was not reported. These results again indicated that oxidative stress is not the primary mechanism of cytotoxicity, but is the result of mitochondrial interactions with NP. It seems that the interaction of the cationic NP with intracellular mitochondria acts as the starting point for a series of subsequent events. To investigate this cascade of reactions further, tumor necrosis factor-alpha (TNF-α) was measured as a biomarker of the inflammatory injury caused by the

intracellular ROS production,[19] especially in macrophage cells. Induction of the TNF-α was only caused by the cationic NP. This is also in line with data reported before.[19-21]

Taken together, these detailed investigations on Si NP and Ge NP provided data from which surface charge-specific interactions of NP could be seen with cells at different levels. The results further indicated that oxidative stress inflicted by intracellular ROS may not be the starting point of toxicity but may arise from the initial interactions of NP with mitochondria. Surface charge was identified as one of the crucial factors determining cytotoxicity of NP. This may have important implications for the development of NP for future medical or, food-related applications. It was reported in literature that cationic NP showed a higher cytotoxicity as well as cellular uptake when compared to the anionic NP.[22, 23] Hence, the knowledge obtained from the present work can be used in the development of new NP that are biocompatible with minimal toxicity. It was shown in Chapter 4 that, by steric shielding (Ge NP-TMPA), the toxicity of Ge NP could be decreased. The results shown in Chapter 5 of this thesis (see below) also reveal that by simple steric shielding of the positive charge, the cytotoxicity of PNP could be curbed. Similarly, by intelligent chemical engineering the surface characteristics can be modulated in a way that could enhance the biocompatibility of NP.

In order to gain more insight into the interactions of NP with cellular systems, tri-block copolymer NP were chosen as a tool for investigation (Chapter 5). The reason for this choice of PNP was that the versatility in tri-block copolymer synthesis allowed us to obtain an interesting collection of polymers that could successfully be modified to have additional properties, like fluorescence. During the synthesis of the polymer, a fluorescent probe was incorporated in the middle block, which made these polymers fluorescent and thereof also the PNP derived from them through nanoprecipitation in water. An advantage of fluorescent PNP is that they can be easily traced in biological systems by confocal laser scanning microscopy (CLSM), which is a powerful technique for investigations of cellular systems. The PNP derived from the tri-block copolymers can not only be rendered fluorescent, but also be functionalized with a variety of terminal groups with different charges. For this, the terminal hydroxyl groups of the tri-block copolymer were converted into amine or carboxylic acid groups, rendering the PNP positive or negative in water. Interestingly, PNP with both a permanent positive charge and additional steric shielding could be prepared by reacting a terminal chloroacetyl group with dimethylethanolamine, or pyridine to give ammonium terminal groups.[8]

The results obtained in Chapter 5 indicated that, as with the Si NP, only the cationic PNP showed cytotoxicity and induction of intracellular ROS production in both Caco-2 and NR8383 cells. Interestingly, the cytotoxicity of the cationic PNP decreased with increasing steric bulk around the positive charge. Kim et al.[24] recently reported similar findings for gold NP. This is intriguing since it shows that the shielding of the charge is also important for the cytotoxicity of PNP. This can have implications for cationic NP that have significant potential for biomedical or food-related applications, but for which the applicability is limited due to their cytotoxicity. By shielding the cationic charges as ammonium groups their applicability could be increased.

Since these tri-block copolymer NP were fluorescent, extensive studies with CLSM were performed (Chapters 5, 6) in order to understand how surface charge and particle size influence the cellular uptake of the different NP. It was found that cationic NP showed much more interaction with the cellular membranes than the negative ones (hydroxyl and carboxylic acid terminated). A possible explanation may lie in the electrostatic attraction between the cationic NP and the negatively charged cell membrane.[25-27] This is a very interesting point for

understanding the pathway through which toxicity is exerted by cationic NP. Some groups have done extensive computer modeling of such interactions between cell membrane models (like anionic lipid bilayers) and cationic NP.[28] These studies showed that the surface charge of the NP had a major effect on these interactions. Computational chemistry showed that from a thermodynamic point of view, cationic NP not only attach themselves to the cell membrane more easily than anionic ones, but also cross the cell membrane faster and enter the cells more easily.[29]

Various groups have recognized the role of cell membrane-bound clathrin and caveolin receptors in the endocytic cellular uptake of NP,[30-32] although systematic investigations with well-characterized NP, carrying different surface charges, have not been reported. It can be presumed that for different surface charge-carrying PNP, different cell membrane-bound receptors can play a role in their cellular interactions. To investigate this, clathrin and caveolin receptors were selectively blocked and their role in the cellular uptake of different PNP was quantitatively assessed by CLSM studies. A clear difference in the interactions of the PNP with the clathrin and caveolin receptors was found, defined by the PNP surface charges. The cellular uptake process of cationic PNP was found to be more dependent on clathrin and that of anionic PNP more dependent on caveolin receptors (Chapters 5, 6).[8] To investigate the role of other cell membrane-bound receptors in the cellular uptake of PNP, mannose receptors - which are exclusively expressed only in few cells lines (like NR8383 cells) - were also selectively blocked (Chapter 6). It was found that the mannose receptors played an important role in the uptake of especially hydroxyl-terminated PNP.

Apart from surface charge, the size of NP has been claimed to influence cytotoxicity.[33, 34] This may be due to the increasing number of reactive groups of the NP that is expressed on the surface of the NP with decreasing size. Hence, smaller NP are comparatively more reactive than bigger ones. In literature, it is reported that smaller NP showed higher cytotoxicity and experience higher cellular uptake compared to the bigger NP.[35, 36] However, there are indications that there is a size threshold for NP, which results in an optimum size for cellular uptake of NP. Although this size threshold is not clearly determined, a commonly accepted size range is between 30-60 nm.[37] Hence, NP with sizes that fall outside this size range, show relatively lower levels of cellular uptake. This size threshold concept was also supported by recent computational modeling studies where in fact NP with ~25 nm radius (i.e. ~50 nm in size) were found to have the maximum chances for getting internalized by cells, because this size fits optimally with most of the cell membrane-bound receptors.[38] It can be understood that the presence of such size threshold once again points towards a delicate interaction between NP and the cells and rationalize the selection of NP, which fall within these size thresholds. Interestingly, the smaller NP of the two sizes of tri-block copolymer NP (45 and 90 nm) (Chapter 6), or polystyrene NP (50 and 100 nm) that were tested, also fell within this optimal size range. It was found that smaller PNP were not only more cytotoxic (in case of cationic PNP) but also showed higher cellular uptake (for all surface charges) compared to the bigger ones. These findings are in line with our expectations and can help in designing future NP for especially medical or food-related applications. This optimal size range for better cellular uptake of NP and toxicity can be a guideline for chemical engineers for designing and synthesizing NP. Besides for cellular uptake, the size of the PNP also played an important role in their interaction with specific cell membrane-bound receptors. For example, smaller (45 nm) and bigger (90 nm) PNP were found to be more reactive towards the clathrin and caveolin receptors, respectively. This size

dependency is again of importance for application of biocompatible PNP. A better understanding of the interaction of specific cell membrane-bound receptors with PNP can help in designing PNP with a better target specificity and higher bioavailability. However, an increased bioavailability may also result in a higher toxicity. This can be an interesting direction for future research, to carefully and intelligently design PNP, for which the advantages outweigh the drawbacks.

A detailed discussion on the role of cell membrane-bound receptors in the cellular uptake of PNP is given in Chapters 5 and 6. Surface charge and the chemistry of the terminal functional groups appeared to have a significant effect on the interaction with the cellular receptors. For example, mannose receptors were found to play a dominant role in the cellular uptake of hydroxyl-terminated PNP. Normally, sugar molecules with their hydroxyl groups are the common substrates for mannose receptors. Therefore, it is possible that the hydroxyl-terminated PNP interacted more strongly with these mannose receptors than the other PNP. Similar types of surface charge-driven interactions of PNP with different cell membrane-bound receptors were also reported by other groups and our data are in line with literature reports.[39-41]

To confirm that these surface charge-based effects on cytotoxicity and cell membrane-bound receptor-mediated interactions of PNP are not only limited to tri-block copolymer NP, fluorescent polystyrene NP of different surface charges (positive and negative) and sizes (50 and 100 nm) were also investigated (Chapters 7, 9 and 10). Overall, the results agreed well with the results obtained for the tri-block copolymer NP. Since it was shown that PNP have different interactions with clathrin, caveolin and mannose receptors, it can be assumed that PNP can also have different interactions with other cell membrane-bound receptors. It is known that different multi drug resistance (MDR) transporters are present on the apical and basolateral sides of monolayers of Caco-2 cells grown on transwell inserts. These MDR transporters are involved in the export of molecules (including important anti-cancer drugs, antibiotics and other xenobiotics) from the intestinal cells to either the blood side or back into the intestinal lumen. In tumor cells their activity may cause multidrug resistance[42,43] and their presence in intestinal cells may cause decreased or enhanced bioavailability depending on whether transport is back to the intestinal lumen or to the blood side.[44,45] Hence, such Caco-2 monolayers grown on transwell inserts provide an adequate in vitro system for testing the interactions of PNP with different MDR transporters (Chapter 7).

It was found that cationic PNP, apart from crossing the Caco-2 monolayers more efficiently compared to the anionic ones, also effectively blocked the transporters present on the apical side of the cells, while anionic PNP had inhibitory effects more on the transporters present on the basolateral side of the cells. This can have implications especially for the development of new food or medical technology-based NP, since it is important to understand the interactions of these NP with the gut enterocytes. Given their role in the excretion of many bio-active compounds, a selective inhibition of these MDR transporters based on the specific surface charge of the PNP, can, in principle, be exploited to increase the bioavailability of drugs. If further research shows that this hypothesis is correct, this can lead to a decreased cost-benefit ratio for application of these drugs as well as a reduction of adverse drug effects due to decreased dose regimes. Interestingly, our initial research with quercetin gave indications that this approach could be successful. Quercetin is a flavonoid molecule that is present in green vegetables and it is popular as a natural antioxidant and thus widely used as an anti-aging agent.[46] Upon co-administration of quercetin with PNP with different surface charges on the

apical side, an increased or decreased amount of quercetin could be recovered from the basolateral compartment depending on the type of MDR transporters inhibited by the PNP. Hence, an initial indication that this strategy to increase the bioavailability of molecules by targeting specific MDR transporters by PNP, could be obtained. However, this needs to be further explored before the possibility of such an application of PNP can be considered. The results of Chapter 7 also revealed that co-administration of PNP and quercetin influenced the bioavailability of different PNP across the Caco-2 monolayers. As quercetin is a known inhibitor of various MDR transporters itself,[47] this showed that different PNP can act also as substrates for the MDR transporters, reconfirming the importance of the interactions between PNP and cell membrane-bound receptors.

In order to assess the bioavailability and biodistribution of tri-block copolymer NP in vivo, an experiment with male Fisher 344 rats was performed (Chapter 8). The rats were given oral gavages of aqueous dispersions of both cationic and anionic fluorescent tri-block copolymer NP (45 nm). At several time points after exposure, blood samples were taken and 6 h after exposure, the rats were sacrificed and the different organs (liver, lungs, kidneys, brains, intestines, spleens) and tibial tissues were collected. The PNP content of all samples was determined by fluorescence. The results showed an initial increase of PNP in blood, followed by a gradual decline. After 24 h, the maximum deposition of PNP was found in the liver, followed by kidney and spleen. Interestingly, a small amount of cationic PNP entered the brain. This finding is important as it showed that cationic PNP can cross the blood-brain barrier (BBB). This capability of crossing the BBB by cationic PNP can be exploited in future for developing PNP that are targeted for delivery of medicines in the cerebral tissues. Unfortunately, it is difficult to compare our data with literature, since animal experiments with NP through oral exposure are very rare as most studies were performed via parenteral routes (like intravenous and intraperitoneal administration).[48] However, even after parenteral exposure, the maximum accumulation of NP was reported in the liver, followed by kidney and spleen. Looking at the physiological perspective, this is not totally unexpected, as after becoming bioavailable in blood, it is likely that NP will be preferentially distributed to highly blood-perfused organs, like kidney, liver and spleen. In a recent study,[49] where NP were administered through oral exposure, similar distribution patterns with liver and kidney showing the largest deposition of the administered NP, followed by spleen and to some extent brain, was reported. Our results matched well with this study. A point of debate may be the inconsistency between in vitro and in vivo data. For example, the in vitro data obtained with Caco-2 cell monolayers suggested that cationic NP were more toxic and were more capable of crossing the intestinal barrier compared to negatively charged NP. However, from in vivo studies, no significant difference in the absorption of cationic and anionic NP could be observed. A reason for this discrepancy between in vitro and in vivo data may be due to the intrinsic physiology of the gut. The gastrointestinal tract is flushed with mucous, and it is possible that the PNP after oral exposure become covered with a superficial layer of mucous which masks the effects of surface charge. So, the bioavailability of PNP, which may be a net outcome of the interactions of PNP with mucous as well as their cellular uptake and excretion by these intestinal cells, can be influenced by surface charge of the PNP. An alternative explanation for the similar bioavailability of positive and negatively charged PNP in vivo may be that cationic PNP, although having a greater capability of crossing the intestinal barriers, also showed higher entrapment in the negative mucous layer,[50] while the situation is opposite for

anionic PNP. The result of these two opposing effects can be an explanation for overall match in bioavailability of cationic and anionic PNP.

To investigate in some more detail, the possible role of formation of reactive oxygen species (ROS) and oxidative stress as a causative factor of cytotoxicity of polystyrene NP, in Chapter 9 of the thesis, a carefully designed experiment was performed where the cytotoxicity patterns of cationic polystyrene NP (anionic polystyrene NP did not show any cytotoxicity) were compared to that of: (1) the mitochondrial ETC disrupting agent 2,4-dinitrophenol and (2) the oxidative stress inducing hydrogen peroxide. In addition the protective role of increased levels of cellular antioxidants, vitamin C and E, as well as the effects of increased and decreased levels of intracellular GSH on the toxicity exerted by these three factors was included in the comparisons. Interestingly, the data for the cationic polystyrene NP on the cytotoxicity as well as on the protective effects of vitamin E and C and the consequences of increased as well as decreased cellular GSH levels resembled those obtained for 2,4-dinitrophenol and not the results obtained for hydrogen peroxide. This knowledge coupled with the current data on surface charge-driven interactions between mitochondria and cationic polystyrene NP led to the conclusion that for cationic polystyrene NP, oxidative stress rather played a subsidiary or secondary role in causing cytotoxicity. However, the existence of oxidative stress in the cells after exposure to cationic polystyrene NP should not be neglected and more research is warranted to understand the true role of oxidative stress. For example, although not a primary mechanism of cytotoxicity for polystyrene NP, the induction of intracellular ROS and subsequent oxidative stress can still be pivotal in causing other types of toxicities, like genotoxicity. The knowledge on such implications of oxidative stress in the context to nanomaterial safety deserves attention.

With this broad range of information available, it becomes necessary to assemble the different scattered pieces of data in a proper way, so that the entire process through which the cytotoxicity of NP occurs, becomes understandable (Chapter 10). To illustrate this, it is not exactly known what the consequences are of the interactions of the PNP with the intracellular mitochondria. From our data on Si NP, Ge NP and tri-block copolymer NP, it was found that especially cationic NP disturb the mitochondrial membrane potential. Therefore, both the mitochondrial membrane potential and cellular ATP content were measured after exposure to polystyrene NP of different surface charges (Chapter 10). Additionally, a surge in cellular free calcium content was found upon exposure to cationic PNP.[51, 52] This also seemed to identify mitochondria as an important intracellular target organelle for PNP. As we found that cationic PNP can hamper the homeostasis of mitochondrial physiology by interfering with its membrane potential, it is possible that the calcium stored within the intracellular mitochondria is released in the cytoplasm and causes the increase in cytoplasmic free calcium levels. The increase in intracellular calcium concentration can then activate apoptotic pathways. This was checked by monitoring the caspase-3 enzyme activity, which is a reliable biomarker for activation of cellular apoptotic processes. It was found that an increase in the cellular caspase-3 activity occurred after exposure to cationic PNP. The increased cytoplasmic free calcium levels may lead to the activation of apoptotic processes. Assembling these pieces of data together, a picture emerged where the intracellular mitochondria were the most important target organelle for PNP.

A common point of debate is why only cationic NP show signs of toxicity as well as higher cellular uptake in comparison to anionic ones. From CLSM studies, it was found that the cationic PNP showed stronger interaction with peripheral areas of the cells whereas the anionic PNP

were rather diffusely spread across the cytoplasm (Chapters 5, 6, 10). A clear explanation for this surface charge-specific phenomenon remains elusive. A survey of different biologically active molecules (like antibiotics) shows that most of these molecules (like penicillin, chloramphenicol, anticancer agents) are alkaloids, meaning that they carry nitrogen atoms which can render them cationic in aqueous solutions. It is often stated that cationic molecules, or cationic NP, show stronger electrostatic attractive interactions with cell membranes simply because of the negative charge of cell membranes. For anionic NP the situation is reverse as now there is an electrostatic repulsive force between them. For cationic NP the electrostatic attraction between the NP and the cell membrane in fact facilitates the interaction between them by decreasing the energy barrier.

A less understood topic is the observed pattern of intracellular distribution of cationic and anionic PNP. CLSM studies showed that especially for anionic PNP, small vesicular structures could be observed inside the cells (Chapter 10), whereas the cationic PNP were spread evenly across the cytoplasm, although both showed the propensity for receptor-based uptake in small vesicular-like lysosomal structures. An explanation put forward by some groups[53, 54] to explain this disparity in the intracellular distribution is that the lysosomal structures containing NP have an acidic interior. Because of their positive surface charges, the cationic NP further increase the amount of positive ions inside the lysosomal structures and decrease their stability. As a result, the lysosomal structures may rupture and release the cationic NP inside the cytoplasm. In contrast, the negative charges on the anionic NP stabilize the lysosomal vesicles and hence the lysosomal structures can maintain their structural integrity inside the cells.

Although it is known that cationic NP show stronger interactions with cell membranes, the nature and outcome of such interactions was largely unknown. Some groups[55] suggested, based on computational studies, that purely as a result of electrostatic attractions, cationic NP caused formation of pouches in the lipid bilayer structures and become embedded in the cell membranes. These pouch-like structures then detach from the cell membranes to enter the cells and leave pores or holes in the cell membrane. Recently, the creation of holes in the cell membrane by cationic NP was suggested, although direct evidence for creation of such holes was missing.[56] With atomic force microscopy (AFM), we were able to map the topography of the surface of viable NR8383 cells and to image the damage to surface continuity created on the cell membranes by the cationic PNP (Chapter 10). For the anionic PNP this was not observed. This once again showed the significant interactions of cationic NP with the cell membrane. Interestingly, it was also found that in contrast to anionic NP, the cationic NP increased the overall roughness of the cell membrane. This may have explicit consequences for the cytotoxicity of NP. Both the holes in as well as the compromised surface continuity of the cell membranes play a role in the toxicity of such NP.

From the results discussed above, an overall picture of the series of events that follow the cellular exposure to different charged NP emerges. Upon integration of the lessons learned so far, it can be stated that the interactions of NP with cellular systems are quite complex. The interactions with different organelles, like intracellular mitochondria, may act as a starting point of the toxicity paradigm. Production of ROS can cause oxidative stress, although from the available data, it seems that oxidative stress is not the primary cause of cytotoxicity for polystyrene NP.

In summary, with these extensive series of systematic experiments, we tried to probe the interactions between NP and biological systems, both in vitro and in vivo. Intracellular mitochondria seem to be one of the most important target organelles for the NP and disturbance of the mitochondrial membrane may act as a starting point for the disruption of the ETC, induction of ROS production (oxidative stress), decrease in ATP production (causing ATP depletion), increase in the cytoplasmic free calcium concentration, resulting in triggering of apoptotic pathways. The chain of events starts with the surface charge-specific interactions of NP with biomembranes. Especially cationic NP can cause damage to the lipid membrane structures, causing the toxicity of the NP to exacerbate. Apart from surface charge, size of the NP also plays an important role in toxicity as well as cellular uptake. Cell membrane-bound receptors play an important role in the cellular uptake of NP and both surface charge and size influence these interactions. The effect of NP on the MDR receptors in the gut enterocytes can possibly be used in manipulating the bioavailability of ingredients applied orally. This offers perspectives for the development of such food-based applications of NP in future.

Integrating these findings, it can be stated that the work described in this thesis successfully probed the influences of some of the surface properties (like surface charge) and physical properties (like particle size) of different NP on the interactions with cells as well as their toxicities. A better insight into the mechanistic aspects of the toxicity of NP could be achieved based on the data reported in this thesis. With the data and analyses reported in this thesis, the knowledge on the toxicity of NP as well as on the intriguing complexity of the cellular interactions, was enhanced. This work may provide vital clues for future research. Since the work also included in vivo experiments, an idea on the bioavailability of PNP after oral exposure can be gained. These data can be pivotal in planning further strategic research in designing smarter and tailor-made NP, meant for specific purposes, along with superior biocompatibility.

Future perspectives

Although the present thesis has extended the understanding and prediction of the influences of some of the surface properties (like surface charge) and physical properties (like particle size) of different NP on the interactions with cells as well as their toxicities, several issues remain to be elucidated to fully understand the hazards of NP to human health and the environment. The current section presents some considerations on future topics of importance in this field.

1. The toxicity of NP needs to evaluated in terms of surface properties of both the NP (like crystallinity, porosity, surface roughness) as well as of the cells (like lipid structure of cell membranes, rigidity, types of receptors present etc.). Indications were repeatedly gathered, as mentioned in this thesis, that the surface chemistry and properties of both the NP and the cells play an important role in determining the interactions. In future investigations, a great deal of importance should be devoted towards exploring these surface-based interactions, as the cellular events start only after the surfaces of the cells and the NP come in contact.

2. Fortunately, with the advanced software available now, more extensive use of molecular modeling is advocated, in order to understand the crucial interactions between the lipid bilayer membrane structure of cells and the reactive surfaces of the NP.

3. It would also be interesting to investigate the mechanism of cytotoxicity of the NP deeper. In this regard, the use of physiologically based pharmacokinetic (PBPK) modeling should be promoted. Recently, some predictions on NP bioavailability and in vivo distribution based on PBPK calculations have emerged[57,58] and the results were very promising. A simultaneous use of PBPK modeling along with in vitro experiments with well-characterized NP could provide a valuable contribution in the field of alternatives for animal testing, since such combined in vitro-in silico approaches were recently shown to be able to predict in vivo dose response curves for toxicity without the need for animal experiments.[59]

4. Although intracellular mitochondria were identified as an important component of the entire toxicity-causing cascade, a cell-signaling mechanism was also found to be existing. It would be exciting to decipher the cell-signaling pathway into more detailed steps, and to exactly know the order of the events and the molecular messengers involved. As the cell membrane-bound receptors (like clathrin, caveolin) were found to play an important role in the cellular interactions of NP, it can be interesting to investigate this in more detail. This would not only supply critical basic knowledge, but would also clarify interactions between different cell membrane-bound receptors and NP that can be further exploited in targeted, NP-mediated drug delivery. Hence, knowing the nature and intricacies of such interactions may open up new avenues for designing NP meant for specific purposes.

5. It was shown in this thesis (Chapter 7) that, depending on surface charge and particle size, polymer NP can influence the functioning of ABC transporters. The activity of these transporter proteins constitutes one of the major reasons for causing drug resistance by decreasing the cellular levels of drugs. It was also found that the interaction of polymer NP with ABC transporters can influence the bioavailability of physiologically relevant

molecules, like carcinogens or bioactive food ingredients. This should be followed up in future to better define possible food-drug, food-food or drug-drug interactions due to application of NP formulations.

6. The synthesis of tri-block copolymer, as described in Chapters 5 and 6, can be improved in many ways. Due to the flexibility of block co-polymer synthesis tailor-made polymer NP for different purposes can be obtained. A simple variation, like altering the PEG chain length, results in a change in the size of NP. Furthermore, the terminal hydroxyl groups can for example be tagged with fluorescent or radioactive material (like radioactive carbon) which makes the NP detectable and quantifiable. Especially, for research under in vivo conditions, this can strongly enhance the applicability of these NP. Similarly, by engineering the polyester middle-block, the biodegradability of the tri-block copolymers can be increased. Other variations in polymer nanoparticles include incorporation of isotopes for PET imaging, crosslinking groups to increase the stability or the use of biodegradable constituents to allow time-released degradation and possibly time-released loss of enclosed drugs.

7. One of the major concerns in risk assessment of NP lies with the fact that the amount of in vitro data largely outweighs the available in vivo data. Hence, the validation of the in vitro data remains far from satisfactory. Given the fact that at the present state-of-the-art risk assessment practice still requires in vivo data, the limited availability of in vivo data and of methods to extrapolate the in vitro data to the in vivo situation acts as a barrier in the risk assessment. It is recommended that more in vivo experiments should be performed in future or that methods to extrapolate in vitro concentration response curves to in vivo dose response curves should be further developed to bridge this gap between these two testing systems,

8. It is quite difficult to adequately characterize the NP in cell culture medium, which makes it very hard to understand what is actually being tested. For example, the NP increase in size due to protein adsorption, immediately after mixing with the cell culture medium. This alters their surface properties (like surface charge) as well as their physical characteristics (like particle size). For a clear understanding of the toxicity of NP it is therefore of utmost importance that the NP are well-characterized, both before and after being suspended in cell culture medium. It should be noted that cell culture media, like F12-K or DMEM, contain many different types of molecules, like proteins, amino acids, salts etc., which makes them very complicated systems to properly characterize the NP in. This may hamper in situ characterizations, but then at least ex situ characterizations after exposure to such a medium are critical to at least find out what the actual nature of the NP under study is in the relevant media. Similar uncertainties regarding proper characterization of NP can be observed for food-based formulations, where it is largely unknown how the local milieu in the human gastro-intestinal tract (like mucous layer) changes the physical and surface characteristics of NP. In future investigations, this is an important issue that should be dealt with.

9. In continuation to the previous statement, it should also be mentioned that in situations where the surfaces of NP are altered due to surface adsorption or deliberate engineering (like functionalization), it is crucial from a toxicological point of view to have a clear idea of the properties of the surface coating. As mentioned in this thesis (Chapter 4), surface coating with biocompatible materials (like dextran) can alleviate the toxicity of NP. This

shows great promise for future and such engineering with surface properties of NP should be followed up with further research.

10. One of the most understated facts about nanotoxicological research is the health hazard that NP can pose from environmental contamination. Eyeing the increased use of NP in industry, food or medical applications, fortunately some policies and guidelines trying to regulate the uses of NP had already surfaced. The regulatory aspect of use of NP can be expected to improve significantly in future. Unfortunately, the situation is yet rather bleak as far as environmental exposure is concerned. Although, some research had ushered in such directions, especially in nano-ecotoxicology, mostly the research is focused on aquatic toxicology. On a critical survey, a significant vacuum with research in other forms of environmental pollution caused by the NP can be noted. For example, soil contamination with NP, like silver NP,[60] C60,[61] can occur which can exert toxic effects on soil organisms, like earthworm *Lumbricus rubellus*. Compared to the need and demand of the situation, very little data is actually available addressing these issues.

11. A rather confusing fact regarding toxicological assessments of NP is that there is insufficient understanding of the dosimetry, or the way in which dose metrics influence the dose response curves for cytotoxicity. Although many factors (like surface charge, charge density, size, surface area, surface functionalization etc.) have been identified as having an influence on cytotoxicity of NP, none of the factors by itself showed a linear correlation with toxicity. It is possible that, instead of a unique factor, multiple factors simultaneously determine the cytotoxicity of NP. In order to obtain a proper risk assessment, it is very important that this problem is considered in future.

The complexity of the mechanisms behind the potential toxicity or non-toxicity of NP is great – not only is it very large, but it also provides an excellent field of play for extensive basic studies that have a clear eye to societal relevance. Improved use of the interplay between detailed toxicology and tailor-made chemistry will thereby also allow the improved and safer use of NP, and as such bring closer one of the promises of 21st century nanotechnology: tailor-made functionality delivered at precisely the right biomolecular or physiological level.

References

1. Rosso-Vasic M, Spruijt E, van Lagen B, De Cola L, Zuilhof H; *Small* 2008, 4:1835-1841.
2. Rosso-Vasic M, Spruijt E, Popovic Z, Overgaag K, van Lagen B, Grandidier B, et al.; *J. Mater. Chem.* 2009, 19:5926-5933.
3. Ruizendaal L, Pujari SP, Gevaerts V, Paulusse JMJ, Zuilhof H; *Chem-Asian J.* 2011, 6:2776-2786.
4. O'Farrell N, Houlton A, Horrocks BR; *Int. J. Nanomed.* 2006, 1:451-472.
5. Zhang X, Brynda M, Britt RD, Carroll EC, Larsen DS, Louie AY, et al.; *J. Am. Chem. Soc.* 2007, 129:10668-10669.
6. Louie A; *Chem. Rev.* 2010, 110:3146-3195.
7. Bhattacharjee S, de Haan LH, Evers NM, Jiang X, Marcelis AT, Zuilhof H, et al.; *Part. Fibre Toxicol.* 2010, 7(25).
8. Bhattacharjee S, Ershov D, Gucht Jvd, Alink GM, Rietjens IMCM, Zuilhof H, et al.; *Nanotoxicology* 2011, *Early Online (DOI: 10.3109/17435390.2011.633714)*:1-14.
9. Thevenot P, Cho J, Wavhal D, Timmons RB, Tang L; *Nanomed-Nanotechnol.* 2008, 4:226-236.
10. Choi JE, Kim S, Ahn JH, Youn P, Kang JS, Park K, et al.; *Aquat. Toxicol.* 2010, 100:151-159.
11. Foucaud L, Goulaouic S, Bennasroune A, Laval-Gilly P, Brown D, Stone V, et al.; *Toxicol. In Vitro* 2010 24:1512-1520.
12. Mocan T, Clichici S, Agoşton-Coldea L, Mocan L, Şimon Ş, Ilie I, et al.; *Acta Physiol. Hung.* 2010, 97:247-255.
13. Stone V, Donaldson K; *Nat. Nanotechnol.* 2006, 1:23-24.
14. Fahmy B, Cormier SA; *Toxicol. In Vitro* 2009, 23:1365-1371.
15. Nadia B, Wided K, Kheira B, Hassiba R, Lamia B, Rhouati S, et al.; *Acta Biol. Hung.* 2009, 60:385-398.
16. Salnikov V, Lukyánenko YO, Frederick CA, Lederer WJ, Lukyánenko V; *Biophys. J.* 2007, 92:1058-1071.
17. Xia T, Kovochich M, Liong M, Zink JI, Nel AE; *ACS Nano* 2007, 2:85-96.
18. Schaeublin NM, Braydich-Stolle LK, Schrand AM, Miller JM, Hutchison J, Schlager JJ, et al.; *Nanoscale* 2011, 3:410-420.
19. Xia T, Kovochich M, Brant J, Hotze M, Sempf J, Oberley T, et al.; *Nano Lett.* 2006, 6:1794-1807.
20. Liu R, Zhang X, Pu Y, Yin L, Li Y, Liang G, et al.; *J. Nanosci. Nanotechnol.* 2010, 10:5161-5169.
21. Lee H-M, Shin D-M, Song H-M, Yuk J-M, Lee Z-W, Lee S-H, et al.; *Toxicol. Appl. Pharmacol.* 2009, 238:160-169.
22. Ruizendaal L, Bhattacharjee S, Pournazari K, Rosso-Vasic M, de Haan LHJ, Alink GM, et al. *Nanotoxicology* 2009, 3:339-347.
23. Villanueva A, Canete M, Roca AG, Calero M, Veintemillas-Verdaguer S, Serna CJ, et al.; *Nanotechnology* 2009, 20:115103.
24. Kim C, Agasti SS, Zhu Z, Isaacs L, Rotello VM; *Nat. Chem.* 2010, 2:962-966.
25. Verma A, Stellacci F; *Small* 2010, 6:12-21.
26. Liu L, Xu K, Wang H, Jeremy Tan PK, Fan W, Venkatraman SS, et al.; *Nat. Nanotechnol.* 2009, 4:457-463.
27. Arvizo RR, Miranda OR, Thompson MA, Pabelick CM, Bhattacharya R, Robertson JD, et al.; *Nano Lett.* 2010, 10:2543-2548.
28. Ginzburg VV, Balijepalli S; *Nano Lett.* 2007, 7:3716-3722.
29. Ke PC, Lamm MH; *Phys. Chem. Chem. Phys.* 2011, 13:7273-7283.

30. Zhang LW, Monteiro-Riviere NA; *Toxicol. Sci.* 2009, 110:138-155.

31. Thurn KT, Arora H, Paunesku T, Wu A, Brown EMB, Doty C, et al.; *Nanomed-Nanotechnol.* 2011, 7:123-130.

32. Lühmann T, Rimann M, Bittermann AG, Hall H; *Bioconjugate Chem.* 2008, 19:1907-1916.

33. Kawata K, Osawa M, Okabe S; *Environ. Sci. Technol.* 2009, 43:6046-6051.

34. Greish K, Thiagarajan G, Herd H, Price R, Bauer H, Hubbard D, et al.; *Nanotoxicology* 2011.

35. Asharani PV, Lian Wu Y, Gong Z, Valiyaveettil S; *Nanotechnology* 2008, 19:255102.

36. Keelan JA; *Nat. Nanotechnol.* 2011, 6:263-264.

37. Auffan M, Rose J, Bottero JY, Lowry GV, Jolivet JP, Wiesner MR; *Nat. Nanotechnol.* 2009, 4:634-641.

38. Zhang S, Li J, Lykotrafitis G, Bao G, Suresh S; *Adv. Mater.* 2009, 21:419-424.

39. Nel AE, Madler L, Velegol D, Xia T, Hoek EMV, Somasundaran P, et al.; *Nat. Mater.* 2009, 8:543-557.

40. Zhang Y, Yang M, Park J-H, Singelyn J, Ma H, Sailor MJ, et al.; *Small* 2009, 5:1990-1996.

41. Patel J, O'Carra R, Jones J, Woodward J, Mumper R; *Pharm. Res.* 2007, 24:343-352.

42. Brand W, Padilla B, van Bladeren PJ, Williamson G, Rietjens IMCM; *Mol. Nutr. Food Res.* 2010, 54:851-860.

43. Brand W, van der Wel PAI, Rein MJ, Barron D, Williamson G, van Bladeren PJ, et al.; *Drug Metab. Dispos.* 2008, 36:1794-1802.

44. Brand W, Schutte ME, Williamson G, van Zanden JJ, Cnubben NHP, Groten JP, et al.; *Biomed. Pharmacother.* 2006, 60:508-519.

45. Schutte ME, Freidig AP, van de Sandt JJM, Alink GM, Rietjens IMCM, Groten JP; *Toxicol. Appl. Pharmacol.* 2006, 217:204-215.

46. Boots AW, Haenen GRMM, Bast A; *Eur. J. Pharmacol.* 2008, 585:325-337.

47. Kioka N, Hosokawa N, Komano T, Hirayoshi K, Nagate K, Ueda K; *FEBS Lett.* 1992, 301:307-309.

48. Soo Choi H, Liu W, Misra P, Tanaka E, Zimmer JP, Itty Ipe B, et al.; *Nat. Biotechnol.* 2007, 25:1165-1170.

49. Schleh C, Semmler-Behnke M, Lipka J, Wenk A, Hirn S, Sch Ffler M, et al.; *Nanotoxicology* 2011.

50. László S; *J. Control. Rel.* 1997, 46:233-242.

51. Zhang H, Xia T, Meng H, Xue M, George S, Ji Z, et al.; *ACS Nano* 2011, 5:2756-2769.

52. Wani MY, Hashim MA, Nabi F, Malik MA; *Adv. Phys. Chem.* 2011.

53. Zhao F, Zhao Y, Liu Y, Chang X, Chen C, Zhao Y; *Small* 2011, 7:1322-1337.

54. Panyam J, Zhou W-Z, Prabha S, Sahoo SK, Labhasetwar V; *FASEB J.* 2002, 16:1217-1226.

55. Lin J-Q, Zheng Y-G, Zhang H-W, Chen Z; *Langmuir* 2011, 27:8323-8332.

56. Hong S, Leroueil PR, Janus EK, Peters JL, Kober MM, Islam MT, et al.; *Bioconjugate Chem.* 2006, 17:728-734.

57. Lin P, Chen JW, Chang LW, Wu JP, Redding L, Chang H, et al.; *Environ. Sci. Technol.* 2008, 42:6264-6270.

58. Lee HA, Leavens TL, Mason SE, Monteiro-Riviere NA, Riviere JE; *Nano Lett.* 2009, 9:794-799.

59. Louisse J, de Jong E, van de Sandt JJM, Blaauboer BJ, Woutersen RA, Piersma AH, et al.; *Toxicol. Sci.* 2010, 118:470-484.

60. Shoults-Wilson WA, Reinsch BC, Tsyusko OV, Bertsch PM, Lowry GV, Unrine JM; *Nanotoxicology* 2011, 5:432-444.

61. van der Ploeg MJC, Baveco JM, van der Hout A, Bakker R, Rietjens IMCM, van den Brink NW. *Environ. Pollut.* 2011, 159:198-203.

Samenvatting

Door de unieke eigenschappen van nanodeeltjes (NP), biedt de toepassing hiervan, i.e. de nanotechnologie, een breed scala aan nieuwe mogelijkheden voor toekomstige ontwikkelingen. Helaas gaat de snelle groei van de nanotechnologie, met zijn nieuwe en bijzondere mogelijkheden, gepaard met een gebrek aan kennis over de (toxische) effecten die nanotechnologische producten kunnen hebben op levende organismen en op het menselijk lichaam. Daarnaast is er in deze tak van technologie een gebrek aan diepgaande kennis over onderwerpen die relevant zijn voor de toxiciteit van nanodeeltjes, zoals de karakterisering en analyse van NPs. Bovendien wordt de situatie nog ingewikkelder als men de interacties van NPs met biologische systemen wil karakteriseren en onderzoeken.

In diverse rapporten werd al een indicatie gegeven van de toxische effecten van NPs. Echter, het ontbreken van een goede karakterisering van de NP, vooral in biologische systemen, samen met het gebruik van vele verschillende cellijnen en het gebrek aan coördinatie, leidden ertoe dat een goede evaluatie van de resultaten om tot een eenduidige conclusie te komen moeilijk is. Ondanks een continue stroom van nieuwe gegevens, roept al dit onderzoek meer vragen op dan dat het beantwoordt, zoals hoe de cytotoxiciteit door de NPs op moleculair en cellulair niveau wordt veroorzaakt en wat het effect van fysische eigenschappen (zoals oppervlaktelading, deeltjesgrootte, enz.) op de cytotoxiciteit is. In dit proefschrift worden deze problemen aangepakt met systematisch opgezette experimenten.

Hoofdstuk 1 dient als algemene inleiding van het proefschrift, waar basisbegrippen, probleemverklaringen en aanpak van onderzoek worden geïntroduceerd. Zoals eerder vermeld, is een goede karakterisering van de NPs een probleem dat verder onderzoek vergt, alvorens conclusies getrokken kunnen worden over de toxiciteit van NPs. Eén van de factoren die bijdragen aan de complexe situatie is, dat op grond van een zeer reactief oppervlak, de NPs interacties kunnen vertonen met een breed scala aan biomoleculen (zoals eiwitten). Hierdoor verandert de chemie van het oppervlak van de NPs, met name in biologische medium (zoals celkweekmedium), door processen zoals oppervlakte-adsorptie van proteïnen. Dit is niet alleen van invloed op NPs in een kern-schil structuur, maar ook de manier waarop cellen de NPs "zien". Vandaar dat in dit type onderzoek het belangrijk is te weten waar de cellen werkelijk aan werden blootgesteld. Daarnaast woedt er een belangrijke discussie over de wijze van interactie die leidt tot (cyto)toxiciteit van de NPs. Eerder werd al verondersteld dat oppervlaktelading- en deeltjesgrootte-afhankelijke toxiciteit veroorzaakt wordt door een inductie van oxidatieve stress. Echter, er is een gebrek aan experimentele gegevens die deze hypothesen ondersteunen. In dit hoofdstuk worden deze kwesties, die verband houden met nanotoxicologisch onderzoek, samen met de aanpak besproken.

In de hoofdstukken 2 en 3, wordt de synthese en cytotoxiciteit van silicium nanodeeltjes (Si NP) met covalent gebonden organische monolagen besproken. Deze unieke reeks van goed gekarakteriseerde NPs, die fluorescent en monodispers zijn, heeft vele mogelijkheden voor verdere oppervlaktemodificaties. Vandaar dat Si NP (1,6 ± 0,2 nm) gemaakt zijn met aan het oppervlak een monolaag van amine eindgroepen (kationisch), azide eindgroepen (neutraal) of carbonzuur eindgroepen (anionisch). Deze werden gebruikt voor het testen van de toxiciteit bij rat alveolaire macrofagen NR8383 en menselijke dikke darm adenocarcinoom Caco-2 cellen.

Alleen Si NP met amine groepen aan het oppervlak bleken al bij zeer lage concentraties toxiciteit in beide cellijnen te veroorzaken. De Si NP met azide oppervlaktegroepen vertonen alleen toxiciteit bij veel hogere concentraties. De anionische zuur getermineerde Si NP vertoonden geen cytotoxiciteit. Dit wees in de richting van een oppervlakte lading-afhankelijkheid van de cytotoxiciteit van Si NP. Inductie van oxidatieve stress werd ook waargenomen en in verband gebracht met de kationische Si NPs. Geïsoleerde mitochondriën van ratten werden blootgesteld aan de verschillende Si NPs, waarbij alleen de amine-getermineerde kationische Si NPs inductie van productie van reactieve zuurstof species (ROS) laten zien. Dit gaf de eerste aanwijzingen dat kationische NP waarschijnlijk kunnen interfereren met de elektronen transportketen (ETC) in het buitenste membraan van de mitochondriën en dus dat de inductie van de ROS productie wordt veroorzaakt door een verstoring van het ETC.

In hoofdstuk 4 werd het effect van oppervlakte-eigenschappen (zoals de oppervlakte lading) op de toxiciteit, zoals beschreven in de hoofdstukken 2 en 3, verder uitgebreid door de integratie van een breed scala van halfgeleider quantum dots met silicium en germanium kern, verkregen uit verschillende laboratoria in de VS en Canada. De Si NP en Ge NP werden verkregen in verschillende groottes en met verschillende oppervlaktemodificaties. De NPs werden getest op NR8383 en Caco-2 cellen met een systematische en grote verscheidenheid van toxiciteitstesten. Ook hier blijken alleen de kationische NP tekenen van toxiciteit te vertonen, alsook inductie van cellulaire ROS, afname van het mitochondriale membraanpotentiaal (Ψm), uitputting van de cellulaire ATP voorraad, en stijging van zowel het vrije cellulaire calciumgehalte als de TNF-α productie. Op basis van deze gegevens werd verondersteld dat kationische NPs cytotoxiciteit veroorzaken door te interfereren met de mitochondriale fysiologie. Oxidatieve stress bleek ook aanwezig, hoewel dit een effect geweest kan zijn van mitochondria-NP interacties. Interessant is dat naast oppervlakelading, ook deeltjesgrootte een belangrijke factor in de cytotoxiciteit speelt. De kleinere NPs bleken meer cytotoxisch dan de grotere. Er werd ook waargenomen dat de toxiciteit van kationische NPs afgezwakt zou kunnen worden door een verhoging van de sterische omvang om de positieve lading van de oppervlaktegroepen. De toxiciteit van kationische NPs kan ook worden verminderd door het oppervlak van de NPs te coaten met biocompatibel materiaal, zoals dextran. Uit deze resultaten blijkt het belang van de oppervlaktechemie voor NPs in cel-NP interacties en zou gebruikt kunnen worden bij het vervaardigen meer biocompatibele NPs.

In Hoofdstuk 5 en 6 wordt de synthese van tri-blokcopolymeren met een hydrofoob polyester midden-blok en hydrofiele PEG$_{2000}$ of PEG$_{400}$ eindblokken besproken. De door nanoprecipitatie verkregen monodisperse polymere NPs (PNPs) waren van verschillende grootte (45 en 90 nm), afhankelijk van de aard van de PEG blokken en hebben verschillende oppervlakteladingen (kationische en anionische). Om deze PNP in de cellen waar te kunnen nemen met confocale laser scanning microscopie (CLSM) werd in het middenblok van de tri-blokcopolymeer een fluorescerende label ingebouwd. Met deze PNPs werden vervolgens een reeks systematische cytotoxicologische experimenten uitgevoerd op NR8383 en Caco-2 cellen. Alleen de kationische PNP bleken cytotoxisch te zijn, terwijl de anionische PNP dat niet zijn. Een oppervlakte lading- en deeltjesgrootte- afhankelijke opname van deze PNP werd waargenomen voor celmembraan-gebonden clathrine en caveoline receptoren. De kationische PNPs geven de voorkeur aan de clathrine-afhankelijke endocytische route, de anionische werden vooral opgenomen in de cellen door de caveoline receptoren. De kationische PNPs geven ook een sterkere interactie met het celoppervlak, die voortvloeit uit elektrostatische aantrekking tussen

de kationische PNPs en het anionische celmembraan. De toxiciteit van kationische PNPs zou kunnen worden verzwakt door het verhogen van de sterische bulk rond de kationische lading. In het algemeen geven de kationische en kleinere (45 nm) PNP-deeltjes een hogere cellulaire opname dan de anionogene en grotere (90 nm) PNPs.

In hoofdstuk 7 wordt de interactie tussen verschillend geladen (kationische en anionische) PNPs (tri-blok copolymeer en polystyreen NP) en ATP-binding cassette (ABC)-transporters onderzocht. Hiervoor werden Caco-2 cellen gekweekt als monolagen op transwell inserts voordat ze werden blootgesteld aan de verschillende PNPs. Kationische PNPs vertonen een veel hogere flux in de Caco-2 monolagen dan de anionische PNPs. De verschillende PNPs laten een interactie zien met de verschillende ABC-transporters op een oppervlakte lading-afhankelijke wijze. De kationische PNPs vertonen voornamelijk interactie met P-gps die tot expressie komen op het apicale zijde van de Caco-2 monolaag. Interessant is dat door blokkeren van de verschillende transporters met ABC specifieke remmers, het transport en ook de verdeling van PNP in de Caco-2 monolagen (apicale, intracellulaire en basolaterale compartiment) na 24 uur blootstelling veranderd kan worden. Dit geeft aan dat de PNPs mogelijk kunnen optreden als substraten voor deze verschillende ABC-transporters. De PNP veranderen ook de verdeling van het pro-carcinogeen PhIP over deze Caco-2 monolagen. Hieruit blijkt dat de PNPs mogelijk de opname van verschillende verbindingen, waaronder schadelijke verbindingen zoals PhIP, kan beïnvloeden na orale blootstelling.

Om de in vitro experimenten met Caco-2 monolagen, die blootgesteld zijn aan verschillende PNPs te valideren, werden in een in vivo experiment mannelijke Fischer344 ratten oraal blootgesteld aan monodisperse (45 ± 5 nm) fluorescerende tri-blokcopolymeer NPs die zowel kationische als anionische oppervlakte-ladingen bezaten. Na de toediening werd bloed verzameld door het regelmatig opofferen van de ratten gedurende een blootstelling van 6 uur. Hirna werden verschillende organen (zoals lever, nieren, hersenen, longen, etc.) en tenslotte het bloed en de ingewanden verzameld en onderzocht op hun PNP gehalte door middel van fluorescentie. PNP met beide oppervlakte-ladingen vertoonden absorptie in de darmen na orale blootstelling met een maximum accumulatie in lever en nieren. Er werden ook PNPs aangetroffen in de milt en in de botten. Interessant is dat zowel kationische als anionische PNPs de bloed-hersen barrière (BBB) kunnen oversteken en aangetoond werden in de hersenen. Interessant is dat de oppervlakte lading-afhankelijkheid van de opname, zoals waargenomen in in vitro studies (hoofdstuk 7), ontbrak in de in vivo studie. Een mogelijke verklaring kan zijn dat als gevolg van de aanwezigheid van het slijmvlies in de darm, de PNP een coating krijgen die de oppervlakteladingen op de PNP afschermen en dus een verschil veroorzaakt tussen de in vivo en de in vitro resultaten.

In hoofdstuk 9 wordt een beknopte onderzoek beschreven naar het mechanisme van cytotoxiciteit van polystyreen NP (PSNP) met kationische en anionische oppervlakte-ladingen (50 nm), uitgevoerd op NR8383 cellen. De cytotoxiciteit van kationische PSNP werd vergeleken met die van de mitochondriale ETC verstorende stof 2,4-dinitrofenol (DNP) en het oxidatieve stress-inducerend middel waterstofperoxide. De patronen van dosis-afhankelijke cytotoxiciteit door de kationische PSNPs kwamen overeen met de werking van DNP en niet met die van waterstofperoxide. Nadat de cellen met anti-oxidanten (vitamine E en C) een pre-incubatie hadden ondergaan, was er weinig bescherming tegen de cytotoxiciteit van de kationische PSNP, dit kwam ook weer overeen met het effect van DNP en niet met dat van waterstof peroxide. Op basis van deze observaties werd verondersteld dat het de mitochondriale ETC verstoring en niet

oxidatieve stress fungeert als een startpunt in de toxiciteitcascade veroorzaakt voor kationische PSNP.

In lijn met de resultaten beschreven in hoofdstuk 9, is een diepgaand onderzoek gestart naar het effect van verschillende oppervlakte-ladingen van 50 nm PSNPs (kationische en anionische) op NR8383 cellen. Alleen de kationische PSNPs bleken het cellulaire ATP gehalte uit te putten, de mitochondriale membraanpotentiaal te verlagen, en aan de andere kant de cellulaire ROS levels, het cellulaire vrije calcium en TNF-α, caspase-3 en transcriptiefactor NF-kB niveaus na 4 uur blootstelling te verhogen. Met behulp van atomic force microscopy (AFM) kon de topografie van het NR8383 celoppervlak worden vastgesteld na blootstelling aan kationische en anionische PSNP. Het bleek dat de kationische PSNP schade veroorzaken aan de integriteit van het celmembraan door verhoging van de ruwheid en zelfs het maken van gaten of poriën in het celmembraan. Op basis van deze waarnemingen, kon een route die het werkingsmechanisme van de toxiciteit van kationische PSNP beschrijft worden voorgesteld.

Tenslotte wordt in hoofdstuk 11 een algemene discussie over de analyse van al de resultaten beschreven uit dit proefschrift, samen met enkele toekomstperspectieven.

Appendix A

Supplementary Information for Chapter 3
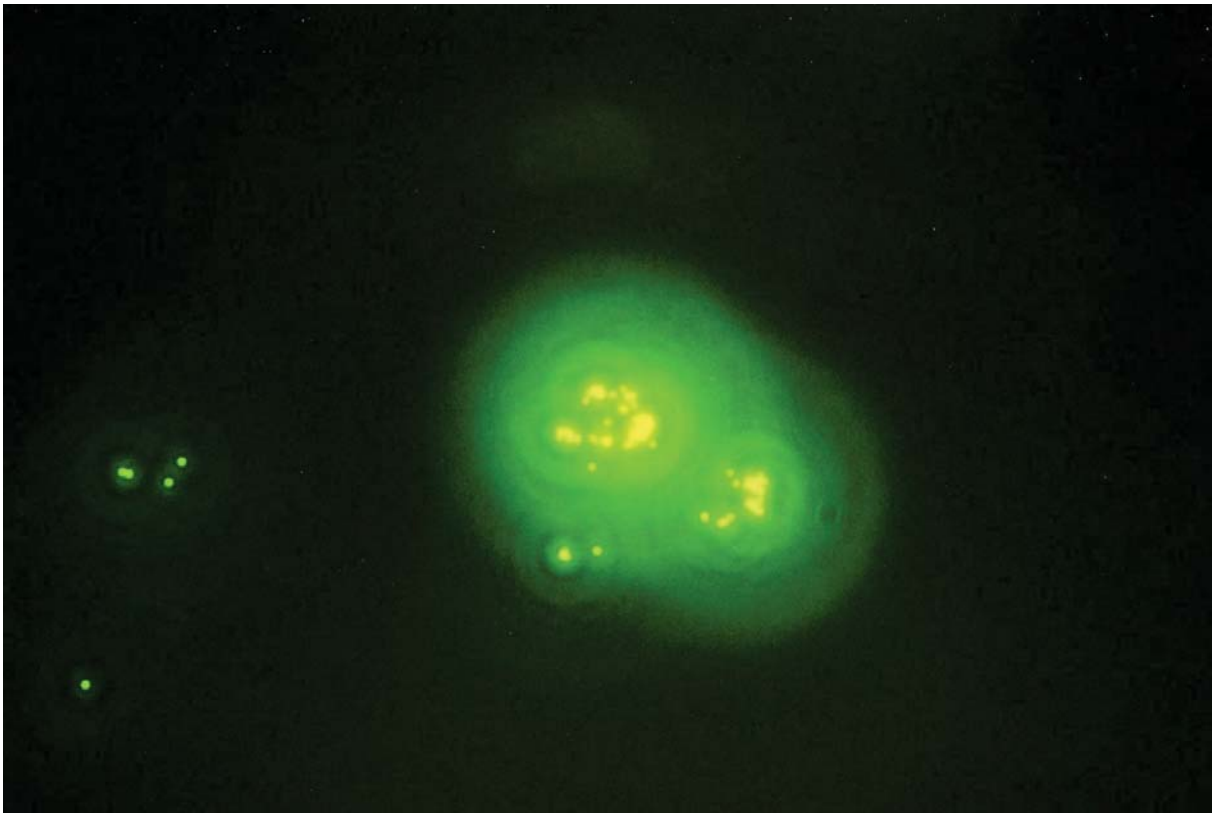
Figure A1: *Fluorescence microscopy picture of NR8383 cells with phagocytosed 1 µm latex beads.*

Appendix B

Supplementary Information for Chapter 5
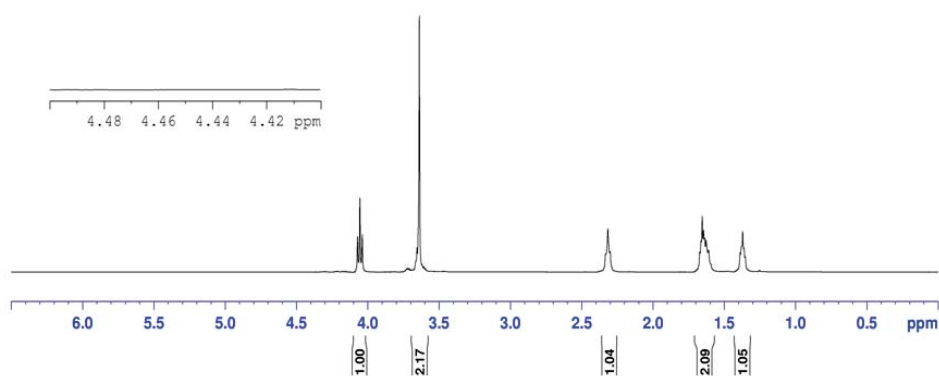
Figure B1: ^1H NMR of PEG$_{2000}$-PHA-PEG$_{2000}$ polymer in CDCl$_3$. Integration of the peaks is used to calculate the average molecular weight.

SEC data of PEG2000-PHA-PEG2000 polymer (in THF)
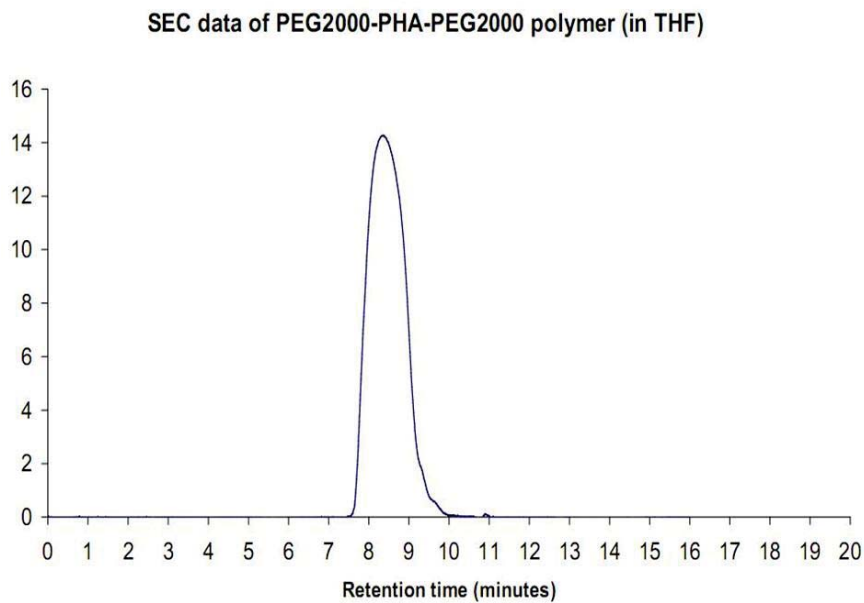
Figure B2*: SEC data of PEG$_{2000}$-PHA-PEG$_{2000}$ polymer in THF.*
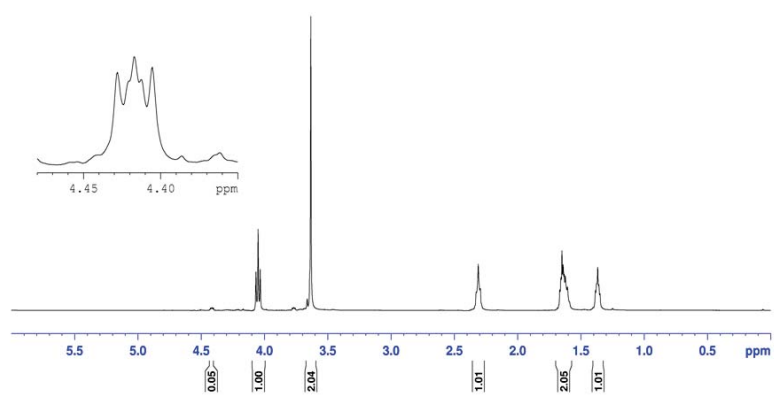
Figure B3*: ^{1}H NMR data of unmodified PEG$_{2000}$-PHA-PEG$_{2000}$ polymer to which TAIC was added; the appearance of the trifurcated peak at δ=4.43 ppm is due to reaction of the free terminal hydroxyl groups with TAIC.*
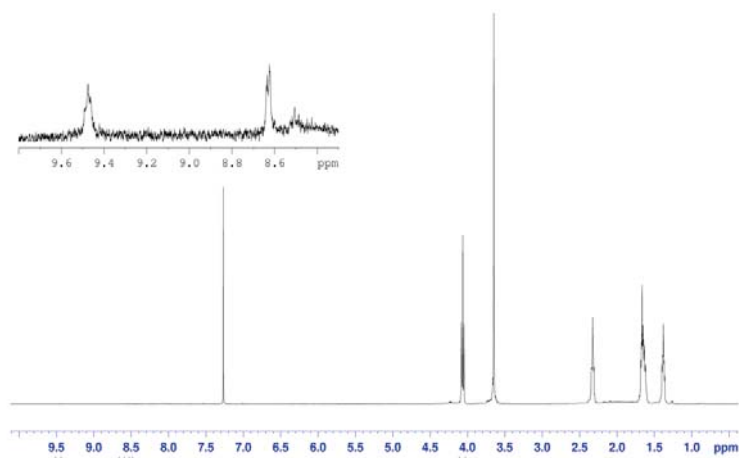
Figure B4: *^{1}H NMR of polymer Pol-Py in CDCl$_3$ showing proton peaks from pyridinium end groups.*
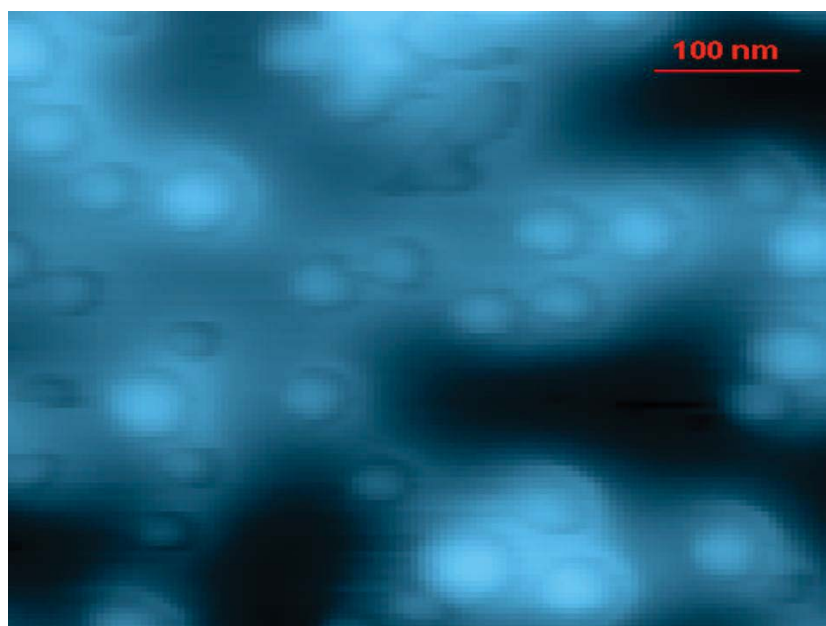
Figure B5: *AFM picture of PNP (45 ± 5 nm) on mica surface in tapping mode.*
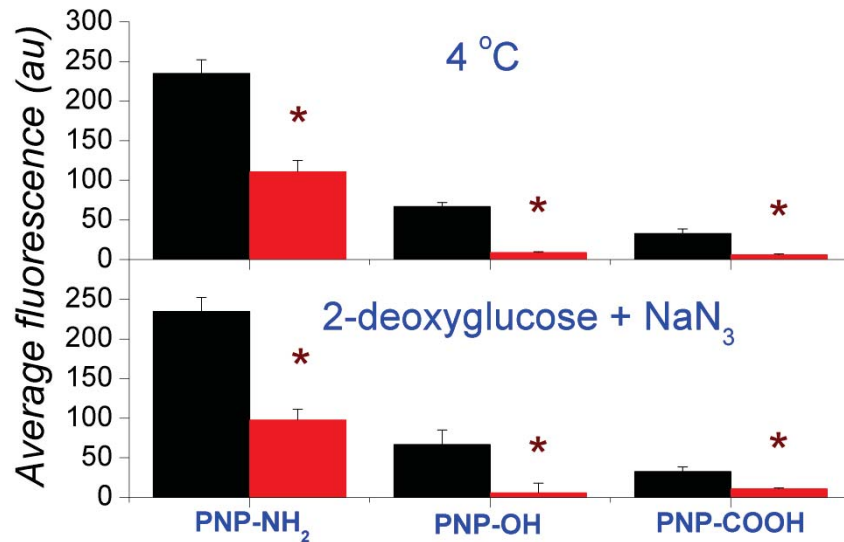
*Figure B6: Average fluorescence from the NR8383 cells after 24 h exposure to different PNP with endocytosis inhibited. The black and red columns represent uptake before and after endocytosis inhibition respectively for each PNP. The results are shown as mean ± SEM of 30 individual cells (n=6). The * symbol signifies results that are statistically different from results before endocytosis inhibition (p < 0.05).*
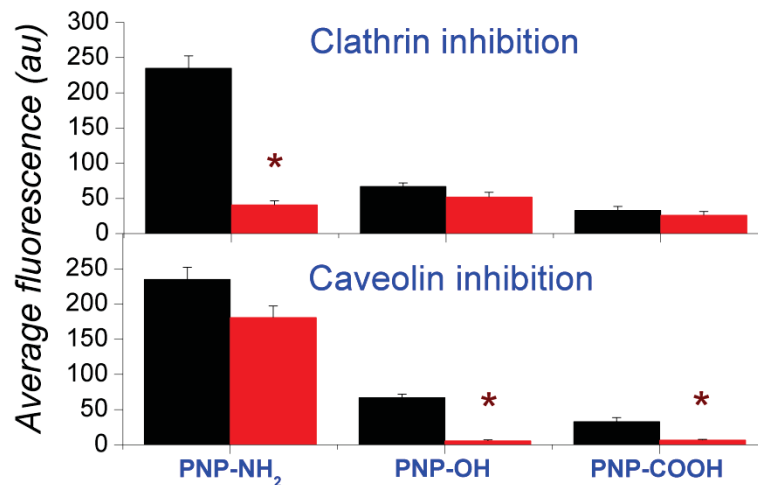

*Figure B7: Average fluorescence from the NR8383 cells after 24 h exposure to different PNP with clathrin and caveolin mediated endocytosis inhibited. The black and red columns represent uptake before and after endocytosis inhibition respectively. The results are shown as mean ± SEM of 30 individual cells (n=6). The * symbol signifies results that are statistically different from results before endocytosis inhibition (p < 0.05).*
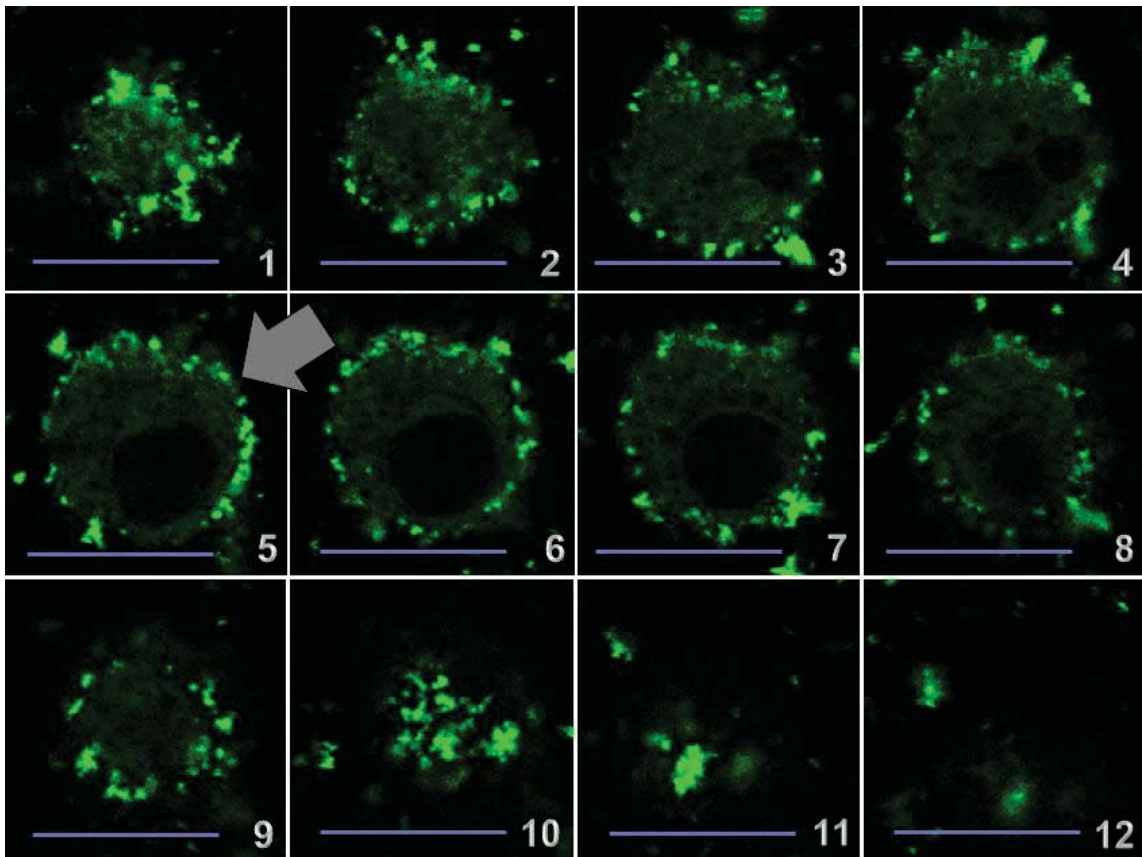
Figure B8*: z-stack image of a NR8383 cell after 24 h exposure to positive PNP-NH$_2$ showing that the PNP were inside the cells and not on the surface. The top left slice (number 1) shows the bottom and the bottom right slice (number 12) shows the top of the cell (λ_{ex} = 488 nm). A halo of fluorescence could be seen from the cellular periphery (arrow) showing more interaction of positive PNP-NH$_2$ with cell membrane compared to other intracellular compartments. Scale bars show 10 µm.*

Appendix C

Supplementary Information for Chapter 6
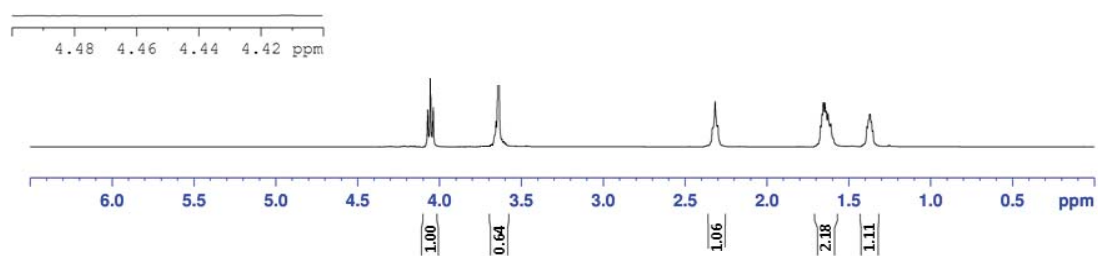
Figure C1: ^1H NMR spectrum of PEG$_{400}$-PHA-PEG$_{400}$ polymer in CDCl$_3$ showing no peak(s) at δ=4.43 ppm.
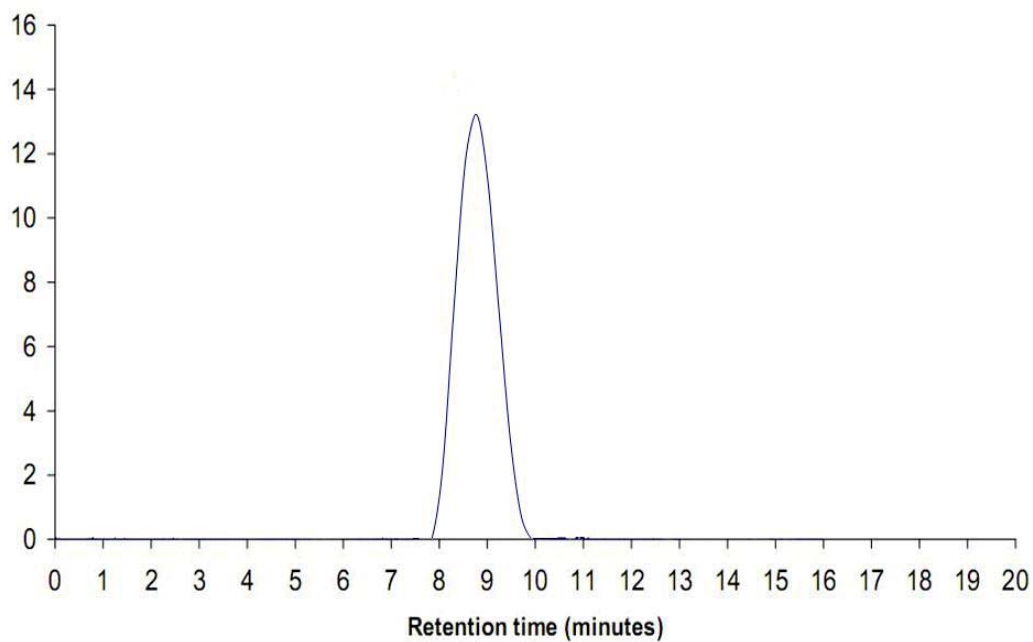
Figure C2: *SEC trace of PEG$_{400}$-PHA-PEG$_{400}$ polymer in THF.*
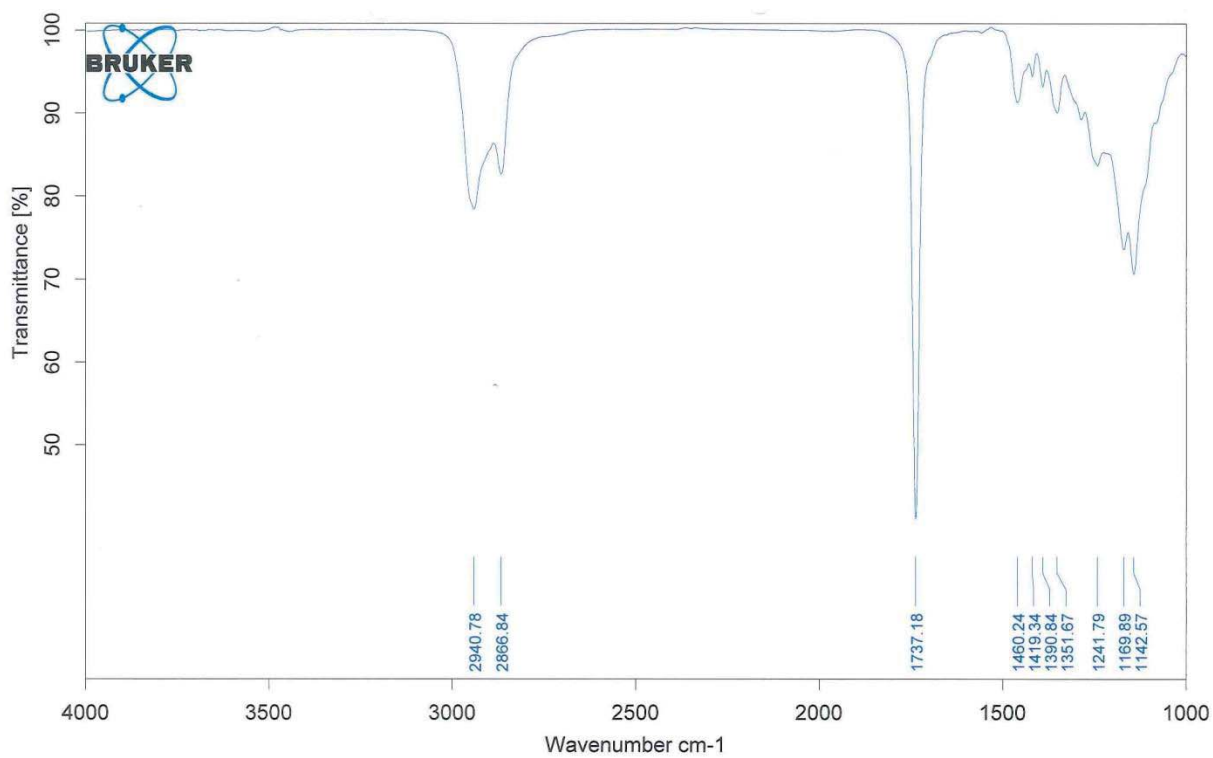
Figure C3: *IR spectrum of Pol$_{400}$ [PEG$_{400}$-PHA-PEG$_{400}$] in carbon tetrachloride (CCl$_4$).*
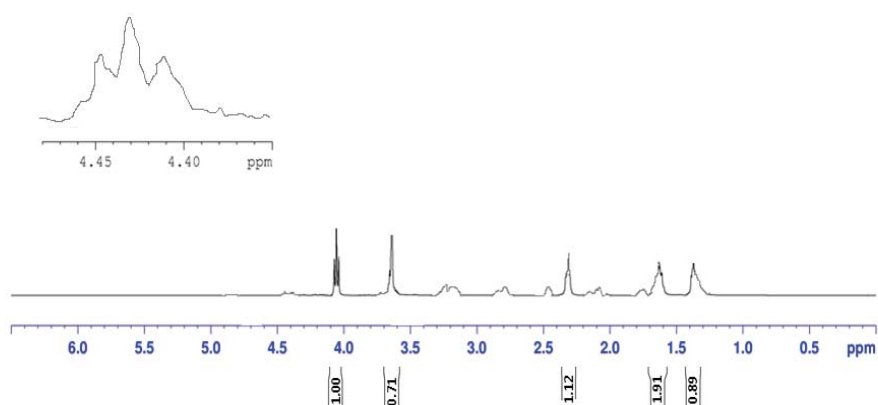
*Figure C4:* *^{1}H NMR spectrum of unmodified PEG$_{400}$-PHA-PEG$_{400}$ polymer to which TAIC is added. The presence of a trifurcated peak at δ=4.43 ppm results from the reaction of the free terminal hydroxyl groups with TAIC.*
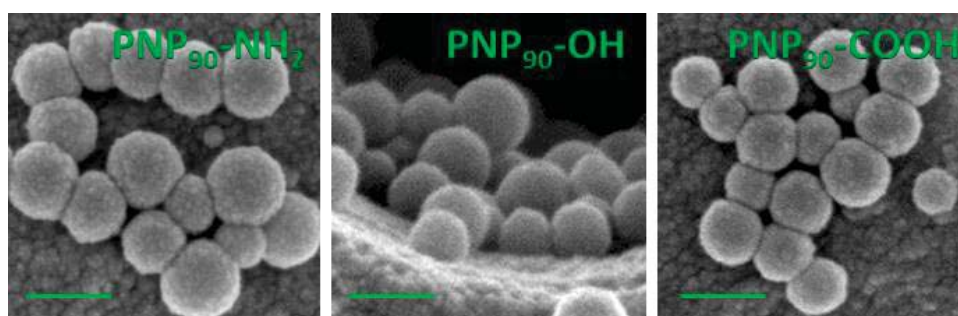

Figure C5: *Scanning electron microscopy pictures of PNP$_{90}$-NH$_2$, PNP$_{90}$-OH and PNP$_{90}$-COOH. Scale bars show 100 nm.*
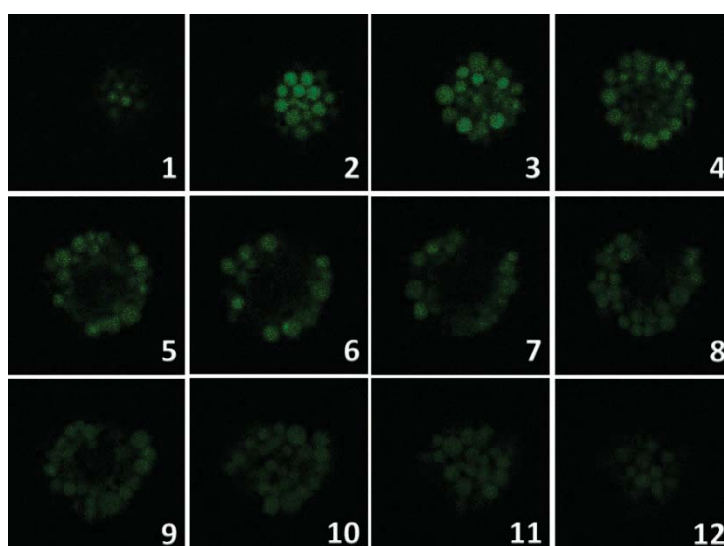
*Figure C6:* *z-stack imaging in NR8383 cells after 24 h exposure to the PNP$_{90}$-OH at 4 °C showing that the PNP were actually inside the cells and not bound to the cell membrane (λ_{ex}=488 nm; λ_{em}=543 nm). Slide 1 showed the bottom and slide 12 showed the top sections of the cell with thickness of each slice ~400 nm.*
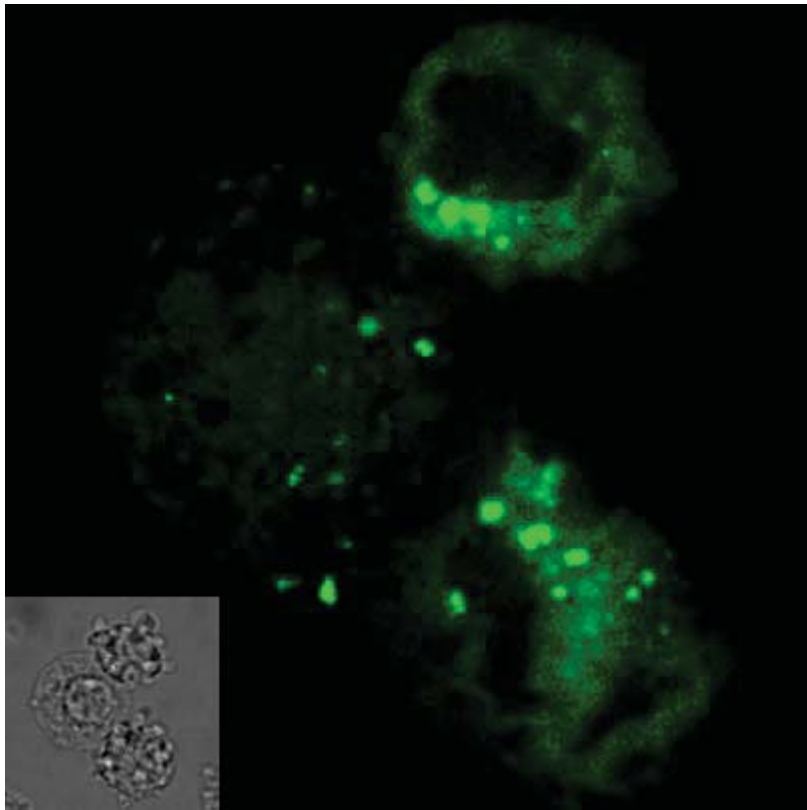
*Figure C7: CLSM picture of some NR8383 cells that have taken up fluorescent $PNP_{90}\text{-}NH_2$.*
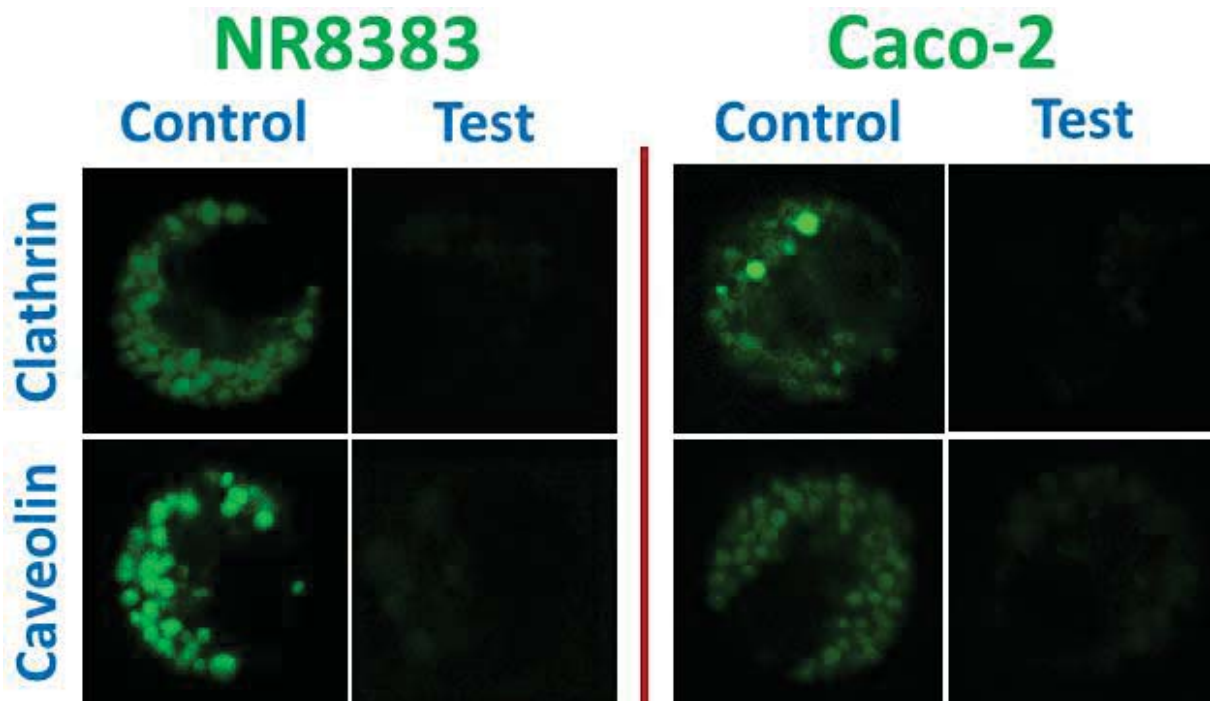
Figure C8: Uptake of green fluorescent transferrin and cholera toxin subunit-B by NR8383 and Caco-2 cells. Control: no blocking of the receptors. Test: Upon selectively blocking the clathrin receptors by hypertonic sucrose or caveolin receptors by MβCD.

Appendix D

## *Supplementary Information for Chapter 7*
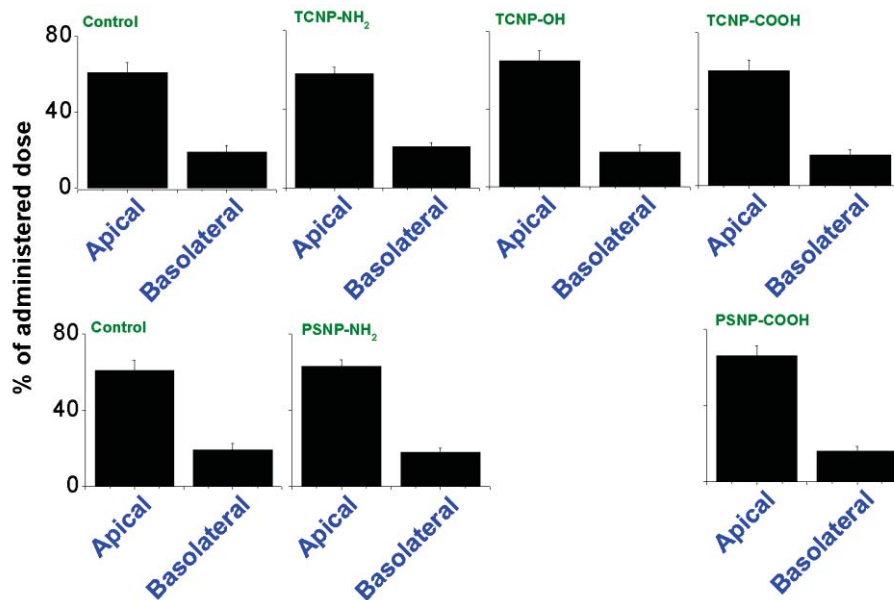
Figure D1: *Control test with passage of lucifer yellow (λ_{ex}=428 nm; λ_{em}=540 nm) across Caco-2 monolayers without and with exposure to different TCNP (upper layer) and PSNP (lower layer) at 1 µg/ml concentration confirming the integrity of the Caco-2 monolayers (n = 3).*
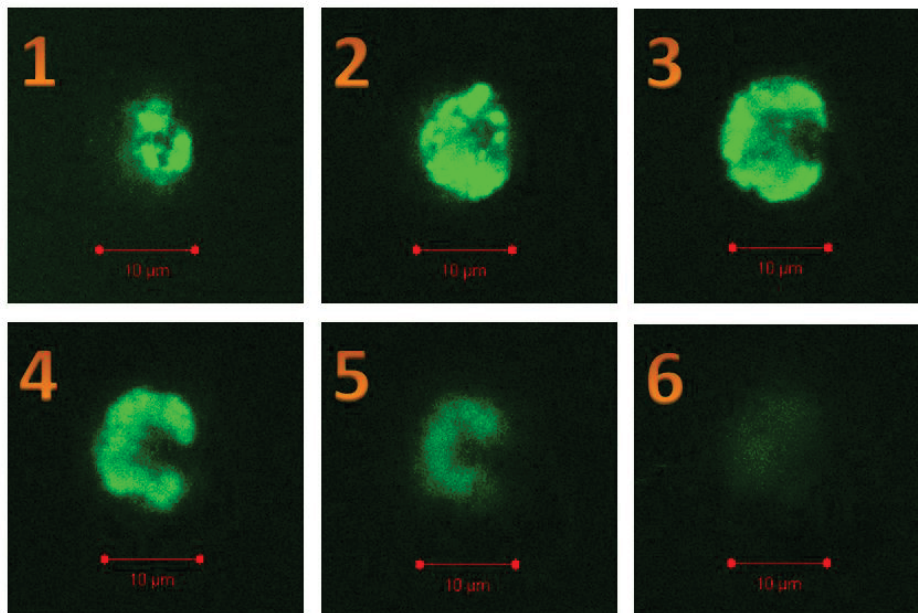

Figure D2: *z-stack imaging of a Caco-2 cell (grown in transwell Caco-2 monolayer) after exposure to positive TCNP-NH$_2$ at 24 h. The slide 1 shows the bottom and slide 6 shows the top section of the cell. Scale bars show 10 µm and embedded in the figures.*

Abbreviations

µm	Micrometer
ABC-transporter	ATP binding cassette-transporter
AFM	Atomic force microscopy
ATCC	American type culture collection
BrdU	5-bromo-2'-deoxyuridine
BSO	Buthionine sulfoximine
$CDCl_3$	Deuterated chloroform
CdSe/ZnS	Cadmium selenide/Zinc sulphide
CLSM	Confocal laser scanning microscopy
DAPI	4',6-diamidino-2-phenylindole
DCFH-DA	2',7'-dichlorfluorescein-diacetate
DLS	Dynamic light scattering
DMEM	Dulbecco's Modified Eagle Medium
DMSO	Dimethylsulfoxide
DNP	2,4-dinitrophenol
DSC	Differential scanning calorimetry
EC50	Half-maximal effective concentration
EFSA	European Food Safety Authority
ETC	Electron transfer chain
F12-K	Ham's F-12K (Kaighn's) medium
FCS	Fetal calf serum
FWHM	Full width half maximum
Ge NP	Geranium nanoparticles
GSH	Glutathione
h	Hour
H_2O_2	Hydrogen peroxide
HBSS	Hank's balanced salt solution
HEK	Human epidermal keratinocyte
IL	Interleukins
iv	Intravenous
$LiAlH_4$	Lithium aluminium hydride
min	Minutes
MTT	3-(4,5-Dimethylthiazol-2-yl)-2,5-diphenyltetrazolium bromide
MβCD	Methyl-beta-cyclodextrin
NAC	N-acetyl cysteine
NAD	Nicotinamide dinucleotide
NEAA	Non-essential amino acid
NF-κB	Nuclear factor kappa-light-chain-enhancer of activated B cells
nm	Nanometer
NMR	Nuclear magnetic resonance
NP	Nanoparticles
ns	Nano-seconds
PAMAM	Poly-amidoamine
PBS	Phosphate buffer saline
PDI	Polydispersity index
PEG	Polyethyleneglycol
PNP	Polymeric nanoparticles
PNP-DMEA	Polymeric nanoparticles-dimethylethanolamine
PNP-Py	Polymeric nanoparticles-pyridinium

ps	Pico-second
PSNP	Polystyrene nanoparticles
PSNP-COOH	Carboxylic acid-terminated polystyrene nanoparticles
PSNP-NH$_2$	Amine-terminated polystyrene nanoparticles
QD	Quantum dots
ROS	Reactive oxygen species
SCQD	Semi-conductor quantum dots
SEC	Size exclusion chromatography
SEM	Standard error of mean
SERS	Surface-enhanced Raman spectroscopy
Si NP	Silicon nanoparticles
Si NP-COOH	Carboxylic acid-terminated silicon nanoparticles
Si NP-N$_3$	Azide-terminated silicon nanoparticles
Si NP-NH$_2$	Amine-terminated silicon nanoparticles
SiCl$_4$	Silicon tetrachloride
t$_{1/2}$	Half-life
TCNP	Tri-block copolymer nanoparticles
TCNP-COOH	Carboxylic acid-terminated tri-block copolymer nanoparticles
TCNP-NH$_2$	Amine-terminated tri-block copolymer nanoparticles
TCNP-OH	Hydroxyl-terminated tri-block copolymer nanoparticles
TEER	Trans-epithelial electrical resistance
TEM	Transmission electron microscopy
THF	Tetrahydrofuran
TNF-α	Tumor necrosis factor-alpha
TOAB	Tetraoctyl ammonium bromide

List of Publications

A. Part of this thesis

1. Ruizendaal L, <u>Bhattacharjee S</u>, Pournazari K, Rosso-Vasic M, De Haan LHJ, Alink GM, Marcelis ATM, Zuilhof H. Synthesis and cytotoxicity of silicon nanoparticles with covalently attached organic monolayers. *Nanotoxicology* **2009**, 3(4):339-347. (**Citations**: 17 as on 31/07/2012).

2. <u>Bhattacharjee S</u>, De Haan LHJ, Evers NM, Jiang X, Marcelis ATM, Zuilhof H, Rietjens IMCM, Alink GM. Role of surface charge and oxidative stress in cytotoxicity of organic monolayer-coated silicon nanoparticles towards macrophage NR8383 cells. *Part. Fibre Toxicol.* **2010**, 7(25). (**Citations**: 18 as on 31/07/2012).

3. <u>Bhattacharjee S</u>, Ershov D, vd Gucht J, Alink GM, Rietjens IMCM, Zuilhof H, Marcelis ATM. Surface charge-specific cytotoxicity and cellular uptake of tri-block copolymer nanoparticles. *Nanotoxicology* **2011**, Advanced online (DOI: 10.3109/17435390.2011. 633714). (**Citations**: 1 as on 31/07/2012).

4. <u>Bhattacharjee S</u>, Ershov D, Fytianos K, vd Gucht J, Alink GM, Rietjens IMCM, Marcelis ATM, Zuilhof H. Cytotoxicity and cellular uptake of tri-block copolymer nanoparticles with different size and surface characteristics. *Part. Fibre Toxicol.* **2012**, 9(11).

5. <u>Bhattacharjee S</u>, Rietjens IMCM, Singh MP, Clark RJ, Atkins TM, Alink GM, Kauzlarich SM, Veinot JGC, Fink MJ, Marcelis ATM, Zuilhof H. The cytotoxicity of surface-functionalized silicon and germanium nanoparticles: the dominant role of surface charges. *Submitted* **2012**.

6. <u>Bhattacharjee S</u>, van Opstal EJ, Alink GM, Marcelis ATM, Zuilhof H, Rietjens IMCM. Surface charge-specific interactions between polymer nanoparticles and ABC transporters in Caco-2 cells. *Submitted* **2012**.

7. <u>Bhattacharjee S</u>, Marcelis ATM, Zuilhof H, Rietjens IMCM, Alink GM. Role of surface charge in bioavailability and biodistribution of tri-block copolymer nanoparticles in rats after oral exposure. *Submitted* **2012**.

8. <u>Bhattacharjee S</u>, Marcelis ATM, Zuilhof H, Alink GM, Rietjens IMCM. Oxidative stress is a secondary mode of action in cytotoxicity of polystyrene nanoparticles. *Submitted* **2012**.

9. <u>Bhattacharjee S</u>, Ershov D, Islam AM, Kämpfer AM, Maslowska KA, vd Gucht J, Alink GM, Marcelis ATM, Zuilhof H, Rietjens IMCM. Surface charge and size-dependent cytotoxicity and cell membrane interaction of polystyrene nanoparticles. *Submitted* **2012**.

B. Not part of this thesis

1. Clift MJD, <u>Bhattacharjee S</u>, Brown DM, Stone V. The effects of serum on the toxicity of manufactured nanoparticles. *Toxicol. Lett.* **2010**, 198:358-365. (**Citations**: 10 as on 31/07/2012).

2. vd Ploeg MJC, vd Berg JHJ, <u>Bhattacharjee S</u>, de Haan LHJ, Ershov D, Fokkink RG, Zuilhof H, Rietjens IMCM, vd Brink NW. Toxicity of nanoparticles towards isolated coelomocytes of the earthworm *Lumbricus rubellus*. *Submitted* **2012**.

Poster/Oral presentations

1. **Nanotoxicology2010** (Poster Presentation); Edinburgh, UK (**Poster**: *Influence of surface charge in cytotoxicity of polymer nanoparticles*).

2. **Fifth International Symposium on Nanotechnology-Occupational and Environmental Health 2011** (Oral talk and Scholarship recipient) Boston, MA, USA (**Title of talk**: *Towards understanding the role of surface charge in cytotoxicity and cellular uptake of tri-block copolymer nanoparticles*).

3. **Biological Implications of Nanoparticles (Minisymposium) 2011**, Lund University, Lund, Sweden (**Title of talk**: *Towards understanding the importance of the interactions between the nanoparticles and cell membrane bound receptors*).

4. **Netherlands Annual Ecology Meeting 2011**, Lunteren, the Netherlands (**Title of talk**: *Oxidative stress: Lessons learned from a nanotoxicology perspective*).

Overview of training activities

Discipline specific activities

Courses
Advanced Organic Chemistry (2009 and 2010)
Risk Assessment (2010)
Toxicogenomics (2011)
Laboratory Animal Science (2011)
Ecotoxicology (2011)
Molecular Toxicology (2011)

Meetings
Nanotoxicology2010 conference in Edinburgh, UK (2010)
5th International Symposium on Nanotechnology-Occupational and Environmental Health in Boston, MA, USA (2011)
Annual NOW Conference Structure and Reactivity, NOW, Lunteren (2009-2011)

General courses

Information Literacy including EndNote Introduction (2011)
Communication in Interdisciplinary Research (2011)
Career Assessment
Philosophy and Ethics of Food Science and Technology (2012)
Career Perspectives (2012)

Optionals

Preparing research Proposal
Analytical Methods in Organic Chemistry (2008)
PhD Study trip to Scotland and North England (2011)
Group Meetings (2008-2012)
Colloquia, Laboratory of Organic Chemistry (2008-2012)
Research in Progress Presentations, Division of Toxicology (2008-2012)
IPOP/BioNano WUR seminars (2009-2010)
KNCV symposium talk (2012)

Sourav **Bhattacharjee**

Sourav Bhattacharjee was born on the 16th September 1978 in Kolkata, India. After finishing his schooling from *Jadavpur Vidyapith*, he joined *Medical College and Hospital Kolkata* in 1997 to study *Bachelor of Medicine and Surgery (MBBS)*. After completion of the MBBS in 2002, he worked for seven months as *Residential House Surgeon (RHS)* in the Dept. of Orthopaedic Surgery of the *Medical College and Hospital, Kolkata*. In 2006 he started pursuing MSc in Biomolecular Sciences/Cell Biology in the *Vrije Universiteit Amsterdam* in the Netherlands. While doing his Masters, he went to Edinburgh (Scotland) and worked in the Napier University in the laboratory of Prof. Vicki Stone. After finishing his MSc in 2008, he joined as a PhD student in a collaborative project between Lab. of Organic Chemistry and Division of Toxicology in Wageningen University, the Netherlands. The most important results obtained in this PhD project are described in this thesis. After PhD, he will work as a post-doctoral research fellow in the *BIOS/Lab-on-a-Chip* group headed by Prof. Albert van den Berg in the MESA+ Institute of Nanotechnology of University of Twente in the Netherlands.

An avid traveller, he has visited more than twenty countries in the Europe as well as other countries like USA, Singapore, UAE. He is a life member of *International Red Cross* as well as member of Royal Australian Chemical Institute, Royal Society of Chemistry (UK), Institute of Nanotechnology (UK), Dutch KNCV. He was member of debate societies and took part in many debate competitions while in college. He is a supporter of *Manchester United FC* in English Premiere League and *Ajax FC* in Dutch *eredivisie*.

ACKNOWLEDGEMENTS

"It was the best of times, it was the worst of times, it was the age of wisdom, it was the age of foolishness, it was the epoch of belief…"

A Tale of Two Cities *(Charles Dickens)*

I still remember the stormy morning of 2008 when I boarded a train to Wageningen from Amsterdam in order to appear in an interview for a PhD position. All I knew that it was a PhD position where nanotoxicology played a significant part along with synthesis of nanoparticles, i.e. the PhD project was a collaborative and interdisciplinary project between disciplines of organic chemistry and toxicology. After more than three years now, here I stand busy writing the final few pages of my thesis. Something that started on a stormy morning of 2008 is about to end in the near future. It has been an incredible journey for the last almost four years and cries for an account on how these few years unfolded with surprises stored in every nook and corner.

Unlike a usual PhD project, I rather had two supervisors and two promoters owing to the equal collaboration between organic chemistry and toxicology with each department pouring over with one supervisor and one promoter. With added statures and reputations as scientists from all these four outstanding people, I must confess that the situation at the start was slightly apprehensive for me and rather nervous. I think it is the right spot in this account to mention these fabulous four persons: from organic chemistry Dr. Antonius T. M. Marcelis (co-promoter) and Prof. dr. Han Zuilhof (promoter) and from toxicology Dr. Gerrit M. Alink (co-promoter) and Prof. dr. Ivonne M. C. M. Rietjens (promoter). This amalgamation of four brilliant scientists always kept my project special for me and I gratefully acknowledge their utmost sincerity, outstanding support and never ending wishes that they bestowed on me throughout my PhD tenure. I think it is absolutely important for a PhD student that he must always be able to look up to his supervisors with respect and dignity. In my case, I simply could do that. For Han, I would like to say that I should rather consider myself lucky if in my entire life I can grab even a quarter of your knowledge. Your knowledge, not only in chemistry, but also in contemporary arts, philosophy, literature is truly outstanding. I thank you for giving me this scope of doing this PhD under your supervision. With Ton, it was a working relation that I would cherish and preserve in my memory. He is one of those supervisors who do not need an appointment to be knocked by the PhD student. It really made my life much easier as I could get his guidance as and when I needed it. With his (Ton) unbeatable patience and cool temperament, I always found it easy to work and move along with my project. The incredible efforts that he put in revising my manuscripts are really something worthy to mention. I would like to thank Gerrit for his ever-friendly gestures and always being in side whenever I required him. I share a very warm personal relationship with him and consider him almost as a "friend, philosopher and guide" whom I can share my problems and seek suggestions. I wish him all the best in his new venture in archaeology which I am sure, he will make it as big as it gets. I look up to Prof. Rietjens as an example of leadership and effectiveness. The whiskers she took before replying mails, initiating the necessary actions and the incomparable speed that she can work with, is very hard to match. I must say that I also like her approach of research which at least for me, worked out well. I must

confess that without her tireless efforts and continuous inspiration, I could not have made even half the publications that I have now.

You four are and will remain within the few of my strongest pillars of life and I would not hesitate a single moment to offer you all with my earnest homage, thanks and greetings. You four are the epitome of virtues and wisdoms and I dream to acquire, at least partially, few of your outstanding qualities in later parts of my life.

My MSc students, who did their thesis under my supervision, deserve nothing lesser than an early mention. To name them: Xue Jiang (China), Nynke M. Evers (Netherlands), Mohamed A. Islam (Bangladesh), Kleanthis Fytianos (Greece), Edward J. van Opstal (USA), Angela A. Kämpfer (Germany) and Katarzyna A. Maslowska (Poland). I want to thank you all from the bottom of my heart. It was like that you all came to my project from different parts of the planet and blessed it with your sincerity and hard work. If I stand strong today with my thesis, it is because of your diligence and cumulative efforts. I am happy to see that you all are pursuing careers in science. Please continue worshipping science as it is the only truth. Maybe, it is through you and all the students you will train yourselves in future, my existence as a scientist will move on irrespective of whether I am there or not.

Dmitry Ershov, a PhD student from Lab. of Physical Chemistry and Colloid Science (WUR), along with his supervisor Dr. Jasper van der Gucht, was an important part of this project. With amazing hardship, Dmitry kept on doing confocal studies and got beautiful pictures for my articles. I am proud that both Dmitry and Jasper got involved in my project. With Dmitry, it is a wonderful friendship and a surprising comfort, which I think also, got reflected over the works that we did over the years. It is exhilarating for me to have both Dmitry and Jasper as my co-authors and I offer you both my sincere thanks and cordial wishes for your future lives.

In the last part of my project, I did an animal experiment and for that I had to work with the Wageningen UR animal housing facility (CKP). I want to extend my thanks to all my colleagues there for their sincere support. I would just like to name Rob, Rene, Wilma, Bert and Lisette as part of that amazing team that helped me going through the task. Thank you all!

Graduate school VLAG and Wageningen University Strategic Research Programme Bionanotehnology are acknowledged for generous funding. I am especially thankful to Fre Pepping, Yvonne Smolders and Vesna Prsic from VLAG for their continued support as and when I needed it. I represented Lab. of Organic Chemistry PhD students in VLAG PhD Council for several months and I would like to thank all my colleagues there for making those months fruitful and effective.

In Toxicology, I am grateful to Laura H. J. de Haan for immense support with work especially in my initial days. My sincere thanks to both Bert and Hans for all the help they offered to me. I also acknowledge the help of Dr. Walter Brand and Dr. Alicia Paini in several small but important things while doing experiments. I would like to extend my love and affection to all other toxicology PhD students. It was an honor working with you all.

In organic chemistry, several people need special mention: Barend van Lagen for all the NMR and fluorescence experiments, Elbert van der Klift and Frank Claasen for size exclusion chromatography and Dr. Marcel Giesbers for AFM. Within staff members, Tom Wennekes needs to be singled out as there was a point of time when he was representing staff members of organic chemistry in VLAG while I was representing the PhD students. On few occasions we had to sort out or rather discuss things out and I can say with no ambiguity that Tom is a great human being. My personal thanks and best wishes go to Maurice Franssen, Teris van Beek, Carel

Weijers, Jos M. J. Paulusse, Ronald and Cees van Rijn. During my teaching classes, I got immense help from Cees van de Haar, Anne-Marie Franssen and Erik van Rozendaal. I would like to express my gratitude to all of them. Nishant Sewgobind and Wouter Biesta did an amazing job in teaching me the Dutch language. It has been a great friendship and I believe that you both are great ambassadors of friendship as well as the people of the Netherlands. Elly Geurtsen and Aleida Ruisch helped me a lot with my official procedures and I would like to thank them very much on this occasion.

My best wishes to all my PhD colleagues in organic chemistry. A special mention for Jaime Garcia Hartjes for the brotherhood with him, sparked by both of us being alumni from the Vrije Universiteit Amsterdam. We both (along with Anke and Willem) were members of the PhD trip organizing board in 2011 to the UK and I must say, that trip was perhaps the happiest phase of my life in Wageningen. My Indian colleagues (Umesh, Satesh, Saurabh, Nagesh, Sidharam and Nagendra) made my life full of laughter which even resulted in a successful *Indian Curry Borrel*. I want to say to the PhD students of organic chemistry that you are the best. On a philosophical note, I would like to make you remember that, this earth is made from the Sun and we all have a Sun inside. With the warmth and light of the Sun within you, I am pretty sure you all will succeed to reach your destinations overcoming all the obstacles that you face. Not merely my wishes, but rather my dreams are with you all!

I gratefully acknowledge two of my Dutch friends, Sjoerd J. Dalmeijer and Gerben Broens, for being an outstanding support throughout my stay in the Netherlands. You are the best two gifts that this country had given me. It was a pure co-incidence that our paths crossed and looking back, I feel proud that it did. You two, being friends, have always uplifted my spirits and morale when it sagged for whatever reasons. Our moments of happiness, unity, laughter, joy, partying, travelling make a nice collage and compel me in believing that such an unconditional friendship is perhaps the holiest possible relationship on this earth. Thanks to both of you for being there always.

I remember some of my family members who were snatched from my life by the brutal truth of death. With heavy heart, I remember my grandparents, both maternal (the late Priyabandhu Chakraborty and late Pratima Chakarborty) and paternal (the late Manindra Chandra Bhattacharjee and late Binapani Bhattacharjee). I also sadly remember the demises of my two uncles: the late Samarendra Chandra Bhattacharyya and late Sudhindra Nath Bhattacharyya, who would have been ecstatic, if alive today. I hope wherever they are, they rest in peace and they bestow their blessings on me so that I can continue doing hard work with honesty and sincerity.

I thank Dr. Rieky van Walraven from the *Faculty of Earth and Life Sciences* in the Vrije Universiteit Amsterdam for her indispensable support throughout my stay as a MSc student and even before joining my PhD in Wageningen. The affection that I got from her as a study coordinator in my MSc student days is something to treasure. I would also like to extend my thanks to Dr. Dirk Bald and Dr. Yves Bollen from the same faculty for their valuable teaching and guidances.

I would like to thank Prof. Vicki Stone for giving me the opportunity to do my MSc thesis in her laboratory way back in 2007. It was one of the most testing periods of my life when being a destitute; I literally used to stroll the streets of Edinburgh, looking for just any opportunity in my career. A scope to work in Prof. Stone's laboratory not only did give my life and career a direction, but also provided me with some sort of an identity. "From Vicki Stone's lab" was a tag

that catalyzed my acceptability and recognition in this field and I do not know how to express my thanks to her for that. Dr. Martin J. D. Clift, my then PhD supervisor, had a significant role in teaching me in my formative days. With the care, affection and guidance he gave me, I am proud to say that Martin was, is and will always be my teacher. For David Brown, I want to say that those simple tips and tricks that I learned from you in laboratory work, still help me. A big thanks to you as well.

My sincere thanks to the people and Governments of both the Netherlands and UK for giving me quality education and international exposure. I am indebted to each and every citizen of these two countries for making this happen.

Last but definitely not the least; I would like to thank my homeland India for giving me my identity as an Indian. It is very hard to explain India and I would not dare it as well. All I can say is that, in spite of whatever drawbacks she has, India is a country of great wisdom. It is a spiritual country and she has proudly taught me to love and care for everyone irrespective of their religion, cast and creed. In simple words there is something very *Indian* about her…an identity which is unique and unparallel. I would like to bow down in front of this great country and cradle of humanity for giving me my life, my family and nurture throughout with her love, wishes, care and support.

In final words, with love, affection and blessings from so many people from different facets of my life, I truly believe that my life is blessed. This PhD is a result of all such stories of outstanding support that I kept on gathering like a selfish giant. All these extraordinary gestures of magnanimity, help and bliss, make me believe in an old Indian saying, "*It is a sin to lose faith on humanity*". This is categorically the essence of not only this PhD, but of my entire bitter-sweet life in spectrum.